Structural and Reactivity Studies of Bis(Imido) Complexes of Molybdenum(VI)

Thérèse Anne Coffey

Supervisor: Dr Graeme Hogarth

Sir Christopher Ingold Laboratories
Department of Chemistry
University College London

October 1997

ProQuest Number: U643798

All rights reserved

INFORMATION TO ALL USERS
The quality of this reproduction is dependent upon the quality of the copy submitted.

In the unlikely event that the author did not send a complete manuscript
and there are missing pages, these will be noted. Also, if material had to be removed,
a note will indicate the deletion.

ProQuest.

ProQuest U643798

Declaration

Except where noted, all the work reported in this thesis was carried out by myself in the Department of Chemistry, University College London, between October 3rd, 1993 and September 30th, 1996. Experiments denoted by an asterisk were performed by Kayode Ajayi, under my direct supervision, as part of his undergraduate project. Molecular orbital calculations were performed by Dr Nik Kaltsoyannis and Woo-Sung Kim. X-ray diffraction crystallography was performed by Dr Graeme Hogarth and Simon Redmond. X-ray powder diffraction was performed by Miss Elizabeth MacLean.

Thérèse Coffey

Dedication

A.M.D.G.

To my family

L.D.S.

Abstract

This thesis concerns the synthesis, structure and reactivity of bis(imido) complexes of molybdenum. Eleven new complexes of the type, $[Mo(NR)_2(S_2CNEt_2)_2]$, are synthesised upon reaction of $[Mo(NR)_2Cl_2(DME)]$ with sodium diethyldithiocarbamate, differing only by the imido substituent.

Crystal structures of $[Mo(N^tBu)_2(S_2CNEt_2)_2]$ and $[Mo(N(2-Me)C_6H_4)_2(S_2CNEt_2)_2]$ exhibit linear-linear imido ligation. The crystal structure of $[Mo(NPh)_2(S_2CNEt_2)_2]$ **1**, re-determined at room temperature, shows bent-linear imido ligation.

VT solution nmr spectroscopy confirms the fluxionality in all complexes. Structural information is discerned from solid-state ^{13}C nmr spectra; a direct relationship between the difference in imido angles and the difference in ppm of the *ipso*-carbon peaks has been established. Absolute imido angles are not calculated but comparing the angle difference with known complexes helps predict their potential reactivity. Of the structurally-unknown complexes, only those arylimido complexes without *ortho*-substituents suggest bending in an imido ligand. MO calculations suggest that, even for **1**, there is negligible preference for linear-linear or bent-linear imido ligation. Other molecular interactions, like crystal packing forces, are cited as the dominant structural influence.

Bis(imido) complexes with different co-ligands and metal centres are reported. It is suggested that $[Mo(NPh)_2(S_2CNMe_2)_2]$ has linear-linear imido ligation, contrasting with **1**.

Reactivity with other simple molecules is investigated, most notable of which is the reaction with hydrogen sulfide to form disulfide complexes $[Mo(NR)(S_2)(S_2CNEt_2)_2]$. Reaction with acids gave bis(amido), imido-amido and also imidotris(dithiocarbamate) cations.

The mechanism of the formation of $[Mo(NPh)(S_2)(S_2CNEt_2)_2]$ upon reaction of phenyl isocyanate with $[Mo(O_2)(S_2CNEt_2)_2]$ is studied.

Acknowledgements

I would like to thank my supervisor Dr Graeme Hogarth for his inspiration, his patience and good humour. I have really enjoyed working for you and I'm sure I'll never have another boss like you. P.S. Congratulations on becoming a father.

To all my friends in Labs 243/5, particularly Simon and Graham, who have suffered me for longer than they or I care to mention; I hope we all had some fun together. Outside the Lab, Ashley, Elizabeth, Kit, Mick and Nicola have all helped make postgrad life especially enjoyable.

Thankyou also to those who have helped in technical and academic matters - especially to the ULIRS team of Patrick Barrie, Abil Aliev and David Butler.

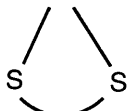Finally, I would like to acknowledge both the EPSRC and my parents for funding.

Index

Abbreviations and Symbols

Ar	2,6-diisopropylphenyl
e^-	electron
ether	diethylether
petrol	40/60 petroleum ether
DME	dimethoxyethane
thf	tetrahydrofuran
etc	diethyldithiocarbamate, $[S_2CN(C_2H_5)_2]$

also in diagrams by $S \diagdown \diagup S$

mtc	dimethyldithiocarbamate, $[S_2CN(CH_3)_2]$
Me	methyl
Et	ethyl
Ph	phenyl
^{t}Bu	*tert*-butyl
^{i}Pr	isopropyl
adm	1-adamantyl
uv	ultraviolet
nmr	nuclear magnetic resonance (spectroscopy)
s	singlet
d	doublet
t	triplet
q	quartet
m	multiplet
δ	chemical shift
ppm	parts per million
J	coupling constant
Hz	Hertz
VT	variable temperature
CPMAS	Cross Polarisation Magic Angle Spinning
NQS TOSS	Non-Quaternary Suppression TOtal Suppression of Sidebands
ir	infra-red (spectroscopy)
w	weak
m	medium
s	strong
vs	very strong
υ	stretching frequency
uv-vis	ultraviolet-visible (spectroscopy)

Mass Spec.	mass spectrometry
EI	electron impact
FAB	fast atom bombardment
MO	molecular orbital
M	metal (general)
M=N	metal-imido
Cp	η^5- cyclopentadienyl (C_5H_5)
Cp*	η^5- cyclopentamethyldienyl (C_5Me_5)
X	anionic ligand (general)
S.S.B.	Spinning side bands

Compound numbers

* indicates new complexes synthesized in this thesis

1	[Mo(NPh)$_2$(etc)$_2$]
2*	[Mo(N^{t}Bu)$_2$(etc)$_2$]
3*	[Mo(N(2-Me)C$_6$H$_4$)$_2$(etc)$_2$]
4*	[Mo(N(3-Me)C$_6$H$_4$)$_2$(etc)$_2$]
5	[Mo(N(4-Me)C$_6$H$_4$)$_2$(etc)$_2$]
6*	[Mo(N(2-F)C$_6$H$_4$)$_2$(etc)$_2$]
7	[Mo(N(2,6-^{i}Pr$_2$C$_6$H$_3$))$_2$(etc)$_2$]
8	[Mo(N(2,6-Me$_2$C$_6$H$_3$))$_2$(etc)$_2$]
9*	[Mo(N(2,4-Me$_2$C$_6$H$_3$))$_2$(etc)$_2$]
10*	[Mo(N(3,4-Me$_2$C$_6$H$_3$))$_2$(etc)$_2$]
11*	[Mo(N(3,5-Me$_2$C$_6$H$_3$))$_2$(etc)$_2$]
12*	[Mo(N(2,6-F$_2$C$_6$H$_3$))$_2$(etc)$_2$]
13	[Mo(N(2,6-Cl$_2$C$_6$H$_3$))$_2$(etc)$_2$]
14*	[Mo(Nadm)$_2$(etc)$_2$]
15*	[Mo(NC$_6$D$_5$)$_2$(etc)$_2$]
16*	[Mo(NC$_6$F$_5$)$_2$(etc)$_2$]
17*	[Mo(NPh)$_2$(mtc)$_2$]
18*	[Mo(N^{t}Bu)$_2$(mtc)$_2$]
19*	[Mo(N^{t}Bu)$_2$(S$_2$C(OEt)$_2$)$_2$]
20*	[Mo(NPh)$_2$(S$_2$PPh$_2$)$_2$]
21*	[Cr(N^{t}Bu)$_2$(etc)$_2$]
22*	[Cr(N^{t}Bu)$_2$(mtc)$_2$]
23*	[Mo(O)(N(4-Me)C$_6$H$_4$)(etc)$_2$]
24	[Mo(NS)(etc)$_3$]
25*	[Mo(O)(N(2,6-F$_2$C$_6$H$_3$))(etc)$_2$]
26*	[Mo(NHAr)$_2$(etc)$_2$]$^{2+}$
27*	[{Mo(N(2,6-^{i}Pr$_2$C$_6$H$_3$))$_2$(etc)(μ-MoO$_4$)$_2$}$_2$]
28*	[Mo(NHAr)(NAr)(etc)$_2$]$^+$
29*	[Mo(NAr)(NHAr)(mtc)$_2$]$^+$
30	[Mo(N^{t}Bu)(etc)$_3$]$^+$
31*	[Mo(NH^{t}Bu)(N^{t}Bu)(etc)$_2$]$^+$
32	[Mo(NPh)(S$_2$)(etc)$_2$]
33	[Mo(N^{t}Bu)(S$_2$)(etc)$_2$]
34	[Mo(N(2-Me)C$_6$H$_4$)(S$_2$)(etc)$_2$]
35	[Mo(N(2,6-^{i}Pr$_2$C$_6$H$_3$))(S$_2$)(etc)$_2$]
36	[Mo(N(2,6-Me$_2$C$_6$H$_3$))(S$_2$)(etc)$_2$]
37*	[{Mo(N(2,6-^{i}Pr$_2$C$_6$H$_3$))$_2$(etc)}$_2$(μ-S)(μ^2-η^2-S$_2$)]
38	[Mo(N(2,6-Cl$_2$C$_6$H$_3$))(S$_2$)(etc)$_2$]
39	[Mo(N(2,6-^{i}Pr$_2$C$_6$H$_3$))$_2$(mtc)$_2$]

Chapter 1   Introduction

1.1   General

The focus of this introduction is the chemistry of imido and (bis)imido complexes of Group 6 metals. Topics discussed include bonding, syntheses, structural studies, spectroscopy and reactivity. A brief introduction to multiply bonded ligands is offered. Examples of complexes with different metals may be used and analogies are drawn with oxo complexes, as the oxo and imido moieties are isoelectronic and also because such oxo complexes have been extensively studied. The dithiocarbamate ligand will be considered specifically with reference to its bonding and potential reactivity. Concise introductions begin each chapter drawing on particularly relevant work. Finally, note that (Ar) always refers to the 2,6-diisopropylphenyl group.

The chemistry of imido complexes has only developed recently; the first complex was synthesized in 1956, namely $[OsO_3(N^tBu)]$[1,2].

$$OsO_4 \ + \ ^tBuNH_2 \longrightarrow \quad + \quad H_2O$$
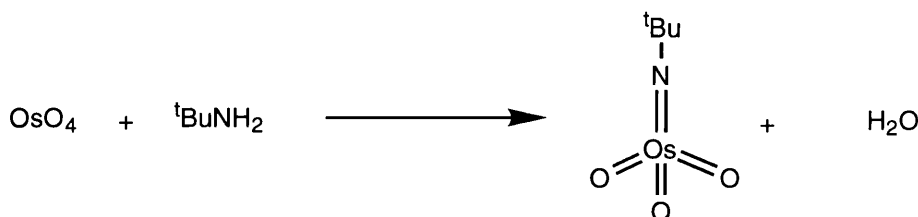
Sharpless later surmised that this complex would add across a double bond (just as for OsO_4) to form β-amino alcohols, allowing direct cis-addition of oxygen and nitrogen moieties across a double bond[3,4].
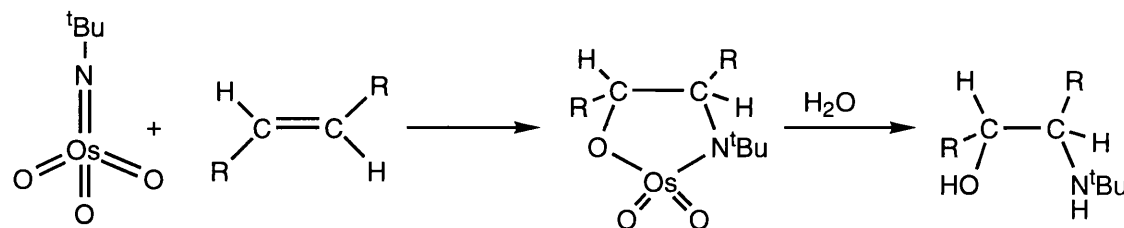
In recent years, there has been a resurgence of interest in imido complexes. They are thought to be intermediates in some catalytic reactions, eg. production of acrylonitrile from propene, ammonia and water[5] and feature in ROMP catalysis[6]. There have been two fairly comprehensive reviews on this subject - published in 1980[7] and in 1994[8] - and a book entitled "Metal-Ligand Multiple Bonds" was published in 1988[9].

1.2 Multiply-Bonded Ligands

The imido ligand is isoelectronic with the well-known oxo, sulfido and alkylidene ligands, when considered as closed shell anions. The differences between these ligands results from changes in π-donating ability of the coordinate atom, polarisability and changes in electronegativity, which are themselves affected by other substituent groups and the metal centre. They do share some characteristics - namely, stabilizing transition metals in high-oxidation states, utilisation of their metal-ligand multiple bond in catalytic cycles and having the inherent unsaturation in the multiple bond which is a potential reaction site. This commonality is a consequence of $d\pi$-$p\pi$ bonding in these complexes.

Oxo ligands are formally doubly-deprotonated water molecules (O^{2-}); they are strong π-donor ligands mainly found when stabilizing high oxidation-state metal complexes. The metal should be a π- acceptor and adequately electron-deficient to allow charge distribution:

$$M^z\text{—}O^- \rightleftharpoons M^{z-1}\text{=}O \rightleftharpoons M^{z-2}\text{≡}O^+$$
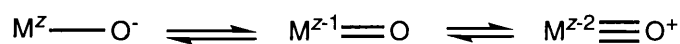
Doubly-bonded oxo ligands have bond lengths of 1.6-1.8Å and show bands in the ir spectrum between 850-1000 cm^{-1} - both being indicative of their multiple bond character. Metal-oxo compounds are regularly used in organic synthesis, to effect epoxidations and oxidation generally. For example, $[Cr(O)_2(ONO_2)_2]$[10] and porphyrin complexes of ruthenium that use atmospheric oxygen as their co-oxidant[11] have both been used to facilitate the epoxidation reaction.
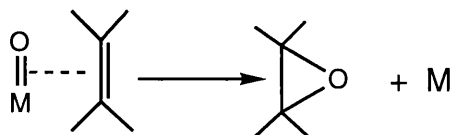
A further example is the selective epoxidation of allylic alcohols with *tert*-butyl hydroperoxide with a vanadium oxo catalyst[12].
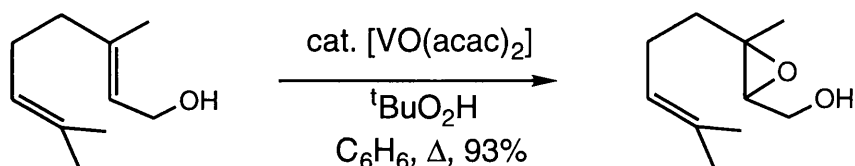
A classic example of oxidation involving a metal-oxo complex is the cis-1,2-diolisation of alkenes using osmium tetroxide, OsO_4. Although intense debate about its mechanism continues, it is believed to proceed via a 4-membered oxa-metallcycle

---

transition state and another ligand, such as pyridine, triggers rearrangement to the osmium chelate; in the process, Os(VIII) is reduced to Os(VI)[13].
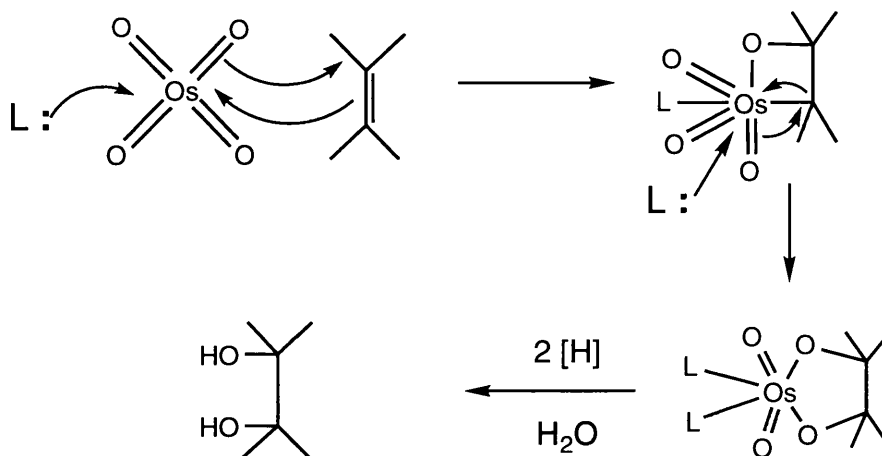
Holm's 1987 review cites many examples of metal-centred oxygen atom transfer reactions[14] and states that, "[Mo] lies at the epicentre of oxo transfer chemistry. More oxo compounds have been prepared and characterized, more oxo transfer reactions are known, and more catalytic systems based on these reactions have been devised than for any other element." The example shown below illustrates the transfer of oxygen to phosphine, reducing the metal from Mo(VI) to both Mo(IV) and to Mo(V) in the dimeric complex[15,16]. Such dimer formation is a frequent occurrence as the reduced species may also attack the bis(oxo) complex as well as the phosphine.

$$Ph_3P \ + \ [Mo(O)_2(etc)_2] \longrightarrow Ph_3P{=}O \ + \ [Mo(O)(etc)_2] \ + \ [Mo_2O_3(etc)_4]$$
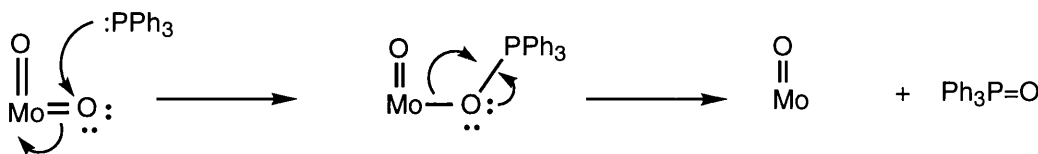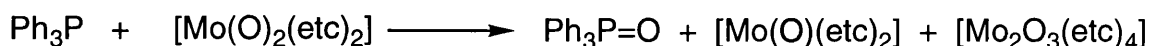
Molybdenum dioxo complexes are particularly studied as they are thought to be involved in the active site for enzymic activity in biological systems.

Alkylidene ligands ([M]=CRR') are divided into two classes - Fischer-type and Schrock-type. In simple terms, the Fischer-type alkylidene (the "carbene") has π-donor sustituents, often a heteroatom (i.e. oxygen, nitrogen or sulphur - e.g. [(CO)$_5$CrC(OMe)(Me)] -see below), and these ligands bind to low oxidation-state metal centres; bonding is dominated by a single dative bond from an occupied orbital on the ligand and stabilized by π back-bonding from filled metal d-orbitals. Fischer-

type complexes may be expected to be quite inert as the lone electron pair on the heteroatom may be used to fill the vacant orbital at the alkylidene carbon atom. However, as that carbon atom is electrophilic, it is readily attacked by nucleophiles.

$$Cr(CO)_6 + MeLi \longrightarrow \left[(CO)_5Cr = C \begin{smallmatrix} O^- \\ Me \end{smallmatrix} \right] Li^+ \xrightarrow{Me_3O^+BF_4^-} (CO)_5Cr = C \begin{smallmatrix} OMe \\ Me \end{smallmatrix}$$

$$(CO)_5Cr = C \begin{smallmatrix} OMe \\ Ph \end{smallmatrix} + EtNH_2 \longrightarrow \left[(CO)_5Cr - \underset{Ph}{\overset{NHEt}{C}} - OMe \right]^- EtNH_3^+ \longrightarrow (CO)_5Cr = C \begin{smallmatrix} NHEt \\ Ph \end{smallmatrix}$$
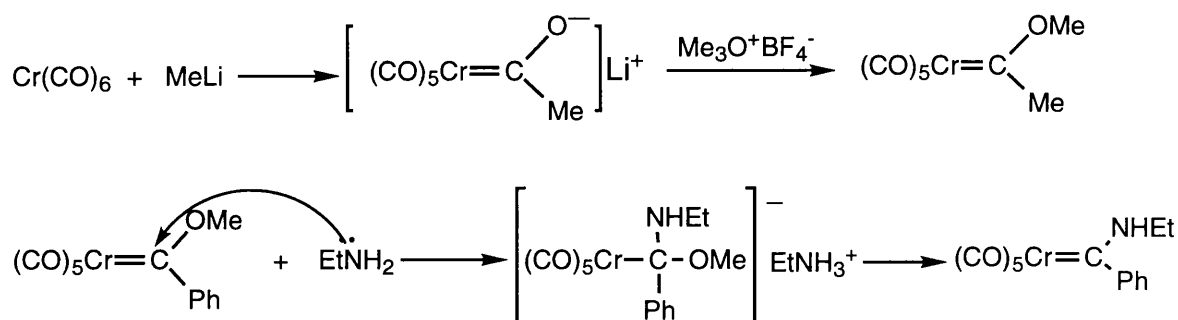
Schrock-type alkylidenes have no heteroatom substitution and bind to high oxidation-state metal centres. The bonding in these cases is thought to be formed by a full sp^2 orbital donating its π-electron density to an empty metal d-orbital (plus π-donation from the carbon p_z orbital). There, the alkylidene carbon atom is nucleophilic, i.e. electrophiles may be added.

$$[TaCp_2Me_2]^+ \xrightarrow[-H^+]{base} \underset{Cp}{\overset{Cp}{>}} Ta \begin{smallmatrix} CH_2 \\ Me \end{smallmatrix}$$

$$({}^tBuCH_2)_3Ta = C \begin{smallmatrix} H \\ {}^tBu \end{smallmatrix} + O = C \begin{smallmatrix} H \\ R \end{smallmatrix} \longrightarrow R'_3Ta - \underset{H}{\overset{{}^tBu}{C}} - \underset{R}{\overset{H}{C}} - O^-$$

$$R'_3Ta = O \quad + \quad \underset{H}{\overset{{}^tBu}{>}} = \underset{R}{\overset{H}{<}}$$
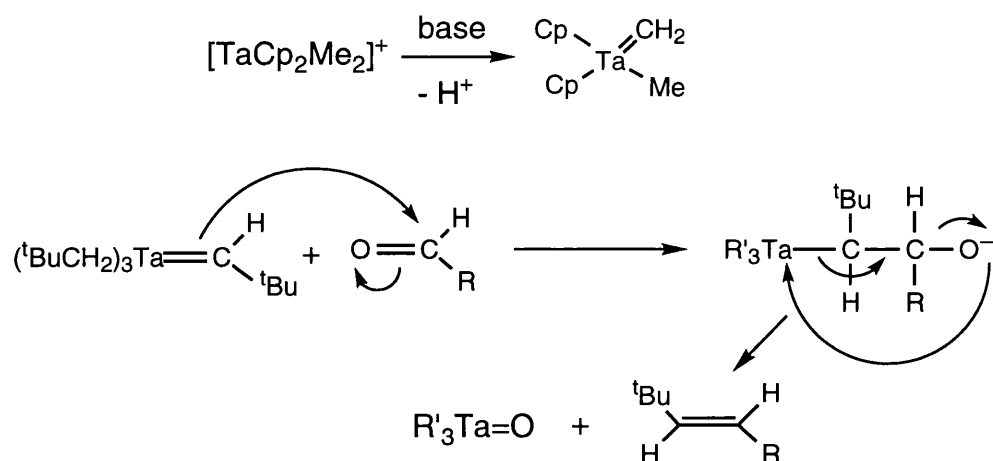
Schrock-type alkylidenes' reactivity may be compared to that of Wittig reagents, c.f.

$$Ph_3P = C \begin{smallmatrix} R \\ R \end{smallmatrix} \xrightarrow{RCHO} Ph_3P = O + \underset{R}{\overset{R}{>}} = \underset{R}{\overset{H}{<}}$$
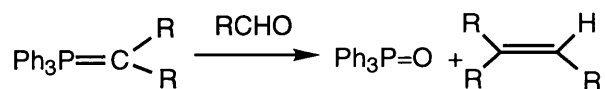
An important difference between the alkylidene and the imido (and oxo) ligand is that the former cannot form a second π-bond to the metal centre.

Finally, the <u>sulfido ligand</u> is of particular interest to this work due to its importance in much of the earlier, related research performed in this laboratory. Sulfur ligands can be made from many sources - hydrogen sulfide, thiols, elemental sulfur, thiocyanates and sulfites. Their negative charge and the high polarizability of their

---

electrons provide the opportunities for bridging. Molybdenum-sulfur complexes are known for their great versatility in bonding, chemical reactivity and redox chemistry. One factor in this is due to the closeness in energy of S, Mo(IV), Mo(V) and Mo(VI) energy levels[17]. Polysulfides are well known, particularly as binary metal sulfides, e.g. $[MoS_4{}^{2-}]$, and in mineralogical and biological systems. Sulfide ligands (S^{2-}) tend to bridge two or more metal centres rather than form terminal ligands. An illustration of the sulfide ligand's versatility can be seen when bridging two metal centres; as seen below, it can act as a 2, 4 or 6 electron donor.
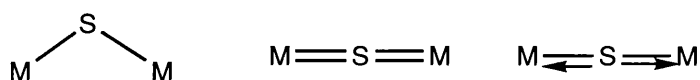
The disulfide ligand $(S_2{}^{2-})$ is very versatile in its coordination modes - ten in all, so far - based on its ability to bind side-on or by bridging metal centres (M–S–S–M) with sulfur's remaining lone electron pairs available for further bonding. The most common bonding mode is that of side-bound coordination to one metal centre as a η^2-ligand. Other modes shown are $\eta^1–\eta^1$, $\eta^2–\eta^2$ and one which shows end-on coordination.

$[Mo(NPh)(S_2)(etc)_2]$[18] $[Ru_2(NH_3)_{10}(S_2)]^{4+}$ [19] $[Mo_2(S_2)_6]^{2-}$ [20] $[Cp^*{}_2Cr_2(S_2)_2S]$ [21]
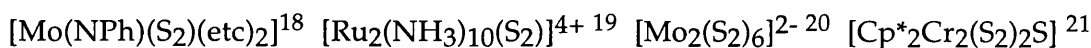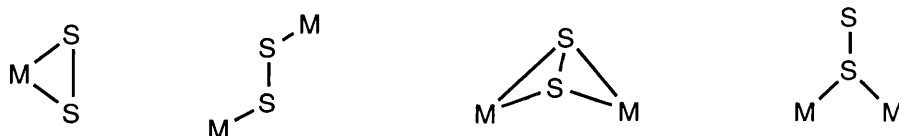
This last example is of note as it displays more than one bonding mode for sulfur[21]:
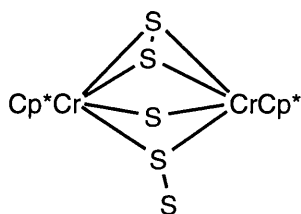
In the ir spectrum, S–S stretches fall between 480 - 600 cm^{-1} and structurally, S–S bond lengths usually vary from 1.98 to 2.15 Å. The $\eta^2–\eta^2$ ligand (the third bonding mode illustrated above) binds asymmetrically to the metal centres. Its S-S bond length is slightly shorter than the usual 1.98 to 2.15 Å. Furthermore, as may be expected, its frequency in the ir spectrum is generally higher than for the normal, side-bound coordination. Synthesis has been achieved by reacting a metal complex with elemental sulfur, direct substitution with another disulfide salt and by reaction with other common sulfur-containing reagents. Further, earlier in this laboratory, a series of

disulfide complexes was obtained upon reaction and decomposition of dithiocarbamate ligands[18,22].

$$[Mo(O)_2(etc)_2] \xrightarrow[\text{toluene, 3d, } \Delta]{\text{RNCO}}$$
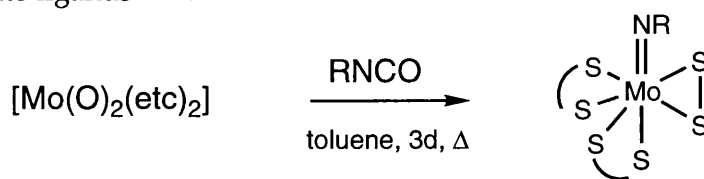
1.3   The Imido Ligand

The imido ligand may be formally regarded as a doubly-deprotonated amine, RN^{2-}. One of its facets is that it can act as a "spectator" ligand. This means that it can vary its electron-donation to the metal centre and still remain bound, while not actually participating in a chemical reaction. The effect is well documented for bis(oxo) complexes and is assumed for bis(imido) complexes[23-25]. By changing the bond order of the multiply-bonded ligand, so the activation barrier to a chemical reaction may be lowered. A monoxo (or monoimido) complex must overcome a high activation barrier upon reaction due to complete loss of its π-donor from the high-valent metal centre. In contrast, when there is another multiply-bonded ligand, the bond order drops and as one π-donor leaves the complex, so the other can donate more strongly to the metal centre - i.e. the activation barrier is lower.

high activation barrier

low activation barrier
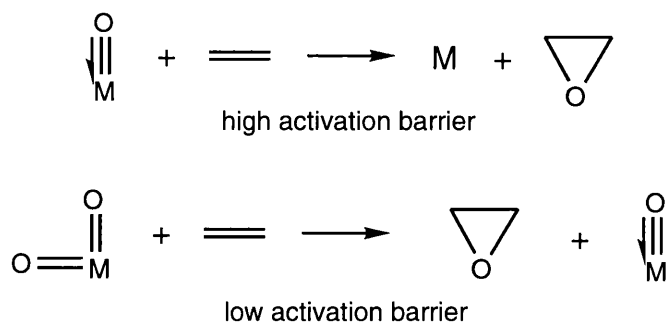
Bonding may be considered using valence-bond (VB) theory or molecular orbital (MO) theory but, as will be discussed later in detail, when considering bis(imido) complexes MO theory affords the most accurate picture. The somewhat simplistic VB description of bonding suggests *sp* hybridization about the nitrogen atom for a linear ligand with 1 σ and 2 π bonds; the bent ligand has sp^2 hybridization with only 1 σ and 1 π bond. Considering the ligands to be neutral, the linear ligand is a four-electron donor and the bent a two-electron donor. A third possibility is where the ligand is a two-electron donor but linearity is kept because symmetry forbids electron donation.

M=N $\diagup$ R

N (sp^2)
2e⁻ donor

M=N—R

N (sp)
2e⁻ donor

M≡N—R

N (sp)
4e⁻ donor
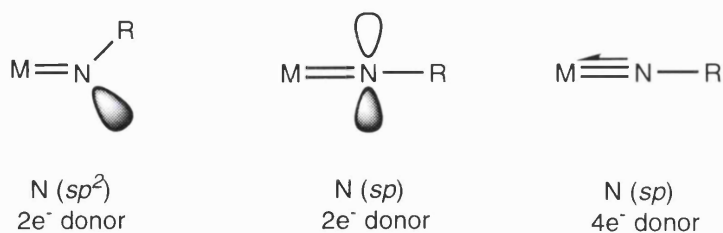
Gibson and co-workers wished to support the idea that the nitrogen atom of a bent imido ligand is sp^2-hybridized[26]. They synthesised two similar complexes, [Mo(N-2,6^{i}Pr$_2$C$_6$H$_3$)$_2$(L)] and [Mo(N-2,6^{i}Pr$_2$C$_6$H$_3$)(CHCMe$_2$Ph)(L)], where L is a tridentate pyridinediolate ligand.

N
O
144.8°
O—Mo
164.7° N(1)

bis(imido)

N
O
H
O—Mo—C
CMe$_2$Ph
N 141.0°
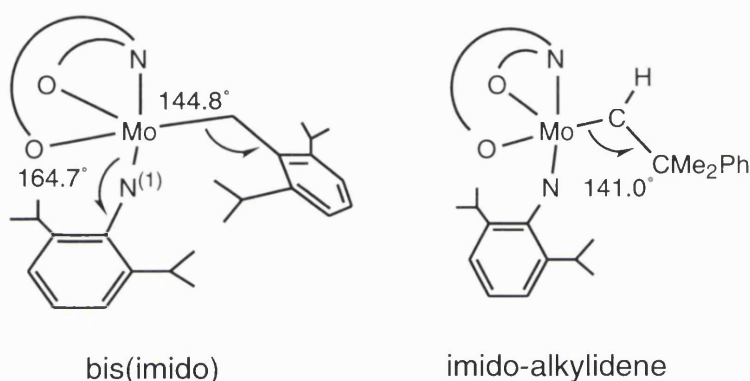
imido-alkylidene

The imido bond angles in the bis(imido) complex were 164.7(4)° (axial) and 144.8(5)° (equatorial); with ample space available, steric interactions could not be the reason for the bending. The alkylidene complex was of similar geometry (angles 141.0(2) for the alkylidene and 172.5(2)° for the imido). Further, the equatorial alkylidene ligand bends towards the axial linear imido ligand as had happened in the bis(imido) complex. As the angle for the alkylidene was similar to related imido-alkylidene complexes[27,28] where the carbon has already been established as sp^2-hybridized, by implication, the bent imido ligand in Gibson's complex would also have a sp^2-hybridised nitrogen atom.

Most monoimido complexes may be understood using this simplistic approach, especially with regard to the third model (above), where lone pair donation from the nitrogen to the metal occurs. Following this, a simple relationship between bond order and bond lengths or angles may be expected. However, this is not the case and, as stated above, MO theory is better used in trying to understand these relationships, especially with multiple imido complexes. Studies on bonding in bis(imido) complexes shall be considered in Chapter 2.

Many theoretical studies have been undertaken on the bonding of imido complexes. Nugent and co-workers found that the charge on the imido nitrogen decreased on going downward and to the right in the periodic table due to changes in the relative energies of atomic orbitals involved in the $N(p) \rightarrow M(d)$ interaction[29]. In particular, Cundari has published three papers devoted to the electronic structure and reactivity of transition metal complexes[30-32]. In the first, he concluded that there are eight possible resonance structures that contribute to a metal-imido bond. These structures differ in whether the σ- or π-bond is dative or covalent or back-bonding, etc.; of these eight, three are the major contributors - the polarized triple bond (covalent σ-, covalent π- and a dative π-bond), a σ-ylide (dative σ- and two covalent π-bonds) and a σ,π-ylide (dative σ-, dative π- and a covalent π-bond). (Note that Cundari considers a dative bond to be a ligand to metal interaction.) These last two resonances had not been considered in previous literature.

where covalent bond = — ; dative bond = ◄—
and lowest bond is the σ bond and the higher two, π
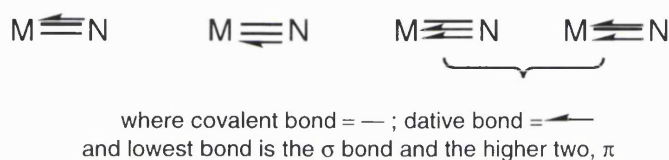
The diagram below is a schematic representation of the most important molecular orbitals in a transition metal imido complex[30].
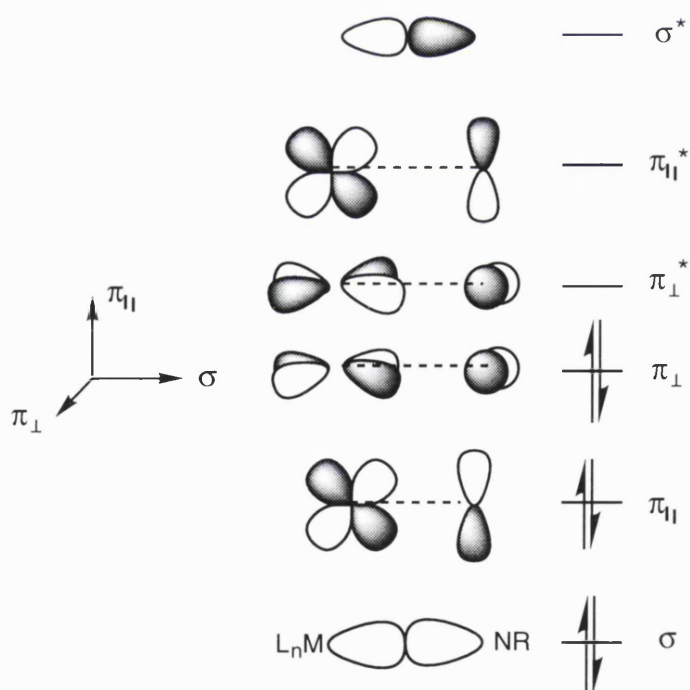
The simple MO diagram below represents an octahedral metal-imido complex, where the imido ligand is linear[9]. The metal d-orbitals, already divided into non-bonding t_{2g}

and σ^* character e_g sets, have their symmetry lowered further upon introduction of the linear imido ligand.
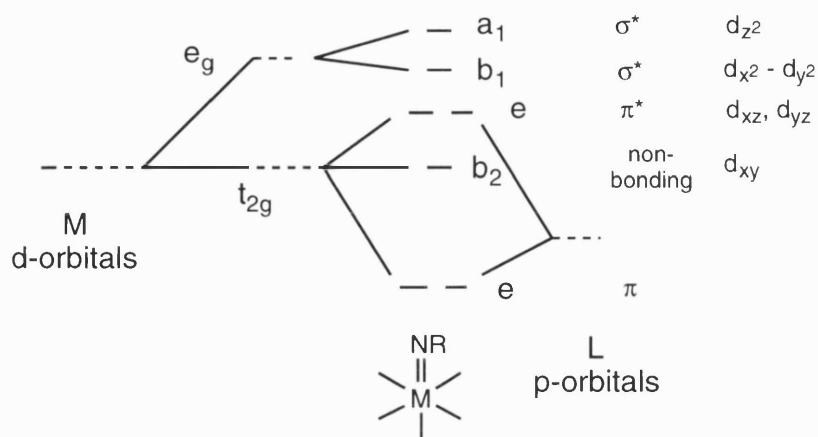
The t_{2g} orbitals are split because two of them are involved in π-bonding. (Taking z to be the M-L bond axis, d_{xz} and d_{yz} are the two bonding orbitals.) Where there is more than one multiply-bonded ligand, the complex should adopt the geometry that minimises the population of the antibonding orbitals and maximises those for bonding.

1.4 Bonding Modes of the Imido Ligand

There are five known bonding modes for the imido ligand which are shown below.

| terminal linear | terminal bent | doubly-bridging | triply-bridging | quadruply-bridging |
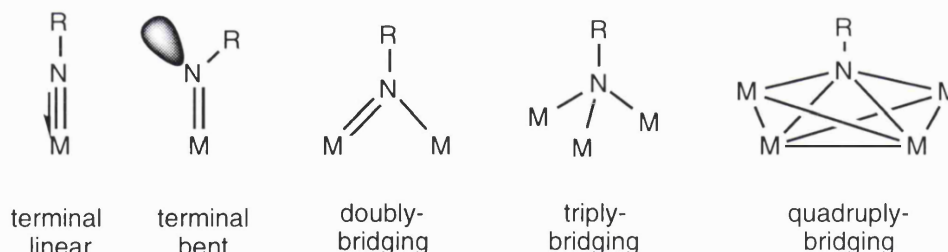
For the first two modes, an analogy may be drawn with the better-known nitrosyl ligand. When linear, the nitrosyl ligand formally donates three electrons to the metal centre; when bent, the ligand only donates one electron.
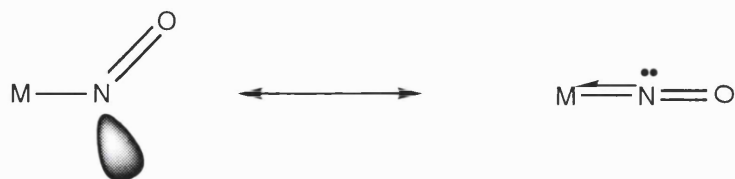
A typical linear nitrosyl complex is $[Cr(NO)(CN)_5]^{3-}$ and a bent complex (with an angle of 123°) is $[Ir(NO)Cl_2(PPh_3)_2]$[33]. Further, there are bis(nitrosyl) complexes that

exhibit one linear and one bent nitrosyl ligand, e.g. $[RuCl(NO)_2(PPh_3)_2]^+$ which was shown by nmr studies to have the nitrosyl in the bent or linear site with rapid exchange between the two[34-36].

The majority of imido complexes display the terminal linear bonding mode where the ligand acts as a four-electron donor. "Linear" is quite a loose description as the metal-nitrogen-carbon angle subtended may vary from 180° to 150° and still be regarded as linear[37]. Some examples are shown below - $[Os(NAr)_3]^6$ and $[Mo(N^tBu)(S_2)(mtc)_2]^{22}$

Note the osmium complex is trigonal planar with a two-fold axis through Os, N(2), C(21) and C(24). The imido angles are 178.0(5)° and 180.0(3)° for Os-N(1)-C(11) and Os-N(2)-C(21), respectively. In the other complex, the imido angle is 168.7(2)°.
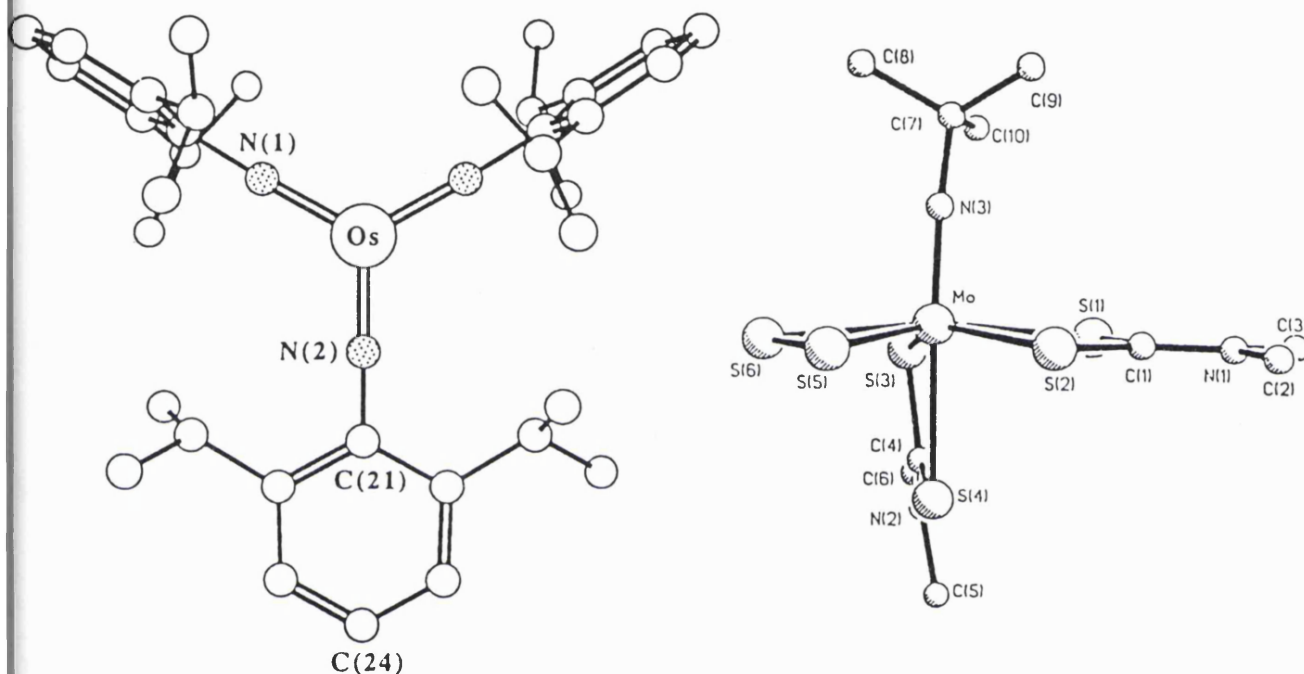
In contrast, examples of bent imido ligation are rare, except where the bending has been forced by steric constraints. The classic example of a naturally bent imido ligand is in $[Mo(NPh)_2(etc)_2]^{38}$. Here, one imido angle subtends 139.4(4)° and the other 169.9(4)°; this will be discussed in greater detail later. Another example is $[Mn(N^tBu)_3Cl]$ where the imido angles vary from 138.5(3) to 141.8(3)°. This is explained by the necessary electron localization for the metal centre to reach its 18-electron configuration[39].

As stated earlier, some complexes have bent imido ligands brought about by steric constraints, i.e. as part of a chelating ligand . The first example of such a

---

chelating ligand incorporating an imido moiety was reported by Minelli and coworkers [40]. Here, 2-aminothiophenol was reacted with [MoOCl$_2$(etc)$_2$] to give [MoCl(etc)$_2$(N,S-NC$_6$H$_4$S)], with a imido angle of 137.7° and Mo-N bond length of 1.744(6)Å.
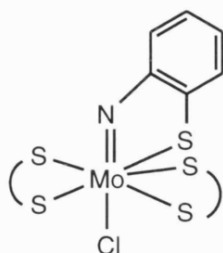
Imido ligands may bridge two, three or four metal centres. When bridging two metal centres (particularly found for those with more than two d-electrons), the ligand acts as a four-electron donor (with the lone electron pair participating in the π-bonding [6]). In the course of their cooperative reactivity studies, Baranger and Bergman synthesized the bridging-imido complex, [Cp$_2$Zr(μ-N^{t}Bu)-Ir(Cp*)][41].
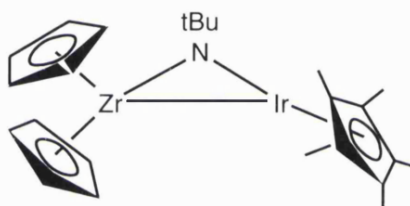
This bimetallic complex is designed to exploit the complementary reactivities of the metal centres; the imido ligand is important as it prevents dissociation upon cleavage of the metal-metal bond. Further, the imido ligand is relatively inert compared to the unsaturated metal centres. The nitrogen is planar suggesting that the nitrogen lone pair has been donated into empty orbitals of the metal centre(s). A second example of bridging-imido ligands is the diimido complex [MoO(etc)(μ-NC$_6$H$_4$Me-o)]$_2$[42].
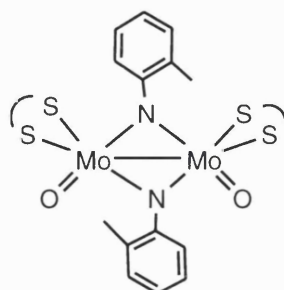
The imido groups span the molybdenum centres approximately symmetrically. The Mo$_2$N$_2$ core is puckered, the dihedral angle between the planes being 149.2°. The

majority of such dimeric complexes are symmetrically bridged, but there are some examples of unsymmetrical bridging, e.g. $[Mo(N^tBu)(\mu-N^tBu)(CH_3)_2]_2$[43]. This structure has a crystallographic centre of symmetry. Relevant bond lengths are : Mo(1)-N(1) 1.730 (2)Å, Mo(1)-N(2) 1.819 (2) Å and Mo(2)-N(2) 2.322 Å. These are approximately the typical bond lengths for a triple, double and single Mo-N bond, respectively. (The bond angle Mo(1)-N(1)-C is 167.4°, deviating from linearity.)
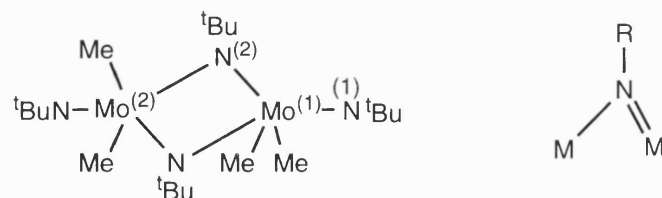
The reason for the adoption of symmetric versus unsymmetric arrangements has been investigated using MO theory, specifically by comparing the above compound with the symmetrically- bridged $[(Me_2N)_2Zr(\mu-N^tBu)]_2$[44]. The two compounds are similar (both d^0-metals and nominally isoelectronic) but due to the different nature and location of the terminal ligands there is significantly different bonding in the bridging regions. This is such that the bridging region of the unsymmetrical molybdenum complex is "antiaromatic" and therefore there is localized bonding with alternating short-long bond lengths; in the zirconium complex, the bonding is delocalized ("aromatic").

Imido ligands may bridge three or four low-valent metal centres. The small number of d-electrons in the metal orbitals reduces the affinity for metal-nitrogen π-bonding and thus, the imido ligand bonds to multiple metal centres. There are several examples of a triply bridging imido ligand of which two are outlined here. Thus, $[Re(N^tBu)_3Cl]$ and $[Co_2(CO)_8]$ react to give the μ_3-imido cluster $[ReCo_3(\mu_3-N^tBu)_2(CO)_{10}]$. The metal atoms are in a butterfly-type arrangement with two carbonyls bridging between the cobalt atoms and one imido group asymmetrically capping each face[45].
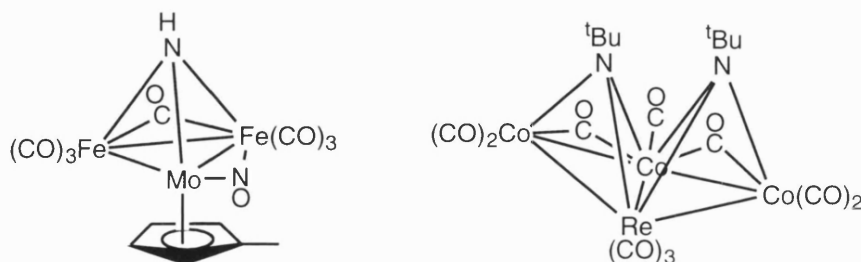
The second example shows a trinuclear complex $[(\eta^5\text{-}CH_3C_5H_4)Mo(\mu_3\text{-}NH)(\mu_2\text{-}NO)(\mu_2\text{-}CO)Fe_2(CO)_6]$ where the imido ligand bridges such as to form a pyramidal core with the metal atoms[46]. Quadruply-bridging imido complexes are quite rare, one example being shown below[47] -
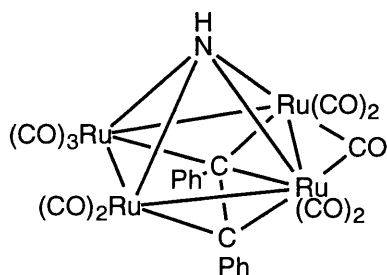
1.5   Synthesis

The most widely utilised routes to introduce an imido ligand into a compound are *via* reaction with amines, isocyanates or azides. An early review by Cenini and La Monica[48] gave prominence to the use of azides and isocyanates although, as stated above, the first synthesis of an imido moiety was *via* an amine. Wigley categorized imido synthesis by seven reaction processes, subdivided further into a number of routes with numerous examples[8]. This classification is:

(A) - Cleavage of the Nitrogen-α-Substituent;

(B) - Metathesis Reactions with No Change in Oxidation State of the Metal;

(C) - Oxidations using Organic Azides, Azo Compounds and Related Species;

(D) - Use of Nitriles;

(E) - Electrophilic Attack on a Nitrido Moiety;

(F) - Rearrangement of a Metallaaziridine and

(G) - Miscellaneous.

Of these, syntheses with amines, isocyanates or azides are the most common and are classic examples of the first three routes. Using an <u>amine</u> and metal oxide produces water so a drying agent must also be used; however, the variety of (primary) amines available is far wider than those of isocyanates.
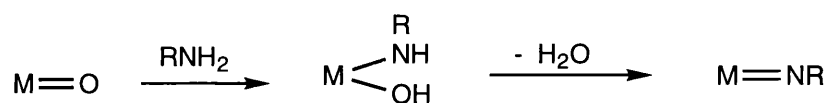
Among early examples were rhenium-imido complexes, initial reactions being successful only with aryl amines but alkylimido complexes were made successfully later on.

$$[Re(O)Cl_3(PEt_2Ph)_2] + PhNH_2 \quad \rightarrow \quad [Re(NPh)Cl_3(PEt_2Ph)_2] \text{ [49]}$$

$$[Re_2O_3(etc)_4] + 2\ PhNH_2 \quad \rightarrow \quad [Re(NPh)(etc)_2]_2O \text{ [50]}$$
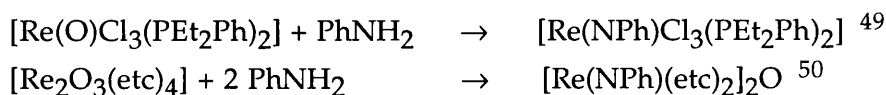
Similar reactions occur with non-oxo ligands -especially halides - and also with amides, silylamines and sulfinylamines, e.g.

$$[Cp^*_2TaCl(thf)] + LiNHPh \quad \rightarrow \quad [Cp^*_2Ta(NPh)H] \text{ [51]}$$

$$[CrO_2Cl_2] + 2\ ((Me_3Si)NH^tBu) \quad \rightarrow \quad [Cr(N^tBu)_2(OSiMe_3)_2] \text{ [52]}$$
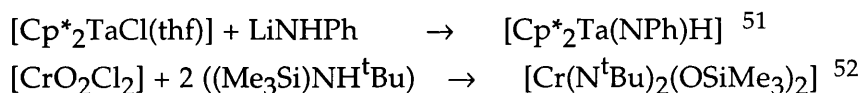
This latter complex was one of the earliest bis(imido) complexes to be synthesized; of interest is the substitution of the chlorides and also, conversion of the oxo ligands to oxosilanes.

Isocyanates have been widely used to introduce the imido ligand. One advantage is that gaseous carbon dioxide is the by-product . With isocyanates, the reaction process can either be via oxidative-addition or via a metathesis reaction with no change in the metal centre's oxidation state. The use of isocyanates was pioneered by Kolomnikov and co-workers in converting $[L_2Cl_3Re(O)]$ to $[L_2Cl_3Re(NR)]$[53]. The following examples illustrate the oxidative-addition reaction of an isocyanate with a low-valent metal centre :

$$[Ru_3(CO)_{12}] + PhNCO \quad \rightarrow \quad [Ru_3(CO)_{10}(NPh)] \text{ [48,54]}$$

$$[WCl_2(PMePh_2)_4] + RNCO \quad \rightarrow \quad [W(NR)(CO)Cl_2(PMePh_2)_2] \text{ [55]}$$
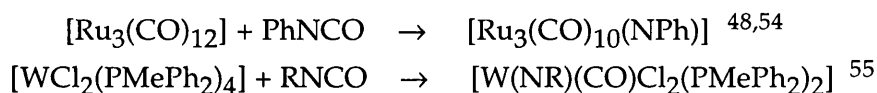
In earlier work in this laboratory, the metathesis-type reaction was performed - a general scheme is shown below for imido synthesis upon reaction of isocyanates with the molybdenum(VI) bis(oxo)bis(dithiocarbamate) complex $[Mo(O)_2(etc)_2]$ giving the molybdenum(VI) imido-disulfide product, $[Mo(NR)(S_2)(etc)_2]$[18,22]. A study of this reaction mechanism is discussed in Chapter 5, only a brief synopsis being given here. Initial substitution of an oxo ligand produces an oxo-imido species; double sulfur-carbon bond cleavage of a dithiocarbamate ligand yields the disulfide ligand and with further attack by dithiocarbamate, the approximately octahedrally-coordinated complex is made.
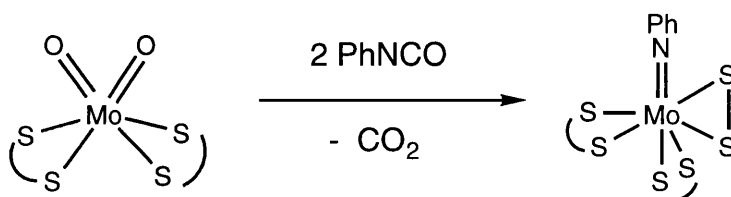
Oxo for imido substitution is believed to occur via a [2+2] cycloaddition mechanism, yielding a four-membered metallacycle; this can then lose carbon dioxide to give the imido complex or lose isocyanate and revert back to the oxide.

$$Mo{=}O \xrightarrow[\text{- }CO_2]{\text{+ RNCO}} M{=}NR$$

with the central metallacycle intermediate:

$$M\underset{N}{\overset{O}{\diamond}}C{=}O$$
$$\text{R}$$

labeled with + RNCO / - RNCO on the left and - CO$_2$ on the right.
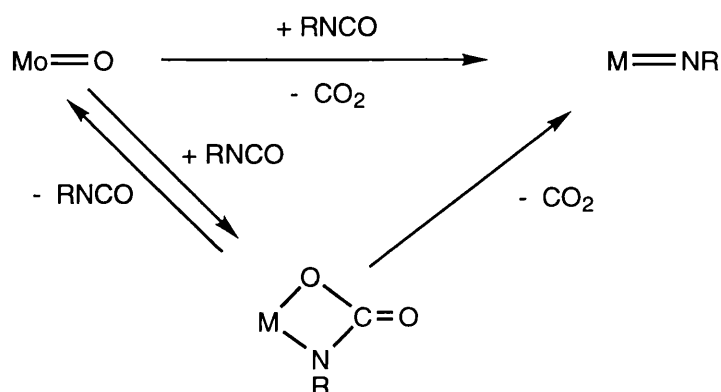
Although this mechanism is not proven, a metallacycle of the type shown above has been isolated after reaction between phenyl isocyanate and with [Cp$_2$Mo(O)] to produce [Cp$_2$Mo{OC(O)NPh}][56]. It is noteworthy, however, that this does not break down to the complex, [Cp$_2$Mo(NPh)], which has been made independently[57].

$$Cp_2Mo\underset{\underset{Ph}{N}}{\overset{O}{\diamond}}C{=}O$$
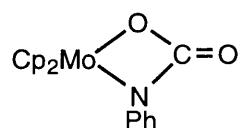
A related example is the formation of the ureato compound [Mo$_2${μ-NPh)(μ-PhNC(O)NPh}(NPh)$_2$(etc)$_2$] upon phenylisocyanate insertion into [Mo(μ-NPh)(NPh)(etc)]$_2$[42]. Here, the isocyanate inserts into a bridging imido ligand, a reaction which is reversible, such that after vigorous reflux and cooling, the dimeric product is recovered. Ureato compounds have been formed previously using isocyanates[58] but this was the first demonstration of its reversible nature.
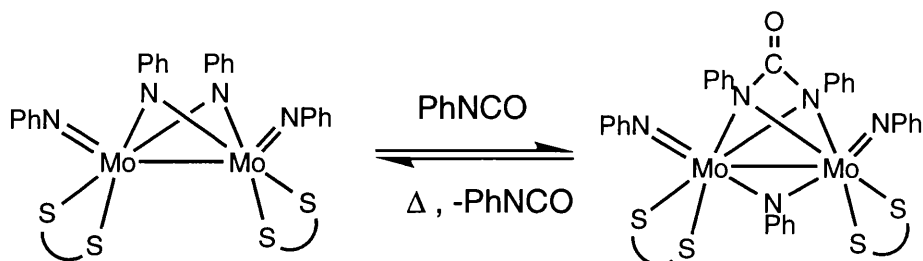
Other related reagents like phosphinimines (R$_3$P=NR), carbodiimides (RN=C=NR) and other compounds with an E=N moiety are also known to participate in metathesis reactions to produce an imido complex with no change in the metal oxidation state.

Finally, the third popular way to introduce the imido ligand is via thermodynamic or photochemical activation of azides, to give dinitrogen and the imido moiety. Production of dinitrogen allows easy product isolation and there is also a large driving force for these exothermic reactions. Both monoimido and bis(imido) complexes have been prepared in this manner[38]; e.g.

$$[Cp^*_2V] + PhN_3 \rightarrow [Cp^*_2V(NPh)] \quad [59]$$

$$[Mo(CO)_4Cl_2] + NH_4[S_2P(OEt)_2] \xrightarrow{\quad PhN_3 \quad} [Mo(NPh)\{S_2P(OEt)_2\}_3] \quad [60]$$
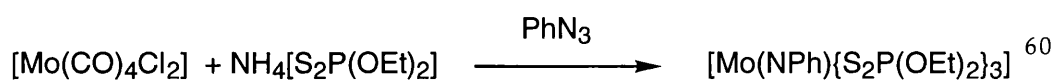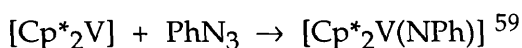
The above examples illustrate just three routes amongst many which have been used in mono and multiple imido ligand synthesis. To synthesise bis(imido) complexes, isocyanates, azides or amines are often used and such routes shall be considered in greater detail in Chapter 2.

Synthesis of mononuclear complexes with more than two imido ligands has developed recently - in 1991, yellow crystalline $[Li(thf)_4][W(NAr)_3Cl]$ was obtained upon reaction of LiNHAr with $[W(NAr)_2Cl_2(thf)_2]$[61]. The anion is tetrahedral with three equivalent imido ligands about the tungsten metal centre. Tris(imido) complexes of molybdenum have also been developed following similar experimental procedures. However, this anion slowly reacts with the amine by-product to give the thermodynamically stable bis(imido)-bis(amido) product $[Mo(NAr)_2(NHAr)_2]$[62]. Finally, tetrakis(imido) complexes have been synthesized- Wilkinson and co-workers made and characterized the dilithium salt of $[W(N^tBu)_4]^{2-}$. Only one of its imido ligands is linear [(176.6(6)°)], while the other three are bent, angles varying between 134.4(5) - 139.6(5)°[63].

1.6   Structural Studies

The majority of imido complexes are octahedrally-coordinated (usually with some degree of distortion) - not surprising given the good orbital overlap for σ- and π-bonding. Other common geometries are square pyramidal and tetrahedral. Whatever their coordination geometry, the vast majority of imido complexes exhibit the terminal linear bonding mode, as described earlier. One trend to note is that the angle about the imido nitrogen deviates less from linearity as the steric bulk of the imido substituent increases. Part of this may be attributed to the avoidance of unfavourable steric interactions with other co-ligands[64].

Linearity is a loose geometric description for the majority of terminal imido ligands. Gibson has suggested that the term "linear" may be applied to a wide range of bond angles, from 180° down to 150° - the variation primarily due to interligand

interactions and crystal-packing forces rather than any great electronic perturbation. His justification of this is the complex [Mo(NAd)(NC$_6$F$_5$)Cl$_2$(dme)] (Ad=1-adamantyl) the X-ray structure of which has two molecules in the asymmetric unit[65]. In one, the imido angles are comparable - for the adamantyl, 160.0(2)° and for the pentafluorophenyl, 162.8(2)°, however, in the second, the adamantyl angle is 172.6(2)°, while the other angle is 152.0(2)°. This wide range of angles illustrates well the "softness" of the imido angle in the consideration of terminal imido ligands[37].

i) 160.0(2)°
ii) 172.6(2)°

i) 162.8(2)°
ii) 152.0(2)°
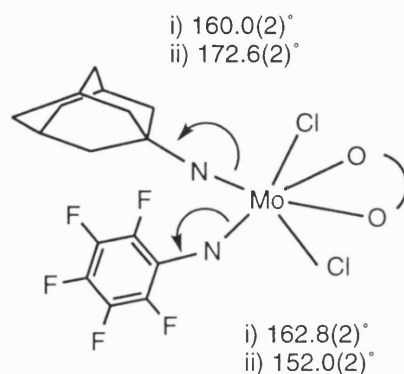
There are several examples of transition metal complexes containing only imido ligands - Nb, Re, Os and the group VI metals. The first homoleptic imido complex of Tc, [Tc$_2$(NAr)$_6$], was synthesized by reacting a THF solution [Tc(NAr)$_3$I] with sodium metal; it 'adopts an unprecedented "ethanelike" structure'[66] with imido angles of 167.6(3)°. The metal-metal bond lies on a crystallographic S$_6$ axis, making the imido ligands symmetrically equivalent and needing a staggered arrangement.
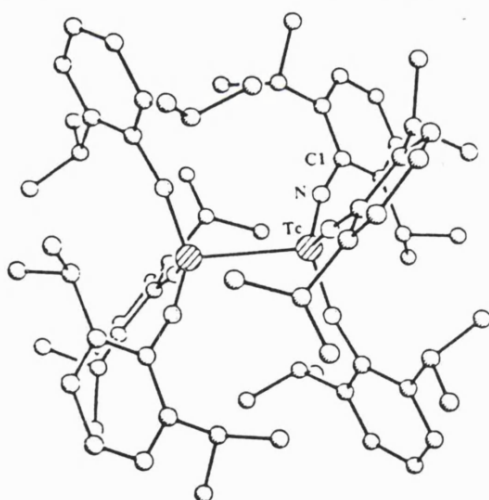
Its structure is very unusual as all other structurally characterized M$_2$E$_6$ complexes (where E is a dianionic ligand) have adopted the edge-bridged tetrahedral dimeric structure, shown below. However, Bryan and Burrell's molecular mechanics calculations have indicated a strong preference for the ethanelike structure adopted.

ArN、   /NAr
    Tc
    | \   Ar
    N   N
    Ar |
        Tc
ArN /   \ NAr

E   E   E
 \\ / \ //
  M——M
 // \ / \\
E   E   E
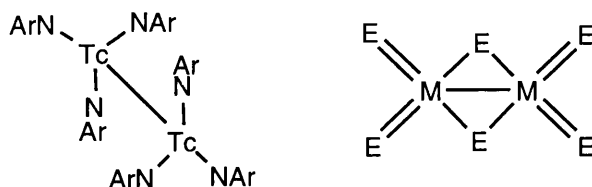
Bent complexes have also been crystallographically characterized - several of which have been referred to earlier. Bis(imido) complexes were predicted to have bent-linear structures satisfying the 18-electron rule, as found in the structure of [Mo(NPh)$_2$(etc)$_2$][38]; however, the vast majority of bis(imido) complexes have adopted a "linear-linear" geometry.

Metal-ligand distances are often suggestive of the bond order, especially for metal-oxo or organometallic complexes. The variation in an imido bond length is very small - of the order of tenths of angstroms, at most - and there is no noticeable difference between alkyl and aryl substituents *per se*. Imido bond lengths range from 1.6 to over 1.8 Å for a terminal ligand; obviously, bridging imido ligands can be even longer. Molybdenum monoimido complexes mostly cover a much narrower range from 1.72 to 1.79 Å. However, as may be expected, bent ligands have a longer Mo-N distance than in a linear ligand. The electron-donating ability of the substituents also affects the bond length but, after considering such small distances, a more significant effect is observed in a co-ligand *trans* to the imido ligand.

The *trans* influence is the ability of a ligand to lengthen the bond of the ligand *trans* to it; this lengthening is usually accompanied by the other ligands bending away from the multiply-bonded ligand. Steric and electronic factors have been cited but steric reasoning cannot always be used to explain a complex's structural features. The influence is really due to the fact that the two ligands interact with the same metal orbital; the more one ligand dominates this orbital, the weaker the other one will be. It is difficult to measure the degree of *trans* influence in a given complex, but lengthening can be very slight or up to 10% of the metal-ligand distance[9].

Imido ligands have a smaller *trans* influence than oxo ligands. This is illustrated by comparing the structures of the complexes [Mo(O)(η^2-S$_2$)(etc)$_2$][67] and [Mo(NR)(η^2-S$_2$)(S$_2$CNR'$_2$)$_2$][22] for which R' = Et, R = Ph and for R' = Me, R = ^{t}Bu and 2,6-^{i}Pr$_2$C$_6$H$_3$, the geometries are very similar except for the metal-sulfur bond length in the dithiocarbamate ligand trans to the multiply-bonded ligand. For the oxo, the Mo-S length is 2.663(6) Å and in the phenylimido, the length is 2.605(1) Å. The methyldithiocarbamate complexes still have shorter lengths than the oxo complex with 2.636(1) and 2.612(1) Å, respectively. It is of interest to note, though, that in the bis(imido) complex, [Mo(NPh)$_2$(etc)$_2$], contrary to the usual behaviour in metal-oxo complexes, it is the bent ligand with the longer metal-nitrogen vector that exerts the

greater *trans* influence - the linear imido has a lengthening effect on the trans Mo-S bond of 0.15 Å which is only half of that effected by the bent ligand[38].

1.7   Spectroscopy

Most of the standard spectroscopic techniques have been used in some part to identify imido compounds, although, uv-vis spectroscopy has not been extensively used. Techniques discussed below include ir and various nmr spectroscopies.

In contrast to molybdenum-oxo complexes, the use of <u>infra-red</u> spectroscopy for imido chemistry is limited because of doubtful assignments of the M-N vibration mode. Different contributions to the literature over several years have not reached agreement on such a stretching frequency for the imido moiety, as there is considerable coupling of the M-N and N-C stretching frequencies and to other vibrations of the alkyl or aryl group. ^{15}N-labelled studies have been undertaken with differing results. Dehnicke and Strahle studied the series [Cl$_3$V(NX)] (where X = Cl, Br or I)[68] and concluded that the "υ(MN)" stretch moved from 1107 to 963 cm^{-1} along the series and that the "υ(X-N)" stretch appeared between 510 and 390 cm^{-1}. They further stated that organoimido complexes would have higher υ(MN) energies, in the region of 1200-1300 cm^{-1}. In contrast, Osborne and Trogler made the reverse assignations after studying [Cp*$_2$V(NPh)] and [Cp*$_2$V(^{15}NPh)][69], suggesting that the metal-nitrogen stretch was in the lower frequency band. A more recent study by Williams and coworkers compared the calculated and observed vibrational modes for a series of complexes - [Ta(X)Cl$_3$], where X = N, NMe, NtBu and NPh[70]. They concluded that there is no single mode solely attributable to M=N, but there are at least three with significant M=N character. The main M=N mode, coupled with C-N, C-C and C-H modes, lies at ~ 1300 cm^{-1}; furthermore, arylimido complexes have higher stretching frequencies than alkylimido complexes. So, it is seen that care must be taken in assigning bands to imido ligands, but nevertheless, many authors have been content to take the presence of a band in the region of 1200 - 1300 cm^{-1} as indication of an imido moiety in their molecule[7].

Solution nmr spectroscopy is a very useful tool to aid characterization but care must be taken to ensure that the nmr solvent does not itself react with the target complex. Further precautions are often taken to eliminate moisture, often with the use of specially-modified tubes and with careful drying of the solvent.

^{1}<u>H nmr spectroscopy</u> has been widely used in the characterization of imido complexes. Wigley states that either upfield or downfield shifts of the α protons are observed and do not always correspond to its acidity[8]. However, after scanning the literature, one noticeable feature is that in arylimido complexes, the protons located at the 2- and 6- positions on the ring are usually shifted downfield. Ring protons usually

appear in the region δ 6.5 - 8.0 ppm (4- position most upfield and 2/6- position most downfield).

$H^{2,6}$ $\delta \approx 7.2 - 7.7$ ppm

$H^{3,5}$ $\delta \approx 6.9\text{-}7.4$ ppm

H^{4} $\delta \approx 6.5 - 7.1$ ppm
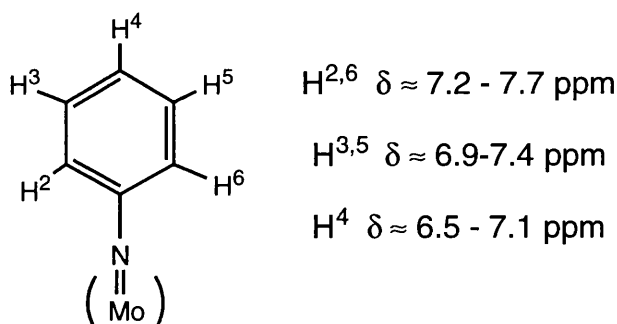
^{13}C nmr spectroscopy is also much used for characterization. With both alkylimido and arylimido complexes, the signal for the ipso-carbon (α to the imido nitrogen) is shifted downfield from the β-carbons or other carbon atoms in the ring. Typical δ values for the ipso-C are 150 - 160 ppm (aryl) or 70-80 for the α-C in *tert*-butyl and adamantyl complexes; other carbons lie in the expected ranges. Nugent and co-workers suggested that the difference in chemical shifts of C_α and C_β for *tert*-butylimido ligands are indicative of an approximation of the electron density residing at the imido nitrogen; this was expressed as: $\Delta = C_\alpha - C_\beta$. A series of complexes were studied, some of which are tabled below[29], and a correlation between nucleophilic and electrophilic behaviour is noticeable. An increase in electron donation from nitrogen to the metal centre appears to cause an upfield shift for the α-carbon and a downfield shift for the β-carbon. Consider especially the electrophilic ligand in [Os(N^{t}Bu)O$_3$] with $\Delta = 55$ while the nucleophilic ligand in [Ph$_3$P=N^{t}Bu] has a significantly smaller value ($\Delta = 16$).

	δ, C_α	δ, C_β	Δ
OsO$_3$(N^{t}Bu)	82.7	27.5	55
OsO$_2$(N^{t}Bu)$_2$	75.1	29.6	46
Ph$_3$P=N^{t}Bu	51.9	36.0	16
Cr(OSiMe$_3$)$_2$(N^{t}Bu)$_2$	77.8	31.3	47
Mo(OSiMe$_3$)$_2$(N^{t}Bu)$_2$	68.8	32.2	37

The identity of the metal centre and other ligands can also affect Δ. Another study on the series [(R$_3$SiO)$_2$M(N^{t}Bu)$_2$] (M = W, Mo, Cr) showed Δ increases as the metal centre's electronegativity increased. As the number of imido ligands increases in a given complex, so the π-bond order decreases, electron density usually increases about the imido nitrogen and so the value of Δ falls.

^{14}N/^{15}N nmr spectroscopy has been used to distinguish bent and linear bonding modes of nitrosyl and diazenide ligands[71,72]. For these ligands, strong deshielding occurs in the bent ligand and differences have been observed between measurements in solution and the solid state; in particular when fluxionality was observed in a complex with one linear and one bent nitrosyl ligand[34,36]. However, in contrast to the nitrosyl and diazenide ligands, the shift ranges for bent and linear ligands are indistinct as deshielding on bending is only small. The range for a terminal imido ligand is δ -92 to +156 ppm. Other components to the complex affect the imido's chemical shift - the metal, *trans*- and co-ligands, oxidation state of the complex and the alkyl or aryl group of the imido ligand itself. Mason and co-workers have studied the nitrogen nmr spectroscopy of several imido complexes[73], including the known bent-linear complex, [Mo(NPh)$_2$(etc)$_2$]. Even with the nitrogen-15 enriched complex, only a singlet resonance was observed for the imido nitrogen (at δ 9.6 ppm), reflecting its fluxionality in solution. Such fluxionality was found in other compounds, e.g. [Re(^{15}NPh)(OEt)(etc)$_2$][73] or [Os(O)$_2$(N^{t}Bu)$_2$][74], where another imido or alkoxide ligand was involved in the fluxional motion.

^{95}Mo nmr spectroscopy has been used extensively for bis(oxo) complexes but the first study on imido complexes was only performed in 1985. Enemark and co-workers considered a series of monooxo, nitrido and phenylimido complexes, the majority of which were seven-coordinate and possessing at least two chelating dithiocarrbamate ligands[75].

L = O, NPh (1+),   L = O, NPh
N, NO, NS   X= Cl, Br
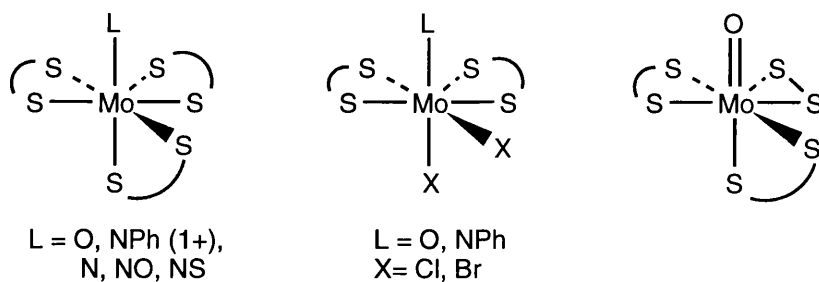
Of the complexes studied, the imido complexes had the lowest chemical shifts, ranging from -294 to -218 ppm, compared to 80 to 182 ppm for analogous oxo complexes. Replacement of the dithiocarbamate ligand by halides deshielded the metal centre, giving a downfield shift. Line widths were shown to be affected by the coordination sphere and steric bulk of the ligands.

Finally, solid state nmr spectoscopy (both ^{13}C and ^{15}N) has not previously been used for the specific structural study of imido complexes. Appendix I offers a concise introduction to the different techniques that are commonly used.

The reactivity of the imido ligand is affected by a combination of electronic and steric effects that control the $M(d) \leftarrow N(p)$ π-interaction, such as the metal centre, its oxidation state and the nature of co-ligands. It has been shown that for transition metal monoimido complexes π-donation to the metal centre by the ligand increases up and left to right across the the transition metals, due to better energetic match of the d and p orbitals. The diagram below shows a simple model of bonding of the ligand, showing three possible situations A, B and C[9].
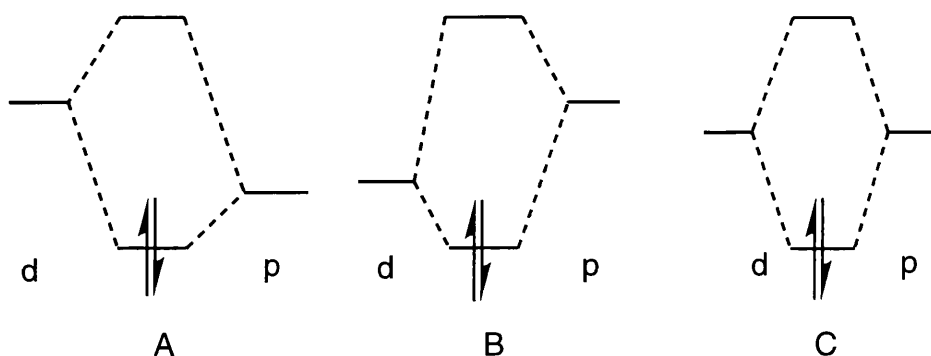
In the first extreme (A), the MO is ligand-based, acting as a closed-shell anion, being a π-donor and hence it is nucleophilic in nature. The LUMO is then localized on the metal centre and is vulnerable to nucleophilic attack. In contrast, in (B), the HOMO is metal-based, leaving the ligand-dominated LUMO empty and the ligand acts as an electrophile. The third situation (C) is more likely where the metal and ligand are engaged in covalent bonding, thus reducing the reactivity of both the metal centre and the ligand. The reactivity of an imido complex can be categorised into reactions with electrophiles and nucleophiles, imido transfer, reactions of the imido substituent and/or the co-ligands.

Reactions with Electrophiles

The most common electrophile used to attack an imido complex is the proton, resulting in amination or removal of the ligand[8]. Until this decade, the sole successful reaction with an alkyl electrophile was the addition of methyl bromide to $[Mo(NPh)_2(etc)_2]$[76], resulting in loss of a single imido ligand.
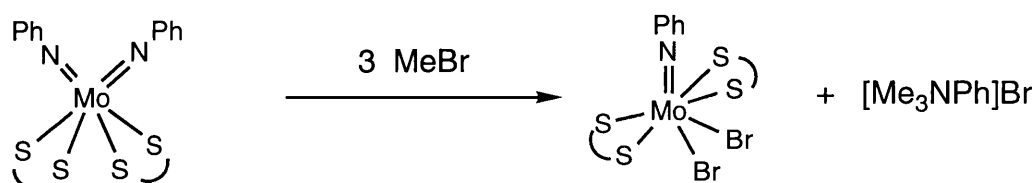
Later, in 1991, Bergman and co-workers reported a series of "pogo-stick" complexes, [Ir(NR)Cp*] (where R = ^{t}Bu, SiMe$_2$^{t}Bu, 2,6-Me$_2$C$_6$H$_3$ and 2,6-^{i}Pr$_2$C$_6$H$_3$), synthesized via amines or lithium amides; the aryl complexes could also be produced on reaction of the tert-butyl complex with an arylamine[77].

$$[Cp*Ir(N^{t}Bu)] \xrightarrow[C_6D_6]{ArNH_2} [Cp*Ir(NAr)] + {}^{t}BuNH_2$$
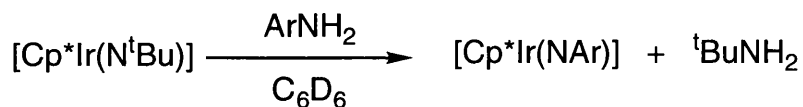
They described the imido ligand as acting as a weak base or nucleophile and insertion reactions were successfully performed with a wide range of simple organic molecules, some of which are shown in the diagram below.
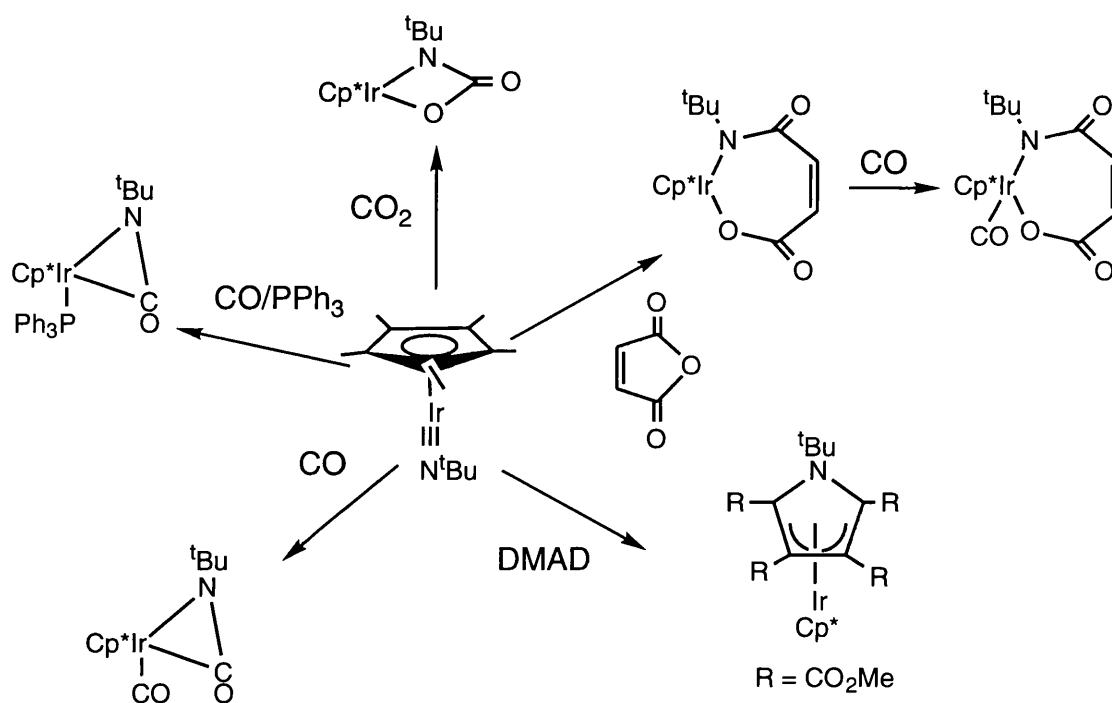
The reaction with the alkyne, DMAD, to form a η^4-pyrrole ligand is of note; the pyrrole has formed from the the imido ligand and two alkyne molecules. Another reaction with an alkyne was observed earlier in this laboratory, when a slight excess of DMAD was combined with [Mo(NPh)(S$_2$)etc$_2$]. The product obtained has been structurally characterized as [Mo{SC(R)=C(R)NPh}-{η^4-SC(R)=C(R)C(NEt$_2$)S}etc] where R = CO$_2$Me[22,78].

R=CO$_2$Me
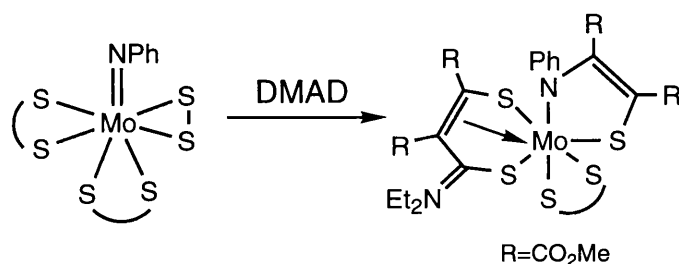
However, the vast majority of imido complexes show no activity towards alkenes or alkynes, with reaction occurring at other multiply-bonded sites.

A final class of electrophilic reactions is imido "exchange" upon reaction of a complex with another amine. One example has already been discussed above in the synthesis of Bergman's "pogo-stick" complexes. It is postulated to proceed by coordination of the entering amine, proton transfer to the other imido ligand, followed by α-elimination of the *tert*-butylamine. This exchanging reaction has also been used successfully by Gibson and co-workers to make mixed bis(imido) complexes from the easily-synthesisable intermediate, [Mo(N^{t}Bu)$_2$Cl$_2$.DME][65]. Other electrophilic reactions have been performed with isocyanates, carbon dioxide and carbodiimides; the electrophilic carbon attacks the imido nitrogen to produce metallacycles.

Reactions with Nucleophiles

The classic nucleophilic reactions are those leading to imido transfer upon reaction with a phosphine. This has been observed many times for the analagous oxo transfer[79]. Chelating sulfur ligands are noted as particularly suitable for these reactions, primarily due to their stabilizing ability.
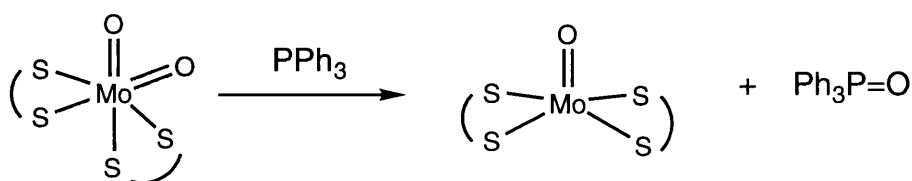
Harlan and Holm investigated imido group transfer both to and from molybdenum complexes[80]. Using [Mo(NTs)$_2$(etc)$_2$] and its oxo-imido relative, they were able to establish a catalytic cycle with phosphines, by monitoring with ^{31}P nmr spectroscopy. Furthermore, they discerned that the more basic phosphines favoured imido over oxo transfer.

$$\text{Mo(NTs)}_2\text{(etc)}_2 \quad + \quad \text{R}_3\text{P} \quad \longrightarrow \quad \text{Mo(NTs)(etc)}_2 \quad + \quad \text{R}_3\text{P=NTs}$$

$$\text{Mo(NTs)(etc)}_2 \quad + \quad \text{X=NTs} \quad \longrightarrow \quad \text{Mo(NTs)}_2\text{(etc)}_2 \quad + \quad \text{X}$$

$$\text{X=NTs} \quad + \quad \text{R}_3\text{P} \quad \longrightarrow \quad \text{R}_3\text{P=NTs} \quad + \quad \text{X}$$
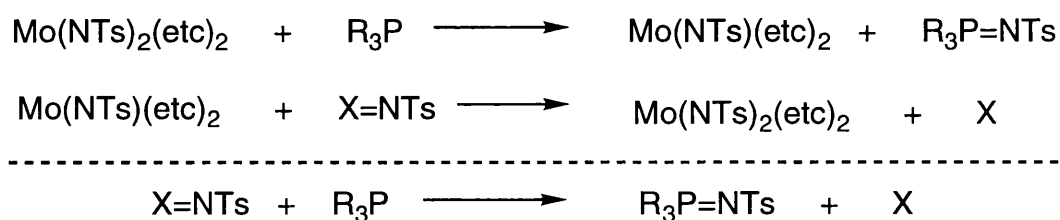
Schrock and co-workers reacted [Os(NAr)$_3$] with less sterically demanding phosphines (PMe$_3$ and PMe$_2$Ph) and trimethyl phosphite to produce *trans*-bis(imido)bis(phosphine) complexes and observed the phosphinimine by ^{1}H nmr spectroscopy. A crystal structure with dimethylphenylphosphine ligands was performed, showing the complex to be square-planar with nearly-linear ligands ($\angle$Os-N-C = 177.9(5)°)[6].

$$[\text{Os(NAr)}_3] \quad + \quad \text{PMe}_2\text{Ph} \quad \longrightarrow \quad \underset{\text{NAr}}{\overset{\text{ArN}}{\text{PhMe}_2\text{P}-\text{Os}-\text{PMe}_2\text{Ph}}} \quad + \quad \text{PhMe}_2\text{P=NAr}$$
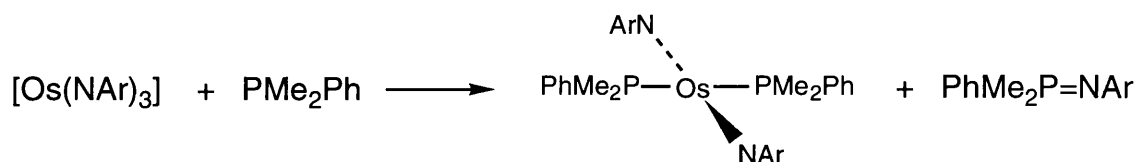
A clear example of imido transfer is recent work performed by Shapley and co-workers during their investigations of the complex, [CpOs(NMe)(CH$_2$SiMe$_3$)$_2$] [SO$_3$CF$_3$][81]. Upon reaction with triphenylphosphine, the phosphinimine is produced; this is confirmed when the imido is isotopically-labelled and the phosphinimine identified as Me^{15}N=PPh$_3$. Here the phosphine acts as both a base and a nucleophile, as it also abstracts a proton in the formation of another product. The methylene amido complex formed (A) is not an intermediate in this reaction as it does not react with phosphine or its protonated form. The authors believe that the nucleophilic phosphine attacks the electrophilic imido ligand to form an unstable phosphinimine and loses (MeN=PPh$_3$).

R=CH$_2$SiMe$_3$ (A)
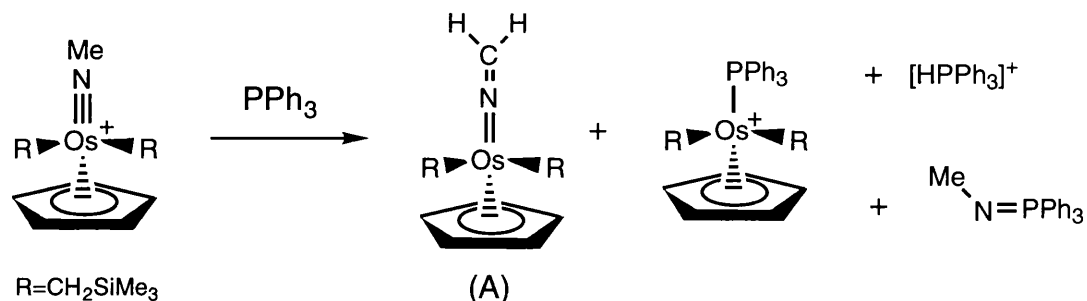
This complex can also react with electrophiles such as ethene. Due to the stability of the imido ligand, it is often the other co-ligands in a complex that will react. For example, the imido ligands in the complexes [Mo(MeCp)(NR)Cl$_2$] (R = Ph or ^{t}Bu) have

---

been shown to be inert towards a number of reagents like sodium amalgam in the presence of other neutral ligands and chlorine[82].
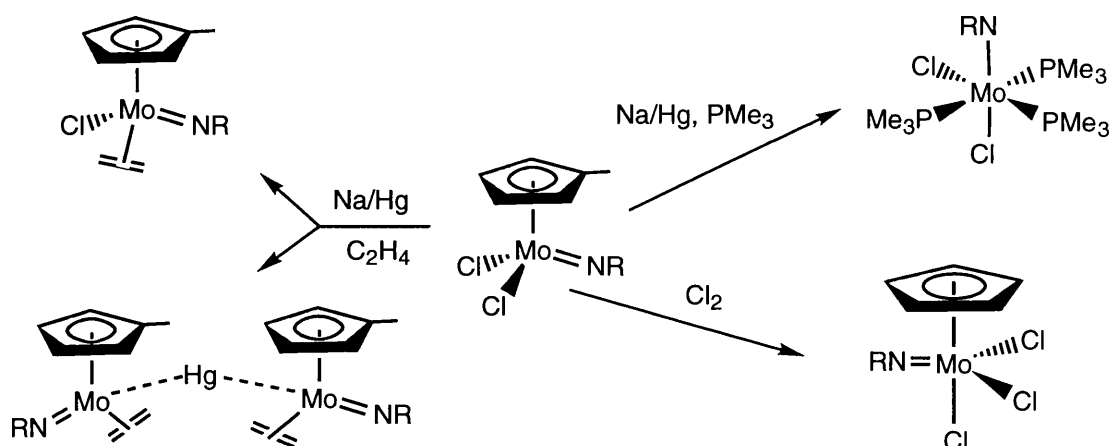
1.9   The Dithiocarbamate Ligand

This ligand is a singly-charged, potentially bidentate ligand consisting of a S-C-S backbone, the central carbon atom of which carries an amido moiety. Several resonance forms may be drawn:
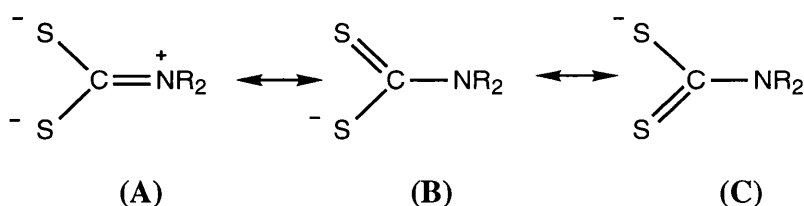
Sulfur atoms are usually thought to be soft but as seen in resonance structure (A), the π-electrons from nitrogen can be delocalized onto the sulfur atoms, making the ligand a strong σ-donor. That is, these sulfur atoms become "hard" and stabilize higher oxidation states, e.g. Mo(VI).

Dithiocarbamate salts are synthesised by reaction of carbon disulfide with a secondary amine in the presence of an alkali-metal hydroxide. Primary amines may be used but the products are unstable and usually react further to give the isothiocyanate.

$$R_2NH \ + \ CS_2 \ + \ MOH \ \xrightarrow{\ H_2O\ } \ [R_2NCS_2]^- \, [M]^+ \ + \ H_2O$$
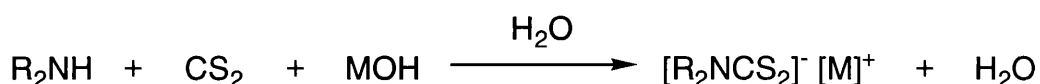
The ligand may bind in a unidentate or chelating fashion, which may be distinguished by both ir and nmr spectroscopy. When unidentate, there will only be a single bond between carbon and nitrogen in the ligand, so rotation will be free about

this bond and nmr spectra will be independent of temperature. When chelating, there will be some double bond character (as shown in the resonance forms below) between carbon and nitrogen and so rotation about this bond will be restricted. When the temperature is raised, rotation about the bond becomes easier and so the nmr spectra are temperature-dependent[83]. Complexes whose C-N stretching frequencies lie between 1500 and 1525 cm^{-1} have considerable double bond character[84]; other ranges suggested in the literature are less than 1545 cm^{-1} for bidentate and greater than 1545 cm^{-1} for monodentate binding[83]. The frequencies of (C—S) bands fall between 990-1002 cm^{-1}.

chelating
hindered rotation

unidentate
facile rotation
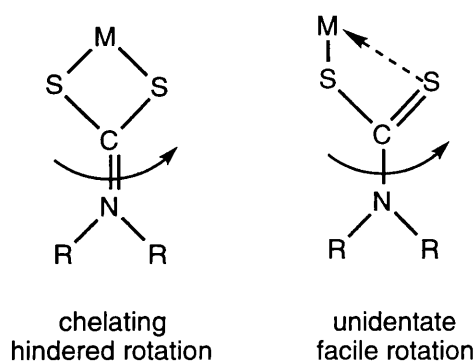
The metal dithiocarbamates are important because of their high covalency and ground state delocalization. This delocalization results from the interaction of the lowest-occupied π-MOs of the ligands with the metal p-orbitals of appropriate symmetry producing a low-lying MO delocalized over the whole complex. Electrochemical data is consistent with this concept of strong σ-donor properties being dominant over weak π-back donation, producing complexes that are fairly easy to oxidize but difficult to reduce.[85] However, not only do dithiocarbamate ligands stabilize high oxidation-state metal centres but they also support low oxidation states, e.g. [Ni(etc)$_2$]$^-$, and unusual sterochemical configurations. However, although dithiocarbamates are usually stable, they often decompose under acidic conditions[86,87].

Chapter 2   Synthesis and Structural Studies

2.1   Introduction

The first mononuclear bis(imido) complex, [Os(O)$_2$(N^{t}Bu)$_2$], was made by reacting osmium tetroxide with *N-tert*-butylphosphinimine[88]. It reacts with alkenes to form diamines. From this first reaction has sprung a great interest in the reactivity and catalytic activity of these complexes, most notable of which is ROMP catalysis[89].

Bis(imido) complexes are known for a wide range of transition metals - V[90], Ta[91], Cr[52], Mo[38,92,93], W[52,94], Re[95], Ru[96] and Os[6,88,97]. Of these, the Cr triad is the most prevalent and it is these group 6 metal complexes that shall be the focus of this chapter.

The first group (VI) bis(imido) complex, [Cr(N^{t}Bu)$_2$(OSiMe$_3$)$_2$], was reported in 1979 by Nugent and Harlow[52,98], formed on reaction of chromyl chloride with *tert*-butyl(trimethylsilyl)amine. This was swiftly followed by the first molybdenum bis(imido) complexes, [Mo(NPh)$_2$(etc)$_2$] (1) and [Mo(N(4-Me)C$_6$H$_4$)$_2$(etc)$_2$] (5), which were originally synthesised by the oxidative-addition reaction of [Mo(CO)$_2$(etc)$_2$] with phenylazide and *para*-tolylazide, respectively[38,76]. The potentially hazardous nature of this reaction led to investigations of alternative synthetic routes. Earlier in this laboratory, reflux of [MoO$_2$(etc)$_2$] with 2,6 - disubstituted aryl isocyanates in toluene afforded, after three days, the bis(imido) complexes [Mo(NAr)$_2$(etc)$_2$] (7) (where Ar = 2,6-^{i}Pr$_2$C$_6$H$_3$), [Mo(N(2,6-Me$_2$C$_6$H$_3$))$_2$(etc)$_2$] (8) and [Mo(N(2,6-Cl$_2$C$_6$H$_3$))$_2$(etc)$_2$] (13)[64,92]. Disadvantages of this route are the high temperature needed, the number of other products formed and the limited number and type of complexes that can be made due to the stability of the desired product; separation from other co-products is only achieved by column chromatography.

Synthesis of bis(imido) complexes has been achieved through several routes, including use of isocyanates[92], phosphinimines[88], silylamines[74] and imido exchange with other complexes[99]. The most successful introduction of two imido ligands, however, is *via* amines. A series of bis(imido) complexes has been synthesised, upon reaction of primary amines with molybdate[27,100]. With time, this synthesis has been refined and developed to allow the facile synthesis of a wide range of bis(imido) complexes, with both identical and different imido substituents[101].
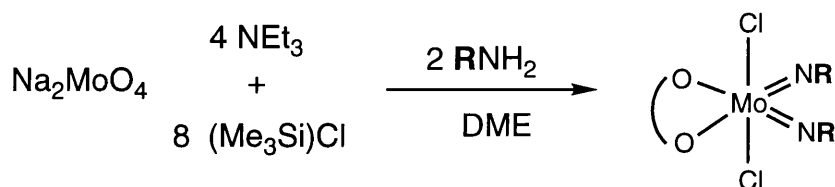
Trimethylsilylchloride "mops up" water formed on reaction of the amine with the molybdate salt, while the triethylamine reacts with any hydrogen chloride formed. The DME complexes formed are highly moisture-sensitive and are handled exclusively in an inert atmosphere. Synthesis is reported on quite a large scale (~ 70 g from 20 g of starting material) and reaction yields are generally high, often upwards of 95%. Characterization of these complexes is mainly achieved by ^{1}H and ^{13}C nmr spectroscopy, showing peaks for the imido ligands, while exchange of DME on the nmr timescale has been observed[100]. This synthesis has been extended to rhenium but not to the other members of Group VI, namely, chromium and tungsten. The crystal structure of one bis(imido) DME complex has been reported by Gibson - [Mo(NC$_6$F$_5$)(Nadm)Cl$_2$(DME)][65]. As discussed in the Introduction (Section 1.6), there are two molecules in the asymmetric unit and the imido angles range from 172.6(2)° to 152.0(2)°.

Further bis(imido) complexes may be synthesised from these and similar precursors. In particular, tetrahedral, coordinatively-unsaturated molybdenum bis(imido) complexes are prone to substitution. Sundermeyer and co-workers have studied the bonding capability of imido complex fragments and produced high-low valent bimetallic complexes in the development of cooperatively reactive complexes for the activation of smaller molecules. Many of their complexes were formed on reaction of the unsolvated analogue, [Mo(NR)$_2$Cl$_2$], with carbonyl metallates[102,103], two of which are shown below;
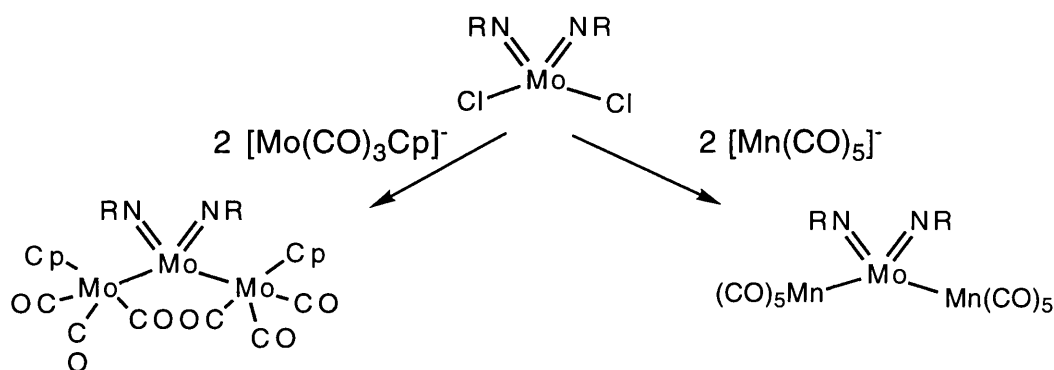
Structures of several mononuclear bis(imido) complexes have now been determined. The near majority of complexes have a linear-linear structure, although the imido angles cover a wide range from 155 to 180°. The imido ligands are always *cis* to one another in a group(VI) metal-centred complex. This is due to the symmetry (and geometry) of the metal d-orbitals available for bonding. However, in group (VIII) complexes, the imido ligands may be *trans* to one another, as in [Os(NAr)$_2$(PMe$_2$Ph)$_2$]. Interestingly, Schrock and co-workers also synthesised [Os(NAr)$_2$(etc)$_2$] and suggested that its imido ligands were also *trans* to one another, though they did not determine its crystal structure[6].

Many complexes are only four-coordinate (as is true for chromium and tungsten) and adopt a tetrahedral geometry, e.g. $[Mo(N^tBu)_2\{\eta^2-(N,O)-{}^tBuNC(O)NH^tBu\}_2]$ with imido angles 170.4(8) and 159.7(8)° [93], and for $[Cr(N^tBu)_2(2,4,6-Me_3C_6H_2)_2]$, 159.8(3) and 159.4(3)° [104]. Recent examples of six-coordinate, octahedral complexes include $[Mo(NAr)_2(etc)_2]$ (7), with identical imido angles of 169.9(2)°, $[W(NPh)_2Cl_2(bipy)]$ with 165.3(9) and 166.3(8)° [105], and the mixed-imido $[W(NPh)(N^tBu)Cl_2(bipy)]$ complex (160.8(8) and 165.1(9)°)[106].
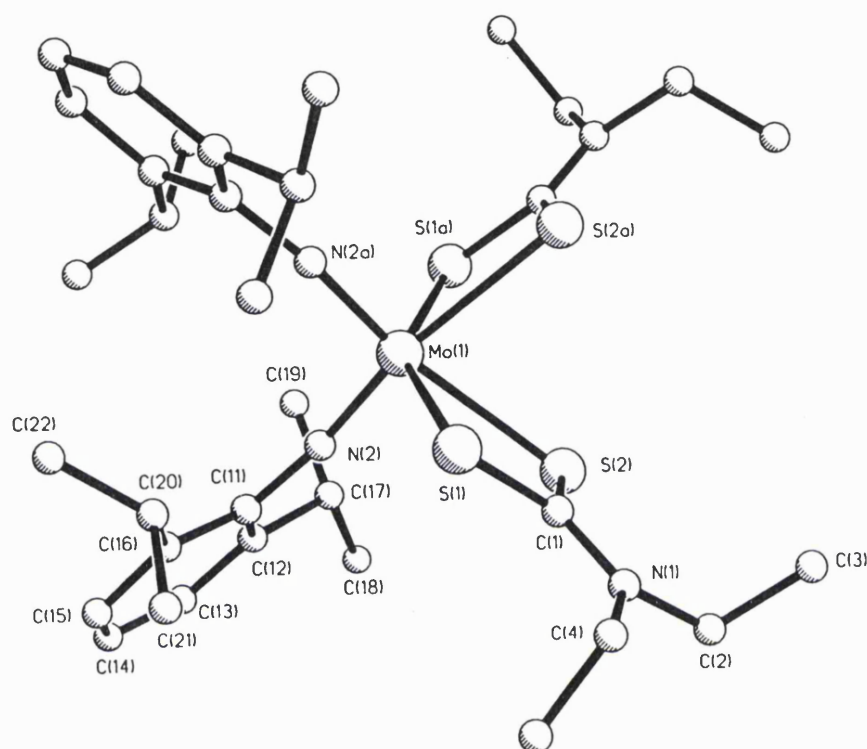
Structure of $[Mo(NAr)_2(etc)_2]$ 7

Very few complexes have a bent imido ligand. The first bis(imido) complex said to show a bent ligand, with an imido angle of 155.1(8)°, was $[Os(O)_2(N^tBu)_2]$[74]. The tert-butyl group on the bent ligand is disordered in this tetrahedral structure. The other ligand has an imido angle of 178.9(9)°. The optimum geometry calculated for this complex gives imido angles of 163 and 177°, but a steric interaction between the butyl substituents occurs on bending of one ligand towards the other. This led the authors to conclude that intramolecular forces dominate the actual structure adopted. By recent definition of linearity[65], though, it is unclear that this structure has a truly bent ligand. Apart from 1, the only other complex that certainly exhibits a bent terminal ligand is the five-coordinate, $[Mo(NAr)_2(L)]$ (where L is a tridentate pyridinediolate) with angles of 164.7(4) and 144.8(5)°[26].

The classic bent-linear complex is that of $[Mo(NPh)_2(etc)_2]$ (1). Its structure, determined at -80°C, is essentially octahedral with the imido ligands in a *cis*

---

conformation. It shows both types of imido ligation with imido angles of 139.4(4) and 169.4(4)° [38]. Bond lengths are 1.789(4) and 1.754(4) Å for the bent and linear ligands, respectively.

Structure of $[Mo(NPh)_2(etc)_2]$ **1**
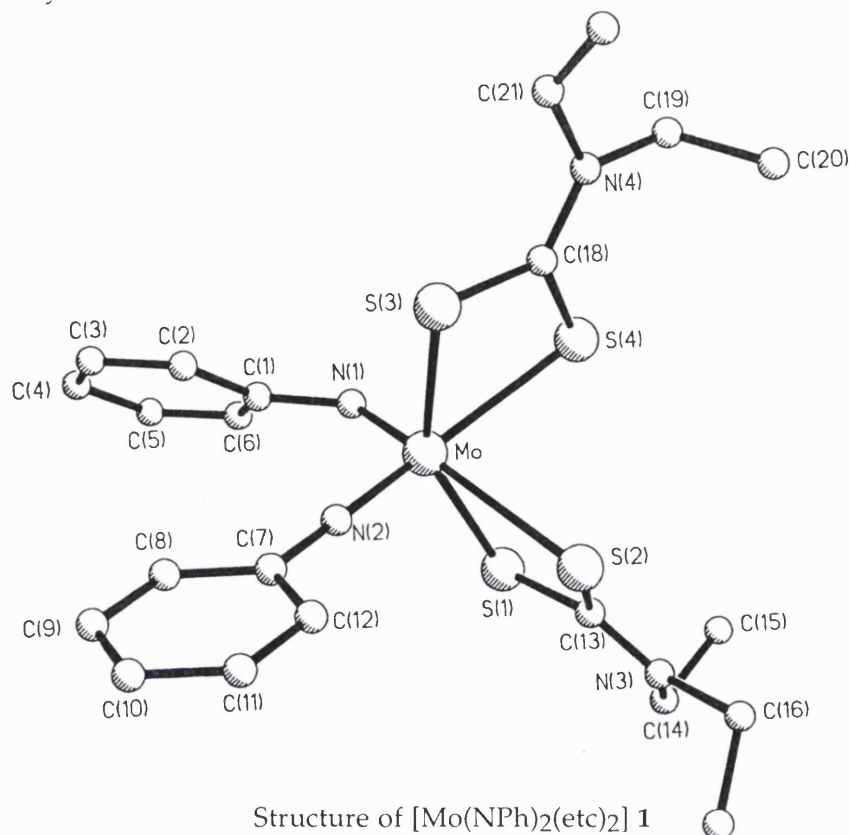
On realization of the bent-linear imido complex, $[Mo(NPh)_2(etc)_2]$ **(1)**, Haymore, Maatta and Wentworth started a debate about <u>bonding</u> by imido ligands, using both symmetry and molecular orbital descriptions to explain their molecular structure[38]. To satisfy the eighteen-electron rule, only six electrons need be donated to the metal centre by the imido ligands. The bent-linear structure of **1** is allowed by placing an electron pair in a metal-ligand non-bonding orbital, thus making the linear imido ligand donate four electrons and the bent, only two. Thus, a double bond has formed between molybdenum and nitrogen accompanied by significant bending at the nitrogen. The authors suggest three structures that could possibly be adopted, of which the first two broadly describe the molecular structure of **1**.
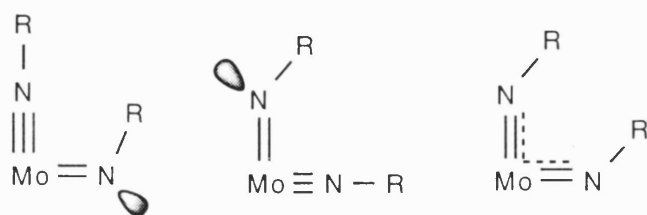
The third structure is described as double half-bent. This suggests that the structural and electronic properties of each imido ligand is intermediate between its possible extremes. This is exemplified by $[Mo(O)_2(S_2CN^nPr_2)_2]$ in that it has identical molybdenum-oxo bond lengths (1.695(5) Å) and very similar molybdenum-sulfur bond lengths, (2.621(2), 2.681(2) Å), *trans* to the oxo ligands[107]. Considering MO calculations of dinitrosyl complexes, especially $[Ru(NO)_2(etc)_2]$[108], similarities were noted for this latter structure to $[Mo(O)_2(S_2CN^nPr_2)_2]$, leading to postulations of intermediate bond order (of 2.5) and lengthening of molybdenum-sulfur bonds *trans* to the imido ligands (with a greater *trans* influence exerted by the bent imido ligand).

This, essentially, valence-bond description of bonding in bis(imido) complexes justified the structure of **1**, but ruling that a linear ligand was always a four-electron donor started to cause problems in satisfying the eighteen-electron rule. Some years later, Hogarth, Green and co-workers synthesised $[\{Mo(\eta\text{-}C_5H_4Me)(NPh)(\mu\text{-}NPh)\}_2]$[109]. Its crystal structure showed essentially linear imido ligands (173.6(2)°) and the flat $[Mo_2(\mu\text{-}N)_2]$ core. This initially suggested that each imido ligand should donate four electrons to the metal centre. Formally, this would exceed the eighteen-electron count at each metal centre but, using symmetry-based MO arguments and extended Hückel calculations, they showed that an imido ligand could donate just three electrons to the complex.

The six frontier orbitals of the metal-cyclopentadienyl fragment had been previously studied[110]. Based on C_{5v} symmetry, the orbitals were identified as: high energy $2a_1$ (mainly metal s and p atomic orbital character), degenerate e_1 set (metal d and p orbitals) and the lowest energy set of ($1a_1$ and e_2), arising from metal d-orbitals, being non-bonding orbitals. With two such molybdenum fragments, twelve molecular orbitals arise although one of these is at such a high energy level (being out of phase) that it would almost certainly be non-bonding in any interaction. Considering then the imido ligands, after accounting for σ-bonding, of the twelve orbitals they offer for interaction with the metal fragment, only two sets are of matching symmetry with the metal orbitals. This leaves one metal-based and two ligand-based orbitals to be non-bonding with regard to molybdenum-nitrogen interactions. Thus, Green and co-workers were able to satisfy the eighteen-electron rule at each molybdenum centre for $[\{Mo(\eta\text{-}C_5H_4Me)(NPh)(\mu\text{-}NPh)\}_2]$ because of the electrons provided by the four imido ligands for bonding interactions - four from each bridging imido and three from each terminal imido; the metal-metal bond provides the last electron for each metal centre.

Extending their analysis with MO calculations, now based on the complex $[\{Mo(\eta\text{-}C_5H_5)(NH)(\mu\text{-}NH)\}_2]$, they showed three MOs, between the bonding and antibonding orbitals, non-bonding in character (for metal-ligand). Two of these were ligand-based and contained approximately equivalent contributions from the terminal and bridging imido ligands. Thus, one electron from each imido ligand is not used in

the molybdenum-nitrogen bond - i.e. the phenylimido ligand acts as a three-electron donor. (The third orbital was assumed to form the metal-metal bond.)

This intermediacy of electron donation is reflected in the structure of [Mo(NAr)$_2$(etc)$_2$] (7)[92]. In contrast to 1, 7 shows two linear imido ligands (169.9(2)°) with molybdenum-nitrogen bond lengths 1.766(2) Å which are between those of 1 - 1.754(4) and 1.789(4) Å (from low-temperature X-ray crystallography determination). As explained in the Introduction, molybdenum-nitrogen imido bond lengths only vary by very small amounts (~ 0.1 Å) so a better insight is gained on consideration of the molybdenum-sulfur bonds *trans* to each imido. In 1, the bond *trans* to the bent imido is considerably longer than that *trans* to the linear ligand (2.755(2), 2.602(2) Å). However, in 7, the molybdenum-sulfur bond length is 2.672(1) Å - again, intermediate between those in 1.

To summarise, many different bis(imido) complexes have already been synthesised in a number of ways, the most common of which involves using amines. In particular, complexes of the type [Mo(NR)$_2$Cl$_2$(DME)] undergo facile substitution of their co-ligands to form a wide range of bis(imido) complexes. Studies into metal-imido bonding using MO calculations have shown that where more than one imido ligand is present, a linear ligand donates only three electrons to metal-imido bonding; the other enters a non-bonding orbital. Structural determination by X-ray crystallography has, on the whole, shown these complexes to have both imido ligands linear and in a *cis* conformation.

Only one six-coordinate group VI bis(imido) complex shows a bent imido ligand - [Mo(NPh)$_2$(etc)$_2$][38]. A similar complex, [Mo(NAr)$_2$(etc)$_2$], has both imido ligands linear[92]. The focus of this chapter, then, is the effect of a change in the imido substituent, R, on the structure of the complex, [Mo(NR)$_2$(etc)$_2$].

2.2   Synthesis of DME complexes, [Mo(NR)$_2$Cl$_2$(DME)]

A recent reaction using the same synthesis with a highly sterically-demanding amine, 2,4,6-triphenylaniline, gave the oxo-imido complex, [MoCl$_2$(O)(N(2,4,6-Ph$_3$C$_6$H$_2$))(DME)][111], the identity of which was confirmed by X-ray crystallography. The imido bond length and angle (1.756(7) Å, 172.2(7)°) are very similar to those of the linear imido ligand of 1. The bonding could conveniently fit the valence-bond description with the imido as a four-electron donor and the oxo ligand as a two-electron donor. However, as discussed above, the bonding need not be regarded strictly in this manner as some metal-orbital sharing should occur between these two *cis*-orientated π-donor ligands. Galindo and co-workers did make their intended

bis(imido) DME complex, [Mo(N(2,4,6-Me$_3$C$_6$H$_2$))$_2$Cl$_2$(DME)]. Then, in a ligand redistribution reaction with [Mo(O)$_2$Cl$_2$(DME)], they produced the oxo-imido complex, [Mo(O)(N(2,4,6-Me$_3$C$_6$H$_2$))Cl$_2$(DME)]; this was presumed to be formed by a concerted oxo and imido transfer reaction, aided by the lability of the DME co-ligands[112].

mes = 2,4,6-Me$_3$C$_6$H$_2$
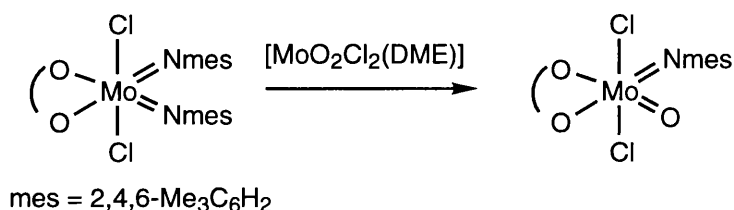
For this work, though, a wide range of bis(imido) DME complexes were synthesised as precursors to molybdenum bis(imido) bis(dithiocarbamate) complexes. The imido substituents are as those drawn on the next page. All complexes were synthesised following Gibson's method, as illustrated above[101]. Care was taken to ensure the solution mixture does not reflux as this led to product contamination. For synthesis of the *tert*-butyl and adamantyl complexes, heating of the solution mixture was not required. The high product yields secured in this synthesis are obtained after several extractions of the reaction residue with ether. Recrystallization usually produced fine, microcrystalline samples of the complexes. The complexes were highly moisture-sensitive and could only be handled in an inert atmosphere, either in a dry glove-box or by rigorous use of Schlenk techniques.

Characterization of the previously-characterized DME complexes was by ^{1}H nmr spectroscopy; data were compared with those in the literature[100]. New complexes were not fully characterized as they were regarded simply as precursors to the dithiocarbamate complexes. However, the proton nmr of one new complex [Mo(N(2,4-Me$_2$C$_6$H$_3$))$_2$Cl$_2$(DME)] is described here. The (OCH$_2$) ethyl protons are represented by a broad peak at 3.47 ppm, while the methyls of the solvent ligand are observed as a singlet at 3.29 ppm. The three aryl protons are observed as two doublets and a singlet at 7.53, 6.65 and 6.64 ppm, respectively. The *meta-* and *para-* methyl substituents are at 2.51 and 1.99 ppm, respectively. The correct identification of these DME complexes was assumed upon the characterization of the respective dithiocarbamate complexes subsequently formed. However, analysis by ^{13}C solid-state nmr spectroscopy on some of these complexes is reported below.

2.3   Synthesis of Dithiocarbamate Complexes, [Mo(NR)$_2$(etc)$_2$]

Use of bis(imido) DME complexes as synthons for new bis(imido) complexes is well established. Facile displacement of the chloride and solvent ligands from these

precursors allows formation of a wide range of bis(imido) complexes. It is easy to envisage the detachment of the DME ligand when in solution, leaving the reactive, coordinatively-unsaturated, four-coordinate molybdenum complex, $[Mo(NR)_2Cl_2]$. Indeed, this has been performed many times, notably in the development and synthesis of imido-alkylidene complexes. Rapid substitution with monoanionic monodentate ligands, often alkoxides, affords four-coordinate complexes of the type, $[Mo(NR)_2X_2]$. It is simple to extend this synthesis to use monoanionic, bidentate co-ligands, like dithiocarbamates. Recently , the reaction of such a complex with thallium acetylacetonate, Tl[acac], has been reported, producing the six-coordinate, octahedral (C_2) complex, $[Mo(Nmes)_2(acac)_2]^{112}$. Its proposed symmetry is based on signals observed in the ^1H and $^{13}C\{^1H\}$ nmr spectra.
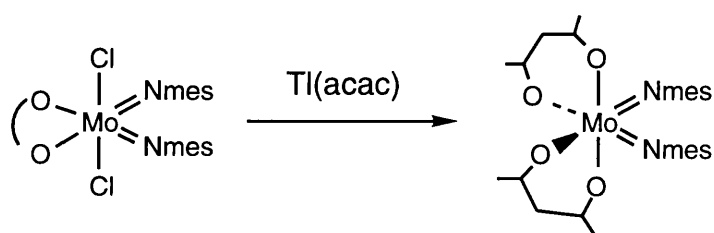
Bis(imido) complexes, reported in this work, were synthesised by the addition of a dithiocarbamate salt to bis(imido) DME precursor and stirred in ether for twelve hours. The product was extracted from the solution with ether and benzene, and purified by recrystallization from ether. This synthetic route was followed to produce sixteen complexes, eleven of which are new. The imido substituents, shown below (N in the 1-position), are chosen for the variety of their steric and electronic effects.
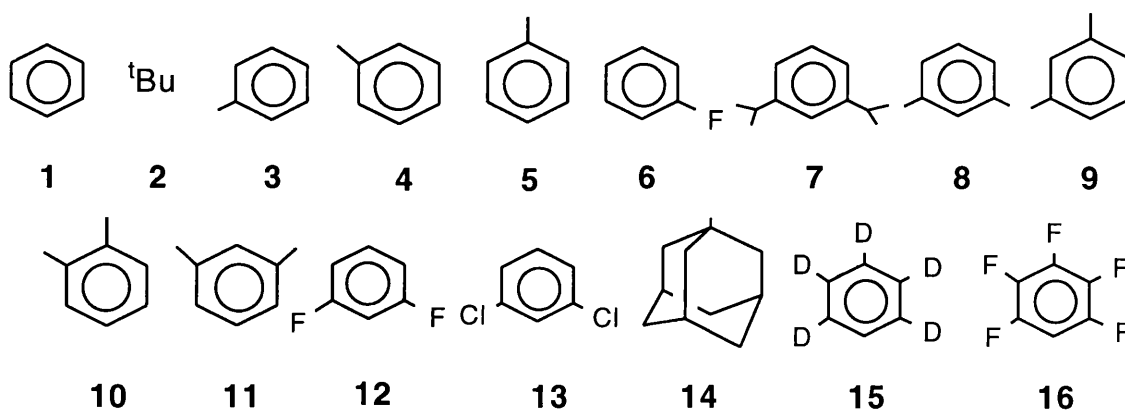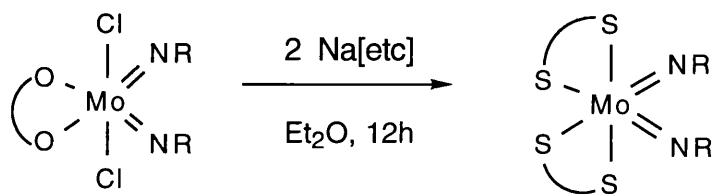
In the solid state, all aryl complexes are dark red, except for **11** which is purple and **13** which is brown-black. The two alkyl complexes, **2** and **14**, are both orange. Complex **15** was synthesised in response to the MO calculations and so is discussed in the last section of this chapter. Most are highly moisture-sensitive, especially when in solution. This sensitivity is not, however, found at all for arylimido complexes with substituents in 2 and 6 positions on the ring. Indeed, the *tert*-butylimido and arylimido complexes with a single substituent in the *ortho* position (**2, 3, 9** and **13**) are stable in solution for a few hours when exposed to air. Highly pure and extremely dry crystalline samples of all complexes are stable in the solid-state for several hours, at least.

Initially, the dithiocarbamate source was the ammonium salt, NH$_4$[etc]. However, this substance suffers from being highly hydroscopic, so reactions were not always successful, usually suffering from hydrolysis/decomposition and leading to low yields. The sodium salt was the next obvious choice though dehydration in a vacuum oven was unsuccessful (unlike sodium dimethyldithiocarbamate). Finally, a suitable dehydration process was found[84] - heating the salt at 80°C under a continuous vacuum of 10^{-2} atm - and henceforth, the sodium salt was used in all reactions. This did reduce product decomposition, though reaction yields were still low. A new extraction process was devised. Firstly, the ethereal solution containing the product was filtered (leaving a residue of sodium chloride); more product is extracted from the filtrate using benzene. Finally, the product is purified by recrystallization in ether, affording product yields of around 50%.

2.4   Characterization and Solution Nmr Studies

Characterization was principally by ^{1}H and ^{13}C nmr spectroscopy. Other techniques added supplementary information, though of these, ir spectroscopy was the least informative. The absence of peaks in the 850-950 cm^{-1} region indicates a lack of molybdenum-oxo bonds, while dithiocarbamate presence was confirmed with absorptions about 1500 cm^{-1}; finally, all show peaks in the 1230-1280 cm^{-1} region which were taken to confirm the presence of an imido ligand. EI mass spectra show molecular ions for all complexes, though, curiously, FAB mass spectra give molecular ions of higher weights.

The majority of complexes have their nmr spectra recorded using d^6-benzene. Some of the highly stable complexes (**2, 7, 8** and **13**) may be recorded in CDCl$_3$. Other complexes, though, are susceptible to reaction with chlorinated solvents. This is clearly demonstrated by a sealed sample of **3** in CDCl$_3$, which changes colour from dark-red to orange-red over some days.

Room temperature ^{1}H nmr spectra consist of simple, sharp peaks for both the dithiocarbamate and imido ligands. A 1:1 ratio of imido and dithiocarbamate peaks

confirms the presence of a bis(imido) complex. Considering the dithiocarbamate ligand, the ethyl protons are always observed as a quartet between 3-4 ppm and the methyl protons by a triplet at 1-2 ppm. The aryl proton peaks usu ally fall in quite a narrow region from 6.8 - 7.4 ppm. The methyl substituents in **4, 5, 10** and other similar complexes give rise to singlets, which are observed close to 2 ppm. The *tert*-butylimido ligands in complex **2** give rise to a singlet, while the adamantyl ligands in **14**, show two singlet peaks for the CH and one set of CH$_2$ protons at 2.01 and 2.35 ppm, respectively. The second set of CH$_2$ protons are represented as a pair of doublets with second-order coupling (at 1.50 and 1.58 ppm).

The simplicity of the peaks for the imido substituents suggests that the imido ligands are equivalent. A typical spectrum is shown below to illustrate the simplicity and general pattern found in the spectra of these complexes.
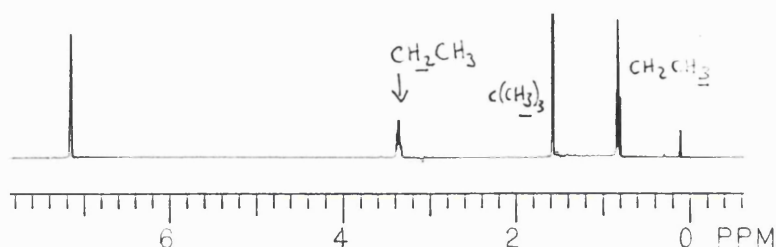
Spectrum of [Mo(N^{t}Bu)$_2$(etc)$_2$] **2**

As may be expected, with fluoroimido complexes (as in **6** and **12**), some fluorine-proton coupling is observed and chemical shifts are somewhat different compared to non-fluorinated complexes. Comparing the protons in **6** to the normal regions outlined above, a triplet, possibly attributable to the *para*-H, shifts upfield to 6.44 ppm. A multiplet (possibly consisting of a triplet or doublet of triplets) is also shifted upfield considerably to 6.6-6.7 ppm and finally, a triplet likely to account for the *ortho*-H, has shifted downfield to 7.54 ppm.

The ^{13}C{^{1}H} solution spectra also display a rather consistent pattern of peaks. Those observed around 125-128 ppm are attributed to unsubstituted aryl carbons. The *ipso*-carbon always appears in the 154-160 ppm region, with the exception of fluoroimido complexes where it shifts upfield as far as 136 ppm (as in **16**). Other imido carbons are usually methyls and their peaks are observed in the 20-30 ppm region, downfield of those in the co-ligand. In the non-aryl complexes, the α-carbon lies near 70 ppm. A proton-coupled spectrum was necessary for a more reliable assignment of peaks to different carbons in the bis(adamantyl) complex, **14**. Dithiocarbamate ligands are indicated by characteristic peaks. The carbon in the backbone of the ligand gives rise to a peak around 200 ppm while the methylene and methyl carbons appear around 40-45 ppm and 12-15 ppm, respectively.

Some of these complexes (**7, 8** and **13**) have been synthesised previously in this laboratory in the reaction of arylisocyanate with $[Mo(O)_2(etc)_2]^{64,92}$. Proton nmr spectra of these complexes showed broad peaks, especially for the ethyl protons of the dithiocarbamate ligand, indicative of fluxional processes. Analysis of VT nmr for **7** showed that the protons of the aryl ring changed little between 253K and 373K. However, the dithiocarbamate ligands' motion was frozen out. On warming, peaks for the methyls of the isopropyl groups on the imido and on the dithiocarbamate broadened and coalesced before sharpening into a single peak for each type. On cooling though, two different signals are shown for each type, motion being frozen out (on the nmr timescale).

Similar VT nmr spectroscopy was performed on **1** and **3**. All show that the peaks of the aryl protons hardly change on cooling and warming, so the fluxionality of the bent-linear configuration is maintained, even at very low temperatures.
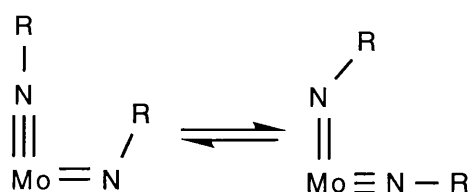
The VT $^{13}C\{^1H\}$ nmr spectra of **1** and **3** confirm that of the VT ^1H nmr experiments. A single peak for the *ipso*-carbon is observed for both complexes, even at temperatures of -80°C. This suggests that the imido ligands are highly fluxional when in solution, even at very low temperatures.

As above, the dithiocarbamate ligand's fluxionality is evident in the ^1H nmr spectra; freezing of the co-ligand motion is observed by multiple peaks for the ethyl and methyl protons while these same peaks broaden and coalesce into a single peak on warming. As alluded to in the Introduction, there is restricted rotation of the ethyl and methyl groups about the ligand's carbon-nitrogen backbone, reflective of its double-bond character . Thus, on cooling, the freezing out of motion of the ethyl and methyl protons is observed in nmr spectra.
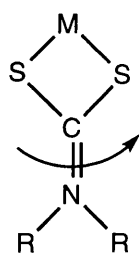
In trying to discern structural information from solution nmr spectroscopy, it may be thought better to use ^{14}N or ^{15}N nmr spectroscopy to distinguish imido

environments. Such nmr experiments were not performed for these complexes given the experiences of Bradley, Mason and co-workers when they investigated nitrogen nmr spectroscopy as a probe of bonding, bending and fluxionality of the imido ligand[73]. They analysed 1 and even enriched the complex with ^{15}N. Even still, there was a single resonance for the imido nitrogen, again, confirming the complex's fluxionality in solution. Thus, solution nmr spectroscopy proves useful only in the characterization of bis(imido) complexes and does not elicit any structural information.

2.5   Structural Studies

The effects of varying imido substituents have been considered previously, with reference to both structure and reactivity. Schrock and Gibson's groups have both studied four-coordinate metal bis(imido) complexes, especially with reference to alkene metathesis. Schrock observed that five-coordinate complexes of the type, $[W(NAr)_2(PR_3)_2(L)]$ would form when L was a relatively small ligand (like ethene) and the imido substituent is the large 2,6-diisopropylphenyl group[113]. However, Gibson was able to keep the four-coordinate geometry using $tert$-butylimido ligands in forming $[Mo(N^tBu)_2(PMe_3)(C_2H_4)]$[101,114]. The authors (Gibson $et~al.$) reason this observation citing the greater steric flexibility of the aryl substituents. These could re-orientate themselves to allow optimal positioning and coordination of the other co-ligands. In contrast, the $tert$-butyl ligands do not have such flexibility and so, do not allow an expansion in coordination to the molybdenum centre.

Gibson's group has also investigated competition between different imido ligands and its consequential structural effects[115]. In particular, $[Mo(NAr)(N^tBu)Cl_2(DME)]$ was synthesised and its crystal structure determined. The distorted octahedral structure shows imido angles of 174.3(2) and 157.9(2)° for the aryl- and non-arylimido ligands, respectively. The aryl nitrogen-molybdenum bond length at 1.753(2) Å is longer than that for the $tert$-butyl ligand (1.728(2) Å). This is thought to arise from competition for one of the imido nitrogen's p-orbitals between the metal and $ipso$-carbon. This interaction also favours linearity in the ligand, as the nitrogen becomes sp-hybridised. The more bent $tert$-butylimido also exerts a greater $trans$ influence than the aryl ligand (on oxygen atoms of the DME ligand).

Earlier in this chapter, the possibility of an imido ligand acting as a three-electron donor was explained by one-electron from each ligand entering a non-bonding orbital while the other three interacted with the appropriate metal d-orbital. Gibson suggests that if the two imido substituents are identical then the strength of the metal-nitrogen π-bonds should be the same but on introducing a different substituent, the degeneracy of orbitals is removed and will allow a stronger interaction with just one of

the imido ligands. The phenyl ring re-orientates itself so as to allow greater overlap of the p-orbitals of the nitrogen and its *ipso*-carbon. Consequently, its metal-nitrogen interaction drops and lets the *tert*-butylimido nitrogen form a stronger π-bond to the metal centre. Thus, an electronic preference has developed for the orientation of the phenyl ring.

Finally, the structural influences of the *tert*-butyl and *para*-tolylimido substituents were evaluated in the mononuclear, monoimido complexes, $[Ti(NR)Cl_2(py)_3]^{116}$. The *para*-tolylimido complex was formed by imido exchange on reaction of the *tert*-butyl complex with the *p*-toluidine. The lack of *ortho*-substituents minimises any steric contribution to the structure, allowing the evaluation to be based only on electronic effects. The authors state that the butyl ligand exerts the greater structural influence, due to the greater lengthening of the *trans* titanium-nitrogen bond (of the pyridine).

In the following discussion, two techniques, namely X-ray crystallography and solid-state nmr spectroscopy, are used to show the structural effects of different imido substituents, based on analysis of the complexes synthesised during this work.

2.6   Solid State Structures - Crystallography

The crystal structures of these complexes are of interest as they can be directly compared with that of the parent complex of this series, $[Mo(NPh)_2(etc)_2]$ **(1)**. This was the first complex to show a truly bent imido ligand with an imido angle of 139.4(4), as discussed and illustrated earlier[38]. Earlier in this laboratory, $[Mo(NAr)_2(etc)_2]$ **(7)** $(R=2,6-^iPr_2C_6H_3)$was shown to have a linear-linear structure, both imido angles being 169.9(2)° [92]. Crystal structure determinations of **8** $(R=2,6-Me_2C_6H_3)$ and **13** $(R=2,6-Cl_2C_6H_3)$ also showed the imido ligands as linear-linear[64]. Crystallographic details are tabled below for **7** and **8**, for comparison with other structures[64].

Crystals for each of these were grown in air - upon diffusion of methanol into a dichloromethane solution of the complex. Given the moisture-sensitivity of the majority of these complexes when in solution, crystal formation had to occur in an inert atmosphere. Attempts to grow crystals have been made by using the solvent diffusion process in a glove-box and also by recrystallization from ether at low temperatures (-30° C). This process only proved successful for crystal formation of **1** (dark-red) and **2** (orange). After several attempts at using these two methods, crystals of **3** (red-brown) were eventually grown in air upon diffusion of petrol into a benzene solution of the complex.

Crystal Structures of 1, 2 and 3

The first structure determined was that of **3** and is shown overleaf. The geometry is approximately octahedral and the imido ligands bend towards one another. Again, the imido conformation is linear-linear though, the angles at each nitrogen are slightly different - 166.8(6) and 175.1(4) °. The molybdenum-nitrogen lengths at 1.776(5)and 1.757(6) Å, for the less linear and linear ligands, respectively, are within the usual range[8]. We have already dismissed molybdenum-nitrogen bond lengths as useful indicators of bond order. More information can be discerned from bond lengths *trans* to the imido moiety. The molybdenum-sulfur bond lengths of those *cis* to the imido ligands are 2.462(2) and 2.458(2) Å. However, the bending of one imido ligand is reflected in the lengthening of the molybdenum-sulfur bond *trans* to it, compared to the other *trans* to the more linear one - 2.682(2) against 2.654(2) Å. Such behaviour is also shown in **1** where the *trans* molybdenum-sulfur bond lengths are 2.755(2) and 2.602(2) Å. Admittedly, the difference in bond lengths is not as significant for **3** as it is for **1**, though the difference in angles is only 8.3°, not 30.0°.

The structure of the non-aryl complex **2** was determined and again, has an approximately octahedral coordination geometry with both ligands linear. The difference in angle is even more pronounced than in **3**. The imido angles are now 162.5(7) and 173.2(8)°, differing by 10.7°. Again, the *trans* molybdenum-sulfur bonds are elongated to different extents, at 2.719(2) and 2.694(2) Å.

Finally, although the structure of **1** had already been determined by Haymore, Maatta and Wentworth, it was performed at -80°C - presumably to reduce the fluxional movement of the dithiocarbamate ligands. When the structure was determined at room temperature, the changes in angles and bond lengths were insignificant. The imido angles are now 141.8(4) and 170.4(5)° although the *trans* molybdenum-sulfur bonds are longer, at 2.761(2) and 2.603(2) Å. This new structural determination is shown overleaf.

In all structures, there is nothing remarkable about the dithiocarbamate ligands. There is no large variation in bite angles, with S-Mo-S ranging from 67.4 to 69.5°. The greatest difference between the two angles in a single complex is observed for **1** (69.51(4) and 67.60(5)°). This is to be expected as the larger *trans* influence of the bent imido ligand should also push away ligands *cis* to it.
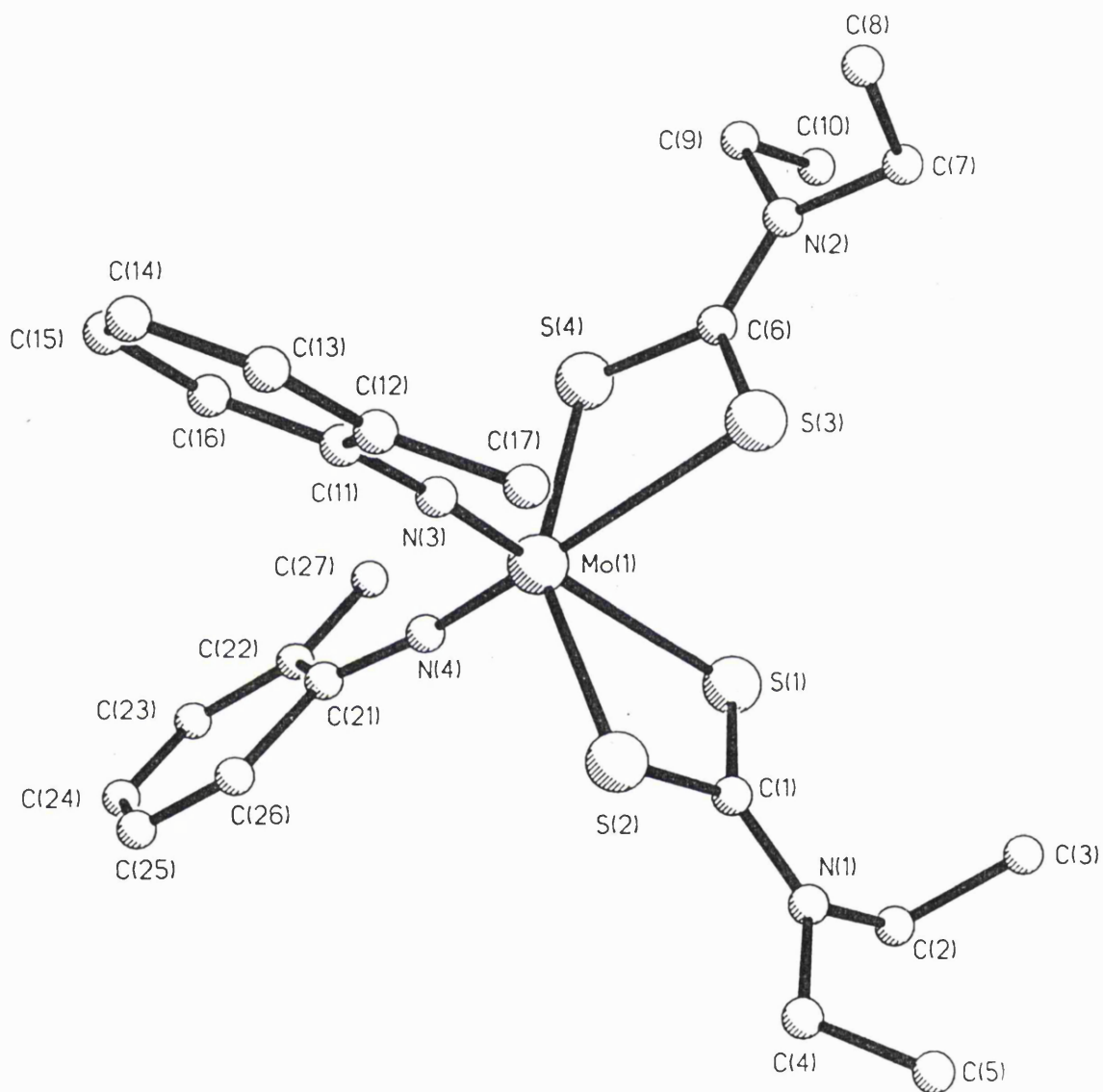
Structure of [Mo(N(2-Me)C$_6$H$_4$)$_2$(etc)$_2$] **(3)**
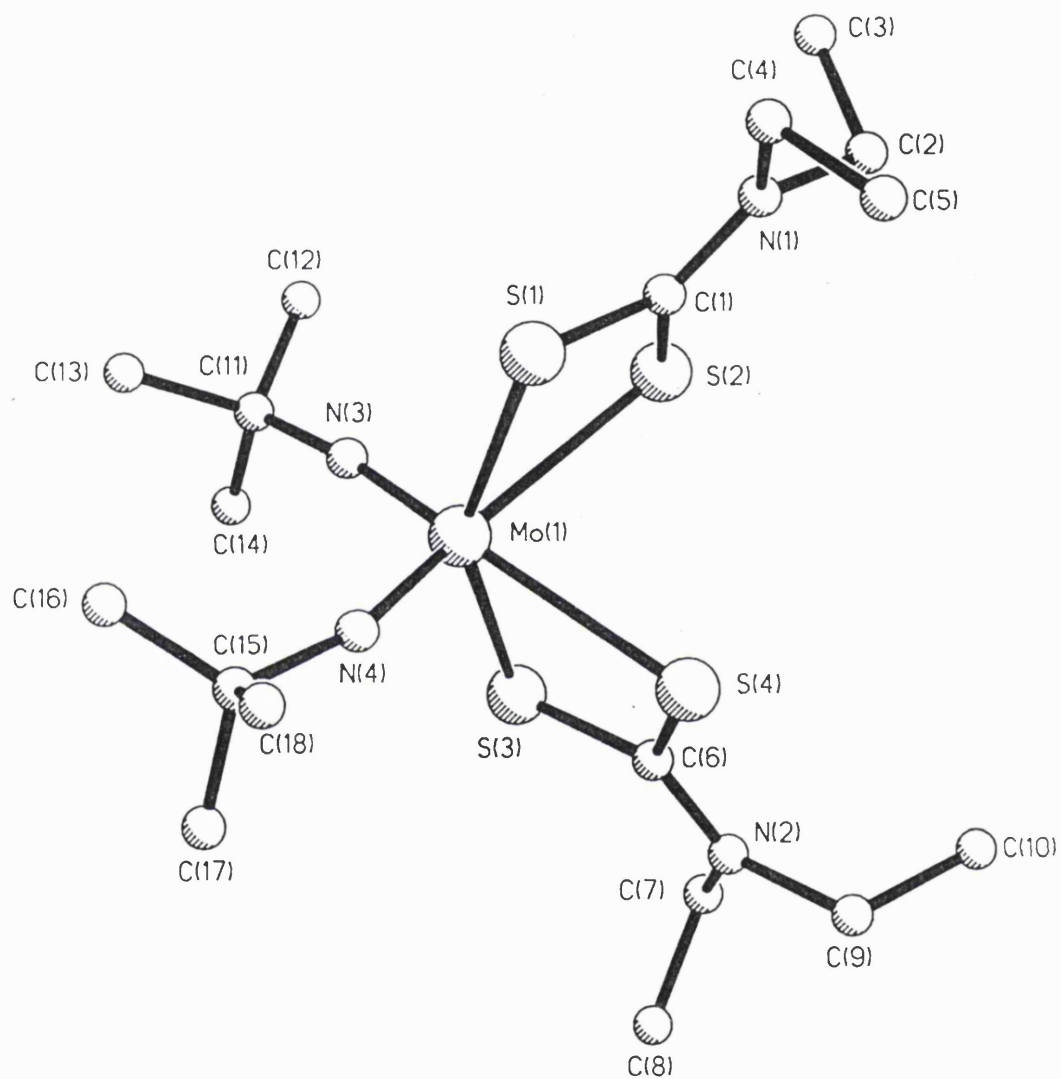
Structure of [Mo(N^{t}Bu)$_2$(etc)$_2$] **(2)**
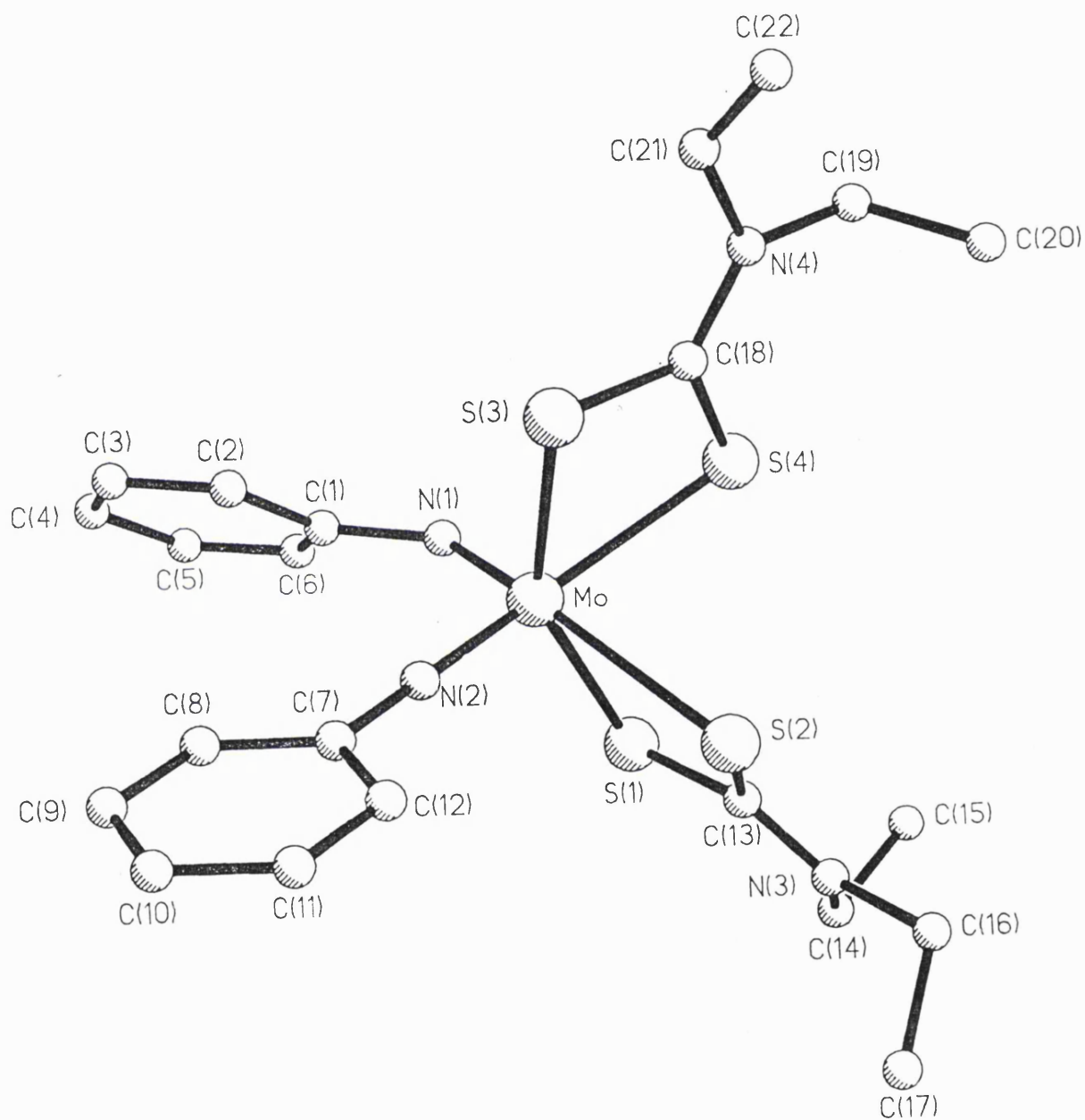
Structure of [Mo(NPh)$_2$(etc)$_2$] **(1)**

This table, below, of crystallographic parameters may be used for comparison between the different structures. It has been argued that the steric effect of a substituent in the *ortho*-position on the ring makes the imido ligands linear-linear. The observation appears to be borne out here, though the increase in bending of one of the imido ligands accompanies a decrease in the steric influence of the imido substituent.

	1 (-80°C)	1 (25°C)	2	3	7	8
Mo-N(1)-C	139.4(4)	141.8(4)	162.5(7)	166.8(6)	169.9(2)	162.0(6)
Mo-N(2)-C	169.4(4)	170.4(5)	173.2(8)	175.1(4)	"	162.8(6)
Mo-S(1)$_{trans}$	2.755(2)	2.761(2)	2.719(2)	2.682(2)	2.672(1)	2.685(2)
Mo-S(2)$_{trans}$	2.602(2)	2.603(2)	2.694(3)	2.654(2)	"	2.684(2)
Mo-N(1)	1.789(4)	1.776(5)	1.753(7)	1.776(5)	1.766(2)	1.770(6)
Mo-N(2)	1.754(4)	1.749(5)	1.721(8)	1.757(6)	"	1.756(6)
N-Mo-N	103.5(2)	103.5(2)	107.3(9)	105.7(3)	104.7(1)	102.5(3)

Note that the numbers attached to N and S, in the table, are only for distinguishing between the two ligands - (1) referring to the ligand with the smaller imido angle. They are not related to the numbering in the crystal structures.

Frustrated by failure to grow crystals of complexes with substituents in the *meta-* or *para-* positions on the aryl ring, it is evident (see below) that the only complex to adopt a bent-linear structure is the first such complex synthesised, namely 1.

2.6   Solid State Nmr Spectroscopy

Given the difficulty of forming single crystals of these complexes coupled with their high fluxionality in solution, we looked for another way of gaining any structural information for these complexes in the solid-state - namely, solid-state nmr spectroscopy. An introduction to this technique is offered in Appendix I. The nucleus of choice would be nitrogen but it is very difficult to measure this without sample enrichment of ^{15}N. The expense of such enriched amines ruled out any possible synthesis and, hence, useful analysis in this way. However, relying on the natural abundance of ^{15}N within the complex, the spectrum of 7 was measured over a day and, as expected, a single peak for the imido nitrogen was observed at 77.4 ppm. The dithiocarbamate nitrogen was observed at -210.8 ppm. Before the crystal structure of 3 was determined, attempts were made to analyse its structure using ^{15}N solid-state nmr spectroscopy (natural abundance). After the sample had run continuously for four days, the result was still ambiguous though for the optimistic, two peaks for the imido nitrogens could be discerned at 67 and 55 ppm. The *tert*-butyl complex 2 was also analysed by ^{15}N (natural abundance) solid-state nmr spectroscopy, though on this occasion, no peak was found at all for the imido nitrogen. It was unfeasible to run

nmr experiments for such long periods, especially when no meaningful result or analysis could be drawn from the spectra.

In contrast, the duration of a ^{13}C solid-state nmr experiment is usually, at longest, a few hours though a good indication can be obtained in minutes. Furthermore, although no information could be obtained concerning the imido nitrogen itself, the ^{13}C spectra nmr reveals information about the environments of those carbons directly attached to the imido nitrogen - namely, the *ipso*-carbon (of the aryl ring) or the α-carbon (in non-aryl complexes).

The first complexes analysed were those with known structures - **7** and **8**. As expected, there is only one peak for the *ipso*-carbon in **7**, reflecting the single environment experienced by these atoms (and the imido nitrogens) in the crystal structure. Similarly to the solution nmr spectrum, peaks for the other carbons are observed - those in the *meta* and *para*-positions of the aryl ring at around 125 ppm; those for the *ortho*-position are shifted downfield slightly; the dithiocarbamate ethyl and methyl carbon peaks are at 45 and 13 ppm, respectively; while the various carbons in the isopropyl groups lie in the range of 21 to 30 ppm. No extra peaks for the *ipso*-carbon are observed in the spectrum for **8**.

The next spectra analysed were those of **2** and **3**. Two peaks are evident for the α- and *ipso*-carbons, respectively. Thus, there is evidence of significantly different environments and hence, different geometries of the imido ligands in these complexes. The last complex to be analysed was **1**. This also shows two peaks for its *ipso*-carbon, though significantly, the separation between them is considerably greater than for either **2** or **3**. A selection of spectra are shown later in this chapter, illustrating the different peaks seen in the *ipso*-carbon region. The table below details the relevant nmr and crystallography data.

	ipso/α-C δ 1 (ppm)	*ipso*/α-C δ 2 (ppm)	difference, Δ δ	Mo-N(1)-C	Mo-N(2)-C	difference, Δ °
1	161.4	156.4	5.0	139.4(4)	169.4(4)	30.0
2	71.7	69.7	2.0	162.5(7)	173.2(8)	10.7
3	158.5	157.2	1.3	166.8(6)	175.1(4)	8.3
7	153.9	153.9	0	169.9(2)	169.9(2)	0
8	157.5	157.5	0	162.0(6)	162.8(6)	0.8

Note that the numbering of the peaks does not mean they have been assigned to a specific ligand.

The differences in angles and the differences in chemical shift of the *ipso*-carbons are compared in the graph shown (overleaf) and a direct relationship is found between these two parameters.

difference in imido angle v. difference in chemical shift
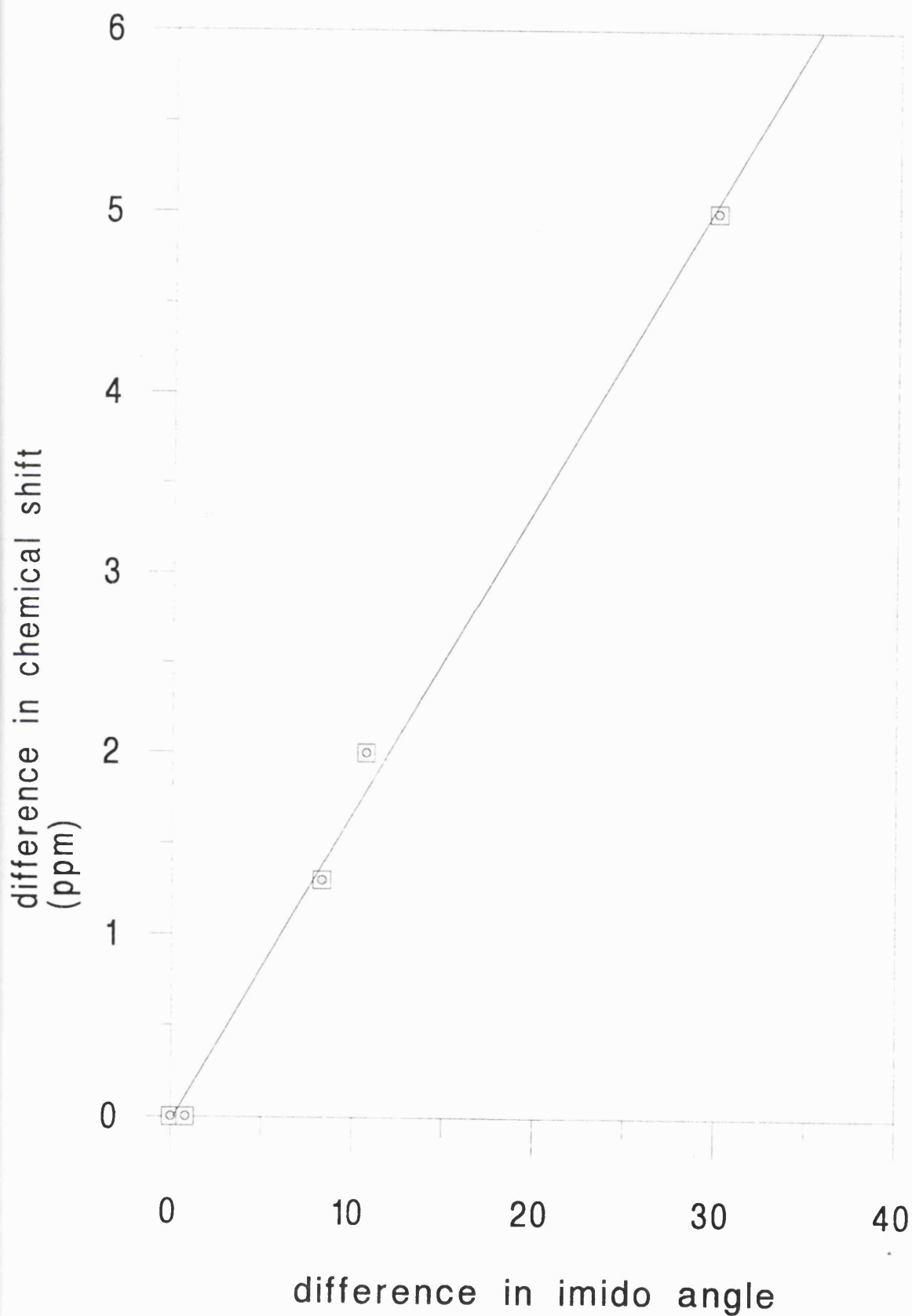
Consequently, nearly all the other complexes were analysed. Using the difference in their chemical shifts for their *ipso*/α-carbons, the difference in their imido angles was calculated. The data and the calculated angle difference is tabulated below. Unfortunately, a sufficiently pure sample of **4** was never obtained for the nmr experiment.

	ipso/α-C δ 1 (ppm)	*ipso*/α-C δ 2 (ppm)	difference, Δ δ	calculated difference, Δ °
5	155.5	151.7	3.8	23.1
6	151.0	-	0	0
9	155.5	-	0	0
10	158.2	155.4	2.8	17.0
11	160.4	156.8	3.6	21.4
12	136.2	-	0	0
14	71.7	-	0	0
16	133.8	-	0	0

Analysis of the table shows that all complexes whose imido groups have a substituent in the 2-position (on the ring) (**6, 9, 12, 16**) have identical environments for the *ipso*/α-carbons, indicative of a linear-linear structure. This is also true for the bis(adamantyl) complex, **14**. Why these complexes show identical imido environments and yet **2** and **3** do not is uncertain. Even the different electron-withdrawing substituents like fluorine have not affected the predicted structure. What must be presumed is that other molecular interactions, like crystal packing forces, must be assuming a dominant role in structural preference.

The only complexes where bending of one of the imido ligands is suggested are those with substituents in the *meta-* or *para-* positions. Indeed, the greatest difference in chemical shifts (and so, implied in imido angles) except for **1**, is for **5** - the *para*-tolyl complex. Considering previous suggestions, the combination of having only one substituent and in the *para-* position makes **5** an ideal candidate to stretch the limits of the angles allowed for a "linear" imido.

It must be emphasised that the graph will only allow the calculation of differences in the imido angles for a given complex and not the absolute angles. Until a crystal structure of **5** is determined, then the cross-over point between a bent-linear and linear-linear structure cannot be evaluated.
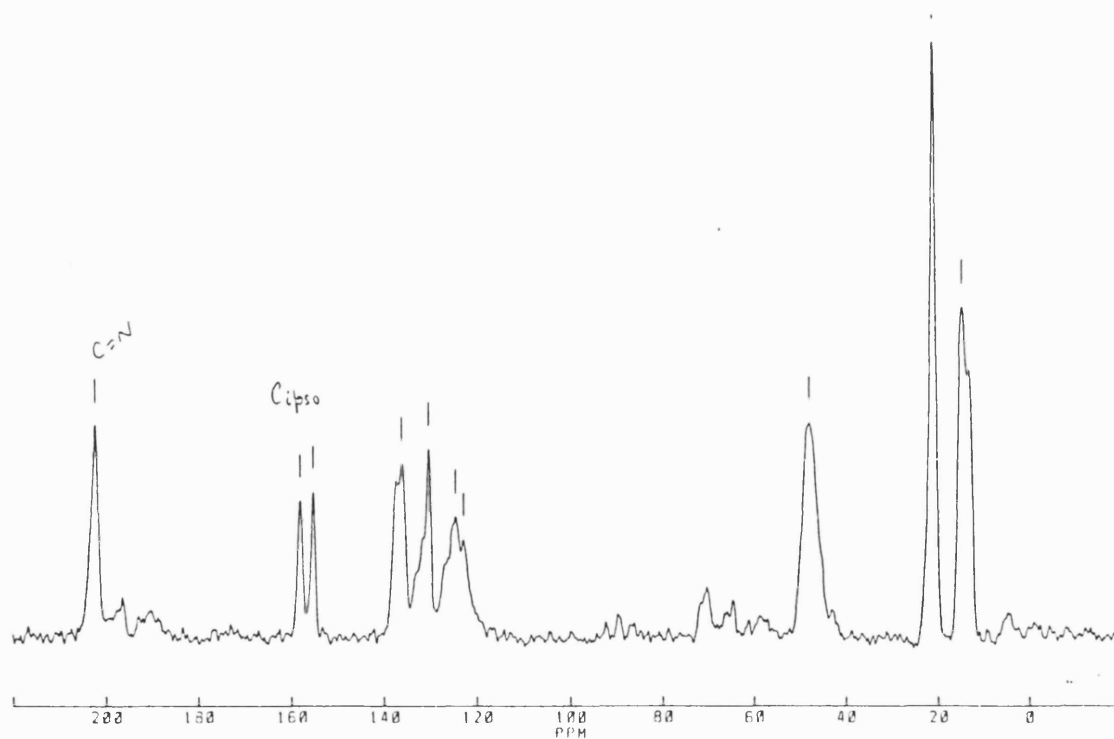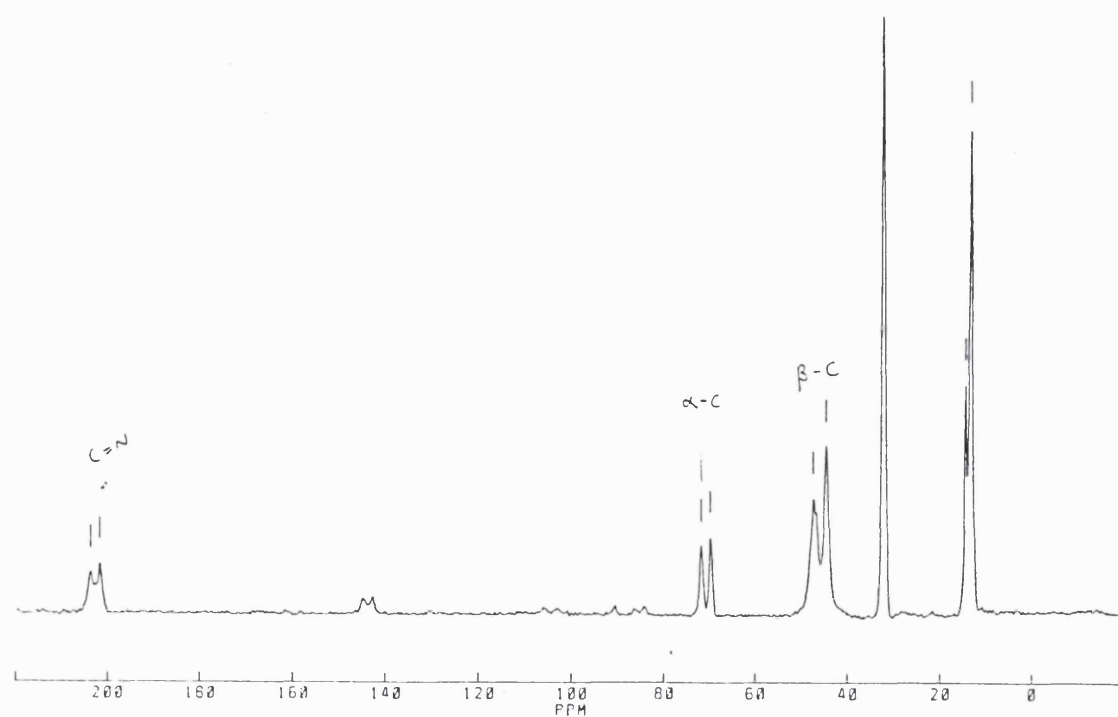
^{13}C Solid-State Nmr Spectra of **2** (above)and **10** (below)

Finally, the structures of some of the DME complexes have been analysed by solid-state nmr spectroscopy; in particular, the DME complexes chosen are the precursors of those dithiocarbamate complexes that show significantly different imido environments. The spectra produced are very interesting as only one peak for the *ipso*-carbons is observed in all complexes. This implies that all the DME complexes analysed adopt a linear-linear structure - even for the bis(phenyl) complex. Thus, it is only on formation of the diethyldithiocarbamate complexes that the geometry of the imido ligation changes.

2.8   Molecular Orbital Calculations

During the course of this work, Woo-Sung Kim, under the supervision of Dr Nik Kaltsoyannis, performed some MO calculations using Extended Hückel theory in his investigation of the structures of these molybdenum bis(imido) complexes. In particular, he studied the conformation of the imido ligand - predicting the amount of bending in a given complex and investigating the competition between intermolecular interactions, e.g. crystal packing forces and intramolecular electronic effects. Extended Hückel theory is a simple model of atomic interactions that takes into account all valence electrons, both σ and π[117]. Computer Aided Composition of Atomic Orbitals[118] was the computer software chosen to allow the pictorialisation of the molecular electronic structure in different formats - Walsh diagrams, MO energy level diagrams and MO contour plots. A summary of their work is presented here as their results were important in designing some experiments for our structural studies.

Ten complexes were chosen, differing in the steric and electronic properties of the imido substituent; the different substituents are shown below. Phenylimido complexes with different metal centres were also selected. At the time of their study, four of these had been synthesised and their structures elucidated by X-ray crystallography. Since that time, three more of the complexes have been synthesised but none have been characterised by X-ray diffraction.
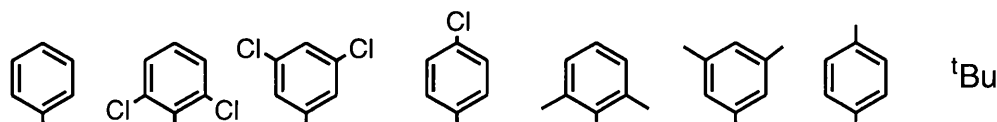
Mo, Cr, W

The total EH energy is the sum of all one-electron energies in the complex. In practice, this does not give the real total energy as it neglects the effects of core electrons and internuclear repulsions. However, when used for comparison with other complexes, it is an adequate measure for differentiating between members of a given series of complexes.

Kim and Kaltsoyannis defined two basis structures - one linear-bent and the other linear-linear. The total energy was calculated for a single molecule of each complex adopting both basis structures. Two complexes (8 and 13) showed a clear energetic preference for the linear-linear structure. Interestingly, all the other complexes had negligible preference for either conformation. Most importantly, the classic bent linear bis(imido) complex 1 is calculated to show little preference for either conformation and thus, intramolecular forces must be important in determining its solid-state structure. Finally, for 2, the preference for the linear-linear structure is significantly larger than for other complexes (though much less than for 8 and 13), with the difference in energies at > 0.5 eV.

Once the energies had been considered, six deformations to the basis structures were calculated, two of which shall be considered in detail - bending of one imido group towards the other (fixed) in steps of 5°, i.e. going from linear-linear to linear-bent, and rotation of a single imido ligand in steps of 20°. In the following Walsh diagrams, the dotted line represents the total energy (TE). The optimum conformation of the ligand is where the total energy is at a minimum.
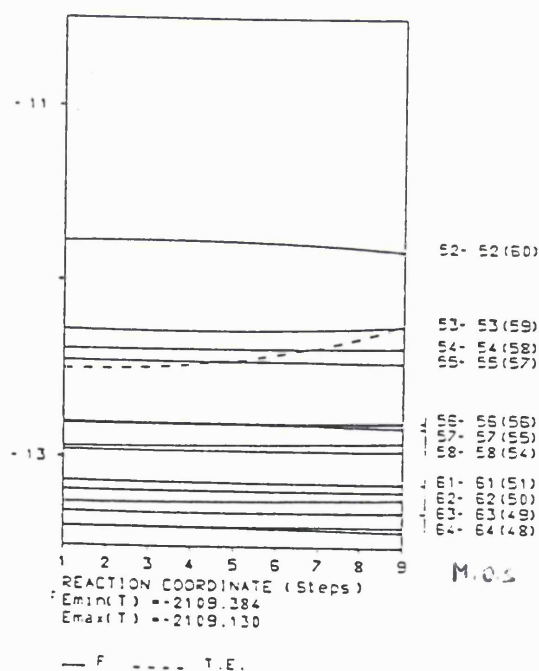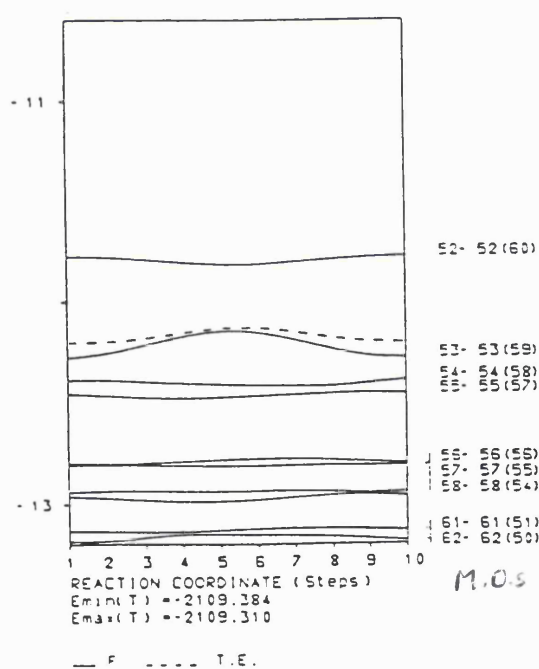
(i)   (ii)

Walsh diagrams for the bending and twisting deformations in 1

(i) bending one imido ligand towards the other (which is fixed linear)

(ii) twisting of one imido ligand while the other is fixed bent

The first complex studied was the bis(phenylimido) complex, **1**. On bending one ligand towards the other, there was a slight increase in the TE, though not as great as when bending away from the second ligand. This is reflected in the crystal structure where the two groups bend towards one another. On rotation of one imido ligand, an increase is seen in the TE line between the fourth and sixth steps. A similar calculation with one ligand bent showed a similar TE change but the increase between the fourth and sixth steps was considerably greater than previously seen, indicating that rotation of the phenyl ring up to 80° is facile. Again, this is demonstrated in the crystal structure which shows the relative alignment of the linear imido ligand to be rotated by 80°. Calculations with chromium and tungsten metal centres produced almost identical results.

The EH calculations accurately predicted the orientation of the imido groups relative to one another in the other complexes studied, giving a fair indication for the structure adopted. In conclusion, then, only arylimido ligands with substituents in the 2- and 6- positions had a clear energetic preference for the linear-linear structure. All others, including the known bent-linear bis(phenylimido) complex **1**, had no strong preference for either structure and bending is predicted to occur with relative ease. Thus, physical effects, like crystal packing forces, should have a dominant effect on the structure adopted for each molecule. This notion has already been expressed by Gibson and co-workers who argued that imido ligands with angles as small as 155° could still be regarded as "linear", the small angle being due to crystal-packing forces[37].

Further to these investigations, the experiments in Chapter 3 were devised, varying both the metal centre and the co-ligands. Before moving on though, a final test of the phenylimido's structural preferences was applied by using d^5-aniline to synthesise [Mo(NC$_6$D$_5$)$_2$(etc)$_2$] **(15)**. The ^{1}H nmr spectrum only showed the ethyl and methyl hydrogens of the dithiocarbamate ligand but the ^{13}C solution nmr spectrum was characteristic and almost identical to that of **1**. Its identity was confirmed by the EI mass spectrum, showing a strong parent peak and fragmentation of a deuterated-imido and a dithiocarbamate ligand.

The ^{13}C solid-state nmr spectrum of **15** duly showed the presence of two peaks for the *ipso*-carbon 4.9 ppm apart - again, nearly identical to that for **1**. Thus, this slight alteration to the imido complex's composition had not been sufficient to change its structure. Of note, again, was its DME precursor's solid-state spectrum showing only one peak for the *ipso*-carbon, suggesting a linear-linear structure.

2.9   Summary

Sixteen complexes of the type, $[Mo(NR)_2(etc)_2]$, have been synthesised, differing only by the change in imido substituent, R. Eleven of these complexes are new and have been characterized. Crystal structures have been obtained for two of these new complexes, 2 and 3; both display a linear-linear conformation of their imido ligands. The crystal structure of 1 was re-determined at room temperature and its structure was confirmed to be bent-linear. VT solution nmr spectroscopy showed these complexes to be fluxional, even at very low temperatures. This failure to discern any structural information led to analysis by solid-state ^{13}C nmr spectroscopy. This technique showed a direct relationship between the difference in imido angles (of the two ligands) and the difference in ppm of the *ipso*-carbon peaks. Thus, although actual imido angles were not actually calculated for complexes, this difference in angle was helpful in assessing the similarity to known complexes and hence, their possible reactivities. Of those complexes with unknown structures, only arylimido complexes with ring substituents in the 3,4 or 5- positions suggested any bending of an imido ligand. Finally, MO calculations proposed that, even for 1, there was negligible preference to have either linear-linear or bent-linear imido ligation. Other molecular interactions, like crystal packing forces, were cited as the dominant factor for adoption of a given structure.

Chapter 3 Other Metals and Ligands

3.1   Introduction

The MO calculations on **1** and **2**, discussed in the previous chapter, have suggested that there is little preference for bent-linear or linear-linear imido ligation in molybdenum bis(imido) complexes. Intrigued by this observation, further experiments were conceived to test the preferred geometrical ligation in bis(imido) complexes. We were especially interested in the bis(phenylimido) complexes since **1** shows a bent-linear conformation, when Walsh diagrams suggest the energy difference between a bent-linear and a linear-linear conformation is very small. This suggests that other interactions like crystal packing forces are a dominant factor in this case. In the previous chapter, the imido substituent was altered, using substituents with different steric and electronic effects. In this chapter, changes in ancillary ligands are investigated. Furthermore, the MO calculations showed little change when the metal centre was changed for chromium or tungsten, so we wondered if the same ligands would adopt the same geometry at a different metal centre.

The other bidentate ligands used were chosen for their similarity to the diethyldithiocarbamate ligand, namely they are all univalent, bidentate sulfur ligands - [S,S'(X)]. The three selected were dimethyldithiocarbamate $[S_2CN(Me)_2]^-$, diphenyldithiophosphinate $[S_2PPh_2]^-$ and ethyl xanthate $[S_2COEt]^-$.

| dimethyl-dithiocarbamate | diphenyl-dithiophosphinate | ethyl xanthate |
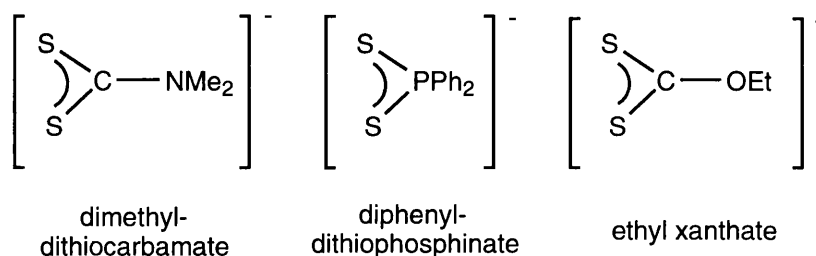
The dimethyldithiocarbamate ligand was chosen because of its great similarity to the standard co-ligand, the only difference being the reduction in steric bulk. In earlier work in this laboratory, imido-disulfide complexes were synthesised with both diethyl- and dimethyldithiocarbamate ligands. The change in this ancillary ligand did not affect the reaction nor the general geometry of the complexes formed, as shown in crystal structure determinations[22], while its properties and bonding modes are similar to those of the diethyldithiocarbamate ligand.

The dithiophosphinate ligand is well known. Like dithiocarbamate ligands, it can stabilize low-oxidation state metal centres because π-electrons can flow from sulfur to empty d-orbitals on the phosphorus, allowing the sulfurs to be "hard" and coordinate bidentately to a "hard" metal. Finally, the xanthate ligand may also

delocalize charge onto oxygen, though not as effectively with the phosphorus in thiophosphinate ligands.

All reactions were performed in the same way as the synthesis of diethyldithiocarbamate complexes - i.e. reacting the molybdenum bis(imido) DME complex with a metal salt of the ancillary ligand.

3.2   Other Ligands

The dimethyldithiocarbamate complexes are synthesised in a similar fashion to their ethyl analogues yielding [Mo(NPh)$_2$(mtc)$_2$] (17) and [Mo(N^{t}Bu)$_2$(mtc)$_2$] (18). Carbon analysis was poor for both. Of note is the dark-red colour of 18, being quite different to orange 2. Their poor solublity in common organic solvents hindered extraction and purification, resulting in reduced reaction yields. For the *tert*-butyl complex 18, a singlet at 1.58 ppm was observed for the *tert*-butyl methyl protons in the ^{1}H nmr spectrum, while the methyl protons of the ancillary ligand shift downfield (as expected) to 2.61 ppm. The phenylimido complex 17 shows the expected resonances for the aryl protons (two triplets and a doublet) and, again, the methyl protons of the dithiocarbamate ligand shift downfield to 2.48 ppm. Their insolubility in common solvents have provided an unsurmountable barrier to crystal formation, though analysis by ^{13}C solid state nmr spectroscopy has been possible.

Consider first, complex 18. In the solid-state, two peaks are seen for the α-carbons (69.9, 72.8 ppm), two for the β-carbons of the methyls (31.8, 32.4 ppm), two for the carbons from the backbone of the dithiocarbamate ligand (204.1, 204.9 ppm) and a multiplet of peaks in the range 41.9 to 44.0 ppm for the methyls of the co-ligand. The difference in ppm (Δδ) for the α-carbons is 2.9 ppm, considerably larger than in 2. Using the graph (from Chapter 2), this corresponds to an imido angle difference of 17.8° against the 10.3° observed for 2. Why should there be a greater degree of bending on a small change in the ancillary ligand? It could be argued that although the bent-linear structure is not particularly favoured in energetic terms, the reduced steric presence of the co-ligand provides less hindrance to the 'flipping' motion of the two imido ligands. This apparent increase in bending of one of the imido ligands is intriguing especially when the solid-state ^{13}C nmr spectrum of 17 is analysed.

Remembering then that the two *ipso*-carbon peaks of 1 were 5 ppm apart, the spectrum for 17 only had one *ipso*-carbon peak - i.e the complex must have a linear-linear structure. Thus, a small change in the co-ligand has completely changed the structure of the complex Attempts to grow single crystals of 17 were continually unsuccessful but impetus was given to the synthesis of other bis(phenylimido) complexes.

^{13}C Solid State Nmr Spectrum of [Mo(NPh)$_2$(mtc)$_2$] (17)

Consequently, the analogous <u>diphenyldithiophosphinate</u> complex was synthesised - namely, [Mo(NPh)$_2$(S$_2$PPh$_2$)$_2$] (20). The dark-red solid was isolated from the reaction mixture of [Mo(NPh)$_2$Cl$_2$(DME)] and Na[S$_2$PPh$_2$] and purified by recrystallization of the ethereal solution at -30°C. The purity was confirmed by elemental analysis which was within reasonable error for all elements. As may be expected there is considerable phosphorus-proton coupling evident in the ^{1}H nmr spectrum and, to a lesser extent, in the ^{13}C{^{1}H} nmr spectrum. However, the ^{31}P{^{1}H} nmr spectrum shows a single resonance for the co-ligands at 64.5 ppm; the single phosphorus environment being indicative of either the fluxionality or linearity of the phenylimido ligands.

The complexity in the the ^{1}H nmr spectrum relates more to the thiophosphinate ligands than to the phenylimido ligands, although the *ortho*-protons of the latter are presumed to be hidden under the nmr solvent peak. The *meta*- and *para*-protons of the imido ligands are represented by triplets at 6.84 and 6.66 ppm, respectively. For the thiophosphinate ligand, the multiplet for the *ortho*-protons are shifted downfield and fall in the region 7.98 to 8.06 ppm; this multiplet may be described as a doublet of doublets of doublets. The rest of the co-ligand's protons give rise to a broad triplet at 6.92 ppm - still downfield of their correspondent protons of the imido ligand. In the ^{13}C{^{1}H} nmr spectrum, there is a single resonance for the *ipso*-carbon and coupling is

evident for the thiophosphinate carbons. The resonances for the other imido carbons are found at 126.7 and 123.4 ppm.

In the ^{13}C CPMAS solid state spectrum of **20**, two peaks are observed for the *ipso*-carbons at 156.7 and 155.1 ppm ($\Delta\delta$ = 1.6 ppm). The peaks at 139.0 and 132.3 ppm are attibutable to the co-ligand, while the other imido carbons are further upfield at 128.1 and 124.5 ppm. The difference in imido environments is supplemented by the different phosphorus environments experienced in the solid-state of the co-ligands. Thus, the ^{31}P solid-state nmr spectrum shows two distinct peaks at 66.6 and 65.5 ppm.

Until further crystal structures of the bis(phenylimido) complexes are determined, it is impossible to take the difference in chemical shifts for these other complexes and authoritatively calculate an imido angle difference, based on the graph/relationship demonstrated in the previous chapter. However, it should be possible to infer from this small chemical shift difference of 1.6 ppm that this complex does not adopt a bent-linear structure.

The third co-ligand used is the <u>xanthate</u>. Sodium ethylxanthate is yellow, has a foul smell and is mildly hygroscopic. Water is removed under reduced pressure but the salt is not heated, to avoid decompositon. The same synthetic procedure was followed to form [Mo(N^{t}Bu)$_2$(S$_2$COEt)$_2$] **(19)** though it proved difficult to obtain an analytically pure sample of the phenylimido xanthate complex. With **19**, extraction and purification in a suitable solvent was not easy. The complex dissolved in both ether and petrol so all solvent was removed under reduced pressure. The complex was, eventually, recrystallized from pentane.

Proton nmr experiments, performed in either CDCl$_3$ or C$_6$D$_6$, give very simple spectra. Interestingly, the chloroform solution is orange, whilst the benzene solution is dark-red. A considerable solvent effect is observed for the xanthate ligands. The *tert*-butylimido methyl protons are observed by a single resonance at 1.38 ppm in C$_6$D$_6$ and at 1.40 ppm in CDCl$_3$. However, the xanthate methylene and methyl protons are shifted by 0.45 and 0.63 ppm, respectively, on the solvent changing from C$_6$D$_6$ to CDCl$_3$.

A proton-coupled ^{13}C nmr spectrum was needed to distinguish between the α-carbon of the *tert*-butylimido ligand and the (OCH$_2$) carbon of the co-ligand. This allows assignment of the single resonance at 71.9 ppm to the imido ligand and the resonances centred on 69.1 ppm to the (OCH$_2$) carbon. Other resonances are observed downfield at 226.4 ppm (for the carbon in the xanthate backbone) and upfield at 30.9 ppm for the imido β-carbons and 13.5 ppm for the xanthate methyl carbons. The solid-state FLIP nmr spectrum shows a single resonance for the α-carbon, though another peak is close to it, that of the (OCH$_2$) carbon. This is confirmed in the NQSTOSS spectrum which again shows a single resonance for the α-carbon.

3.3   Other metals

Several <u>tungsten</u> bis(imido) complexes have previously been synthesised. Acting as the gateway to this chemistry is the complex $[W(NAr)_2Cl_2(DME)]$ which is, in turn, made from either tungsten dioxodichloride, tungsten oxotetrachloride or $[W(NAr)Cl_4].thf^{28}$. However, atttempts to prepare this DME intermediate during this work proved unsuccessful; no excuse is offered nor has any obvious fault in the procedure been unearthed. Frustrated by failure with tungsten, efforts were made to synthesise the <u>chromium</u> analogue.

Gibson and co-workers had already tried and failed to make the chromium DME complex but they had successfully synthesised $[Cr(N^tBu)_2Cl_2]$ *en route* to the development of new alkene polymerisation catalysts[119]. Following their synthetic route, the initial chromium bis(imido) complex $[Cr(N^tBu)_2(OSiMe_3)_2]$ was made upon reaction of of chromyl chloride with the silylamine, as originally performed by Nugent and Harlow[52]. This was then converted to the dichloride $[Cr(N^tBu)_2Cl_2]$ after reaction with boron trichloride. Reacting this four-coordinate complex with sodium diethyldithiocarbamate yielded a dark red product, characterized as $[Cr(N^tBu)_2(etc)_2]$ **(21)**. The methyldithiocarbamate complex $[Cr(N^tBu)_2(mtc)_2]$ **(22)** was synthesised in a similar manner.
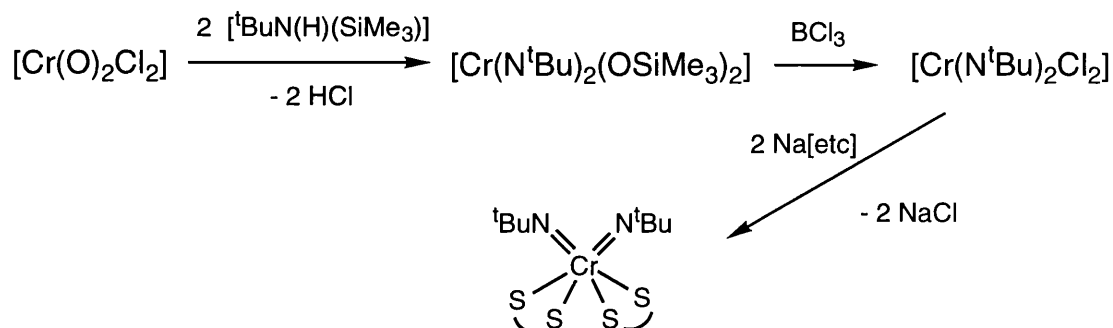
Considering **22** first, the ^1H nmr spectrum is very simple showing two singlets , one for the methyls of the *tert*-butylimido at 1.57 ppm and the other for the co-ligand at 2.57 ppm. The elemental analyses obtained were unsatisfactory for a bis(imido) complex, but consistent with an oxo-imido product. This may be the product of hydrolysis during recrystallization. The $^{13}C\{^1H\}$ spectrum shows a singlet at 77.8 ppm for the α-carbon. In the solid-state, two peaks at 78.6 and 76.8 ppm show different environments for the two imido ligands. The chemical shift difference of 1.8 ppm, if related to the graph in Chapter 2, corresponds to a difference in imido angles of 10.6°. Different environments are also observed in the ancillary ligands and in the methyl groups of the *tert*-butylimido ligands.

The ^{1}H nmr spectrum of **21** is also simple, consisting of the normal singlet (at 1.56 ppm) for the *tert*-butylimido protons and the quartet and triplet for the co-ligand's protons. The EI mass spectrum shows the molecular ion at 490 with an excellent fragmentation pattern; five further peaks testify to the fragmentation of imido and dithiocarbamate groups. A strong stretch at 1264 cm^{-1} in the ir spectrum and several stretches in the 1420-1500 cm^{-1} region further indicate the presence of imido and dithiocarbamate groups. The ^{13}C{^{1}H} spectrum shows the imido α- and β-carbons clearly at 77.7 and 30.4 ppm, respectively. The carbon from the co-ligand's backbone is in its usual region at 203.2 ppm. In the FLIP spectrum, there are some resonances at 75.6 and 72.8 ppm, though these disappear in the NQSTOSS spectrum. Given the resonance at 77.7 ppm in the solution spectrum, caution forbids definite assignment of these peaks to the α-carbon, even if citing the change in metal centre as a reason for its shift downfield, . The methyl carbons of the *tert*-butylimido ligand are evident at 31.3 ppm indicating that the sample had not decomposed.

Attempts to grow single crystals proved unsuccessful. However, given that the crystal structure of its molybdenum analogue, **2**, has been determined, it is possible to determine if the structure of the two are the same by using powder X-ray diffraction. A simple introduction to this technique is offered in Appendix II. As with crystallography, the diffraction pattern depends on the unit cell. However, in simple terms, if the two complexes have the same structure, then the majority of peaks in the powder spectra should be the same. The experiments were performed and the spectra are shown overleaf. By simple comparison of the two, it appears that they do not have the same structure.

The first arylimido complexes were synthesised quite recently upon reaction of [Cr(N^{t}Bu)$_2$Cl$_2$] with 2,6-Me$_2$C$_6$H$_3$NCO[120]. Several attempts have been made to form the phenylimido analogues by an imido exchange reaction using amines. An intractable mixture forms on reaction of aniline with **21**. A highly insoluble, black solid forms on reaction of aniline with [Cr(N^{t}Bu)$_2$Cl$_2$]. No useful analysis of this solid has been secured though.

In summary, several new bis(imido) complexes have been synthesised using different co-ligands and a different metal centre. No crystal structures have been determined though analysis by ^{13}C solid state nmr spectroscopy has revealed that a change in co-ligand can dramatically alter the structure of a bis(imido) complex. This is suggested for [Mo(NPh)$_2$(mtc)$_2$] **21** which adopts a linear-linear conformation unlike the bent-linear conformation of the similar complex, [Mo(NPh)$_2$(etc)$_2$] **1**.
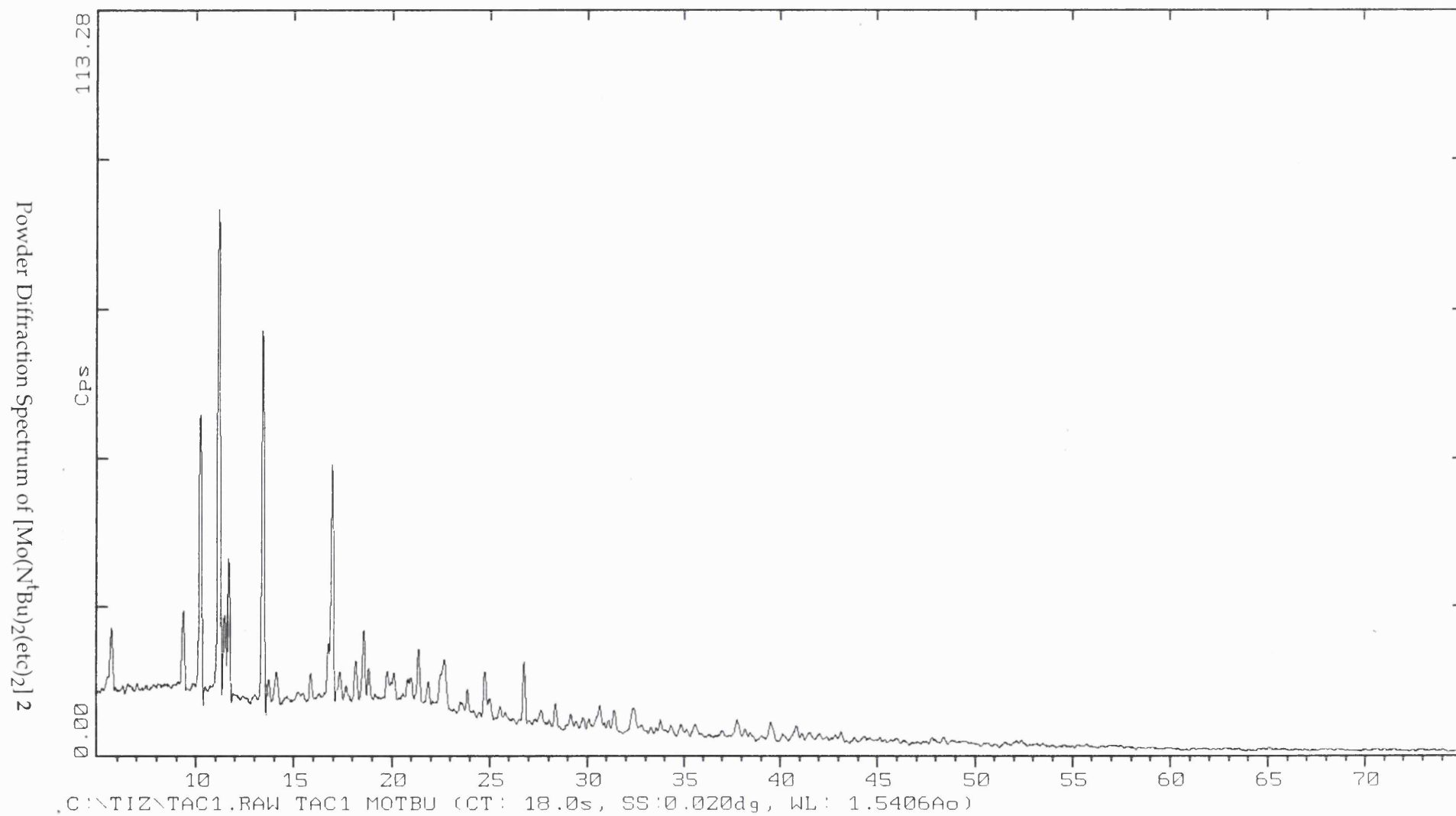
113.28

Cps

0.00

10   15   20   25   30   35   40   45   50   55   60   65   70

C:\TIZ\TAC1.RAW TAC1 MOTBU (CT: 18.0s, SS:0.020dg, WL: 1.5406Ao)

Other Ligands and Metals
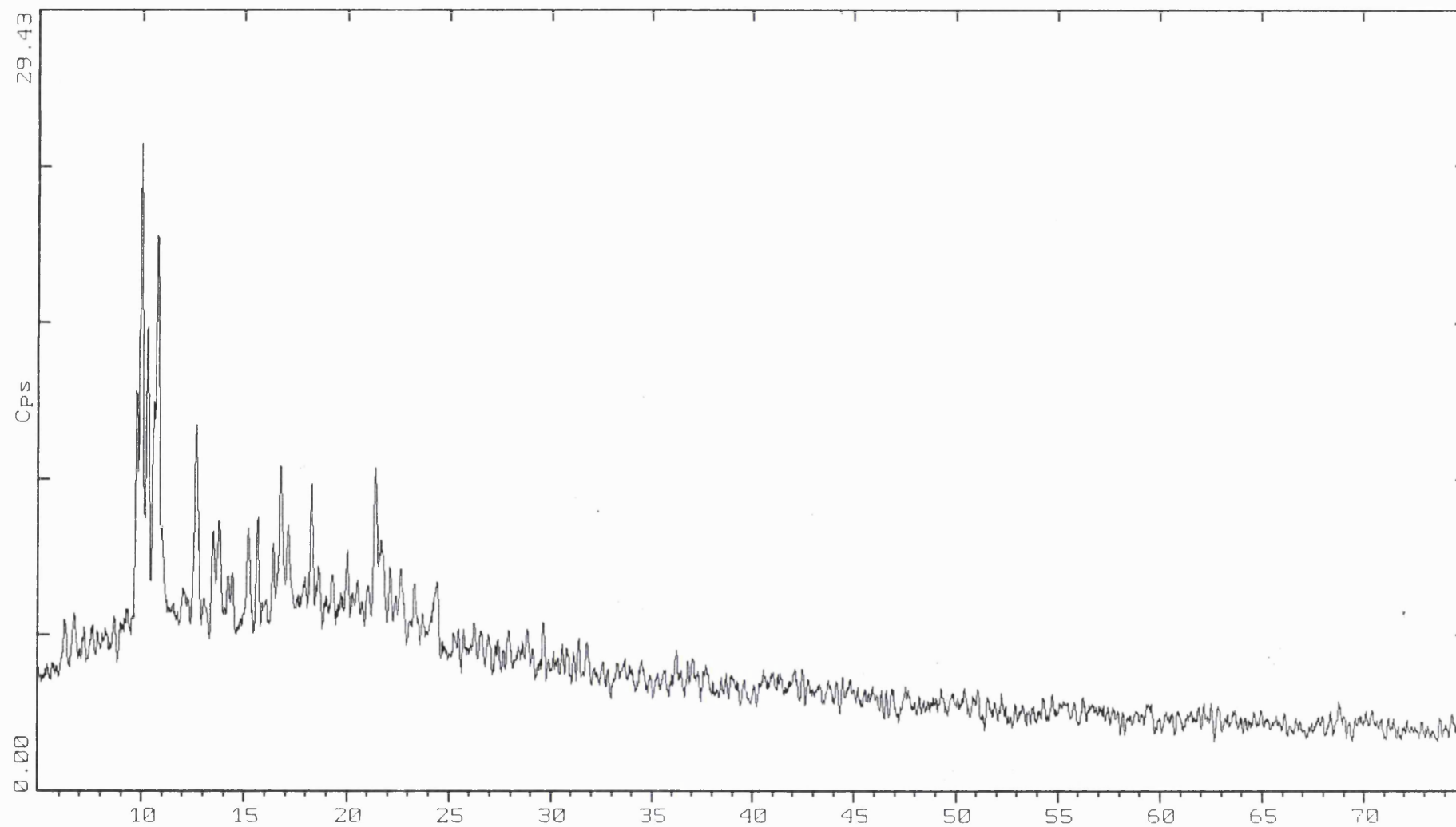
Powder Diffraction Spectrum of [Mo(N^{t}Bu)$_2$(etc)$_2$] 2

Powder Diffraction Spectrum of $[Cr(N^tBu)_2(etc)_2]$ 21

Chapter 4   Reactivity of Bis(imido) Complexes

4.1   Introduction

Various reactions previously performed to discover the range of reactivity of the imido ligand were introduced in Chapter 1. The substantive of this chapter will focus exclusively on the reactivity of the mononuclear bis(imido) complexes, $[Mo(NR)_2(etc)_2]$. Several substituents have been used but it is mainly the phenyl and *tert*-butyl complexes **1** and **2**, respectively, that have been subject to investigation. Some reactivity studies have already been performed previously in this group[64] and used for comparison with studies conducted by Haymore and Maatta[121]. In contrast to the inertness of the majority of monoimido complexes, bis(imido) complexes show greater reactivity. This is due to the ease of displacement of one imido ligand, leaving the other to become a stronger π-donor and stabilize the complex - known as the spectator effect.

The reactivity of bis(imido) complexes was brought to the fore by the discovery of ROMP (Ring Opening Metathesis Polymerisation) catalysis as they are synthetic precursors to active imido-alkylidene catalysts. First observed by Grubbs and co-workers, the use of imido catalysts was developed by Schrock[28,89] and Gibson[119], using complexes of the type, $[M(NR)(CR')(OR'')_2]$ (M is a Group VI metal).
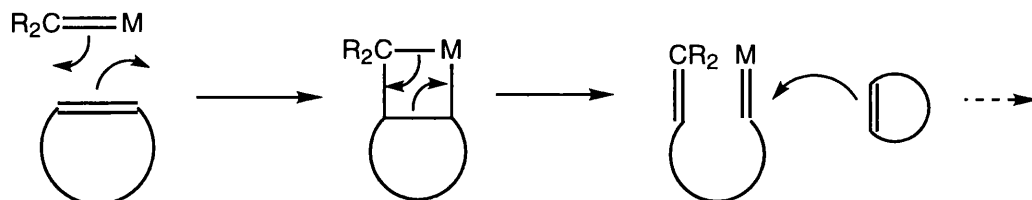
The simplified mechanism above shows alkene metathesis by the alkylidene ligand of the catalyst, driven by the release of ring strain in the organic substrate, starting the formation of a chain; the metal-alkylidene is attacked by another substrate molecule and so the process continues. There are several advantages to ROMP catalysis. The catalyst is "living", continuing to work until all substrate is consumed and thus, polymer chain lengths can be easily controlled. Further, a number of substituents and functionalities on the substrate can be tolerated; different substituents on the catalyst may be used to control various properties of the polymeric product, such as molecular weight, tacticity and strength and flexibility. The activity of these catalysts has been shown to be heavily dependent on the identity of the alkoxide substituent. In contrast, not as much work has been given to role of the imido substituent in these complexes. Generally, bulky aromatic substituents are used for

stability and ease of synthesis, although subsequent syntheses have used both *tert*-butyl[119] and adamantyl[122] ligands.

In studying the catalytic activity of binuclear ruthenium alkylidene catalysts, Grubbs and co-workers observed that although the alkylidene group was singly involved in the metathesis reaction, the presence of an imido ligand enhanced the catalytic performance. They further observed the spectator effect; as the alkylidene is "lost", the π-interaction with the imido ligand is increased and is then lost with alkylidene re-formation. Using a bulky substituent on the imido ligand, they were able to control the stereochemistry and reduce the chance of dimerization[123].

Bis(imido) complexes have not been used in many other organic syntheses but one of note is their use as Lewis acid catalysts for the regioselective ring-opening of epoxides[124]. High-valent imido metal complexes are predicted to be good Lewis acid catalysts, due to their low-lying vacant d-orbitals, helped by their good solubility in a range of organic solvents and their high tolerance of functional groups. The ring-opening of epoxides by trimethylsilyl azide (or an amine) was promoted by using $[Cr(N^{t}Bu)_2Cl_2]$[125], $[Mo(N^{t}Bu)_2Cl_2]$[100], $[W(N^{t}Bu)_2(NH^{t}Bu)_2]$[126] and the monoimido complex, $[Cr(N^{t}Bu)Cl_3(DME)]$[127].

Nu = nucleophile (azide/amine)
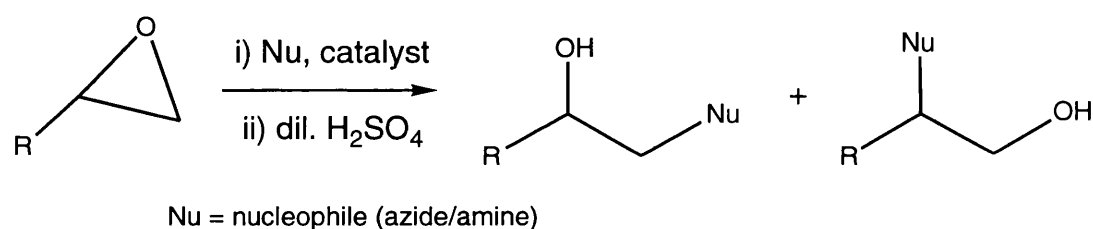
The catalytic activity increases in the order, W $\ll$ Mo $\leq$ Cr - correspondent with the increasing electrophilicity of the metal centre. Bis(imido) catalysts are slower but more selective than the monoimido complexes in producing the 2-azido alcohol.

Bent imido ligands are presumed to show greater reactivity than linear ligands. This increase in reactivity and nucleophilicity may be explained as a combination of several factors: the localization of charge on the imido nitrogen due to the formal presence of a lone electron pair; the greater steric accessibility of the imido nitrogen and the reduction in bond order between molybdenum and nitrogen, allowing easier cleavage.

Maatta and Wentworth studied the reactivity of their infamous linear-bent bis(imido) complex, $[Mo(NPh)_2(etc)_2]$, towards protonation and alkylation[76]. Upon reaction with hydrogen chloride, the imido-dichloride $[Mo(NPh)Cl_2(etc)_2]$ formed, while with tetrafluoroboric acid, the expected $[Mo(NPh)(etc)_3]^{+}$ did not form. However, alkylation with methyl bromide proved successful in removing a single imido ligand to yield phenyltrimethylammonium bromide and the imido-dibromide complex, $[Mo(NPh)Br_2(etc)_2]$. It is proposed that the nucleophilic imido nitrogen (of the bent

ligand) attacks the carbon atom of MeBr to be followed by Mo-Br bond formation; further attack on the alkylating agent leads to formation of another Mo-Br bond and of the salt.

Earlier in this laboratory, the reactivity of the linear-linear bis(imido) complex **7** was briefly investigated[64]. Reaction was unsuccessful with both the unsaturated organic molecule, DMAD, and with methyliodide. The lack of the bent (and more reactive) imido ligand or the steric bulk of the substituents on the aryl ring (hindering attack at the imido nitrogen) may both be responsible for the failures.

4.2   Thermolysis of bis(imido) complexes

The thermal stability of three of these complexes, namely, **3**, **8** and **13** (chosen for their varying steric and electronic factors) was investigated by refluxing for a prolonged period in toluene, with careful exclusion of air. Each was found (by nmr spectroscopy) to be unchanged after thermolysis. This was also found for **1**, being stable in d^8-toluene at reflux for three days. This, then, shows that these complexes are themselves stable and that any reactivity is due only to interaction with the whole complex and not any fragmented parts.

1, 3, 8, 13
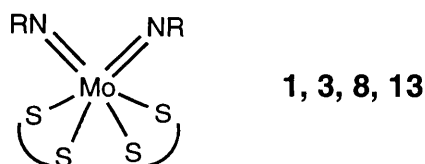
4.3   With air/moisture

Transition-metal imido species are known to be susceptible to hydrolysis, with the exception of Group VIII metals. Osmium bis(imido) complexes form upon reaction of an amine with osmium tetroxide in aqueous solution. This behaviour is exceptional though as the majority of complexes are attacked by nucleophilic water to form the metal oxide and the amine.

$$M = NR \longrightarrow M = O \quad + \quad RNH_2$$
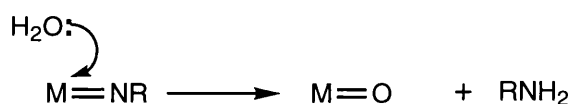
Reaction of [Mo(N(4-Me)C$_6$H$_4$)$_2$(etc)$_2$] with moisture

While preparing **5** from [Mo(N(4-Me)C$_6$H$_4$)$_2$Cl$_2$.DME] and NH$_4$[etc] (as described in Chapter 2), a yellow by-product formed, presumed to be decomposition on exposure to moisture. This was isolated but characterization proved difficult as it was a mixture. A yellow product was separated out and identified as the oxo-imido

species, $[Mo(O)(N(4-Me)C_6H_4)(etc)_2]$ (23). Its ^1H nmr spectrum clearly shows a 1:2 imido-dithiocarbamate ratio, while its ir spectrum shows a strong peak at 910 cm^{-1} and another peak at 1243 cm^{-1}, respectively indicative of molybdenum-oxo and molybdenum-imido moieties. Accurate elemental microanalyses confirmed the identity of 23.

Recrystallisation of the remaining mixture upon slow diffusion of methanol into a dichloromethane solution afforded an orange crystalline complex. The ir spectrum showed a peak at 1260 cm^{-1} suggesting an imido ligand; furthermore, the mass spectrum showed a complex of (m/z) 586 with a fragmentation pattern appropriate for the loss of a single sulfur and another atom. The ^1H nmr spectrum showed three dithiocarbamate ligands but no aromatic protons and, therefore, no imido ligands. Finally, a crystal was selected and, by X-ray crystallography, the complex was identified as $[Mo(NS)(etc)_3]$ (24), whose structure is shown overleaf.

24
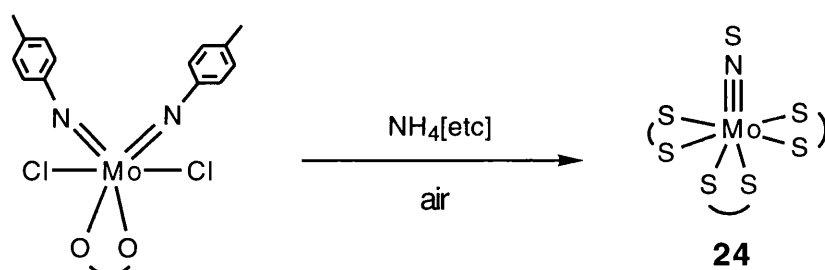
A rationale for the formation of 24 in this manner has not been reached but it is clear that scavenging of dithiocarbamates, accompanied by partial break-up of dithiocarbamate ligands, from other molecules has occurred. This compound had been previously prepared in 1979 by Bishop, Chatt and Dilworth[128] via thermolysis of bis(oxo) complex, $[Mo(O)_2(\eta^2-S_2CNEt_2)_2]$ with trimethylsilyl azide. This and other thionitrosyl complexes have also been synthesized by reacting sulfur sources (like elemental sulfur, isothiocyanates, sulfur dichloride, etc.) with analogous nitrido complexes. The peak in the ir spectrum at 1260 cm^{-1}, originally suggesting an imido ligand, is actually typical for the thionitrosyl ligand. Absorptions due to these ligands can be in the rather wide range of 1065 to 1390 cm^{-1}, and there is no correlation between the stretching frequency and the M-N-S angle[129].

There are many examples now of the thionitrosyl ligand but less than ten of those have been characterized crystallographically. The first crystal structure of one of these compounds, $[Mo(NS)(mtc)_3]$, was determined by Hursthouse and Motevalli [130] and can be compared to our own complex.
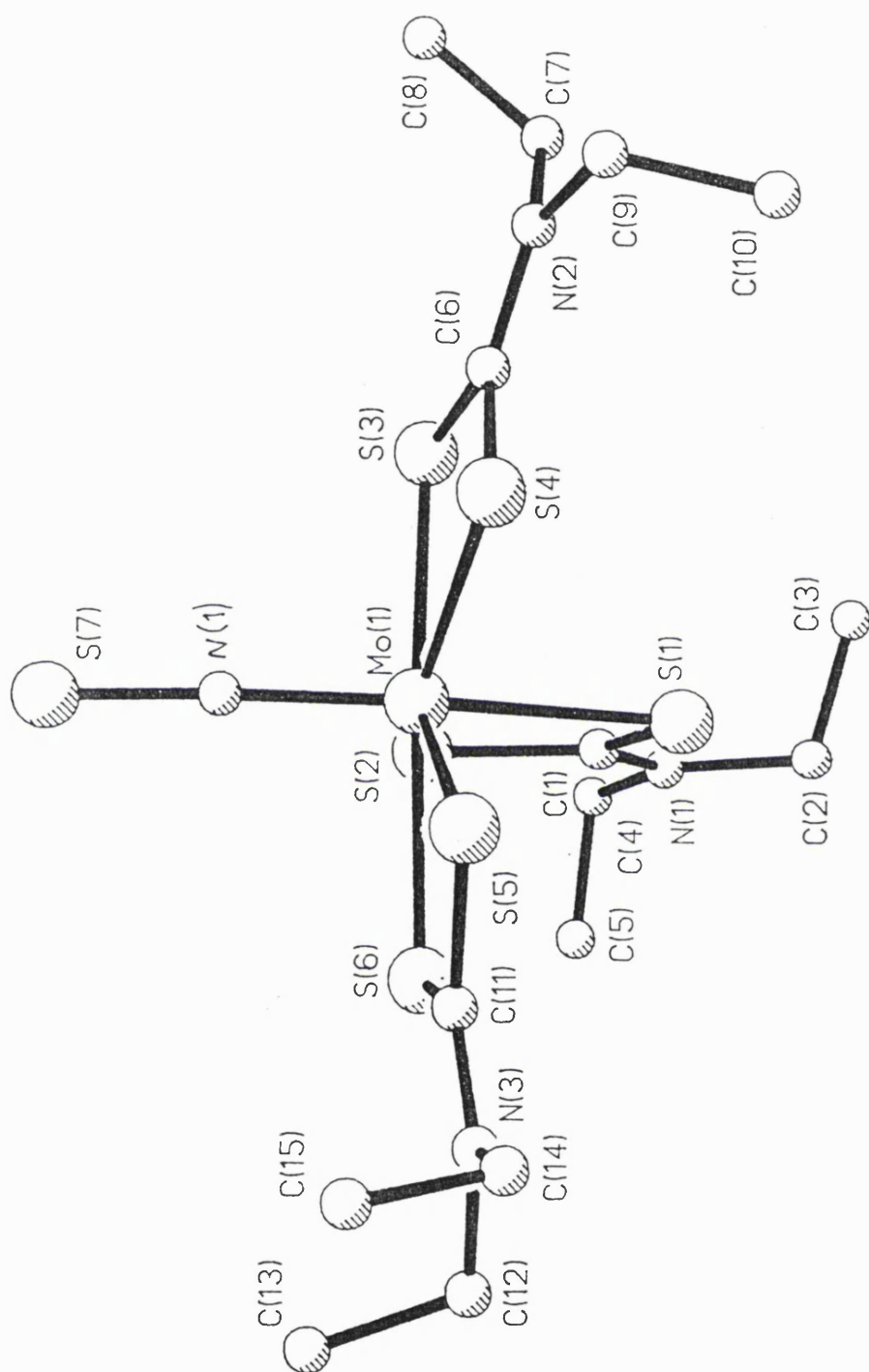
Structure of [Mo(NS)(etc)₃] **24**

The structure of **24** is best described as a distorted pentagonal bipyramid. The thionitrosyl ligand is essentially linear [Mo(1)-N(4)-S(7) 174.8(2)°]; the Mo-N distance is 1.765(4)Å and the N-S distance is 1.568(4)Å - characteristically short for the thionitrosyl ligand. The thionitrosyl ligand fills one axial site while the second is occupied by a sulfur atom, S(1), from the dithiocarbamate ligand *trans* to the thionitrosyl ligand. This Mo-S distance is significantly longer than those in the equatorial sites, due to the *trans* influence of the multiply-bonded thionitrosyl ligand.

This effect has been seen before for [Mo(NS)(mtc)3] and for [Mo^{VI}(N)(etc)3]. Defining Δ= (Mo-S$_{ax}$) - (Mo-S$_{eq}$(average)), for [Mo(NS)(etc)3] Δ= 0.098Å, [Mo(NS)(mtc)3] Δ= 0.087Å and for the analogous nitrido complex [Mo(N)(etc)3], Δ=0.329Å.

The site of this sulfur atom, S(1), is also where the greatest distortion from the bipyramidal structure is seen - [N(4)-Mo(1)-S(1) 164.62(11)°]. It is due to the bite-angle constraint of the dithiocarbamate ligand, when its sulfur atoms are occupying both the axial and equatorial sites. Note finally, that there is disorder in this structure at the C(8) atom. There is a (0.65/0.35) occupancy ratio for C(8)/C(8A) - only C(8) is shown in the structure.

Reaction of [Mo(NR)₂(etc)₂] with moisture to form [Mo(O)(NR)(etc)₂]

As noted earlier, many of the bis(imido) complexes were unstable in solution and decomposition by hydrolysis often resulted to form a yellow solid, isolable from the solution of the bis(imido) complex. The two complexes formally characterized were [Mo(O)(N(4-Me)C$_6$H$_4$)(etc)$_2$] **(23)** and [Mo(O)(N(2,6-F$_2$C$_6$H$_3$))(etc)$_2$] **(25)**. The characterization of **23** was discussed above. The ir spectrum of **25** showed peaks at 886 and 1262 cm^{-1}, again respectively indicative of molybdenum-oxo and molybdenum-imido moieties. The ^{1}H nmr spectrum showed a 1:2 ratio of imido to dithiocarbamate ligands and elemental microanalyses confirmed the identity of the oxo-imido complexes.

23, 25
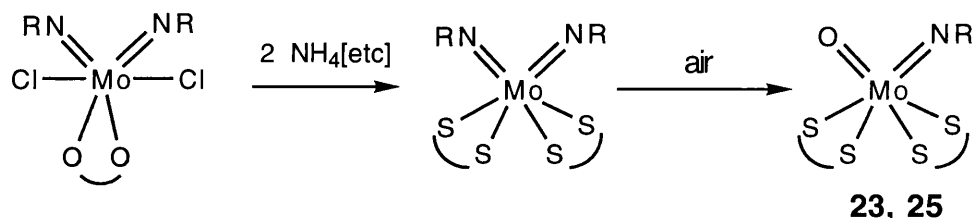
Similar oxo-imido complexes have been previously synthesized. Maatta and co-workers developed two routes - oxidation of [Mo(O)(etc)$_2$] with tolylazide and oxidation of [Mo(N(4-Me)C$_6$H$_4$)(etc)$_2$] by dimethylsulfoxide or oxygen[76,121]. Some recent examples, like [Mo(O)(N(2,4,6-Ph$_3$C$_6$H$_3$)Cl$_2$(DME)][111] referred to earlier in Chapter 2, are of particular interest as they are synthesised following an almost identical methodology to that of our bis(imido) DME complexes. As **23** and **25** had

formed from the solutions of bis(imido) complexes, it is proposed that the hydrolysis occurred after addition of dithiocarbamate salt to the DME complex. As already alluded to in Chapter 2, all the molybdenum bis(imido) DME precursors are highly susceptible to hydrolysis and can only be handled in inert atmosphere. If hydrolysis occurred before dithiocarbamate addition, it is highly improbable that a complex with an imido ligand could be produced. Far more likely is that simple hydrolysis of only one imido ligand of **5** and **12** occurred to give the air-stable **23** and **25**. Further decomposition to the bis-oxo species did not occur.

4.4   With Acids

Imido complexes often undergo facile hydrolysis reactions with acids. However, they may react with different acids in different ways, according to the nucleophilicity of its conjugate base. Thus, [Os(N^{t}Bu)O$_3$] is stable in dilute nitric acid but is hydrolysed by dilute sulfuric acid. The complex [Re(NPh)(PMe$_3$)$_2$Me$_3$] also reacts differently with different acids, as shown below[131];
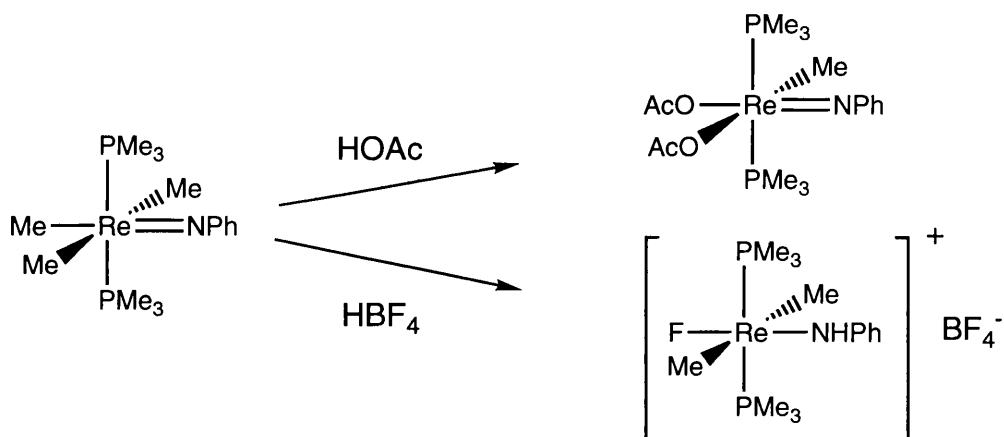
Previous studies with acids have been performed by Maatta and Wentworth[76]. They reacted [Mo(NPh)$_2$(etc)$_2$] **(1)** with hydrogen chloride and tetrafluoroboric acid. With (gaseous) hydrogen chloride, the benzene solution changed colour from red-brown to bright yellow and a flocculent, white precipitate was formed and identified as aniline hydrochloride. The yellow solution was isolated and identified as the imido dichloride complex with a molecule of chloroform, [Mo(NPh)Cl$_2$(etc)$_2$].CHCl$_3$. A similar result occurs with the bis(oxo) complex affording the oxo-dichloride species.
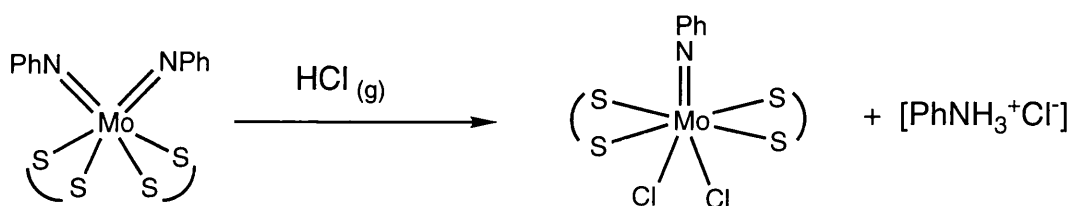
This was assumed to occur by the pathway shown below. Protonation at one of the imido groups leads to an imido-amido cation which immediately has the nucleophilic chloride ion enter its coordination sphere. At this stage, the amido ligand should only donate one electron, while the remaining phenylimido ligand donates four electrons. There is then a lone pair of electrons located on the amido nitrogen, allowing hydrogen chloride to attack once more and the imido dichloride complex forms.
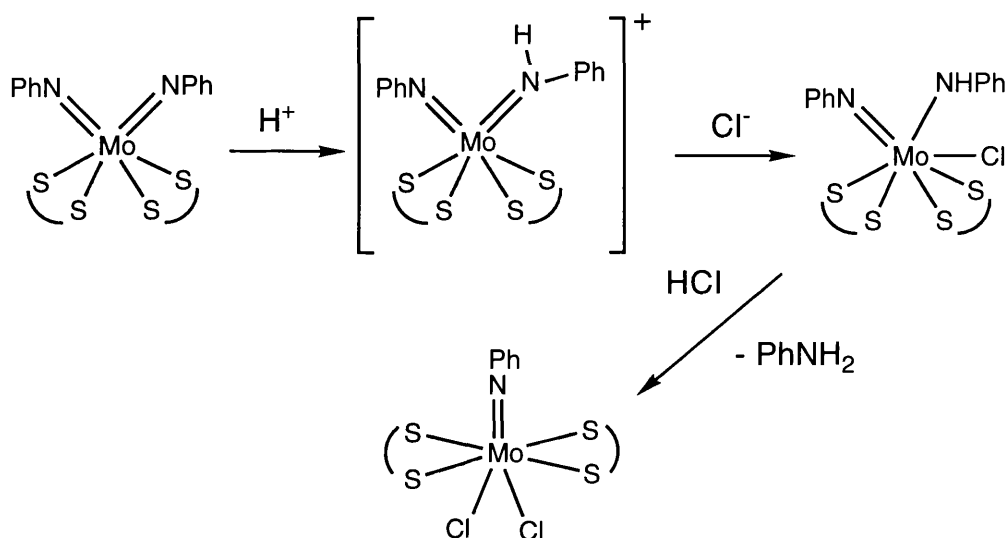
A different reaction was seen (by Maatta) with the two other acids, HPF_6 and HBF_4, where the conjugate bases are less nucleophilic. A cationic species is obtained with both acids but on reaction with the tetrafluoroboric acid, the cation $[Mo(NPh)(etc)_3]^+$ could not be isolated. However, this cation was isolated upon reaction of the imido dichloride complex with hexaflurorophosphoric acid. The structure is assumed to resemble its oxo analogue, as determined by Young and co-workers[132].
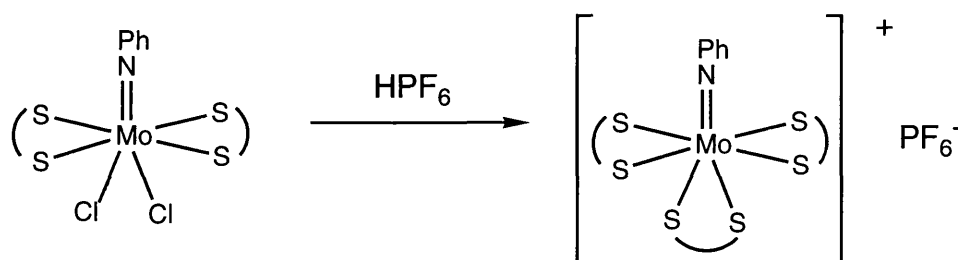
Reaction with HBF₄.Et₂O

Upon reaction of tetrafluoroboric acid with a dichloromethane solution of 7, the solution turned yellow. In the ^1H nmr spectrum, a broad peak at 7.91 ppm is observed suggesting the formation of an amido complex. Whether the complex is mono(amido) or bis(amido) is unclear. The integral of the peak indicates the presence

of two amido protons. Furthermore, there is a 1:1 ratio of dithiocarbamate and amido ligands which suggests the formation of $[Mo(NHAr)_2(etc)_2]^{2+}$ (26).
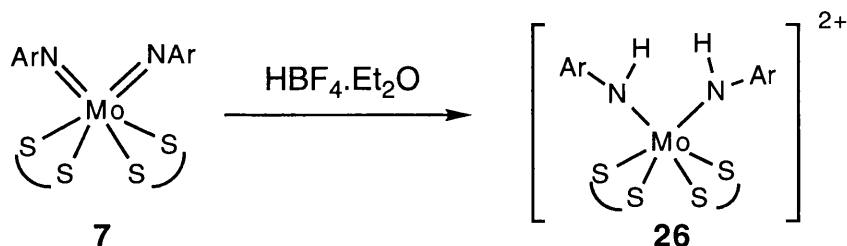
However, there is another possibility where a monoamido complex is formed, $[Mo(NAr)(NHAr)(etc)_2]^+$ (28). The broadness of the peak could be due to proton transfer between the imido and amido ligands. Indeeed, excess acid could be the cause of the signal at 7.91 ppm.
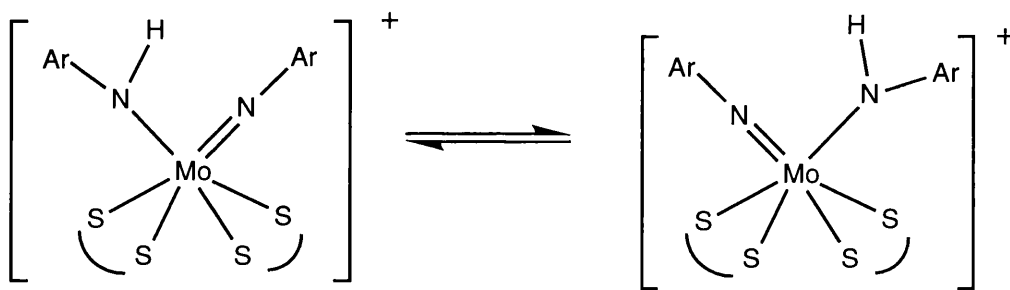
Maatta and Wentworth were not able to isolate an amido species, suggesting that even with an acid with a poorly nucleophilic conjugate base (such as HBF_4), the imido-amido species is highly unstable. Hence, in the absence of a good nucleophile (like Cl⁻), it will attack and scavenge the dithiocarbamate ligand of a neighbouring complex to form the tris(dithiocarbamato) cation. In the case of 26 or 28, the added stability of the complex may be attributable to the bulky imido substituent.

A molybdenum bis(imido)-bis(amido) complex has been prepared previously by Osborne, albeit not by protonation of imido moieties. The complex $[Mo(NAr)_2Cl_2]$.thf was formed upon reaction of aryl isocyanate with $[MoO_2Cl_2]$ in tetrahydrofuran solvent. This was then reacted with a lithium amide to yield $[Mo(NAr)_2(NHAr)_2]$, the arylamine and another molybdenum species[133].
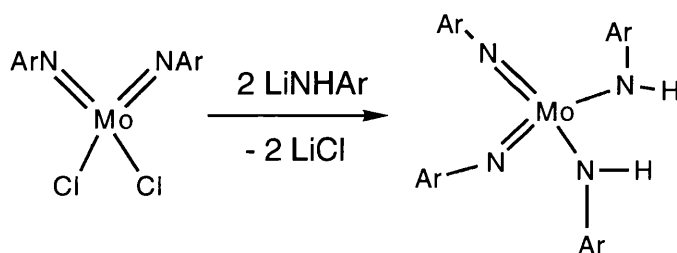
Its structure is tetrahedral about the molybdenum centre with the imido angles (Mo-N-C_{ipso}) at 172.3(3) and 155.7(3)°, and the two amido ligands bent at 134.3(2) and 123.4(2)° (Mo-N-C_{ipso}). In its ^{1}H nmr spectrum, the amido proton is shown by a singlet at 8.03 ppm; with the presence of peaks for the arylimido protons, this shows that the proton is fixed on one ligand, or at least, transfer is not occurring on a nmr timescale.

The amido complex was prepared for crystallization by layering a dichloromethane solution with methanol. After some considerable time, a mixture of yellow needles and orange crystalline solid grew from this solution. The orange solid was analyzed by ^{1}H nmr spectroscopy but could not be characterized and was certainly not **26**. The yellow needles were barely soluble in common solvents, but in the ir spectrum was a Mo=O band at 904 cm^{-1} as well as the expected imido bands (1280, 1263 cm^{-1}). A crystal suitable for X-ray crystallography was selected and the structure was identified as [Mo(N(2,6-^{i}Pr$_2$C$_6$H$_3$))(etc)$_2$(μ-MoO$_4$)]$_2$ (**27**), shown overleaf.

As can be clearly seen, the molecule consists of an eight-membered ring of alternating molybdenum and oxygen atoms. Half the structure is unique, being related to the other half by an inversion centre. The coordination geometry about each metal centre is very different despite the fact they both have (formally) an oxidation state of +6. The first molybdenum atom, Mo(1), has a distorted pentagonal bipyramidal geometry. The imido and one of the bridging oxo ligands take up axial positions, while another bridging oxo ligand and sulfur atoms of the two dithiocarbamate ligands are in equatorial positions. The imido ligand is linear [Mo(1)-N(3)-C(11) 174.2(8)°] and its bond length is typical at 1.740(8) Å. The strong *trans* influence of the imido ligand is seen in comparing the bond lengths of molybdenum to the bridging oxo ligands in their axial and equatorial positions. The axial oxygen, *trans* to the imido ligand, has a considerably longer bond length [Mo(1)-O(1) 2.103(7) Å] than the equatorial oxygen, *cis* to the imido with [Mo(1)-O(2) 1.997(6) Å].

The second molybdenum centre has essentially tetrahedral geometry with the molybdate groups spanning the imido- and dithiocarbamate-stabilized molybdenum centres. The bridging molybdenum-oxygen bond lengths are longer [Mo(2)-O(2) 1.814(6), Mo(2)-O(1A) 1.794(7) Å] and the terminal molybdenum-oxygen bond lengths are shorter [Mo(2)-O(3) 1.710(9), Mo(2)-O(4) 1.698(9) Å] than the average of 1.76 Å found in the free molybdate ion[134]. The core ring of this molecule is in a chair-type conformation. The bridging oxo ligands are not linear; the angles subtended at O(1) and O(2) are 151.1(4) and 150.4(4)°, respectively. The O-Mo-O bite-angles subtended at the molybdenum centres are 84.4(3) and 111.5(3)° (at Mo(1) and Mo(2)).
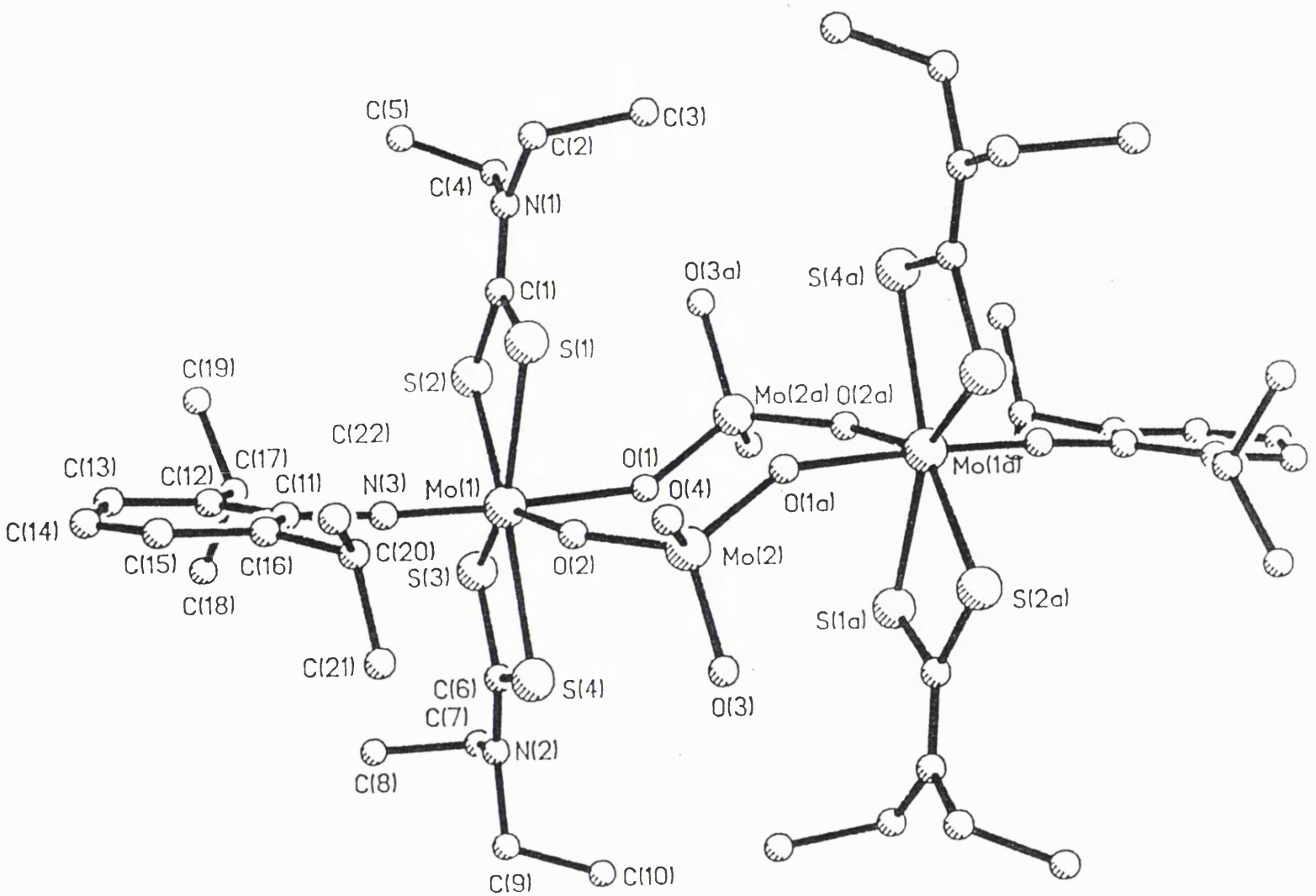
Structure of [Mo(N(2,6-^{i}Pr$_2$C$_6$H$_3$))(etc)$_2$(μ-MoO$_4$)]$_2$ (**27**)

This type of "cyclic" structure has rarely been seen. A similar eight-membered metal-oxo core is found in $[Cp^*_2Ti(\mu\text{-}MoO_4)]_2$, synthesized upon reaction of titanocene dichloride with sodium molybdate, as performed by Floriani and co-workers[135].
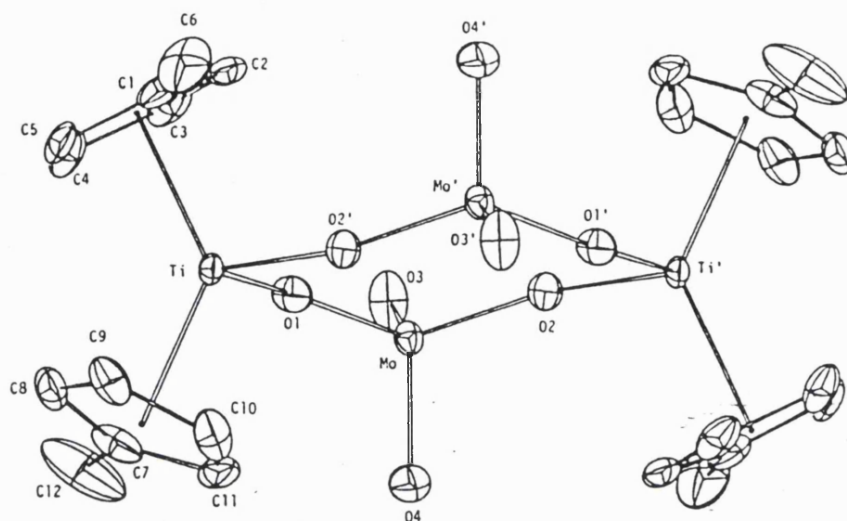
The $Ti_2Mo_2O_4$ ring is similar to that of **27** having bite-angles of 95.9(1) and 114.5(1)° at titanium and molybdenum respectively. However, there is a significant difference in the bond lengths of the metal-oxygen bonds to the non-molybdate centre; these vary by only 0.03Å in the titanium complex but by 0.106Å in **27**. Further, it is of note that the structure of ammonium molybdate consists of an infinite chain of eight-membered Mo_4O_4 rings with alternating tetrahedral and octahedral molybdenum (VI) metal centres; the rings are linked by further oxo ligands bridging the octahedral sites[136]. A Mo_4O_4 ring also forms the heart of the complex $[Mo_4O_{12}(C_{12}H_{30}N_4S_2)_2(C_3H_7ON)_n]$ (where $n \approx 2$)[137]. In the ring, molybdenum-oxo bond lengths alternate with values of 1.80 - 1.81(1) and 2.11 - 2.13(1) Å; the longer lengths are those *trans* to terminal oxo groups.

There appears to be only one previous example of a complex where two molybdenum-imido centres are bridged by a molybdate group. Controlled hydrolysis of $[Mo(CH_2{}^tBu)_2(=CH^tBu)(N^tBu)]$ to produce the molybdate-bridged $[\{Mo(CH_2{}^tBu)_3(N^tBu)\}_2(\mu\text{-}MoO_4)]$ *via* a series of dimeric intermediates was reported by Osborn and co-workers[138]. Here, the geometry of the molybdenum-imido centres is approximately trigonal bipyramidal with the imido and oxo ligands occupying the axial sites. For the molybdate centre, the terminal Mo-O bonds are shorter and the bridging bonds are longer than those of the free molybdate ion, just as in **27**. The stronger π-donor effect of the imido ligand is reflected by the increase in bond lengths to 2.017(3) and 2.031(3) Å for the molybdenum-oxo bonds *trans* to the imido groups. Further, the angles subtended at the bridging oxygen atoms are approximately 159°.
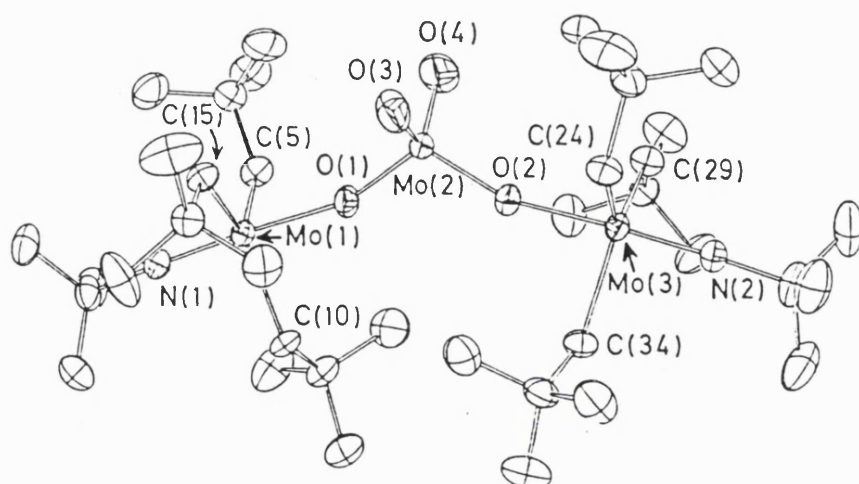
A final example of a molybdate group bridging two metal centres is seen in the structure of $[O_2Mo\{[\mu\text{-}O]Ti(^tBuNPh)_3\}_2]$[139].

How **27** is formed is unclear but a rationale is suggested below.
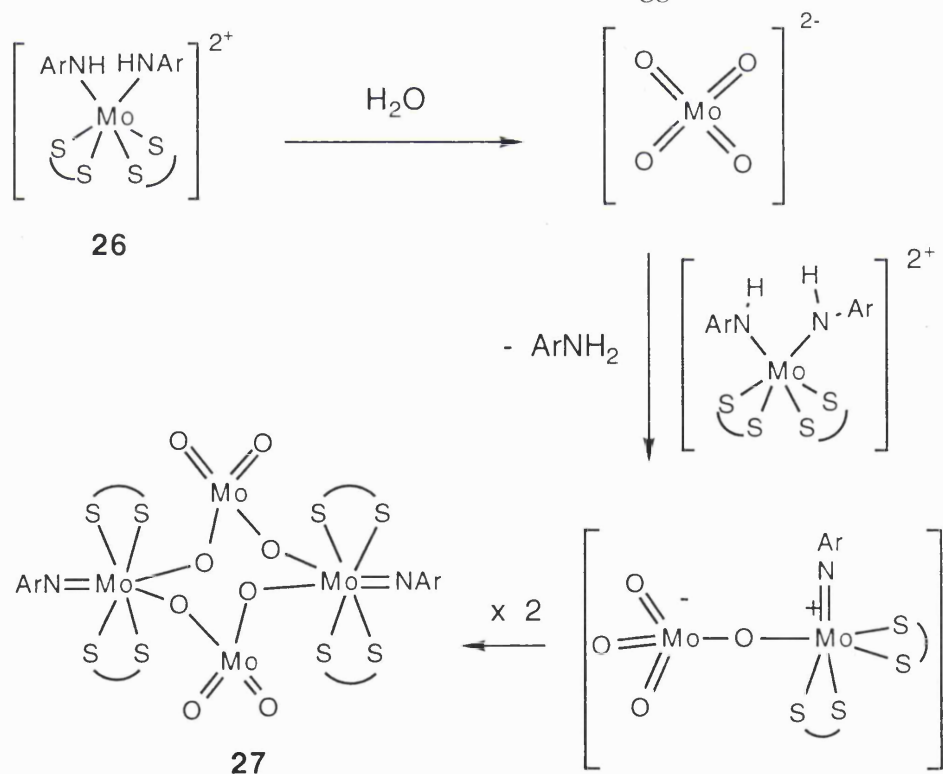
Molybdate is presumed to form in solution upon complete hydrolysis of some molybdenum centres. These then react further with **26**, losing the amido group to give a zwitterionic intermediate, $[Mo(NAr)^+(etc)_2(\mu\text{-}OMoO_3)^-]$ which dimerises to form **27**. Attempts to resynthesize this complex via the original synthetic route failed. Other

synthetic routes were also tried unsuccessfully - e.g. direct addition of sodium molybdate to the imido-dichloride complex or the protonated imido-amido complex. Such failure may be partly due to the poor solubility of molybdate salts in non-aqueous solutions.

Reaction of trifluoroacetic acid with 7 afforded a colour change to yellow. The reaction was monitored by nmr spectroscopy. The ^1H spectrum shows complex peaks for both the methylene and methyl protons of the dithiocarbamate ligand but there is no broad peak indicative of an amido proton. However, the number of aryl protons observed in the spectrum indicates the presence of imido and dithiocarbamate ligands in a 1:1 ratio. Five of the aryl protons are accounted for in a multiplet while the other (4-H on one of the aryl rings) is shown as a triplet. There are two sets of septets for the protons of the isopropyl groups. This suggests that the environment for each arylimido ligand is quite different. The combination of this and the complexity of the peaks suggests an imido-amido complex. However, there is still only one triplet for the methyls of both dithiocarbamate ligands. It may be possible that proton transfer between the principal ligands is on such a timescale that on the nmr timescale, the motion is not frozen out but nor is it averaged out (as suggested above with HBF_4 as the acid). This may be due to the strength of the acid and its counterion's capacity for coordination. Interestingly, the ^{13}C nmr spectrum shows a doubling up of peaks for each expected carbon atom (compared to 7). This may reflect a close relationship between the two ligands and strongly suggests an imido-amido complex, [Mo(NAr)(NHAr)(etc)$_2$]$^+$ (28).
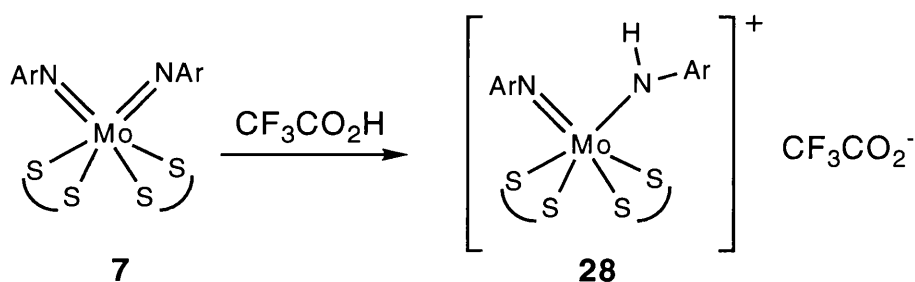
The change in acid (i.e. the change in counterion) can affect the position of the amido proton and indeed, excess acid is observed at >10 ppm, reflecting the exchange that could be occurring between the acid and the amido proton of the complex. The presence of the acid is evident in the ^{13}C nmr spectrum, with significant carbon-fluorine coupling, with quartets at 160.5 and 113.9 ppm.

In order to further investigate the role of trifluoroacetic acid, another bis(imido) was chosen for reaction but on this occasion, the co-ligand was changed from diethyldithiocarbamate to dimethyldithiocarbamate. The resultant proton nmr spectrum is more simple than above. In particular, the isopropyl imido substituents are less complex than that seen in the formation of 28. However, there are still two

distinct signals for the isopropyl proton (CHMe$_2$) and now, there are two signals for the methyls of the dithiocarbamate ligand. This suggests that the imido-amido complex has formed, [Mo(NAr)(NHAr)(mtc)$_2$]$^+$ (29).
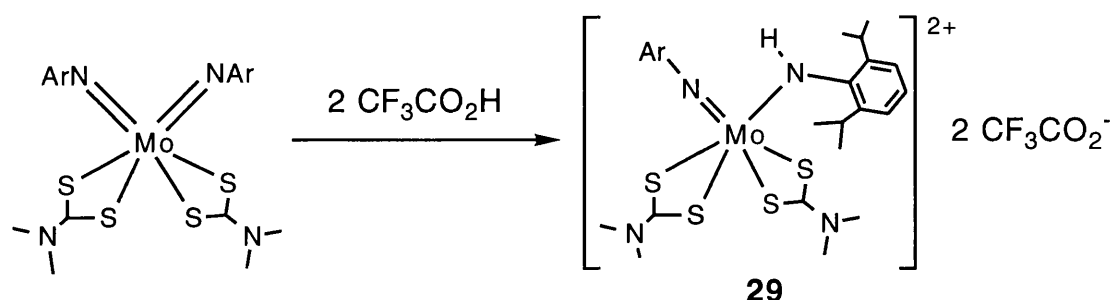
Finally, **7** was reacted with hydrogen chloride for comparison with that of **1** as performed by Maatta and Wentworth. A colour change to yellow was observed and a peak at 7.44 pm could be assigned as an amido proton. What is certain is that no precipitation occurred and the imido-dichloride complex did not form. The rest of the spectrum is not simple and as suggested above, this is what may be expected for an imido-amido complex. Again, the imido-amido cationic complex of **7** must be more stable than that of **1** and is not desperately scavenging for another ligand for stabilization.

Given the high stability of complexes derived from **7**, a different and more reactive imido complex was needed to test the reactivity with acids. The *tert*-butyl complex **2** was also reacted with the two acids, HBF$_4$.Et$_2$O and CF$_3$COOH. Again, both reactions were monitored by ^{1}H nmr spectroscopy. Reaction with HBF$_4$ produced a complicated ^{1}H nmr spectrum but in the mass spectrum, a parent peak of 613 was observed, correspondent with [Mo(N^{t}Bu)(etc)$_3$]$^+$ (**30**). This cation was not reflected clearly in its nmr spectrum. However, it is conceivable that competition occurs between two reaction pathways - namely, formation of the bis(amido) complex or the monoimido-tris(dithiocarbamato) cation. The *tert*-butylimido nitrogen is considerably more basic than that of the arylimido complex. Thus, if the bis(amido) complex forms, proton transfer from one amido group to the other could occur, encouraged by formation and loss of butylamine, followed by scavenging of another dithiocarbamate group. The analogous oxo complex has been shown to form the monoxo-tris(dithiocarbamate) cation; although the oxygen is not so basic, it is sterically more accessible[76].

^tBuN N^tBu
Mo
S S
S S

2

$HBF_4.Et_2O$ →

$\begin{bmatrix} & H & H & \\ ^tBu-N & : & N-^tBu \\ & Mo & \\ S & & S \\ S & & S \end{bmatrix}^{2+}$

$-\,^tBuNH_2$

$\begin{bmatrix} & ^tBu \\ & N \\ & \| \\ S & Mo & S \\ S & & S \\ & S\ S \end{bmatrix}^{+}$

30

$+$

$\xleftarrow{\text{etc}^-}$

$\begin{bmatrix} & ^tBu \\ & N \\ & \| \\ & Mo \\ S & & S \\ S & & S \end{bmatrix}^{2+}$
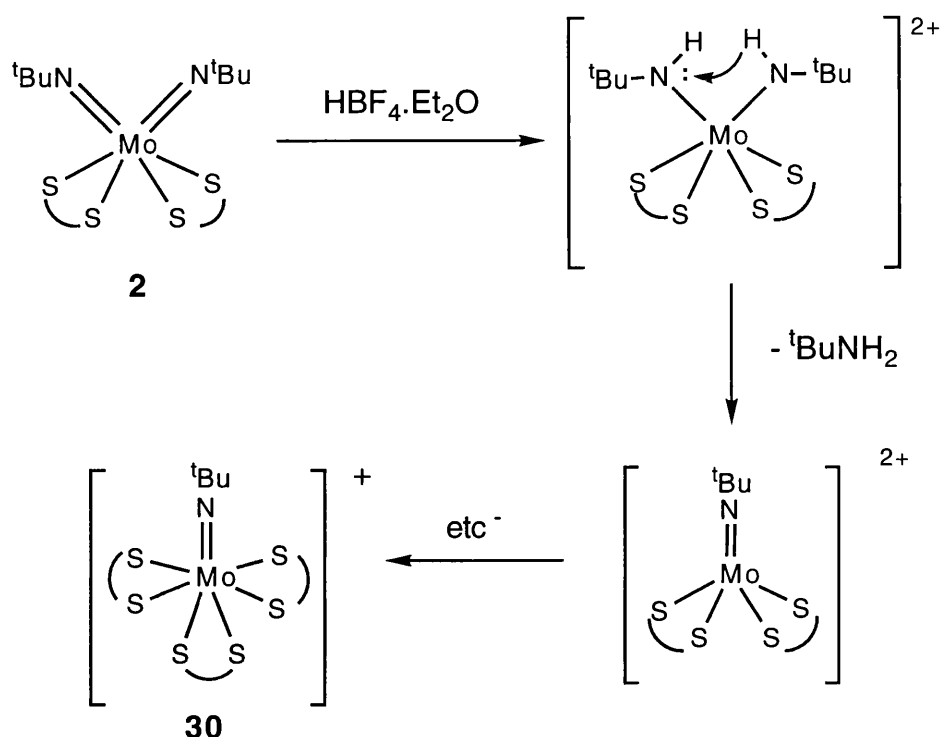
The reaction with CF_3CO_2H affords a change in colour to yellow. It is suggested that the imido-amido complex, $[Mo(N^tBu)(NH^tBu)(etc)_2]^+$ (31), has formed. The reaction appears to stop at this point and again, CF_3COOH being a weaker acid than HBF_4 must contribute to the lack of any further reaction. The ^1H nmr spectrum of 31 shows the methyl protons of both the imido and dithiocarbamate ligands as discrete signals, while methylene protons of the dithiocarbamate ligand are discernible as a quartet. Two discrete singlet resonances are observed for the imido ligands (or, rather, imido and amido ligands) but again, only one environment is indicated for the dithiocarbamate ligands. This suggests that intramolecular proton transfer may be occurring but the nmr timescale is such that the free motion of the dithiocarbamate ligands appears unperturbed.

In conclusion, it has proved difficult to predict the products of reactions of bis(imido) complexes with acids. A subtle interplay between the steric and electronic influences in the complex coupled with the different properties of the acids weighs against prediction of a reaction pathway with any certainty.

4.5   With Chalcogenides

With Hydrogen Sulfide, H_2S

Hydrogen sulfide gas was bubbled through a dichloromethane solution of $[Mo(NR)_2(etc)_2]$ (1, 2, 3, 7 and 8) until the solution was saturated and then left to stir for twelve hours. Uniquely for 2, a change in colour was observed from orange to red (as all other complexes were already a deep-red in dichloromethane.) Products were

separated by column chromatography giving, in most cases, two main products. Other minor products were not characterized.

The major product in all cases was the disulfide, [Mo(NR)(S$_2$)(etc)$_2$] - red for the non-aryl complex and purple for the aryl complexes; namely, [Mo(NPh)(S$_2$)(etc)$_2$] (32), [Mo(N^{t}Bu)(S$_2$)(etc)$_2$] (33), [Mo(N(2-Me)C$_6$H$_4$)(S$_2$)(etc)$_2$] (34) and [Mo(NAr)(S$_2$)(etc)$_2$] (35). For no apparent reason, the reaction did not proceed easily to the disulfide product for 8. This reaction was repeated several times with no success. Finally, after an extended saturation of three minutes and stirring for three days, a small amount of the disulfide (37%) was produced, namely [Mo(N(2,6-Me$_2$C$_6$H$_3$))(S$_2$)(etc)$_2$] (36). In this laboratory, complexes of the type [Mo(NR)(S$_2$)(etc)$_2$] have previously been synthesised by the thermolysis reaction of [Mo(O)$_2$(etc)$_2$] with RNCO in toluene[22]. This route provides an alternative route to their synthesis, and in some cases, with higher yields.

The second product was always orange and eluted from the column with 1:20 methanol / dichloromethane solution. They were shown by mass spectrometry (and for some products by ^{1}H nmr spectroscopy) to contain the species [Mo(NR)(etc)$_3$]$^+$. (Note that this product did not form with 7.) The counterion was never identified, though it is presumed to be the acid's conjugate base, SH$^-$. Results are tabulated below for ease of comparison.
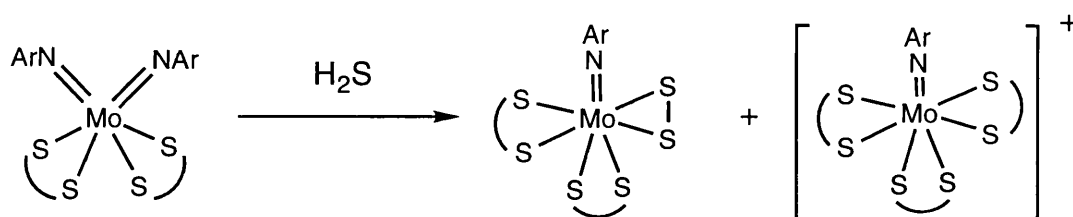
R	saturation time (seconds)	[Mo(NR)(S$_2$)(etc)$_2$] yield (%)	[Mo(NR)(etc)$_3$]$^+$ formation ?
Ph (32)	60	62	✔
2-MeC$_6$H$_4$ (34)	60	83	✔
^{t}Bu (33)	10	58	✔
2,6-Me$_2$C$_6$H$_3$ (36)	120; 180	0; 37	✔
2,6-^{i}Pr$_2$C$_6$H$_3$ (35)	300	68	✘

The introduction of the disulfide ligand to a molybdenum dithiocarbamate complex using hydrogen sulfide has been seen before upon the reaction of [Mo(O)$_2$(S$_2$CN^{n}Pr$_2$)$_2$][67]. It was a rather surprising reaction as, compared to oxygen, sulfur has a greater propensity to bridge metal centres and indeed, the other products of this reaction were a mixture of sulfur-bridged dimers. Dirand-Colin and co-workers suggested that molybdenum was reduced by the hydrogen sulfide, resulting in

formation of H_2S_2. This would convert to higher sulfanes and S_8 which would then react with any metal complex to form the disulfide product. However, this reaction with H_2S was tried unsuccessfully with the analogous diethyldithiocarbamate complex.

Considering the $[Mo(NR)(etc)_3]^+$ products in detail, only the complexes formed from **2** and **8** gave satisfactory ^1H nmr spectra. Good fragmentation patterns were produced by the complexes formed from **1** and **2** in their mass spectra. The counterion was never identified and attempts to form a stable complex with the cation, by reacting the product with NaBPh$_4$ to induce counterion exchange, also failed. This type of imido-tris(dithiocarbamate) cation is well documented[76,140]. A crystal structure of $[Mo(NCPh_3)(mtc)_3]^+$ was presented by Chatt and co-workers[140] with a typical imido length and angle (1.731(2) Å and 175.1(5)°) and the expected lengthening of the molybdenum-sulfur bond of the dithiocarbamate ligand *trans* to the imido ligand (2.606(2) from 2.504(2) Å). It is very similar to the analogous oxo complex reported later by Young and co-workers[132].

A reaction mechanism is suggested here. (Dithiocarbamate ligands are omitted for clarity.)
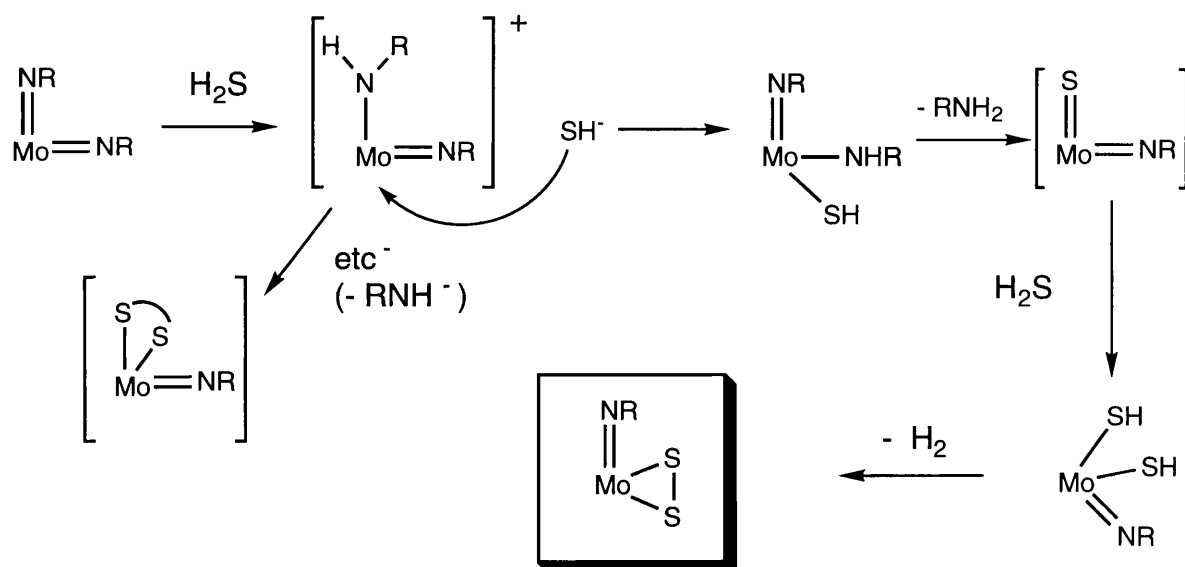
Uniquely for **7**, a further compound was isolated and characterized. The ^1H nmr spectrum of this orange solid indicated the presence of imido and dithiocarbamate ligands in a 1:1 ratio. The spectra were rather complex for the diethyldithiocarbamate ligand, suggesting restricted rotation about the carbon-nitrogen backbone of the ligand. The ir spectrum showed a strong stretch at 1262 cm^{-1} and several very weak stretches in the area about 500 - 600 cm^{-1} region. In the mass spectrum (FAB), a clear parent peak at 935 and its fragmentation pattern showed loss of a single sulfur atom, suggests a complex of formula $[Mo_2(NAr)_2(etc)_2S_3]$ with a single sulfide ligand in the complex. Orange crystals were grown from slow diffusion

of methanol into a dichloromethane solution and characterized by X-ray diffraction as
$[\{Mo(N(2,6^{-i}Pr_2C_6H_3))_2(etc)\}_2(\mu\text{-}S)(\mu^2\text{-}\eta^2\text{-}S_2)]$ (37).
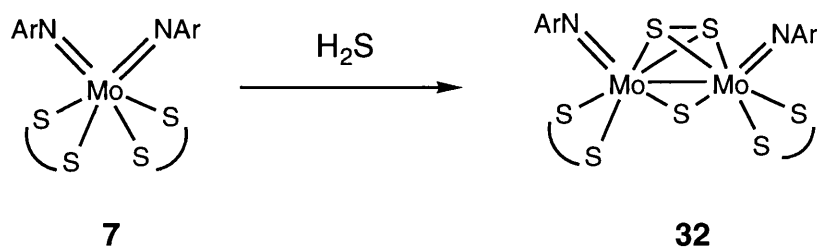
The mode of formation of this trisulfide compound is unclear. It is suggested
that the $[Mo(NAr)(S_2)(etc)_2]$ complex is not an intermediate since when this was
reacted with hydrogen sulfide, the trisulfide complex was not produced.

The structure of **37** (shown overleaf) contains two equivalent molybdenum(V)
centres, each carrying an imido and dithiocarbamate ligand. The imido angles are near
linear at 177.0(9) and 174.4.(9)°; the molybdenum-nitrogen bond lengths are 1.740(1)
and 1.716(9) Å, both typical for molybdenum-imido complexes. They are spanned
approximately symmetrically by a sulfido ligand ([Mo(1)-S(1) 2.349(3)] and [Mo(2)-
S(1) 2.337(3) Å) and asymmetrically by a disulfide ligand.

The asymmetry is rather pronounced with different metal-sulfur bond lengths,
attributable to the different environments experienced by the two sulfur atoms in the
ligand. One atom, S(2), lies roughly in the $Mo_2S(1)$ plane but the other, S(3), lies
2.00Å from the plane. Another difference between them is that S(2) is *cis* to both
imido ligands, while S(3) is *trans* to both. Hence, with the enhanced *trans* influence of
the imido (and, potentially, sulfur) ligands, the metal-sulfur bond lengths are rather
different with S(2) lying closer to the molybdenum centres [Mo(1)-S(2) 2.370(4),
Mo(2)-S(2) 2.383(4)] than S(3) [Mo(1)-S(3) 2.551(5) and Mo(2)-S(3) 2.657(5) Å].

Such pronounced asymmetry for this disulfide ligand is quite rare. In contrast,
the molybdenum-sulfur bond lengths of the disulfide ligand in $[Cp^*_2Mo_2(\mu\text{-}\eta^2\text{-}\eta^2\text{-}$
$S_2)(\mu\text{-}S)_2]$ differ by only 0.006 Å, though the inequality is on average 0.03 - 0.04 Å[21].
Sulfur-sulfur distances in disulfide ligands range from 1.89 to 2.15 Å, though the
average length for this type of ($\eta^2\text{-}\eta^2$) ligand is 2.02(3) Å. The distance in our ligand
is considerably shorter than the average at 1.936(6) Å. The small coordination angle
of this ligand favours a high coordination number at the metal centre; furthermore,
such a high coordination number discourages nucleophilic attack on the metal centre
and hence, helps stabilize the metal-metal bond. Frequencies in the ir spectrum for S-S
range from 480 to 600 cm^{-1}; **37** has a band at 549 cm^{-1} which is confidently assigned
to the disulfide ligand.
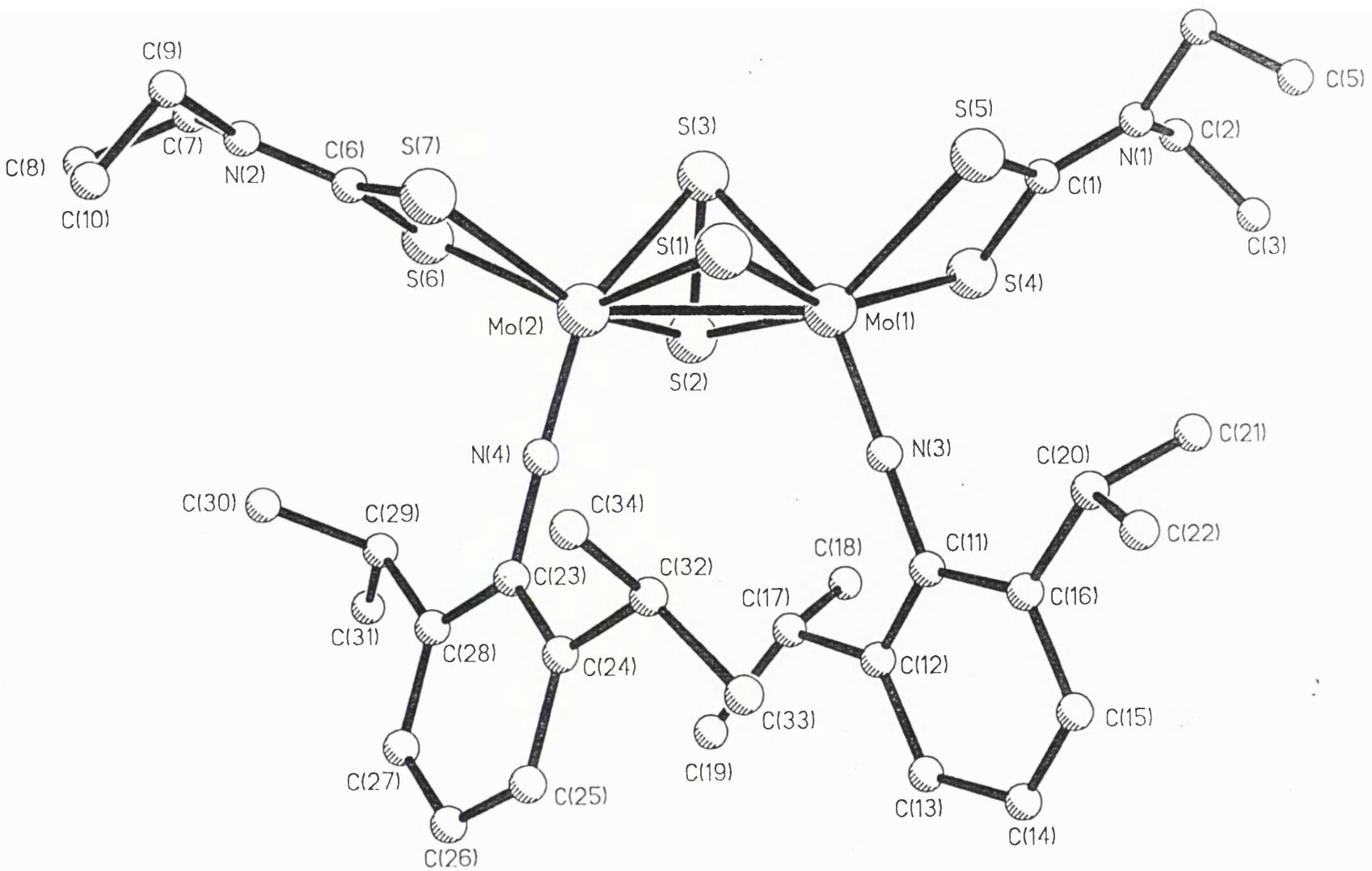
Structure of $[\{Mo(N(2,6\text{-}^iPr_2C_6H_3)\}_2(etc)\}_2(\mu\text{-}S)(\mu^2\text{-}\eta^2\text{-}S_2)]$ (37)
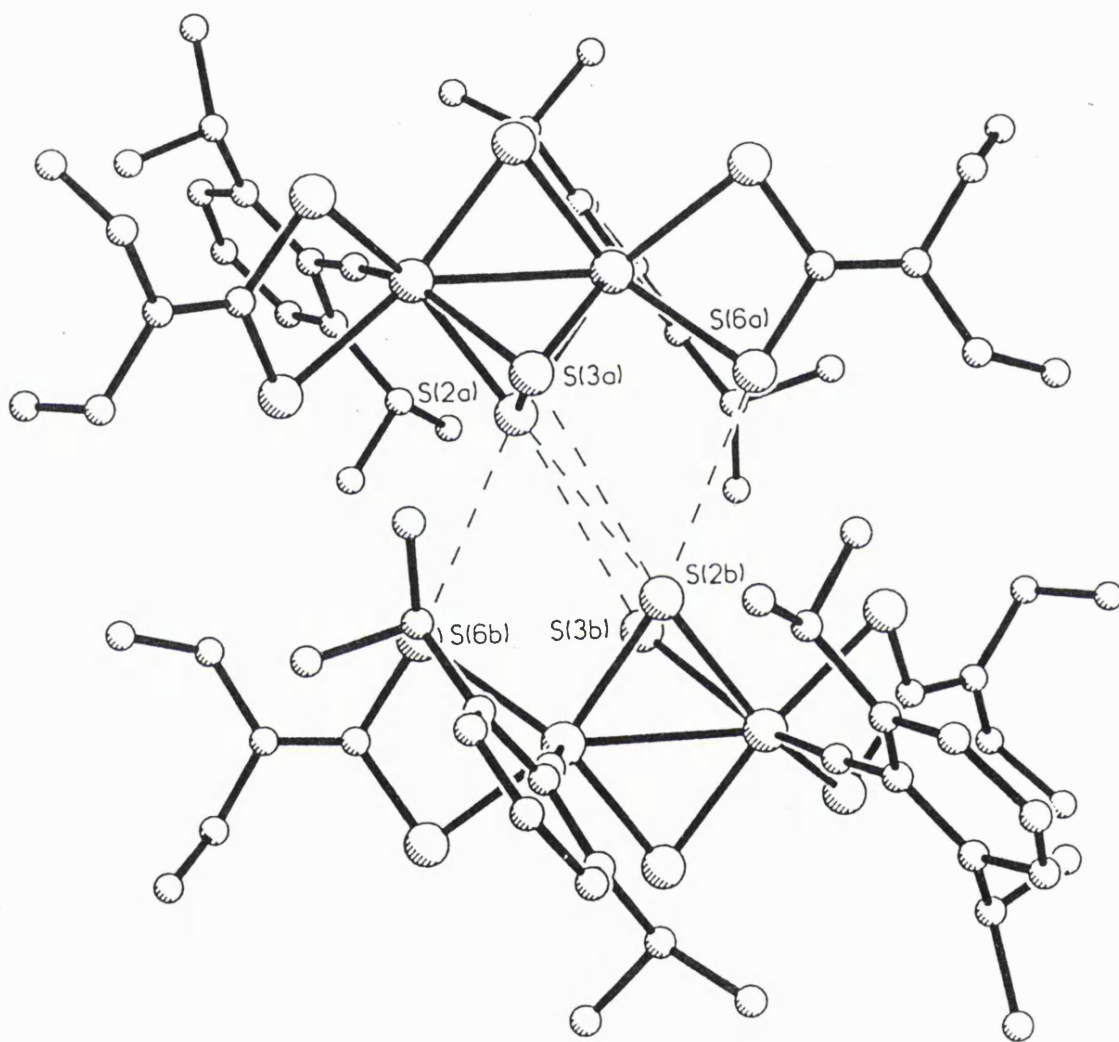
Crystal Packing in **37**

Bonding in these complexes has been compared to that in η^2 side-on MO_2 complexes.

σ and π- bonding in η^2- coordination MS_2 complexes

Where the disulfide ligand is linked to only one metal centre, as in $[Mo(NPh)(S_2)(etc)_2]$ (**32**), then the π-bonding is the major interaction. When bridging two metal centres, as in **37**, this interaction occurs with both metals. If the metal has few d-electrons, then a lower electron density will reside on the ligand when bridging two metal centres rather than when bonded to just one. Depopulation of the π^* orbitals is consistent with the shorter S-S distances and higher (S-S) frequencies of the (η^2-η^2) ligand compared to the (η^2) ligand.

The structure of molybdenum trisulfide has been under investigation since it was first formed in 1825. There have been many previous structural studies using crystallography and various absorptions; the most comprehensive of them (by Chien and co-workers[141]) proposed chains of face-sharing MoS_6 octahedra with alternating long and short Mo-Mo distances with (μ^2-η^2-S_2) ligands across the shorter Mo-Mo distance.

Chien's structure   Hibble's structure

- - - (Mo-Mo) bond
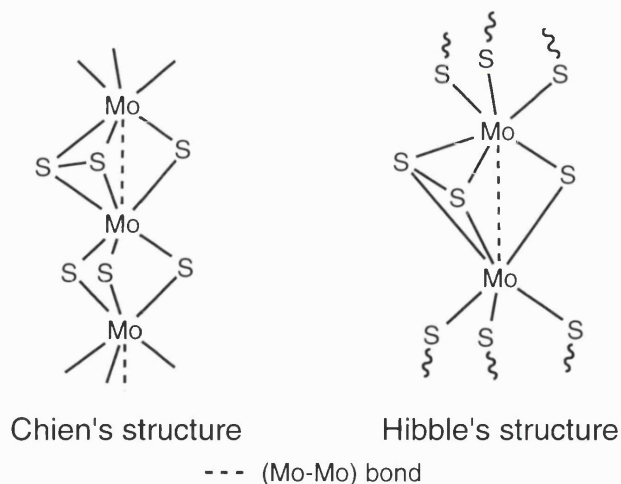
Hibble and co-workers have studied the Mo K-edge EXAFS and S K-edge absorptions of molybdenum trisulfide[142]. They concluded that the structure consists of layers based on building blocks of Mo_2S_9, linked by vertex or edge-sharing of octahedra. Here the molybdenum atoms are close to one another (2.76 Å) and are bridged by sulfido and disulfido ligands. Each molybdenum centre has an octahedral

---

geometry about it and an oxidation state +5 ; the formulation for this structure is $[Mo(S^{2-})_2(S_2^{2-})_{0.5}]$, the diamagnetism completed by a metal-metal bond. Our complex **37** satisfies all the structural features demanded for Hibble's structure. The Mo-Mo bond length is 2.797(2) Å, the asymmetric disulfide ligand and another sulfide ligand linking the metal centres. The chained-layer structure suggested for MoS_3 must be linked by long-range interactions between the Mo_2S_9 building blocks. Again, this is reflected in examination of a packing diagram of **37** (shown above) which shows the presence of weakly bound dimeric units, held together by long-range interactions between the disulfide groups (S⋯S 3.483, 3.566 Å) and also between the disulfide and a dithiocarbamate ligand (S⋯S 3.458 Å).

Other dimeric complexes were also reacted with hydrogen sulfide with limited success. There are differences in the ir spectra of $[\{Mo(O)(etc)(\mu\text{-}NPh)\}_2]$ before and after its reaction with hydrogen sulfide, especially in the region of 400-525 cm^{-1}. A peak at 457 cm^{-1} may be indicative of a Mo=S stretch. Earlier in this laboratory, this stretch has been shown to arise at ~ 478 cm^{-1}[143]. In the ^1H nmr spectrum, the main product formed seems little different from the starting material though resonances of another product with phenylimido ligands are evident. The mass spectrum has a strong molecular ion consistent with the starting material. However, on closer inspection of that region, a second series of peaks centred on 719 may be discerned. This gives a molecular ion consistent with $[Mo_2(O)(S)(etc)_2(\mu\text{-}NPh)_2]$, suggesting that substitution of a single oxo ligand with sulfur has occurred.
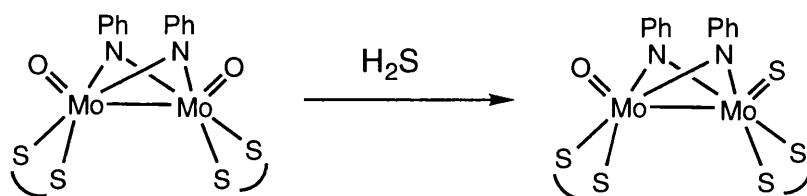
Reaction with the ureato complex $[Mo_2(NPh)_2(etc)_2(\mu\text{-}NPh)\{\mu\text{-}PhNC(O)NPh\}]$[64] did not give rise to any changes from the starting material.

It is interesting to note that not only has hydrogen sulfide acted as a source of sulfur but it has also acted as an acid in producing the tris(dithiocarbamate) ion.

Reactions with Lawesson's reagent

Lawesson's reagent, $[(4\text{-}(OMe)C_6H_4)P(S)(\mu\text{-}S)]_2$[144], has been used as an oxygen/sulfur exchange reagent in organic synthesis[145] and more recently in organotransition-metal synthesis[146].
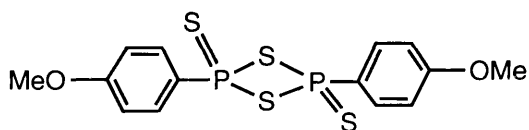
Its chemistry is based on the ligands made available upon fragmentation and is most commonly used, in organic chemistry, for the conversion of the carbonyl group (C=O) to (C=S)[147]. Based on its ability as a sulfur source, it was decided to investigate the conversion of either the oxo or imido ligands in a molybdenum complex to the thio equivalent.

Complex 13 was reacted with Lawesson's reagent and the reaction mixture was purified by column chromatography. ^{1}H nmr spectroscopy indicated the major product to be the imido-disulfide complex, [Mo(N-2,6-Cl$_2$C$_6$H$_3$)(S$_2$)(etc)$_2$] (38), which had already been made in this laboratory[22]. However, its ir spectrum did not match that of an authentic sample. Furthermore, peaks were evident in a ^{31}P nmr spectrum. Finally, both green plates and green needles were grown; a plate was chosen and an X-ray diffraction study performed, confirming the identity of the product as the imido-disulfide complex. Indexing of the green needle gave the same cell parameters as the plate.

The structure of 38 (shown overleaf) is a distorted pentagonal biypramid in which the metal is displaced from the plane of the equatorial sulfur atoms by 0.335 Å. The imido angle is 165.1(8)° and the Mo-N bond length is 1.741(9) Å; the disulfide bond length is 2.033(5) Å. Crystal structures of 36 and of [Mo(NAr)(S$_2$)(mtc)$_2$] showed Mo-N distances of 1.759(4) and 1.734(3) Å, respectively; thus on substitution of the aryl ring with bulky, electron-releasing groups, the imido bond length shortens by 0.025 Å. Here, there is also a shortening of the bond length (by 0.018 Å) so the inclusion of either electron-withdrawing or electron-releasing substituents in the aryl ring results in a shortening of the molybdenum-nitrogen bond. The strong *trans-*influence of the imido ligand is observed again in the lengthening of the Mo-S bond trans to it to 2.591(3) Å, compared to the average of 2.499 Å for the sulfur atoms in equatorial sites. To account for the peaks in the ^{31}P nmr spectrum, it is evident that some phosphorous-containing complex must have eluted concurrently with the disulfide complex. Under close inspection of the crystals, minute red plates were observed, presumed to be this other complex.

13   Lawesson's reagent   38
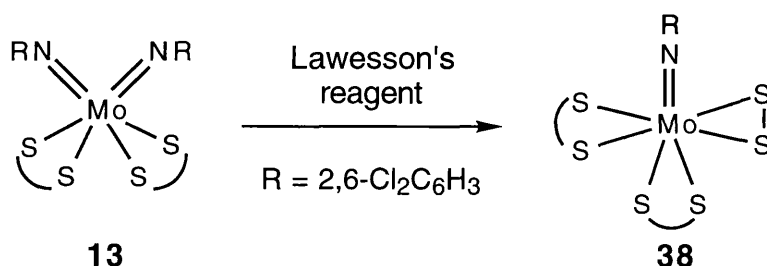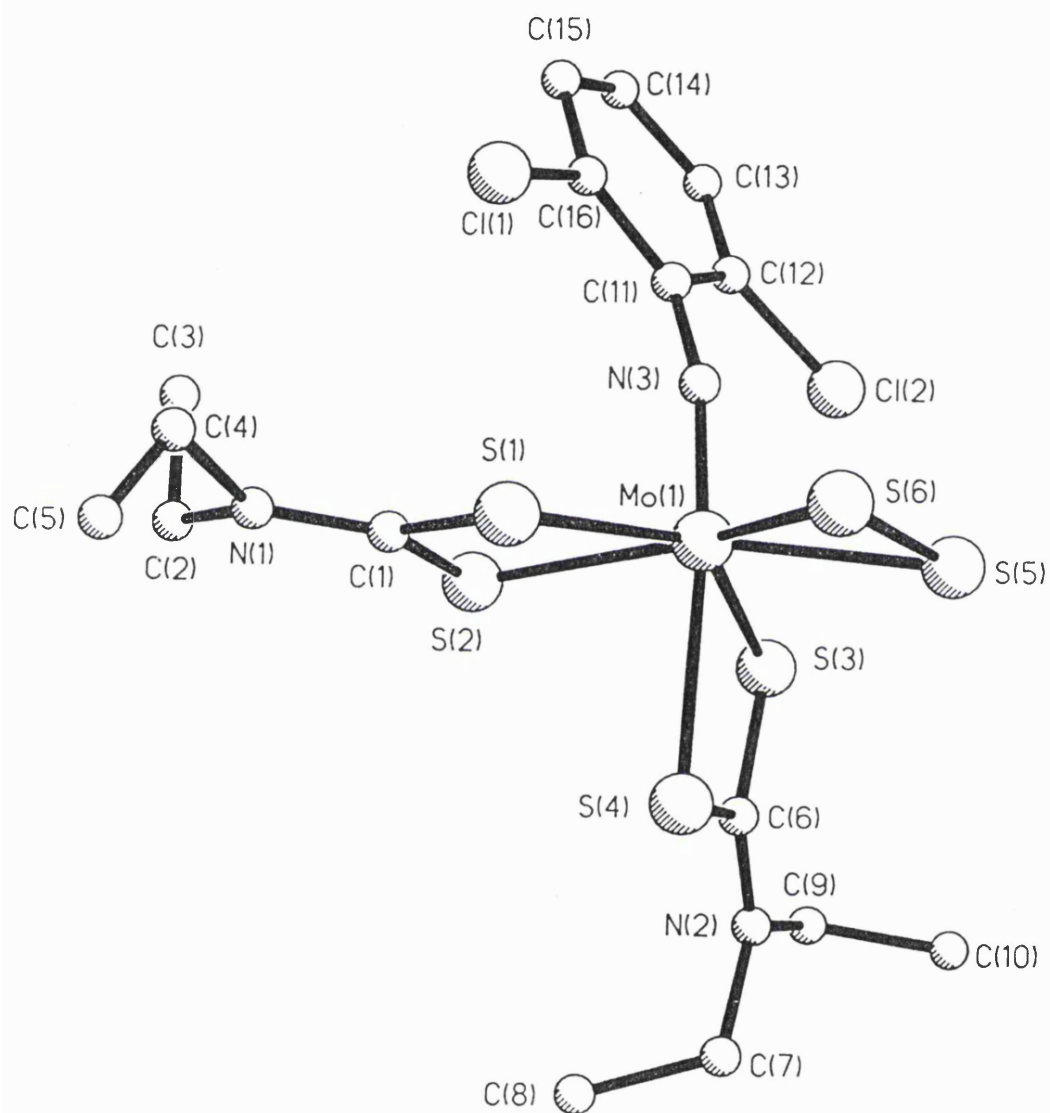
R = 2,6-Cl$_2$C$_6$H$_3$

Structure of [Mo(N-2,6-Cl$_2$C$_6$H$_3$)(S$_2$)(etc)$_2$] (**38**)

Given the difficulty in forming the imido-disulfide from the 2,6-dimethylphenyl bis(imido) complex with hydrogen sulfide, it was reacted with Lawesson's reagent. On this occasion, the imido-disulfide **36** was produced readily; its ^{1}H nmr spectrum correlated with the original data. Two other phosphorous-containing species were produced but we have failed to identify these products. [$MoO_2(etc)_2$] was reacted with Lawesson's reagent but again, the blue [$Mo(O)(S_2)(etc)_2$] did not form.

However, on reaction with the phenylimido ureato complex, the strong peak seen for the carbonyl in the starting material disappears. Furthermore, in the FAB mass spectrum, a peak is observed for the molecular ion of [$Mo_2(NPh)_2(etc)_2(\mu$-NPh){μ-PhNC(S)NPh}]. A strong peak at 794 is consistent with the loss of a dithiocarbamate and the (CS) group from the thioureato complex. Thus, on this occasion, the oxygen of the carbonyl group appears to have been substituted by a single sulfur atom.

It appears then, that Lawesson's reagent is an excellent source of sulfur. Though its reactions may be more time-consuming than the simple reaction with hydrogen sulfide, apart from the disadvantage of formation of co-products, the reagent appears highly successful in its sulfur-transfer role.

Reaction with H₂Se and Se

The development of selenide chemistry has been very slow (compared to sulfide chemistry) due to the difficulty of synthesis of selenide complexes. Hydrogen selenide is an extremely toxic, malodorous and expensive gas which often leads to impure mixtures of products. The gas is usually produced by the reaction of mineral acid on a metal selenide. Elemental selenium and selenium anions have been used with greater effect[148]. There are two types of selenium, the more commonly available of which is a grey, unreactive powder. Selenium nmr spectroscopy is widely used, but is only possible on machines that can reach a very low frequency.

In our synthesis, it has proved difficult to both capture this gas (generated *in situ* on reaction of a mineral acid with mercury- or aluminium- selenide) and provide a driving force for its reaction with the bis(imido) complexes. Reaction of **2** with selenium powder has been tried. The selenium appeared to be consumed during the course of the reaction. However, after some short period, grey powder was observed settling out of the nmr sample.

4.6   With Phosphines

Imido transfer to phosphines is not a new phenomenon for imido complexes although it has been studied far more extensively for oxo complexes. Reaction of three

phosphines (PPh_3, PPh_2Me and PMe_2Ph) was tried with **2**. For the latter two phosphines, only starting material was recovered. However, with triphenylphosphine, another product is formed. Attempts to separate it from the starting materials by using different solvents for extraction was only partially successful. The ^1H nmr spectrum is highly complex showing extensive coupling and broad peaks. The $^{13}C\{^1H\}$ spectrum is not more illuminating. However, the $^{31}P\{^1H\}$ nmr spectrum shows a resonance for the triphenylphosphine and for another species at 25.1 ppm. This is presumed to be the phosphine imine, $[Ph_3P=N^tBu]$.

Triphenylphosphine also reacts with **3**. This reaction was followed by $^{31}P\{^1H\}$ nmr spectroscopy. The colour of the nmr solution changed from the brown to a dark-red; the solution gradually became more transparent as the colour got brighter till it was nearly orange. A resonance at 49 ppm was observed, again, presumed to be that of the phosphine imine, $[Ph_3P=N(2\text{-}MeC_6H_4)]$. A peak assigned to phosphine oxide at 32 ppm gradually emerged in the spectrum.

2, 3
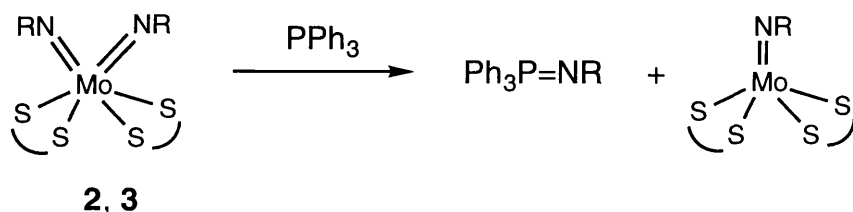
4.7 With Other Molecules

Reactions were tried with several other reagents but for none of these could new products be identified. It is evident that reaction has occurred with some reagents but these products have been highly impure, contaminated with starting material or other by-products, making characterization highly difficult.

With <u>chlorine</u> gas, **2** changed in colour from orange to red - however, the ^1H nmr spectrum was complex and did not correlate simply with the imido-dichloride species. Reaction of chlorine with **1** did not produce the already-known, yellow imido-dichloride product. Instead, a red mixture was produced which could not be separated without visible decomposition.

With ethyldiazoacetate and **1**, the colour changed from red to a dark yellow colour. The proton nmr spectrum revealed a complex mixture of products. Other techniques did not reveal any information on this extremely moisture-sensitive substance. Again, with sodium amalgam, DMAD, metal complex $[Ru_3(CO)_{12}]$, acetylene and hydrogen (with and without photolysis), any products were not identified. On the whole, intractable, impure substances were obtained that did not lend themselves to analysis in any form.

4.8   With Aniline

The exchange of organoimido ligands has been important in the development of mixed-imido complexes as seen earlier. *Tert*-butyl imido complexes can usually be synthesised easily but these imido ligands are then readily displaced by arylamines to form new imido complexes. This use of *tert*-butylamido-arylamine exchange has become quite common for later transition metals, examples of which have already been cited above[37,77]. In both examples, the exchange occurs at a four-coordinate molybdenum species. In the latter, the reaction is proposed to proceed by initial coordination of the amine to the metal centre, followed by proton transfer and subsequent α-elimination of *tert*-butylamine, leaving the new imido complex. Bergman and co-workers observed imido exchange in one of their "pogo-stick" complexes, [(η^6-*p*-cymene)Os(N^{t}Bu)], with 2,6-dimethylphenylamine[149]. The methodology has been extended to earlier transition metals - e.g. addition of an arylamine to a dichloromethane solution of [Ti(N^{t}Bu)Cl$_2$(py)$_3$] and leaving it to stand for a few hours yields the arylimido complex and butylamine[116].

Imido exchange can be initiated by other imido-bearing reagents, such as imines. Recently, Meyer and Cantrell observed both aryl and *tert*-butyl bis(imido) complexes undergoing imido-imine metathesis by ^{1}H nmr spectroscopy[150].

$$R^1 = Ar, {}^tBu; R^2 = {}^tBu, Ph; R^3 = Ph, {}^nPr$$
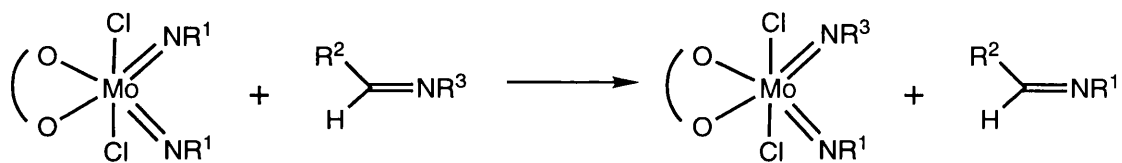
Using alkoxides as co-ligands (instead of chlorides) has no effect on the metathesis. These molybdenum imido complexes catalyse the imine metathesis and do not exhibit the problems of termination or substrate inhibition as is seen for other catalsyts, such as [Cp$_2$Zr(N^{t}Bu)(thf)][151]. Reaction times are very slow, the quickest being eight days and using an excess of imine (12 equivalents). However, the metathesis is very general - the reaction working with a variety of substrates, imido substituent and co-ligands.

In our work, several attempts were made to induce imido exchange. All reactions were monitored by ^{1}H nmr spectroscopy. Some of these experiments were performed in a sealable nmr tube which allowed for additon of extra arylamine. The reaction of **2** with aniline was monitored over a period of two days. After a short time, new peaks not attributable to **2** or aniline started to emerge. These peaks have grown as those of aniline have disappeared and have been correlated with those of **1**.

It has not been possible to definitively assign a peak to the methyls for butylamine. However, given the other peak assignments, it is fair to suggest that imido exchange has occurred.
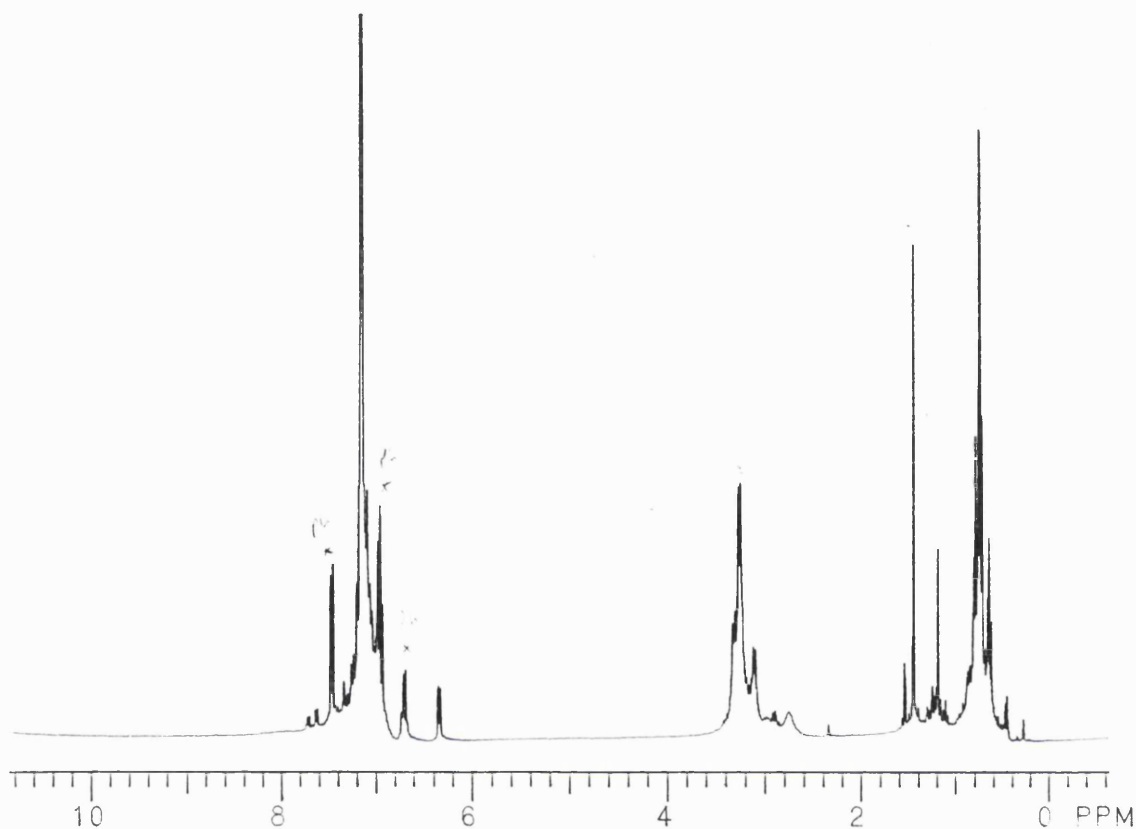
^{1}H nmr spectrum of reaction of **1** with PhNH$_2$ after 24h

To summarise then, in this work, the imido ligand has shown itself to be a highly reactive moiety. The variety of reagents used coupled with the diversity of products formed illustrates well the flexibility of the ligand with regard to electronic and steric factors.

We have discovered only one general reaction process which is the formation of mono(imido)-disulfide complexes **32, 33, 34, 35** and **36** upon reaction of the complexes **1, 2, 3** and **7** with hydrogen sulfide gas and the reaction of **13** with another sulfur source, Lawesson's reagent, to form **38**. A dimeric complex [{Mo(N(2,6-^{i}Pr$_2$C$_6$H$_3$))$_2$(etc)}$_2$(μ-S)(μ^2-η^2-S$_2$)] **37** was also formed upon reaction with **7** and a crystal structure obtained. This had an interesting structure with the two molybdenum centres being bridged by a (μ^2-η^2-S$_2$)- and a (μ-S)- ligand.

The imido's susceptibility to form the oxo moiety (with moisture) is well known. Limited exposure to air led to the formation and characterisation of two oxo-imido complexes, **23** and **25**. Complete hydrolysis and removal of the imido ligands accompanied by partial scavenging of another dithiocarbamate ligand is presumed to be the pathway to formation of the thionitrsosyl complex, [Mo(NS)(etc)$_3$] **24**.

Hydrolysis was also assumed to feature in the formation of the complex, [Mo(N(2,6-^{i}Pr$_2$C$_6$H$_3$))(etc)$_2$(μ-MoO$_4$)]$_2$ **27**, after reaction of **7** with tetrafluoroboric acid. Other reactions with this acid and trifluoroacetic acid led to (imido-amido), bis(amido) and mono(imido)-tris(dithiocarbamato) complexes, **26, 28, 29, 30** and **31**.

Reactions with a number of other reagents have been tried unsuccessfully. The degree of difficulty in handling these highly-moisture sensitive complexes has hindered the progress of identification of several other complexes formed. However, it has led to the discovery of some curious molecules, as shown above.

As a result of earlier work in this group, a general reaction scheme was developed concerning the thermolysis of bis(oxo) complexes of Mo(VI), *viz.* [MoO$_2$(S$_2$CNR'$_2$)$_2$], with organic isocyanates which produces imido-disulfide compounds of the type [Mo(NR)(S$_2$)(S$_2$CNR'$_2$)$_2$][18,22]. Other products formed were tetraethyldithiuram disulfide and compounds of the type [{MoX(μ-X)(S$_2$CNR'$_2$)$_2$}$_2$] (X=O, S or NR) where X varied according to the nature of the isocyanate. Further, when the imido moiety had substituents in its 2- and 6- positions, the bis(imido) complexes [Mo(NR)$_2$(S$_2$CNR'$_2$)$_2$] were also formed.
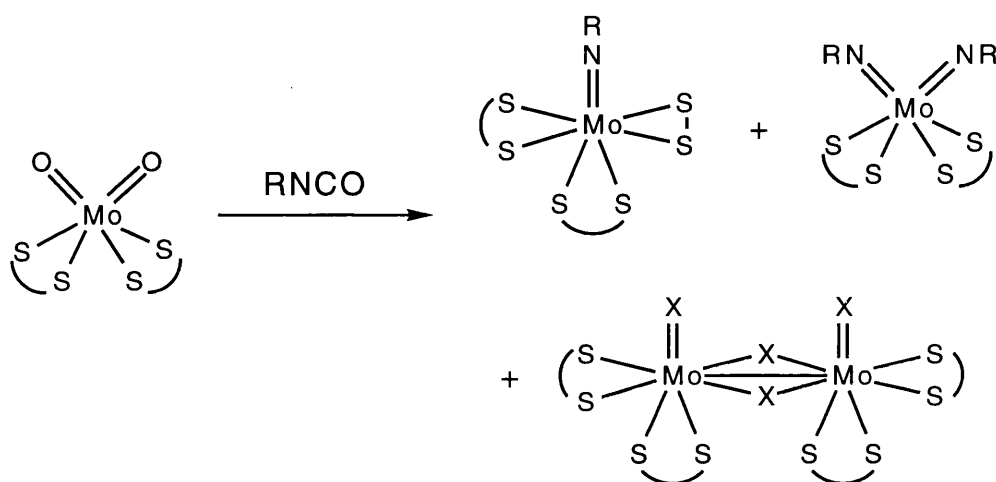
Thus it was decided to investigate the conditions and mechanism for the mode of formation of the imido-disulfide compound.

The key questions to be considered in discerning the mechanism were:

(i)   how is the side-bound disulfide ligand formed?

(ii)   when does the dithiocarbamate cleavage occur - before or after the imido incorporation?

(iii) to identify any intermediates.

The disulfide ligand might be formed via two possible routes - a double sulfur-carbon bond cleavage of a single dithiocarbamate ligand or *via* cleavage of the tetraethyldithiuram disulfide (formed upon dithiocarbamate oxidation). The cleavage of dithiocarbamate ligands is fairly well documented, particularly the single sulfur-carbon cleavage process. This was first noted in 1972 by Weiss and co-workers[152,153]; [Mo^{II}$_2$(μ-O$_2$CMe)$_4$] was reacted with four equivalents of [NH$_4$][S$_2$CN^{n}Pr$_2$] producing the sulfido-bridged dimer [{Mo^{IV}(μ-S)(η^2-SCN^{n}Pr$_2$)(S$_2$CN^{n}Pr$_2$)}$_2$] - an oxidative-addition process at both metal centres.

$$[Mo_2(\mu\text{-}O_2CMe)_4] \xrightarrow[-4\ MeCO_2^-]{4\ [S_2CN^nPr_2]^-}$$
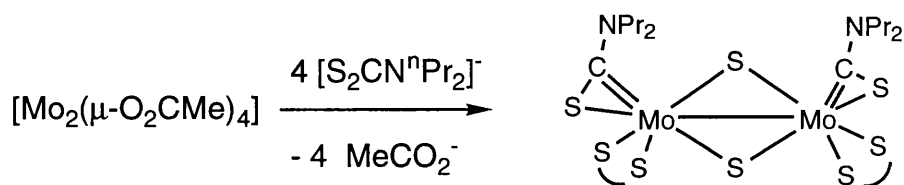
Further cleavage processes have been noted at mononuclear centres - for example, the addition of PEt_3 to $[WS(PhC_2Ph)(S_2CNR_2)_2]$ results in sulfur abstraction and dithiocarbamate cleavage giving $[WS(PhC_2Ph)(\eta^2\text{-}SCNR)(S_2CNR_2)]$[154].

These reactions all result in an increase in the oxidation state of the metal centre. In our system, however, there is no apparent change in the metal's oxidation state as both the starting material and product are molybdenum +(VI). This has been noted previously and, interestingly, it is also an example of the introduction of a sidebound η^2-disulfide ligand from decomposition of a dithiocarbamate ligand. On addition of excess $Na[S_2CNEt_2]$ to $TaCl_5$, two tantalum (V) products are produced - $[Ta(S)(etc)_3]$ and $[Ta(S_2)(etc)_3]$[84,155].

The formation of the disulfide compound suggests that a double carbon-sulfur bond cleavage has occurred; note, however, though that the compound may also be formed by addition of sulfur or sulfur-containing compounds to the monosulfido complex. The organic fragments produced in the sulfur-carbon cleavage are absent from the metal coordination sphere, as is true for our reaction.

Further evidence of the possibility of double sulfur-carbon bond cleavage in a dithiocarbamate ligand is provided by Deeming and Vaish[156]. They reacted $[Ru(CO)_2(etc)_2]$ with $[Ru_3(CO)_{12}]$ to produce $[Ru_5(CO)_{11}(\mu^4\text{-}S)_2(\mu\text{-}CNEt_2)_2]$; on this occasion both sulfur atoms (though only two of four) and the organic fragments are trapped in the metal's coordination sphere.

So it is clear that the disulfide ligand can be formed as a result of double sulfur-carbon bond cleavage. To find out when the dithiocarbamate cleavage occurs, a series of experiments were performed, designed to produce possible reaction intermediates. Some candidates for the intermediates are outlined below:
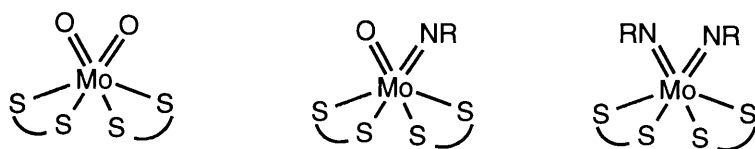
The first to consider is the oxo-disulfide species - that is, whether the dithiocarbamate cleavage occurs before imido incorporation. There are two experiments to ponder here - can this intermediate be made from our starting material and can the final product be made by adding the isocyanate to this proposed intermediate?

Initially, thermolysis of [MoO$_2$(etc)$_2$] alone in toluene for three days was performed. During the reaction a purple colouration was noticed, suggesting the formation of [Mo$_2$O$_2$(μ-O)(etc)$_2$] but after work-up and purification of the mixture by column chromatography, the only product identified was [Mo$_2$O$_2$(μ-O)(μ-S)(etc)$_2$]. Crucially, the first candidate [Mo(O)(S$_2$)(etc)$_2$] was not formed, suggesting that this was not an intermediate.
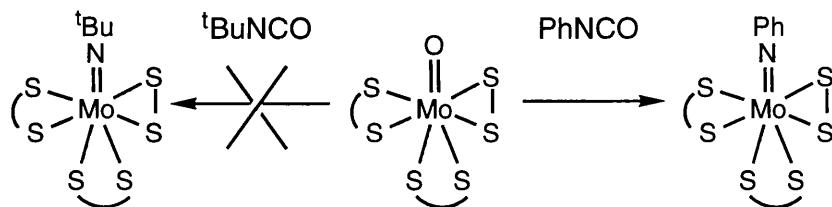
A second experiment was undertaken to further rule out [Mo(O)(S$_2$)(etc)$_2$] as an intermediate. The oxo-disulfide compound was reacted with phenyl isocyanate and the disulfide compound [Mo(NPh)(S$_2$)(etc)$_2$] was duly formed in high yield. However, when *tert*-butyl isocyanate was used in a similar thermolysis, no significant reaction was observed[64]. Thus, this route, dithiocarbamate cleavage followed by imido substitution, was discarded as a general mechanism.

Having concluded that the intermediate must contain an imido moiety, two other candidates were considered- the bis(imido) compound and the oxo(imido) species as pictured above. Bis(imido) compounds have been synthesized *via* this route but only for aryl isocyanates with substituents in the 2 and 6 position[64,92]. However, as referred to in chapter 4, **7**, **8** and **13** were thermolysed alone and no reaction occurred. Further, d^8-toluene solutions of both **1** and **3** were heated for prolonged periods (three days for **3** and five days for **1**) and monitored by nmr spectroscopy. Provided exclusion of air was rigorous, then both samples essentially remained unchanged.

These nmr experiments, then, seem to rule out the bis(imido) compounds as intermediates, leaving [Mo(O)(NR)(etc)$_2$] as the most plausible intermediate. This has been suggested previously in an earlier paper from this group[18].
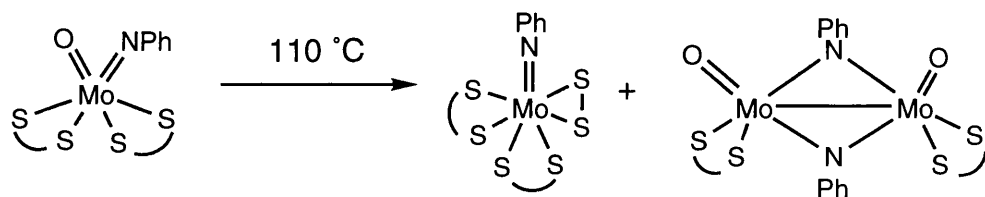
If the known oxo-imido species is the intermediate, loss of a dithiocarbamate ligand (as tetraethyldithiuram disulfide) would give a molybdenum (V) centre which could then dimerise to produce the above dimeric compound.

To check the plausibility of this intermediate, a d^8-toluene solution of [Mo(O)(NPh)(etc)$_2$] (formed on decomposition of 1) was heated in a sealed nmr tube and subsequent changes were monitored by nmr spectroscopy. On refluxing, the solution gradually changed from yellow to green. Accompanying this change in colour was an increase in complexity of the ^{1}H nmr spectrum. Resonances due to [Mo(O)(NPh)(etc)$_2$] diminished while resonances assigned to both [Mo(NPh)(S$_2$)(etc)$_2$] and [Mo$_2$O$_2$(μ-NPh)$_2$(etc)$_2$] appeared. The spectra of these two are highly complex, especially for the ethyl and methyl protons of the dithiocarbamate ligands. This makes full assignment of the spectra difficult, however, it is certain that two new products have formed, whose aryl regions and the general fit of the spectra compare favourably with the two complexes aforementioned. After sixteen hours of thermolysis, the oxo-imido species had completely disappeared. Thus, it has been shown that the oxo-imido compound is an intermediate in the formation of the imido-disulfide and molybdenum (V) dimeric compounds upon the thermolysis reaction of [MoO$_2$(etc)$_2$] with isocyanates and a reaction pathway is suggested below;
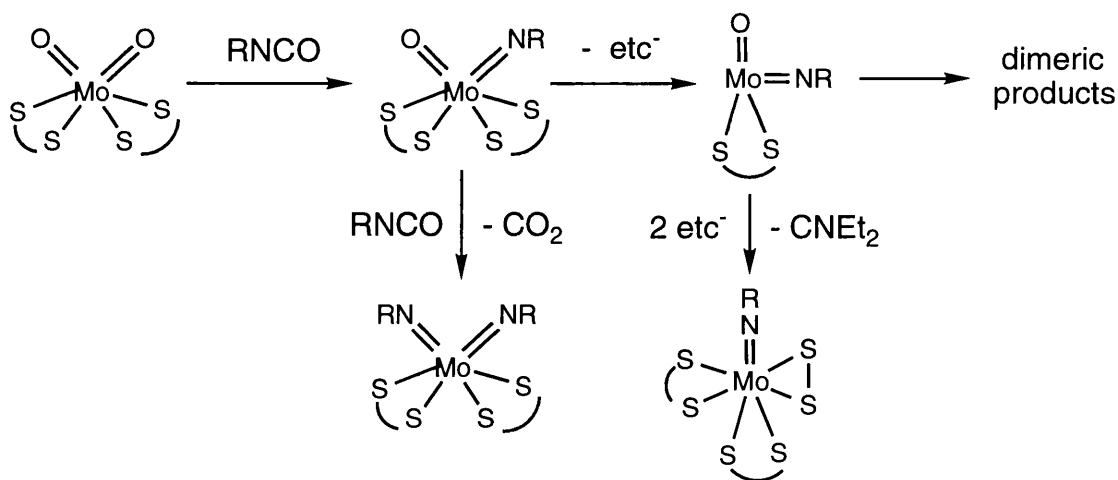
Initial substitution of the oxo for the imido occurs upon reaction with the isocyanate. This is, however, unstable under reaction conditions (refluxing toluene) and undergoes dithiocarbamate loss to give the coordinatively-unsaturated molybdenum (V) complex [Mo(O)(NR)(etc)]. This can then go in two directions - (i) rapid dimerization to give the dimer; (ii) it is attacked by free dithiocarbamate, undergoing oxo subsitution (previously seen at molybdenum (VI) centres by Weiss and co-workers[157]). The double sulfur-carbon cleavage process could also occur at this point, with exclusion of the organic fragment (Et$_2$NC), finally giving the imido-disulfide compound.

Summary

In this thesis, we have introduced a series of new molybdenum bis(imido) complexes of the type, [Mo(NR)$_2$(S$_2$CNEt$_2$)$_2$]. They have been synthesised by addition of a diethyldithiocarbamate salt to the bis(imido) DME complexes, of general formula, [Mo(NR)$_2$Cl$_2$(DME)]. Some of these DME complexes have been prepared previously[100,101], though the majority of those presented in this thesis have not been reported elsewhere. Eleven of the diethyldithiocarbamate complexes are new, differing only by their imido substituents. Only two of these complexes are non-aryl (*tert*-butyl and adamantyl) while the rest are aryl with a combination of electron-releasing and electron with-drawing groups at different positions of the aryl ring. Five of these diethyldithiocarbamate complexes have been synthesised previously, four of which were prepared recently in this laboratory - namely, **3, 7, 8** and **13**[64,92].

The other complex, [Mo(NPh)$_2$(S$_2$CNEt$_2$)$_2$] **(1)**, was synthesised in 1979[38] and was the first complex to show a bent-linear conformation of its imido ligands. This complex was resynthesised during the course of this work and its structure, re-determined at room temperature, was confirmed. Crystal structures of [Mo(N^{t}Bu)$_2$(S$_2$CNEt$_2$)$_2$] **(2)** and [Mo(N(2-Me)C$_6$H$_4$)$_2$(S$_2$CNEt$_2$)$_2$] **(3)** were shown to exhibit linear-linear imido ligation.

Other bis(imido) complexes have also been synthesised with different ancillary ligands - dimethyldithiocarbamate, dithiophosphinate and xanthate. Furthermore, two new chromium bis(imido) complexes have also been prepared, namely [Cr(N^{t}Bu)$_2$(S$_2$CNEt$_2$)$_2$] and [Cr(N^{t}Bu)$_2$(S$_2$CNMe$_2$)$_2$].

VT solution nmr spectroscopy has confirmed the fluxionality of the imido ligands in all complexes. Given the lack of success in growing crystals, solid-state ^{13}C nmr spectroscopy has been used to discern structural information. Using the data from those complexes whose structures are known (**1, 2, 3, 7** and **8**), a direct relationship between the difference in ppm of the *ipso*-carbon (or α-carbon) peaks and the difference in imido angles has been established. Of the structurally-unknown complexes, only those arylimido complexes without *ortho*-substituents suggest bending in an imido ligand.

Of note is that the deuterated phenylimido complex, **15**, is the only other complex which is predicted to have a bent-linear imido conformation, as for **1**. As absolute imido angles are not calculated, it is difficult to suggest where the cross-over point (from linear-linear to bent-linear) in this ppm/angle relationship lies. However, the arylimido complexes with methyl groups in the 3- and 4-positions on the ring are those closest to reaching this status. MO calculations, based on Extended Hückel theory, suggest that, even for **1**, there is negligible preference for linear-linear or bent-

linear imido ligation. Other molecular interactions, like crystal packing forces, are cited as the dominant structural influence.

For those other bis(imido) complexes, the most interesting suggestion (from interpretation of its ^{13}C solid-state spectrum) is that [Mo(NPh)$_2$(S$_2$CNMe$_2$)$_2$] (17) has linear-linear imido ligation, contrasting with its sister complex, 1. Powder diffraction spectra have indicated that the chromium and molybdenum bis(*tert*-butyl) imido complexes do not have the same structure.

Reactivity with other simple molecules has been investigated, with differing amounts of success. The most successful of those studied was the reaction with hydrogen sulfide to form imido-disulfide complexes, [Mo(NR)(S$_2$)(S$_2$CNEt$_2$)$_2$] (32, 33, 34, 35 and 36). A further complex was formed with 7 and identified as the dimeric product 37, [{Mo(N(2,6-^{i}Pr$_2$C$_6$H$_3$))$_2$(etc)}$_2$(μ-S)(μ^2-η^2-S$_2$)], by X-ray crystallography. Reaction of 13 with Lawesson's reagent also produced the imido-disulfide complex 38, [Mo(N(2,6-Cl$_2$C$_6$H$_3$))(S$_2$)(S$_2$CNEt$_2$)$_2$], which was confirmed by X-ray crystallography.

Reaction of 2 and 7 with tetrafluoroboric and trifluoroacetic acids gave a variety of bis(amido), imido-amido and also imido-tris(dithiocarbamate) cations. Hydrolysis and further reaction of the bis(amido) cation of 7 (26) led to the formation of 27, [{Mo(N(2,6-^{i}Pr$_2$C$_6$H$_3$))$_2$(etc)(μ-MoO$_4$)$_2$}$_2$]; its crystal structure showed molybdenum-imido centres to be bridged by molybdate groups. Hydrolysis of the oxo-imido species 23 led to the formation of a thionitrosyl complex 24, [Mo(NS)(etc)$_3$] which was characterized by X-ray crystallography. Reactions of 2 and 3 with triphenylphosphine were monitored by ^{31}P{^{1}H} nmr spectroscopy; in both reactions, a resonance for the relevant phosphine-imine was observed. Exchange of imido substituents was observed by ^{1}H nmr upon reaction of 2 with aniline.

The reaction of a bis(oxo) species, [Mo(O)$_2$(S$_2$CNEt$_2$)$_2$], with isocyanate to form an imido-disulfide complex, [Mo(NR)(S$_2$)(S$_2$CNEt$_2$)$_2$] had been shown (earlier in this laboratory) to be general for a wide range of isocyanates[18,22]. Studying the reaction using phenyl isocyanate, a reaction pathway has been suggested. The intermediate oxo-imido species (formed from the bis(oxo) complex and isocyanate) is unstable in refluxing toluene and loses a dithiocarbamate to form [Mo(O)(NR)(etc)]. From here, rapid dimerization may occur (responsible for the dimeric product also observed) or it may be attacked by free dithiocarbamate, losing its oxo group, and a double sulfur-carbon cleavage of a dithiocarbamate occurs to leave the target imido-disulfide compound, [Mo(NPh)(S$_2$)(S$_2$CNEt$_2$)$_2$].

In short then, a wide range of molybdenum bis(imido) complexes has been made and their structures studied by X-ray crystallography and solid-state nmr

spectroscopy. The structures have been shown to be dependent not only on the imido substituents but also on ancillary ligands. Reactivity studies have been performed to a certain extent, which have highlighted the versatility of the imido ligand.

Chapter 6   Experimental

6.1 General

All preparations were carried out under an atmosphere of dinitrogen using a dual dinitrogen/vacuum line fitted with several two-way tap outlets or a Vacuum Atmospheres HE-493 dry glove-box. A rotary vacuum pump provided a vacuum of approximately 10^{-2} Torr and oxygen-free dinitrogen was obtained from cylinders, used as supplied. Chemicals used were purchased from Aldrich Chemical Co., Fluka, Lancaster Synthesis, Avocado and Janssen and used as supplied, except for: solvents which were dried before use, as detailed below; amines were distilled prior to use; $[NH_4(S_2CNEt_2)]$ was dried under vacuum; $[Na(S_2CNEt_2).3H_2O]$ was dehydrated *in vacuo* whilst being heated at $80\,^\circ C^{84}$ and $[Na(S_2CNMe_2).3H_2O]$ was dehydrated in a vacuum oven. Lecture bottles of gases were bought from Argo. NaS_2PPh_2 was supplied by Simon Redmond; $[Mo(NAr)_2(mtc)_2]$ (**39**) was drawn from stock which had been prepared earlier in this laboratory[64]; Hg_2Se, Al_2Se_3 and Se were supplied by Graham Shaw and Ivan Parkin[158]. Some compounds were made according to literature preparations as detailed in the text below.

Unless otherwise stated, all reactions were carried out in Schlenk flasks sealed with either glass Schlenk caps or rubber 'Subaseals'™. Liquids were transferred via stainless-steel cannulae by excess dinitrogen pressure. Filtration was achieved using such cannulae modified to accept a filter (glass micro-fibre) at one end. Solvents were refluxed over a suitable drying agent under a continuous stream of dinitrogen. Toluene and heptane were refluxed over sodium metal. Dimethoxyethane and tetrahydrofuran were refluxed over potassium metal. Dichloromethane and acetonitrile were refluxed over CaH_2. Diethylether, 40/60 and 30/40 petroleum ethers were refluxed over sodium/potassium (1:3) alloy. Methanol was refluxed over magnesium metal. Hexamethyldisiloxane was distilled. Solvents were then stored in ampoules over 4Å molecular sieves (except toluene and petrol which were stored over sodium metal and acetonitrile and methanol which were not stored over any drying agent). Solvents were degassed thoroughly before use by repeated evacuating and admitting of dinitrogen.

Chromatography was performed on columns of deactivated alumina (6% w/w water) made up with petrol. Solutions were absorbed onto approximately five grammes of alumina before chromatography.

Ultraviolet irradiation was produced by a Hanovia medium-power mercury lamp.

Microanalyses were performed by the in-house microanalytical department. Solid state ^{13}C and ^{15}N nmr spectroscopy was performed by ULIRS on a Bruker MSL300 spectrometer and mass spectrometry (FAB and EI) was performed by ULIRS

and the in-house mass spectrometry department.

Nmr spectra were recorded at 20°C on a Varian VXR400 spectrometer and referenced internally using residual solvent reference. ^{31}P spectra were referenced to a solution of [P(OMe)$_3$]. Air-sensitive samples were prepared in the glove-box in 507-PP tubes which were fitted with a Young's valve™ or which were sealed under vacuum. Chemical shifts (δ) are expressed in ppm and all couplings are in Hertz. Solvents used were CDCl$_3$, C$_6$D$_6$, C$_7$D$_8$, CD$_2$Cl$_2$ and CD$_3$OD. CDCl$_3$ was dried and stored over molecular sieves. C$_6$D$_6$ and C$_7$D$_8$ were dried over Na/K alloy. Note that all spectra were recorded in C$_6$D$_6$ unless otherwise stated. The following convention is used in the assigning of aryl protons in the spectra:
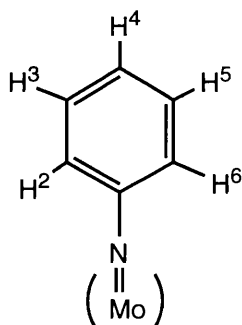
Infra-red spectra were recorded on a Nicolet 205 FT-IR spectrometer as KBr discs (unless otherwise stated). Uv-vis spectra were recorded on a Shimadzu UV-160A spectrometer; samples were prepared in the glove-box in holders fitted with a Young's tap™ (except where otherwise stated). Crystal structures resolved by X-ray diffraction were performed on a Nicolet R3m/V four-circle single crystal diffractometer using the SHELXTL PLUS programme[159] by Graeme Hogarth and Simon Redmond. Crystallographic tables are listed in Appendix III. Powder X-ray diffraction was performed on a Siemens D5000 diffractometer by Elizabeth MacLean. † and ‡ denote complexes originally made by the groups of Schrock and Gibson, respectively (references are provided where appropriate) and * denotes an experiment completed by Kayode Ajayi.

6.2 Synthesis of bis(imido) DME adducts

General Procedure[101]

White anhydrous sodium molybdate (2.00 g, 9.72 mmol) was degassed for several hours in a Schlenk tube with a magnetic stirrer bar. Dimethoxyethane (40 ml) was added and the solution stirred giving a white suspension. Triethylamine (5.4 ml, 38.98 mmol), trimethylsilylchloride (10.0 ml, 78 mmol) and two equivalents of the amine (19.44 mmol) were added via a degassed syringe to the stirring solution. The solution

---

changed colour and became thick with white solid. The solution was left to stir and to heat overnight at 65°C for eighteen hours. The solution (which had again changed colour) was filtered into another degassed Schlenk tube. The remaining solid was washed with diethyl ether until the washings were clear. The washings were transferred to the solution and the residue was discarded. Solvent was removed under reduced pressure from the solution to give a solid which was washed with petrol, dried *in vacuo* and transferred to the glove-box for storage.

† Synthesis of [Mo(NPh)₂Cl₂(DME)]

Two equivalents of aniline (18.54 mmol) was added to sodium molybdate, triethylamine and trimethylsilylchloride in dimethoxyethane, following the general procedure. Initially, the solution changed colour to pale yellow and finally to dark red; a dark red solid was recovered after recrystallization in ether - [Mo(NPh)₂Cl₂(DME)][100](72% yield).

^{1}H nmr obtained was in agreement with original data[100].
^{13}C CPMAS TOSS: 155.4 (ipso-C); 132.4, 130.6, 128.3, 120.9 (aromatic); 72.6 (OCH₂); 66.0, 64.9, 63.4 (OCH₃)

Synthesis of [Mo(N(2-Me)C₆H₄)₂Cl₂(DME)]

Two equivalents of o-toluidine (19.44 mmol) were added to sodium molybdate, triethylamine and trimethylsilylchloride in dimethoxyethane, following the general procedure. The solution changed colour to pale yellow and finally to dark red; a dark red solid was recovered after recrystallization in ether - [Mo(N(2-Me)C₆H₄)₂Cl₂(DME)] (65% yield).

^{13}C CPMAS TOSS: 158.0, 157.4, 156.2, 155.5 (ipso-C); 136.8, 134.3, 132.2, 131.5, 130.2, 127.9(aromatic); 71.3 (OCH₂); 66.6, 65.7 (OCH₃); 19.2 (2-CH₃C₆H₄)

† Synthesis of [Mo(N^{t}Bu)₂Cl₂DME)]

Two equivalents of *tert*-butylamine (18.5 mmol) were added to sodium molybdate, triethylamine and trimethylsilylchloride in dimethoxyethane, following the general procedure. The solution changed colour to deep yellow and a yellow solid was recovered after recrystallization in 30/40 petroleum ether - [Mo(N^{t}Bu)₂Cl₂(DME)][101],[100] (85% yield).

^{1}H nmr data was in agreement with original data[100].
^{13}C CPMAS NQS: 73.0, 72.2 (α-C); 64.9 (OCH₃); 31.4, 30.6 (C(CH₃)₃)

Synthesis of [Mo(N(2,4-Me₂C₆H₃))₂Cl₂DME)]

Two equivalents of 2,4-dimethylaniline (18.54 mmol) was added to sodium

molybdate, triethylamine and trimethylsilylchloride in dimethoxyethane, following the general procedure. The solution changed colour to pale yellow and finally to dark red; a dark red solid was recovered after recrystallization in ether - [Mo(N(2,4-Me$_2$C$_6$H$_3$))$_2$Cl$_2$(DME)] (80 % yield).

nmr: ^{1}H: δ 7.53 (d, 2H, J 7.3, H^6); 6.65 (d, 2H, J 7.3, H^5 - overlapping); 6.64 (s, 2H, H^3); 3.47 (s broad, 4H, OCH_2); 3.29 (s, 6H, OCH_3); 2.51 (s, 6H, (2-CH_3)C$_6$H$_3$CH$_3$); 1.99 (s, 6H, (4-CH_3)C$_6$H$_3$CH$_3$)

Synthesis of [Mo(N(3,4-Me$_2$C$_6$H$_3$))$_2$Cl$_2$(DME)]

Two equivalents of 3,4-dimethylaniline (18.54 mmol) was added to sodium molybdate, triethylamine and trimethylsilylchloride in dimethoxyethane, following the general procedure. The solution changed colour to pale yellow and finally to dark red; a dark red solid was recovered after recrystallization in ether - [Mo(N(3,4-Me$_2$C$_6$H$_3$))$_2$Cl$_2$(DME)] (82% yield).
C$_{20}$H$_{28}$N$_2$O$_2$Cl$_2$Mo$_1$;

Synthesis of [Mo(N(3,5-Me$_2$C$_6$H$_3$))$_2$Cl$_2$(DME)]

Two equivalents of 3,5-dimethylaniline (18.54 mmol) was added to sodium molybdate, triethylamine and trimethylsilylchloride in dimethoxyethane, following the general procedure. The solution changed colour to pale yellow and finally to dark red; a dark red solid was recovered after recrystallization in ether - [Mo(N(3,5-Me$_2$C$_6$H$_3$))$_2$Cl$_2$(DME)] (85% yield).
^{13}C CPMAS: 155.6 (ipso-C); 138.1, 136.2, 130.6, 127.3, 118.6 (aromatic); 71.9 (OCH$_2$); 64.4 (OCH$_3$); 22.2 (3,5-(CH$_3$)$_2$C$_6$H$_3$)

Synthesis of [Mo(N(2,6-F$_2$C$_6$H$_3$))$_2$Cl$_2$(DME)]

Two equivalents of 2,6-difluoroaniline (18.54 mmol) was added to sodium molybdate, triethylamine and trimethylsilylchloride in dimethoxyethane, following the general procedure. The solution changed colour to pale yellow and finally to dark red; a dark red solid was recovered after recrystallization in ether - [Mo(N(2,6-F$_2$C$_6$H$_3$))$_2$Cl$_2$(DME)] (65% yield).

Synthesis of [Mo(N(2-F)C$_6$H$_4$)$_2$Cl$_2$(DME)]

Two equivalents of o-fluoridine (18.54 mmol) was added to sodium molybdate, triethylamine and trimethylsilylchloride in dimethoxyethane, following the general procedure. The solution changed colour to pale yellow and finally to dark red; a dark red solid was recovered after recrystallization in ether - [Mo(N(2-F)C$_6$H$_4$)$_2$Cl$_2$(DME)] (73% yield).

---

† <u>Synthesis of [Mo(N(2,6-Me$_2$C$_6$H$_3$))$_2$Cl$_2$(DME)]</u>[64]

Two equivalents of 2,6-dimethylaniline (18.54 mmol) was added to sodium molybdate, triethylamine and trimethylsilylchloride in dimethoxyethane, following the general procedure. The solution changed colour to yellow and finally to dark red; a dark red solid was recovered after recrystallization in ether - [Mo(N(2,6-Me$_2$C$_6$H$_3$))$_2$Cl$_2$(DME)] (94% yield)[100].

<u>Synthesis of [Mo(N(2,6-Cl$_2$C$_6$H$_3$))$_2$Cl$_2$(DME)]</u>

Two equivalents of 2,6-dichloroaniline (18.54 mmol) was added to sodium molybdate, triethylamine and trimethylsilylchloride in dimethoxyethane, following the general procedure. The solution changed colour from pale yellow to dark red; a brown solid was recovered after recrystallization in ether - [Mo(N(2,6-Cl$_2$C$_6$H$_3$))$_2$Cl$_2$(DME)] (92% yield).

† <u>Synthesis of [Mo(N(2,6-^{i}Pr$_2$C$_6$H$_3$))$_2$Cl$_2$(DME)]</u>

Two equivalents of 2,6-diisopropylaniline (18.54 mmol) was added to sodium molybdate, triethylamine and trimethylsilylchloride in dimethoxyethane, following the general procedure. The solution changed colour to pale yellow and finally to dark red; a red solid was recovered after recrystallization in ether - [Mo(N(2,6-^{i}Pr$_2$C$_6$H$_3$))$_2$Cl$_2$(DME)] (90% yield)[100].

<u>Synthesis of [Mo(N(3-Me)C$_6$H$_4$)$_2$Cl$_2$(DME)]</u>

Two equivalents of m-toluidine (18.54 mmol) was added to sodium molybdate, triethylamine and trimethylsilylchloride in dimethoxyethane, following the general procedure. The solution changed colour to pale yellow and finally to dark red; a brown solid was recovered after recrystallization in ether - [Mo(N(3-Me)C$_6$H$_4$)$_2$Cl$_2$(DME)] (58% yield).

^{13}C CPMAS NQSTOSS: 157.0 (ipso-C); 143.3, 140.8, 139.7 (aromatic); 65.1, 61.3 (OCH$_3$); 21.2 (3-CH$_3$C$_6$H$_4$)

<u>Synthesis of [Mo(N(4-Me)C$_6$H$_4$)$_2$Cl$_2$(DME)]</u>

Two equivalents of p-toluidine (18.54 mmol) were dissolved in dimethoxyethane in a Schlenk tube and added *via* a cannula to sodium molybdate, triethylamine and trimethylsilylchloride in dimethoxyethane, following the general procedure. The solution changed colour to pale yellow and finally to dark red; a brown solid was recovered after recrystallization in ether - [Mo(N(4-Me)C$_6$H$_4$)$_2$Cl$_2$(DME)] (60% yield).

^{13}C CPMAS NQSTOSS: 156.9 (ipso-C); 140.7, 139.5 (aromatic); 65.0, 61.2 (OCH$_3$);

22.5, 21.1(4-CH$_3$C$_6$H$_4$)

Synthesis of [Mo(Nadm)$_2$Cl$_2$(DME)]

Two equivalents of 1-adamantamine (18.54 mmol) were dissolved in a Schlenk tube and added *via* a cannula to sodium molybdate, triethylamine and trimethylsilylchloride in dimethoxyethane, following the general procedure. The solution changed colour to yellow and a yellow solid was recovered after recrystallization in 30/40 petroleum ether - [Mo(Nadm)$_2$Cl$_2$(DME)] (90% yield).

† Synthesis of [Mo(NC$_6$F$_5$)$_2$Cl$_2$(DME)]

Two equivalents of 2,3,4,5,6-pentafluoroaniline (18.54 mmol) was added to sodium molybdate, triethylamine and trimethylsilylchloride in dimethoxyethane, following the general procedure. The solution changed colour to dark red and a dark red solid was recovered after recrystallization in ether - [Mo(NC$_6$F$_5$)$_2$Cl$_2$(DME)][100] (62% yield). ^{13}C CPMAS TOSS: 138.2 (C-F); 131.9 (ipso-C); 72.3 (OCH$_2$); 63.9 (OCH$_3$)

Synthesis of [Mo(NC$_6$D$_5$)$_2$Cl$_2$(DME)]

Two equivalents of 2,3,4,5,6-pentadeuteroaniline (18.54 mmol) was added to sodium molybdate, triethylamine and trimethylsilylchloride in dimethoxyethane, following the general procedure. The solution changed colour to dark red and a dark red solid was recovered after recrystallization in ether - [Mo(NC$_6$D$_5$)$_2$Cl$_2$(DME)] (70% yield). ^{13}C CPMAS TOSS: 155.2 (ipso-C); 130.1(broad), 125.2, 120.4 (aromatic); 72.3 (OCH$_2$), 66.0, 64.8, 63.3 (OCH$_3$)

6.3   Synthesis of bis(imido)bis(dithiocarbamate) complexes
General Procedure

[Mo(NR)$_2$Cl$_2$(DME)] was reacted with two equivalents of ammonium diethyldithiocarbamate or anhydrous sodium diethyldithiocarbamate by stirring in ether in a Schlenk tube. After stirring for twelve hours, the reaction mixture was filtered into another degassed Schlenk tube. The residue was washed with ether and washings transferred to the solution. Most of the solvent was removed under reduced pressure and the compound was left to recrystallize at -20°C. The first recrystallized product was washed with benzene and the mixture filtered. The benzene was removed under reduced pressure, the residue dissolved in ether and left to recrystallize at -20°C.

Synthesis of [Mo(NPh)$_2$(etc)$_2$] (1)

[Mo(NPh)$_2$Cl$_2$(DME)] (4.56 mmol) was reacted with two equivalents of sodium

diethyldithiocarbamate (9.2 mmol) in ether, following the general procedure. Dark red microcrystalline solid was isolated from the ethereal solution and identified as [Mo(NPh)$_2$(etc)$_2$] **(1)** (53% yield). Crystals also grew in the ethereal solution and a suitable one was chosen for X-ray diffraction crystallography.

C$_{22}$H$_{30}$N$_4$S$_4$Mo$_1$;

ir (cm^{-1}): 1501s, 1468m, 1431s, 1383m, 1357w, 1266s, 1207w, 1146m, 1095m, 1068m, 1020m, 803w, 755w, 686m, 670w

nmr: ^{1}H : 7.47 (d, 4H, J 7.3, H^{2,6}); 6.97 (t, 4H, J 7.5, H^{3,5}); 6.70 (t, 2H, J 7.4, H^4); 3.25 (q, 8H, J 7.0, CH_2CH$_3$); 0.74 (t, 12H, J 7.1, CH$_2$CH_3)

^{13}C{^{1}H}: 202.8 (C=N); 158.7 (ipso-C); 128.6, 125.3, 123.4 (aromatic); 46.1 (CH$_2$CH$_3$); 12.1 (CH$_2$CH$_3$)

^{13}C CPMAS TOSS: 200.7 (C=N); 161.5, 156.5 (ipso-C); 130.1; 128.6; 126.7 (aromatic); 47.5, 44.5 (CH$_2$CH$_3$); 13.8, 12.6 (CH$_2$CH$_3$)

Mass Spec.(EI) : M$^+$ 575; fragmentation - 486 (-NPh), 429 (-etc), 397 (-2NPh), 369 (-NPh -etc)

Elemental Analyses - found(calculated)%: C 45.56(45.98); H 5.28(5.26); N 9.63(9.75); S 21.66(22.30)

Synthesis of [Mo(N(^{t}Bu)$_2$(etc)$_2$] (2)

[Mo(N^{t}Bu)$_2$Cl$_2$(DME)] (4.56 mmol) was reacted with two equivalents of sodium diethyldithiocarbamate (9.2 mmol) in ether, following the general procedure. Orange microcrystalline solid was isolated from the ethereal solution and identified as [Mo(N^{t}Bu)$_2$(etc)$_2$] **(2)** (60% yield). Orange crystals grew in this solution and a suitable one was selected for X-ray diffraction crystallography.

C$_{18}$H$_{38}$N$_4$S$_4$Mo$_1$;

ir (cm^{-1}): 1497m, 1429m, 1263s, 1209m, 1097s, 1022s, 802s

nmr: ^{1}H : 3.36 (q, 8H, J 7.0 ,CH_2CH$_3$); 1.57 (s, 18H, C(CH_3)$_3$); 0.82 (t, 12H, J 7.1, CH$_2$CH_3)

^{13}C{^{1}H} : 203.9 (C=N); 71.2 (α-C); 45.8 (CH$_2$CH$_3$); 31.3 (C(CH$_3$)$_3$); 12.4 (CH$_2$CH$_3$)

^{13}C CPMAS: 203.3, 201.4 (C=N); 71.7, 69.7 (α-C); 47.2, 44.4 (CH$_2$CH$_3$); 32.1 (C(CH$_3$)$_3$); 14.3, 13.0 (CH$_2$CH$_3$)

^{15}N CPMAS: 373K: -214.1, -209.1 (C=N); 293K: -214.5, -209.0 (C=N)

Mass Spec. (EI): M$^+$ 536; fragmentation - 465 (-N^{t}Bu), 316 (-N^{t}Bu -etc)

Elemental Analyses - found(calculated)%: C 39.85(40.43); H 6.82(7.16); N 10.22(10.48); S 24.06(23.99)

melting point: 144°C

Synthesis of [Mo(N(2-Me)C$_6$H$_4$)$_2$(etc)$_2$] (3)

[Mo(N(2-Me)C$_6$H$_4$)$_2$Cl$_2$(DME)] (4.56 mmol) was reacted with two equivalents of ammonium diethyldithiocarbamate (9.2 mmol) in ether, following the general procedure. Dark brown microcrystalline solid was isolated from the ethereal solution and identified as [Mo(N(2-Me)C$_6$H$_4$)$_2$(etc)$_2$] (3) (45% yield). A crystal suitable for X-ray diffraction crystallography was grown upon slow diffusion of petrol into a benzene solution of the compound in air.

Note that the compound decomposed when dissolved in CDCl$_3$, even when sealed in an inert atmosphere.

C$_{24}$H$_{34}$N$_4$S$_4$Mo$_1$;

ir (cm^{-1}): 1633w, 1497s, 1432s, 1295m, 1273s, 1206m, 1146m, 1076m, 759m

nmr: ^{1}H (C$_7$D$_8$): 333K: 7.36 (d, 2H, J 7.9, H^6); 6.83 (dd, 4H, J 7.7, H^{3,5}); 6.62 (t, 2H, J 7.4, H^4); 3.33 (q, 8H, J 7.1, CH$_2$CH$_3$); 2.44 (s, 6H, (2-CH$_3$)C$_6$H$_4$); 0.836 (t, 12H, J 7.1, CH$_2$CH$_3$)

213K: 7.55 (d, 2H, J 7.6, H^6); 6.80 (t,2H, J 7.6, H^5); 6.72 (d,2H, J 7.5, H^3); 6.61 (t,2H, J 7.3, H^4); 3.15 (bd, 8H, CH$_2$CH$_3$); 2.53 (s, 6H, (2-CH$_3$)C$_6$H$_4$); 0.57 (d, 12H, J 6.2, CH$_2$CH$_3$)

^{13}C{^{1}H} (C$_7$D$_8$) : 193K: 200.9 (C=N);157.8 (ipso-C); 130.5, 129.2, 126.3 (aromatic); 45.2, 45.0 (CH$_2$CH$_3$); 19.8 (2-CH$_3$(C$_6$H$_4$)); 12.3, 11.6 (CH$_2$CH$_3$)

333K: 203.2 ;158.2; 130.2, 129.9, 126.2; 45.8; 18.9; 12.3

^{13}C CPMAS TOSS: 202.4, 199 (C=N); 158.6, 157.3 (ipso-C); 134.3, 131.6, 130.1, 127.0 (broad), 122.6 (aromatic); 49.1, 45.9 (CH$_2$CH$_3$); 21.2, 19.8 (2-CH$_3$(C$_6$H$_4$)); 14.1, 12.8 (CH$_2$CH$_3$)

^{15}N CPMAS TOSS: 67, 55; -39; -75; -206

Mass Spec.(EI) : M$^+$ 604; fragmentation - 499 (-NAr), 457 (-etc), 352 (-NAr -etc)

Elemental Analyses - found(calculated)%: C 47.77(47.82); H 5.70(5.69); N 9.18(9.29); S 21.33(21.28)

Synthesis of [Mo(N(2,4-Me$_2$C$_6$H$_3$))$_2$(etc)$_2$] (9)

[Mo(N(2,4-Me$_2$C$_6$H$_3$))$_2$Cl$_2$(DME)] (4.56 mmol) was reacted with two equivalents of sodium diethyldithiocarbamate (9.2 mmol) in ether, following the general procedure. Brown microcrystalline solid was isolated from the ethereal solution and identified as [Mo(N(2,4-Me$_2$C$_6$H$_3$))$_2$(etc)$_2$] (55% yield).

C$_{26}$H$_{38}$N$_4$S$_4$Mo$_1$;

ir (cm^{-1}): 1497s, 1474m, 1456m, 1429m-s, 1357m, 1300m, 1274s, 1208m, 1148m, 1092w, 1073w, 814m

nmr: ^{1}H : 7.60 (d, 2H, J 7.9, H^6); 6.74 (d, 2H, J 8.1, H^5); 6.71 (s, 2H, H^3); 3.30 (q broad, 8H, J 6.1, CH$_2$CH$_3$); 2.65 (s, 6H, (2-CH$_3$)C$_6$H$_4$); 2.03 (s, 6H, (4-CH$_3$)C$_6$H$_3$); 0.79 (t, 12H, J 7.0, CH$_2$CH$_3$)

$^{13}C\{^1H\}$: 203.1 (C=N); 156.0 (ipso-C); 134.9, 130.7, 130.6, 127.0, 125.6 (aromatic); 45.7 (CH$_2$CH$_3$); 21.1((2-CH$_3$)C$_6$H$_3$); 19.0 ((4-CH$_3$)C$_6$H$_3$); 12.3 (CH$_2$CH$_3$)

^{13}C CPMAS TOSS: 202.0 (C=N); 155.5 (ipso-C); 138.5, 135.6; 133.9, 132.4; 130.4, 127.6, 126.8 (aromatic); 50.7, 45.7 (CH$_2$CH$_3$); 23.9, 23.3, 21.6, 19.6, 16.8, 13.3, 11.5

^{13}C CPMAS NQSTOSS: 202.0 (C=N); 155.5 (ipso-C);; 138.6, 135.6, 134.0, 132.4 (aromatic); 23.3, 19.6, 16.8; 13.3, 11.4

Mass Spec. (EI): M$^+$ 633; fragmentation - 513 (-NAr); 485, 483 (-etc); 361 (-NAr -etc)

Elemental Analyses - found(calculated)%: C 48.62(49.50); H 5.93(6.07); N 8.57(8.88); S 19.57(20.33)

Synthesis of [Mo(N(3,4-Me$_2$C$_6$H$_3$))$_2$(etc)$_2$] (10)

[Mo(N(3,4-Me$_2$C$_6$H$_3$))$_2$Cl$_2$(DME)] (4.56 mmol) was reacted with two equivalents of sodium diethyldithiocarbamate (9.2 mmol) in ether, following the general procedure. Brown microcrystalline solid was isolated from the ethereal solution and identified as [Mo(N(3,4-Me$_2$C$_6$H$_3$))$_2$(etc)$_2$] (10) (58% yield).

C$_{26}$H$_{38}$N$_4$S$_4$Mo$_1$;

ir(cm^{-1}): 1497vs, 1456m, 1429s, 1384s, 1336m, 1306m, 1275s, 1208m, 1147m, 1022m, 845m, 813m

nmr: ^1H : 7.42 (d, 2H, J 7.1, H^6); 7.41 (s, 2H, H^2); 6.81 (d, 2H, J 7.1, H^5); 3.29 (q, 8H, J 7.0, CH$_2$CH$_3$); 1.91 (s, 6H, (3-CH$_3$)C$_6$H$_3$); 1.84 (s, 6H, (4-CH$_3$)C$_6$H$_3$); 0.77 (t, 12H, J 7.2, CH$_2$CH$_3$)

$^{13}C\{^1H\}$: 203.2 (C=N); 157.8 (ipso-C); 136.3, 134.1, 129.7, 125.2, 121.8 (aromatic); 40.5 (CH$_2$CH$_3$); 19.6 ((3-CH$_3$)C$_6$H$_3$); 19.4 ((4-CH$_3$)C$_6$H$_3$); 12.3 (CH$_2$CH$_3$)

^{13}C CPMAS TOSS: 202.1 (C=N); 158.2, 155.4 (C=N); 136.1, 130.4, 124.6, 122.9 (aromatic); 48.0 (CH$_2$CH$_3$); 21.2 ((3-CH$_3$)C$_6$H$_3$) and/or ((4-CH$_3$)C$_6$H$_3$) ; 14.8 (CH$_2$CH$_3$)

Mass Spec. (EI): M$^+$ 632; fragmentation - 513 (-NAr), 485 (-etc), 397 (-2NAr), 366 (-etc-NAr)

Elemental Analyses - found(calculated)%: C 48.71(49.50); H 6.20(6.07); N 8.69(8.88); S 20.01(20.33)

Synthesis of [Mo(N-3,5-Me$_2$C$_6$H$_3$)$_2$(etc)$_2$] (11)

[Mo(N(3,5-Me$_2$C$_6$H$_3$))$_2$Cl$_2$(DME)] (4.56 mmol) was reacted with two equivalents of sodium diethyldithiocarbamate (9.2 mmol) in ether, following the general procedure. Purple microcrystalline solid was isolated from the ethereal solution and identified as [Mo(N(3,5-Me$_2$C$_6$H$_3$))$_2$(etc)$_2$] (11) (48% yield).

C$_{26}$H$_{38}$N$_4$S$_4$Mo$_1$;

ir (cm^{-1}): 1629m, 1613m, 1596m, 1529s, 1501m, 1456m-s, 1438s, 1382m, 1354m,

1323w, 1274s, 1263s, 1206m, 1146m, 1095s, 1078s, 1021s, 845w, 803m-s

nmr: ^{1}H : 7.21 (s, 4H, H^{2,6}); 6.44 (s, 2H, H^4); 3.29 (q, 8H, J 7.0, CH$_2$CH$_3$); 1.96 (s, 12H, (3,5-CH$_3$)C$_6$H$_3$); 0.77 (t, 12H, J 7.1, CH$_2$CH$_3$)

^{13}C{^{1}H} : 203.1 (C=N); 158.1 (ipso-C); 137.8 (C^{3,5}); 127.3 (C^{2,6}); 121.4 (C^4); 45.8 (CH$_2$CH$_3$); 21.1 ((3,5-CH$_3$)C$_6$H$_3$); 12.3 (CH$_2$CH$_3$)

^{13}C CPMAS TOSS: 201.4 (C=N); 160.4, 156.8 (ipso-C); 139.1, 137.7 (C^{3,5}); 130.7; 124.9(broad) (C^{2,6}); 119.0; 118.1 (C^4); 47.9(broad); 43.9(broad) (CH$_2$CH$_3$); 25.2; 23.7; 22.5 ((3,5-CH$_3$)C$_6$H$_3$); 15.5; 14.7; 12.1 (CH$_2$CH$_3$)

Mass Spec. (EI) : M$^+$ 633; fragmentation - 514 (-NAr); 486,485 (-etc); 398,397,395 (-2NAr); 366 (-NAr -etc)

Elemental Analyses - found(calculated)%: C 48.51(49.50); H 6.11(6.07); N 8.40(8.88)

Synthesis of [Mo(N(2,6-F$_2$C$_6$H$_3$))$_2$(etc)$_2$] (12)

[Mo(N(2,6-F$_2$C$_6$H$_3$))$_2$Cl$_2$(DME)] (4.56 mmol) was reacted with two equivalents of sodium diethyldithiocarbamate (9.2 mmol) in ether, following the general procedure. Dark red microcrystalline solid was isolated from the ethereal solution and identified as [Mo(N(2,6-F$_2$C$_6$H$_3$))$_2$(etc)$_2$] (12) (38% yield).

C$_{22}$H$_{26}$N$_4$F$_4$S$_4$Mo$_1$;

ir (cm^{-1}): 1508vs, 1468vs, 1436s, 1384vs, 1275s, 1265s, 1236m, 1208w, 1019m, 1001s, 965w, 649w

nmr: ^{1}H : 6.37 (dd, 4H, J 7.6, H^{3,5}); 6.16-6.08 (m, 2H, H^4); 3.19 (q, 8H, J 6.7, CH$_2$CH$_3$); 0.72 (t, 12H, J 7.1, CH$_2$CH$_3$)

^{13}C{^{1}H} : 202.6 (C=N); 157.3 (ipso-C); 154.8 (C-F); 128.6, 127.4, 127.2, 124.0 (aromatic); 111.1, 110.9; 45.6 (CH$_2$CH$_3$); 12.2 (CH$_2$CH$_3$)

^{13}C NQS: 201.5 (C=N); 199.5 (C-F); 136.2 (ipso-C); 13.0 (CH$_2$CH$_3$)

Mass Spec. (EI): M$^+$ 647; fragmentation - 520 (-NAr), 500 (-etc)

Elemental Analyses - found(calculated)%: C 39.99(40.87); H 4.10(4.02); N 8.45(8.67); S 20.21(19.81)

Synthesis of [Mo(N(2-F)C$_6$H$_4$)$_2$(etc)$_2$] (6)

[Mo(N(2-F)C$_6$H$_4$)$_2$Cl$_2$(DME)] (4.56 mmol) was reacted with two equivalents of sodium diethyldithiocarbamate (9.2 mmol) in ether, following the general procedure. Dark red microcrystalline solid was isolated from the ethereal solution and identified as [Mo(N(2-F)C$_6$H$_4$)$_2$(etc)$_2$] (6)(42% yield).

C$_{122}$H$_{28}$N$_4$F$_2$S$_4$Mo$_1$;

nmr: ^{1}H : 7.54 (t, 2H, J 7.0, H^3); 6.68 (t, 2H, J 8.0, H^5); 6.64 (t, 2H, J 7.0, H^4); 3.21 (bd, 8H, CH$_2$CH$_3$); 0.73 (t, 12H, J 6.9, CH$_2$CH$_3$) (fourth aryl proton is presumed hidden)

^{13}C CPMAS: 201.2, 199.4 (C=N); 151.0 (C-F); 146.2 (ipso-C); 13.5, 12.8 (CH$_2$CH$_3$)

Mass Spec.(EI): M$^+$ 612; fragmentation - 503 (-NAr), 465 (-etc)

Elemental Analyses - found(calculated)%: C 42.16(43.26); H 4.68(4.62); N 8.75(9.17); S 20.07(21.00)

Synthesis of [Mo(N(2,6-Me$_2$C$_6$H$_3$))$_2$(etc)$_2$] (8)[64]

[Mo(N(2,6-Me$_2$C$_6$H$_3$))$_2$Cl$_2$(DME)] (9.2 mmol) was reacted with two equivalents of sodium diethyldithiocarbamate (9.2 mmol) in ether. After stirring for twelve hours, the reaction mixture had solvent removed under reduced pressure and was separated by column chromatography. The main product was eluted with 3:10 dichloromethane/petrol and identified as [Mo(N(2,6-Me$_2$C$_6$H$_3$))2(etc)$_2$] (8)(80% yield).

^{1}H nmr data was in agreement with original data[64].

^{13}C CPMAS: 199.9 (C=N); 157.5 (ipso-C); 133.3, 128.2, 125.7 (aromatic); 47.5, 46.3 (CH$_2$CH$_3$); 20.3, 18.9 ((2,6-CH$_3$)C$_6$H$_3$); 11.4 (CH$_2$CH$_3$)

Mass Spec. (EI): M$^+$ 633

Elemental Analyses found(calculated)%: C 49.37(50.31); H 5.63(4.55); N 8.68(9.02); S 20.14(20.66)

Synthesis of [Mo(N(2,6-Cl$_2$C$_6$H$_3$))$_2$(etc)$_2$] (13)[64]

[Mo(N(2,6-Cl$_2$C$_6$H$_3$))$_2$Cl$_2$(DME)] (4.56 mmol) was reacted with two equivalents of ammonium diethyldithiocarbamate (9.2 mmol) in ether. After stirring for twelve hours, the reaction mixture had solvent removed under reduced pressure and was separated by column chromatography. The main product was eluted with 3:10 dichloromethane/petrol and identified as [Mo(N(2,6-Cl$_2$C$_6$H$_3$))2(etc)$_2$] (13) (75 % yield). ^{1}H nmr was in agreement with original data[64].

^{13}C CPMAS NQSTOSS: 199.9 (C=N); 152.1 (ipso-C); 134.7, 130.1, 126.9, 123.1 (aromatic); 11.4 (CH$_2$CH$_3$)

Mass Spec.(EI): M$^+$ 712

Elemental Analyses - found(calculated)%: C 37.48(37.09); H 3.94(3.68); N 7.63(7.86); S 18.07(18.00); Cl 19.72(19.90)

Synthesis of [Mo(N(2,6-^{i}Pr$_2$C$_6$H$_3$))$_2$(etc)$_2$] (7)[92]

[Mo(N(2,6-^{i}Pr$_2$C$_6$H$_3$))$_2$Cl$_2$(DME)] (4.56 mmol) was reacted with two equivalents of ammonium diethyldithiocarbamate (9.2 mmol) in diethyl ether[64]. After stirring for twelve hours, the reaction mixture had solvent removed under reduced pressure and was separated by column chromatography. The main product was eluted with 1:4 dichloromethane/petrol and identified as [Mo(N(2,6-^{i}Pr$_2$C$_6$H$_3$))2(etc)$_2$] (7) (85% yield). ^{1}H nmr was in agreement with original data[92].

---

^{13}C CPMAS: 200.3 (C=N); 154.0 (ipso-C); 145.0, 142.2, 126.4, 123.0 (aromatic); 45.8 (CH$_2$CH$_3$); 29.7, 27.7, 27.3, 25.2, 21.1, 14.7 (^{i}Pr); 13.9 (CH$_2$CH$_3$)

Mass Spec.(EI): M$^+$ 744

Synthesis of [Mo(N(3-Me)C$_6$H$_4$)$_2$(etc)$_2$] (4)

[Mo(N(3-Me)C$_6$H$_4$)$_2$Cl$_2$(DME)] (4.56 mmol) was reacted with two equivalents of ammonium diethyldithiocarbamate (9.2 mmol) in ether, following the general procedure. Brown solid was isolated from the ethereal solution and identified as [Mo(N(3-Me)C$_6$H$_4$)$_2$(etc)$_2$] (4)(23 % yield).

C$_{24}$H$_{34}$N$_4$S$_4$Mo$_1$;

ir (cm^{-1}): 1527s, 1458s, 1402s, 1278m, 1205w, 793w

nmr: ^{1}H : 7.02 (d, 4H, J 7.6, H^{2,6}); 6.56 (t, 2H, J 7.6, H^5); 6.49 (s, 2H, H^4); 3.79-3.92 (m, 8H, CH$_2$CH$_3$); 2.24 (s, 6H, 3-CH$_3$); 1.46 (t, 12H, J 7.0, CH$_2$CH$_3$)

Synthesis of [Mo(N(4-Me)C$_6$H$_4$)$_2$(etc)$_2$] (5)

[Mo(N(4-Me)C$_6$H$_4$)$_2$Cl$_2$(DME)] (4.56 mmol) was reacted with two equivalents of ammonium diethyldithiocarbamate (9.2 mmol) in ether, following the general procedure. Brown solid was isolated from the ethereal solution and identified as [Mo(N(4-Me)C$_6$H$_4$)$_2$(etc)$_2$] (5)(20 % yield).

C$_{24}$H$_{34}$N$_4$S$_4$Mo$_1$;

nmr: ^{1}H : 7.50 (d, 4H, J 7.9, H^{2,6}); 6.79 (d, 4H, J 7.9, H^{3,5}); 3.27 (q, 8H, J 7.0, CH$_2$CH$_3$)); 1.9 (s, 6H, 4-CH$_3$); 0.75 (t, 12H, J 7.0, CH$_2$CH$_3$))

^{13}C CPMAS: 203.0 (C=N); 155.5, 151.7 (ipso-C); 46.8 (CH$_2$CH$_3$); 22.0 ((4-CH$_3$) C$_6$H$_4$); 13.4 (CH$_2$CH$_3$)

Synthesis of [Mo(Nadm)$_2$(etc)$_2$] (14)

[Mo(Nadm)$_2$Cl$_2$(DME)] (4.56 mmol) was reacted with two equivalents of sodium diethyldithiocarbamate (9.2 mmol) in ether, following the general procedure. Orange microcrystalline solid was isolated from the ethereal solution and identified as [Mo(Nadm)$_2$(etc)$_2$] (14)(70% yield).

C$_{30}$H$_{50}$N$_4$S$_4$Mo$_1$;

ir (cm^{-1}): 1490s, 1449m, 1426s, 1301m, 1270s, 1211m, 1144m, 1095m

nmr: ^{1}H : 3.40 (q, 8H, J 7.0, CH$_2$CH$_3$); 2.35 (s, 12H, CH$_2$a); 2.01 (s, 6H, CHc); 1.58 (d, 6H, CH$_2$b - 2nd order coupling); 1.50 (d, 6H, CH$_2$b - 2nd order coupling); 0.86 (t, 12H, J 7.0, CH$_2$CH$_3$)

^{13}C{^{1}H} : 204.2 (C=N); 72.1 (C(CH$_x$)$_3$); 45.8 (CH$_2$CH$_3$); 45.0 (CH$_2$a); 36.7 (CH); 30.2 (CH$_2$b); 12.5 (CH$_2$CH$_3$)

^{13}C CPMAS: 202.6 (C=N); 71.7 (C(CH$_3$)$_3$); 45.8 (CH$_2$CH$_3$); 45.6 (CH$_2$a); 37.4 (CH);

30.7; 30.4 (CH_2b); 15.4; 13.1 (CH_2CH_3)

Mass Spec.(EI): M^+ 692; fragmentation 543 (-Nadm)

Elemental Analyses - found(calculated)%: C 51.97(52.15); H 7.31(7.29); N 8.03(8.11); S 18.72(18.56)

Synthesis of [Mo(NC$_6$F$_5$)$_2$(etc)$_2$] (16)

[Mo(NC$_6$F$_5$)$_2$Cl$_2$(DME)] (4.56 mmol) was reacted with two equivalents of sodium diethyldithiocarbamate (9.2 mmol) in ether, following the general procedure. Dark red solid was isolated from the ethereal solution and identified as [Mo(NC$_6$F$_5$)$_2$(etc)$_2$] (16) (28% yield).

$C_{22}H_{20}N_4F_{10}S_4Mo_1$;

$^{13}C\{^1H\}$: 201.3 (C=N); 139.9 (ipso-C); 135.5; 135.3 (aromatic); 45.7, 44.5, 43.0 (CH_2CH_3); 12.1 (CH_2CH_3)

^{13}C CPMAS: 200.9 (C=N); 137.3 (ipso-C); 133.8 (aromatic); 49.9; 46.5 (CH_2CH_3); 14.9, 11.8 (CH_2CH_3)

^{13}C CPMAS TOSS: 200.9 (C=N); 133.7 (ipso-C); 49.8(CH_2CH_3); 14.9, 11.7 (CH_2CH_3)

^{13}C CPMAS NQSTOSS: 200.9 (C=N); 133.8 (ipso-C); 14.9, 11.7 (CH_2CH_3)

Mass Spec.(FAB): M^+ 756; fragmentation - 608 (-etc), 575 (-NAr), 460 (-2 etc), 427 (-NAr-etc)

Synthesis of [Mo(NC$_6$D$_5$)$_2$(etc)$_2$] (15)

[Mo(NC$_6$D$_5$)$_2$Cl$_2$(DME)] (4.56 mmol) was reacted with two equivalents of sodium diethyldithiocarbamate (9.2 mmol) in ether, following the general procedure. Dark red solid was isolated from the ethereal solution and identified as [Mo(NC$_6$D$_5$)$_2$(etc)$_2$] (15) (46% yield).

$C_{22}H_{20}N_4D_{10}S_4Mo_1$;

nmr: ^1H : 3.28 (q, 8H, J 7.1, CH_2CH_3); 0.77 (t, 12H, J 7.2, CH_2CH_3)

$^{13}C\{^1H\}$: 202.8 (C=N); 158.5 (ipso-C); 124.9, 124.7, 124.5; 123.2, 122.9, 122.6 (aromatic); 45.8 (CH_2CH_3); 12.3 (CH_2CH_3)

^{13}C CPMAS TOSS: 200.7; 161.2, 156.3; 129.6 (broad), 125.9, 120.2; 47.5, 44.6; 13.7, 12.6

Mass Spec.(EI): M^+ 584; fragmentation 490 (-NC$_6$D$_5$), 439 (-etc)

Elemental Analyses - found(calculated)%: C 43.44(45.19); H 5.17(6.89); N 9.14(9.58)

6.4   Experimental for Chapter 3
Synthesis of [Mo(NPh)$_2$(S$_2$CNMe$_2$)$_2$] (17)

[Mo(NPh)$_2$Cl$_2$(DME)] (4.56 mmol) was reacted with two equivalents of sodium dimethyldithiocarbamate (9.2 mmol) in ether, following the general procedure. The

compound was not very soluble in ether so the compound was extracted from the residue with benzene and also with dichloromethane. The benzene and dichloromethane solutions had solvent removed under reduced pressure, the residue dissolved in ether and this was also left for recrystallization. Black solid was isolated from the solution and identified as [Mo(NPh)$_2$(mtc)$_2$] (17) (40% yield).

$C_{18}H_{22}N_4S_4Mo_1$;

nmr: ^{1}H : 7.50 (d, 4H, J 8.1, H^{2,6}); 6.98 (t, 4H, J 7.5, H^{3,5}); 6.71 (t, 2H, J 7.5, H^4); 2.48 (s, 12H, NCH$_3$)

^{13}C CPMAS: 199.9 (C=N); 160.3 (ipso-C); 129.5, 128.2, 124.4, 123.8, 116.6 (aromatic); 39.7 (broad)(NCH$_3$)

Mass Spec.(EI): M$^+$ 521; fragmentation - 430 (-NPh), 398 (-mtc)

Elemental Analyses - found(calculated)%: C 39.00(41.69); H 4.22(4.28); N 10.41(10.80)

Synthesis of [Mo(N^{t}Bu)$_2$(S$_2$CNMe$_2$)$_2$] (18)

[Mo(N^{t}Bu)$_2$Cl$_2$(DME)] (4.5 mmol) was reacted with two equivalents of sodium dimethyldithiocarbamate (9.2 mmol) in ether, following the general procedure. Orange solid was isolated from the ethereal solution and identified as [Mo(N^{t}Bu)$_2$(mtc)$_2$] (18) (41% yield).

$C_{14}H_{30}N_4S_4Mo_1$;

nmr: ^{1}H : 2.61 (s, 12H, NCH$_3$); 1.58 (s, 18H, C(CH$_3$)$_3$)

^{13}C{^{1}H} : 204.9 (C=N); 71.1 (C(CH$_3$)$_3$); 40.3 (NCH$_3$); 31.4 (C(CH$_3$)$_3$)

^{13}C CPMAS: 204.1, 203.3 (C=N); 72.8, 69.9 (C(CH$_3$)$_3$); 42.4, 41.9 (NCH$_3$); 32.4, 31.8 (C(CH$_3$)$_3$)

Mass Spec.(EI): M$^+$ 480; fragmentation - 409 (-N^{t}Bu)

Elemental Analyses - found(calculated)%: C 31.78(35.13); H 6.26(6.32); N 10.65(11.71)

Synthesis of [Mo(NPh)$_2$(S$_2$PPh$_2$)$_2$] (20)

[Mo(NPh)$_2$Cl$_2$(DME)] (4.5 mmol) was reacted with two equivalents of sodium dithiophosphinate (9.2 mmol) in ether, following the general procedure. Dark red microcrystalline solid was isolated from the ethereal solution and identified as [Mo(NPh)$_2$(S$_2$PPh$_2$)$_2$] (20) (52% yield).

$C_{36}H_{30}N_4P_2S_4Mo_1$;

nmr: ^{1}H : 8.05-7.99 (ddd, 4H, PPh$_2$); 6.92 (m, 6H, PPh$_2$); 6.84 (t, 4H, J 7.6, H^{3,5}); 6.68 (t, 2H, J 7.3, H^4)

^{13}C{^{1}H} : 158.2 (ipso-C(imido)); 137.9 (d, J 78.9, (S$_2$P-C); 131.3, 126.7, 123.4 (aryl)

^{31}P{^{1}H}: 64.5

^{13}C CPMAS: 156.7, 155.1 (ipso-C(imido)); 139.0 (P-C); 132.3; 128.1; 124.5 (aryl)

^{31}P CPMAS: 66.6, 65.5

Elemental Analyses - found(calculated)%: C̲ 54.86(55.66); H̲ 3.82(3.89); N̲ 3.18(3.61); S̲ 16.41(16.51); P̲ 8.17 (7.97)

Synthesis of [Mo(N^{t}Bu)$_2$(S$_2$COEt)$_2$] (19)

[Mo(N^{t}Bu)$_2$Cl$_2$(DME)] (4.5 mmol) was reacted with two equivalents of sodium ethylxanthate (9.2 mmol) in ether, following the general procedure. Dark red microcrystalline solid was isolated from the ethereal solution and identified as [Mo(N^{t}Bu)$_2$(S$_2$COEt)$_2$] (19) (42% yield).

C$_{14}$H$_{28}$N$_2$O$_2$S$_4$Mo$_1$;

nmr: ^{1}H : 4.12 (q, 4H, J 7.2, OCH$_2$CH$_3$); 1.38 (s, 18H, C(CH$_3$)$_3$), 0.83 (t, 6H, J 7.0, OCH$_2$CH$_3$)

^{1}H (CDCl$_3$): 4.57 (q, 4H, J 7.2, OCH$_2$CH$_3$); 1.46 (t, 6H, J 7.0, OCH$_2$CH$_3$); 1.40 (s, 18H, C(CH$_3$)$_3$)

^{13}C{^{1}H} : 226.4 (S$_2$C); 71.9 (α-C); 69.1 (OCH$_2$); 30.9 (C(CH$_3$)$_3$); 13.5 (OCH$_2$CH$_3$)

^{13}C: 226.4 (S$_2$C); 71.9 (α-C); 70.6, 69.1, 67.6 (t, J 150, OCH$_2$); 32.8, 31.5, 30.3,29.1 (q, , J 128, C(CH$_3$)$_3$); 15.4, 14.1, 12.8, 11.6 (q, J 128, OCH$_2$CH$_3$)

^{13}C CPMAS NQS: 72.6 (α-C); 32.4, 30.2 (C(CH$_3$)$_3$); 15.3 (OCH$_2$CH$_3$)

^{13}C CPMAS FLIP: 225.9 (S$_2$C); 72.5(α-C); 70.8 (OCH$_2$); 32.4, 30.2 (C(CH$_3$)$_3$); 15.3 (OCH$_2$CH$_3$)

Synthesis of [Cr(N^{t}Bu)$_2$(etc)$_2$] (21)

This is a three-stage process.

Synthesis of [Cr(N^{t}Bu)$_2$(OSiMe$_3$)$_2$][72]

A heptane solution of [^{t}Bu(NH)(SiMe$_3$)] (72.0 mmol) was added to a heptane solution of [CrO$_2$Cl$_2$] (13.0 mmol) and the mixture was refluxed for 30 minutes. After cooling, the solution was filtered and the heptane was removed *in vacuo*. The solid was dissolved in hexamethyldisiloxane (~ 20 ml) and left to recrystallize at -20°C. A black crystalline solid (consisting of fine, large needles) was isolated from the solution and identified as [Cr(N^{t}Bu)$_2$(OSiMe$_3$)$_2$].

^{1}H nmr was in agreement with original data.[52]

Synthesis of [Cr(N^{t}Bu)$_2$Cl$_2$][160]

To a dichloromethane solution of [Cr(N^{t}Bu)$_2$(OSiMe$_3$)$_2$] (2.91 mmol) at 0°C was added (dropwise, with stirring and over fifteen minutes) a 1.0 M solution in heptane of BCl$_3$ (3.1 mmol). After addition of BCl$_3$, the mixture was allowed to come to room temperature and was stirred for a further two hours. The solvent was removed *in vacuo* and the solid was left to dry *in vacuo* for a further twelve hours to yield clups of

needles. The solid was extracted with hot heptane; the heptane was removed *in vacuo* and the dark red solid was dried *in vacuo*. This microcrystalline solid was identified as [Cr(N^{t}Bu)$_2$Cl$_2$].

^{1}H nmr was in agreement with original data[160].

Synthesis of [Cr(N^{t}Bu)$_2$(etc)$_2$] (21)

[Cr(N^{t}Bu)$_2$Cl$_2$] (0.94 mmol) was reacted with two equivalents of sodium diethyldithiocarbamate (1.90 mmol) in ether, following the general procedure as outined above (in 6.3). Dark red solid was isolated from the ethereal solution (and from a petrol solution) which was identified as [Cr(N^{t}Bu)$_2$(etc)$_2$] (21)(76% yield).

C$_{18}$H$_{38}$N$_4$S$_4$Cr$_1$;

ir (cm^{-1}): 1653w, 1494s, 1459m, 1429s, 1379m, 1356m, 1301w, 1264s, 1209m, 1147, 1133w, 1094m, 1075m, 1020m, 915w, 803m

nmr: ^{1}H : 3.52 (q, 8H, J 6.7, CH_2CH$_3$); 1.56 (s, 18H, C(CH_3)$_3$); 0.90 (t, 12H, J 6.7, CH$_2$CH_3)

^{13}C{^{1}H} : 203.2 (C=N); 77.7 (C(CH$_3$)$_3$); 46.2 (CH$_2$CH$_3$); 30.4 (C(CH$_3$)$_3$); 12.6 (CH$_2$CH$_3$)

^{13}C CPMAS: 201.4 (C=N); 79.7, 79.0, 76.3, 75.6 (C(CH$_3$)$_3$); 47.4 (CH$_2$CH$_3$); 31.3 (C(CH$_3$)$_3$); 15.2, 14.1; 12.7, 12.1 (CH$_2$CH$_3$)

^{13}C CPMAS (243K) : 201.4 (C=N); 79.9, 79.2 (d, C(CH$_3$)$_3$); 76.1, 75.4 (d); 47.2 (CH$_2$CH$_3$); 31.0 (C(CH$_3$)$_3$); 14.4, 12.0 (CH$_2$CH$_3$)

^{13}C CPMAS NQSTOSS: 201.7 (C=N); 79.6, 79.0 (d); 76.2, 75.6 (d); 31.2 (C(CH$_3$)$_3$); 15.1, 14.2, 12.2 (CH$_2$CH$_3$)

Mass Spec.(EI): M$^+$ 490; fragmentation - 419 (-N^{t}Bu), 348 (-2N^{t}Bu), 342 (-etc), 271 (-N^{t}Bu -etc), 200 (-2N^{t}Bu -etc)

Synthesis of [Cr(N^{t}Bu)$_2$(mtc)$_2$] (22)

[Cr(N^{t}Bu)$_2$Cl$_2$] (1.01 mmol) was reacted with two equivalents of sodium dimethyldithiocarbamate (2.05 mmol) in ether, following the general procedure. A dark red solid was isolated from the ethereal solution which was identified as [Cr(N^{t}Bu)$_2$(mtc)$_2$] (22) (58% yield).

C$_{14}$H$_{30}$N$_4$S$_4$Cr$_1$;

nmr: ^{1}H : 2.80 (s, 12H, NCH_3); 1.57 (s, 18H, C(CH_3)$_3$)

^{13}C{^{1}H} : 204.3 (C=N); 77.8 (C(CH$_3$)$_3$); 41.0 (NCH$_3$); 30.8 (C(CH$_3$)$_3$)

^{13}C CPMAS: 204.4, 201.4 (C=N); 78.6, 76.8 (C(CH$_3$)$_3$); 45.5, 44.4, 39.6, 39.0 (NCH$_3$); 32.1, 31.3 (C(CH$_3$)$_3$)

Elemental Analyses - found(calculated)%: C 29.86(38.71); H 6.72(6.91); N 10.09(12.90); recalculated for [Cr(O)(N^{t}Bu)(mtc)$_2$] - C 31.65; H 5.58; N 11.07

Reaction of [Cr(N^{t}Bu)$_2$Cl$_2$] with PhNH$_2$

[Cr(N^{t}Bu)$_2$Cl$_2$] was reacted with two equivalents of sodium diethyldithiocarbamate in tetrahydrofuran in a Schlenk tube. A moisture-sensitive, black solid was isolated but was insoluble in a wide range of solvents. No further analysis was attempted.

6.5 Experimental for Chapter 4

6.5.1. Thermolysis

Toluene solutions of **3**, **8** and **13** were refluxed (individually) for three days. No colour changes were observed. Solvent was removed from the solution in vacuo. The products were purified by column chromatography; for all, a major band eluted with 3:10 dichloromethane/petrol, identified, in each case, as the starting material. ^{1}H nmr were in agreement with original data.

A d^8-toluene solution of **1** was flame-sealed in a nmr tube. The tube was heated vigorously for three days; refluxing of the solution was noted. The solution was monitored by ^{1}H nmr spectroscopy during the three days. No peaks assignable to new species were observed.
^{1}H nmr was in agreement with data recorded earlier (indicated in 6.3).

6.5.2 Reaction with air/moisture
Synthesis of [Mo(NS)(etc)$_3$] (24)

[Mo(N(4-Me)C$_6$H$_4$)$_2$Cl$_2$(DME)] (4.5 mmol) was reacted with two equivalents of ammonium diethyldithiocarbomate (9.2 mmol) in diethyl ether. After stirring for 12h, a yellow product precipitated from the reaction mixture. The product was isolated and washed with ether. Orange crystals grew upon slow mixing of a dichloromethane solution with methanol in air. The compound was crystallographically characterized as [Mo(NS)(S$_2$CNEt$_2$)$_3$] (24) (16% yield).
C$_{15}$H$_{30}$N$_4$S$_7$Mo$_1$;
Mass spec. (FAB) M$^+$ 586

Synthesis of oxo-imido complexes, [Mo(O)(NR)(etc)$_2$]

General Procedure
In the formation of [Mo(NR)$_2$(etc)$_2$] (**5** and **12**), yellow products precipitated out of the reaction mixture. The products were isolated, washed with petrol and identified as [Mo(O)(NR)(etc)$_2$].
Synthesis of [Mo(O)(N(4-Me)C$_6$H$_4$)(etc)$_2$] (23)
C$_{17}$H$_{37}$N$_3$O$_1$S$_4$Mo$_1$;

---

ir (cm^{-1}): 1519s, 1439m, 1279m, 1243m, 1209m, 1075m, 910s(bd), 835m

nmr:^{1}H: 7.26 (d, 2H, J 7.1, H^{2,6}); 7.07 (d, 2H, J 7.1, H^{3,5}); 3.73-3.80 (m, 8H, CH_2CH$_3$); 2.37 (s, 3H, (4-CH_3)C$_6$H$_4$); 1.31 (t, 12H, J 7.1, CH$_2$CH_3)

Elemental Analyses found(calculated)%: C 39.85(39.77); H 5.64(5.30); N 7.86(8.18); S 24.15(24.97)

Synthesis of [Mo(O)(N(2,6-F$_2$C$_6$H$_3$))(etc)$_2$] (25)

C$_{16}$H$_{23}$N$_3$O$_1$S$_4$Mo$_1$;

ir (cm^{-1}):1523s, 1478m, 1457m, 1439m, 1384s, 1281w, 1262m, 1094m, 1077m, 1019s, 886m, 803m, 466m, 453m

nmr: ^{1}H : 6.08-5.92 (m, 3H, aromatic); 3.24-2.86 (m, 8H, CH_2CH$_3$); 0.76-0.67 (m, 12H, CH$_2$CH_3)

Mass Spec.(EI): M$^+$ 537; fragmentation - 521 (- O); 410 (- NAr)

Elemental Analyses - found(calculated)%: C 35.71(35.88); H 4.81(4.33); N 8.19(7.85)

6.5.3   With Acids

Reactions with tetrafluoroboric acid, HBF$_4$.Et$_2$O

A dichloromethane solution of 7 (4.57mmol) was reacted with a couple of drops of [HBF$_4$.Et$_2$O]. On shaking, the solution turned yellow. Solvent was removed under reduced pressure and the residue was prepared for crystallization. The formation of [Mo(NHAr)$_2$(etc)$_2$]$^{2+}$ (26) or [Mo(NHAr)(NAr)(etc)$_2$]$^+$ (28) is suggested.

nmr: ^{1}H: (CDCl$_3$): 7.91 (bd, 2H, NH); 7.21 (d, 4H, J 7.4, H^{3,5}); 7.14 (t, 2H, J 7.4, H^4); 4.32 (septet, 4H, J 6.8, CH(CH$_3$)$_2$); 4.03-3.72 (m, 8H, CH_2CH$_3$); 1.41 (t, 12H, J 6.8, CH$_2$CH_3); 1.36 (d, 12H, J 6.8, CH(CH_3)$_2$); 1.28 (d, 12H, J 6.8, CH(CH_3)$_2$)

Crystals of [{Mo(NAr)(etc)(μ-MoO$_4$)}$_2$] (27)

Elemental Analyses found(calculated)%:C 34.25(36.31); H 4.98(5.12); N 5.33(5.77)

A dichloromethane solution of 2 was reacted with a couple of drops of [HBF$_4$.Et$_2$O]. By a molecular ion peak of 611, the product was identified as [Mo(N^{t}Bu)(etc)$_3$]$^+$ (30). Mass Spec. (FAB): M$^+$ 611

Reactions with trifluoracetic acid, CF$_3$CO$_2$H

A dichloromethane solution of 7 was reacted with a couple of drops of CF$_3$CO$_2$H. On shaking, the solution turned yellow. Solvent was removed *in vacuo*. The formation of [Mo(NHAr)(NAr)(etc)$_2$]$^+$ (28) is suggested.

nmr: ^{1}H(CDCl$_3$): 7.27-7.05 (m, 5H, aromatic), 6.85 (t, 1H, H^4); 4.09 (septet, 2H, CH(CH$_3$)$_2$); 3.88-3.77 (m, 8H, CH_2CH$_3$); 2.96 (septet, 2H, CH(CH$_3$)$_2$); 1.36 (t, 12H, J

7.0, CH$_2$CH$_3$); 1.28 (d, 12H, CH(CH$_3$)$_2$); 1.19 (d, 12H, CH(CH$_3$)$_2$)

nmr: ^{13}C(CDCl$_3$): 196.3 (C=N); 160.5 (q, J$_{CF}$ 42.9, CF$_3$COO$^-$); 155.4 (C$^{1'}$); 141.9 (C$^{2'}$); 131.4 (C^1); 130.5 (C^2); 128.4 (C$^{4'}$); 124.9 (C$^{3'}$); 124.0 (C^3); 123.3 (C^4); 113.9 (q, J$_{CF}$ 285.4, CF$_3$COO$^-$); 44.4, 43.6 (CH$_2$CH$_3$); 28.7, 28.6 (CH(CH$_3$)$_2$); 25.1, 23.4 (CH(CH$_3$)$_2$); 12.5, 12.4 (CH$_2$CH$_3$)

A dichloromethane solution of [Mo(NAr)$_2$(mtc)$_2$] (**39**) was reacted with a couple of drops of CF$_3$CO$_2$H. On shaking, the solution turned yellow. Solvent was removed *in vacuo*. The formation of [Mo(NHAr)(NAr)(mtc)$_2$]$^+$ (**29**) is suggested.

nmr: ^{1}H(CDCl$_3$): 10.08 (bd, NH or CF$_3$CO$_2$H); 7.48 (t, 1H, J 7.9, H^4); 7.31 (d, 2H, J 7.7, H^{3,5}); 7.27 (t, 1H, J 7.8, H$^{4'}$); 7.15 (d, 2H, J 7.8, H$^{3,5'}$); 3.84 (septet, 2H, J 6.7, CH(CH$_3$)); 3.44 (s, 6H, NCH$_3$); 3.39 (s, 6H, NCH$_3$); 3.03 (septet, 2H, CH(CH$_3$); 1.29 (d, 12H, J 6.8, CH(CH$_3$)$_2$); 1.22 (d, 12H, J 6.8, CH(CH$_3$)$_2$)

A dichloromethane solution of **2** was reacted with a couple of drops of CF$_3$CO$_2$H. On shaking, the solution turned yellow. Solvent was removed *in vacuo*. The formation of [Mo(NH^{t}Bu)(N^{t}Bu)(etc)$_2$]$^+$ (**31**) is suggested.

nmr: ^{1}H(CDCl$_3$): 3.80 (q, 8H, J 7.1, CH$_2$CH$_3$); 1.37 (s, 9H, ^{t}Bu); 1.26 (t, 12H, J 7.0, CH$_2$CH$_3$); 1.14 (s, 9H, ^{t}Bu)

6.5.4. With Chalcogenides

Reactions with Hydrogen Sulfide
General Procedure

A dichloromethane solution (~ 30 ml) of [Mo(NR)$_2$(etc)$_2$] was purged with hydrogen sulfide gas until the solution was saturated (shown when gas started bubbling theough a solution of bleach attached to tap). The solution was then left to stir for twelve hours and then purged with dinitrogen to remove excess H$_2$S. The solvent was removed *in vacuo* and the solid prepared for column chromatography.

Reaction with [Mo(NAr)$_2$(etc)$_2$] (7)

A dichloromethane solution of **7** (0.34 mmmol) in dichloromethane was reacted with H$_2$S for five minutes to obtain a saturated solution and then left to stir for three days, following the general procedure. Elution with dichloromethane/petrol (1:5) afforded a brown band identified as unreacted starting material (19% yield); elution with dichloromethane/petrol (3:10) afforded an orange band (13% yield); elution with dichloromethane/petrol (4:10) afforded a purple band which yielded [Mo(NAr)(S$_2$)(etc)$_2$]^{22} (**35**) (68% yield). Recrystallization of the orange band was

effected upon slow mixing of dichloromethane solutions with methanol producing orange crystals. One of these was selected for X-ray diffraction crystallography and identified as [{Mo(N(2,6-^{i}Pr$_2$C$_6$H$_3$))$_2$(etc)}$_2$(μ-S)(μ^2-η^2-S$_2$)] (32).

C$_{34}$H$_{54}$N$_4$S$_7$Mo$_2$;

ir (cm^{-1}): 1510m, 1459m, 1438m, 1384m, 1262s, 1096s, 1021s, 803s, 669w, 549w, 468w, 454w

nmr: ^{1}H (CDCl$_3$): 6.84 (t, 1H, J 7.5,H^4); 6.81 (t, 1H, J 7.5, H^4); 6.72 (d, 2H, J 7.6, H^{3,5}); 6.68 (d, 2H, J 7.6, H^{3,5}); 4.04-3.88 (m, 4H, C*H*$_2$CH$_3$); 3.79 (septet, 1H, J 6.8, C*H*Me$_2$); 3.66 (septet, 1H, J 6.8, C*H*Me$_2$); 3.43-3.29 (m, 4H, C*H*$_2$CH$_3$); 1.34-1.28 (tx4, 12H, J 7.1, CH$_2$C*H*$_3$); 0.97-0.91 (dx4, 24H, J 6.8, CH*Me*$_2$)

^{13}C{^{1}H} (CDCl$_3$): 207.7, 206.1 (*C*=N); 153.7, 152.1 (ipso-C); 147.9, 146.3 (o-C$_6$H$_3$); 126.6-121.3 (multiple s, aromatic); 45.7-44.5 (multiple s, *C*H$_2$CH$_3$); 28.9-27.4 (multiple s, *C*HMe$_2$); 23.7-23.0 (multiple s, CH*Me*$_2$)

Mass Spec. (FAB): M$^+$ 935

Elemental Analyses - found(calculated)%: C̲ 43.91(43.68); H̲ 5.82(5.78); N̲ 5.74(6.00); S̲ 22.28(23.98)

35 - ^{1}H nmr in agreement with original data[22].

Reaction with [Mo(NPh)$_2$(etc)$_2$] (1)

1 (0.17 mmol) was reacted with H$_2$S for 60 seconds, following the general procedure. Elution with dichloromethane/petrol (2:5) gave a purple band [Mo(NPh)(S$_2$)(etc)$_2$][18] (32) (62% yield) and with methanol/dichloromethane (1:20) an orange band which was identified by mass spectrometry to contain the molecular ion, [Mo(NPh)(etc)$_3$]$^+$(10% yield).

32 - ^{1}H nmr in agreement with original data[18].

[Mo(NPh)(etc)$_3$)]$^+$:Mass Spec (FAB) M$^+$ 637

Reaction with [Mo(N(2-Me)C$_6$H$_4$)$_2$(etc)$_2$] (3)

3 (0.17 mmol) was reacted with H$_2$S for 90 seconds, following the general procedure. Elution with dichloromethane/petrol (3:10) gave a purple band which afforded [Mo(N(2-Me)C$_6$H$_4$)(S$_2$)(etc)$_2$][22] (34) (83% yield) and with methanol/dichloromethane (1:20) an orange band which afforded a compound containing the molecular ion, [Mo(N(2-Me)C$_6$H$_4$)(etc)$_3$]$^+$(15% yield).

34 - ^{1}H nmr in agreement with original data[22].

[Mo(N(2-Me)C$_6$H$_4$))(etc)$_3$)]$^+$:Mass Spec. (FAB): M$^+$ 645

Reaction with [Mo(N^{t}Bu)$_2$(etc)$_2$] (2)

2 (0.37 mmol) was reacted with H$_2$S for 10 seconds, following the general procedure.

A near-immediate colour change from orange to dark-red was observed. Elution with dichloromethane/petrol (3:10) gave a red band which afforded [Mo(N^{t}Bu)(S$_2$)(etc)$_2$][22] (33) (58% yield) and with methanol/dichloromethane (1:20), a brown band which afforded a compound containing the molecular ion, [Mo(N^{t}Bu)(etc)$_3$]$^+$ (30% yield).

33 - ^{1}H nmr in agreement with original data [22].

[Mo(N^{t}Bu)(etc)$_3$)]$^+$: Mass Spec. (FAB): M$^+$ 611

Reaction with [Mo(N(2,6-Me$_2$C$_6$H$_3$))$_2$(etc)$_2$] (8)

8 (0.15 mmol) was reacted with H$_2$S for 180 seconds, following the general procedure. Elution with dichloromethane/petrol (1:4) gave a brown band which afforded unreacted starting material (80% yield) and with methanol/dichloromethane (1:20) an orange band which afforded a compound containing the molecular ion, [Mo(N(2,6-Me$_2$C$_6$H$_3$))(etc)$_3$]$^+$(20% yield).

Mass Spec. (FAB): M$^+$ 659

This reaction was repeated under identical conditions except that the solution was stirred for three days. Elution with dichloromethane/petrol (7:20) gave a brown band which was identified as [Mo(N(2,6-Me$_2$C$_6$H$_3$)(S$_2$)(etc)$_2$] (36). ^{1}H nmr was in agreement with original data[22].

Reaction of [Mo(N^{t}Bu)$_2$(etc)$_2$] (2) with H$_2$Se

Concentrated nitric acid was added dropwise to black Hg$_2$Se or to green Al$_2$Se$_3$. The gas evolved in the flask should be passed through fused CaCl$_2$ and bubbled into the dichloromethane solution of 2 via an upturned filter cannula. However, it is thought that the hydrogen selenide did not have a sufficient driving force through to the schlenk tube. Any reaction was presumed to be that with nitric acid.

Reaction of [Mo(NPh)$_2$(etc)$_2$] (1) with Se

1 (0.5 mmol) was reacted with grey, elemental selenium (1 mmol) in benzene solvent (40 ml). After stirring for twelve hours the solution was still red in colour but all the selenium metal had been consumed. Solvent was removed *in vacuo* and the oily solid was washed with petrol but to no apparent effect. In the glove box, part of the solid was dissolved in ether and left to recrystallize in the freezer. The rest was dissolved in dichloromethane and carefully layered with petrol. No crystals formed. The oily residue was unsuitable for further analysis.

Reactions of other compounds with H_2S

A dichloromethane solution of $[Mo(O)(etc)(\mu\text{-}NPh)]_2$ was reacted with H_2S for 45 seconds, following the general procedure. Starting material was recovered. A trace of another molecular ion was observed in the mass spectrum, consistent with the formula of $[Mo_2(O)(S)(etc)_2(\mu\text{-}NPh)_2]$.

Mass Spec. FAB M^+ 719

A dichloromethane solution of $[Mo_2(etc)_2(NPh)_2(\mu\text{-}NPh)\{\mu\text{-}PhNC(O)CNPh\}]$[64] was reacted with H_2S for 60 seconds, following the general procedure. Only starting material was recovered.

Reactions of bis(imido) and other complexes with Lawesson's reagent

General Procedure

The imido compound and Lawesson's reagent $[\{((4\text{-}CH_3O)C_6H_4)P(S)\}_2(\mu^2\text{-}S)_2]$ were reacted together in toluene solvent and left to heat and stir. Solvent was removed under reduced pressure and the mixture purified by column chromatography.

Reaction with $[Mo(N(2,6\text{-}Cl_2C_6H_3)_2(etc)_2]$

13 was reacted with Lawesson's reagent, following the general procedure.

More than one product formed in a mixture. Separation was difficult and only partially achieved by crystallization. The only product identified was $[Mo(N(2,6\text{-}Cl_2C_6H_3)(S_2)(etc)_2]$ (38). ^1H nmr spectrum correlated to the original data[64]. The other species were indicated in the phosphorus nmr spectrum, but never identified.

$^{31}P\{^1H\}$: 73.6, 73.3, 72.8, 72.7, 72.45, 72..37, 65.6

Reaction with $[Mo_2(etc)_2(NPh)_2(\mu\text{-}NPh)\{\mu\text{-}PhNC(O)CNPh\}]$

A dichloromethane solution of the ureato complex was reacted with Lawesson's reagent, following the general procedure. Mainly starting material was recovered. A second product formed had a mass spectrum consistent with $[Mo_2(etc)_2(NPh)_2(\mu\text{-}NPh)\{\mu\text{-}PhNC(S)CNPh\}]$.

Mass Spec (FAB) M^+ 794

ir (cm^{-1}): 1652w, 1596w, 1518w, 1437w, 1262s, 1096s, 1023s, 803s, 753w

Reaction with $[Mo(O)_2(etc)_2]$

A dichloromethane solution of the bis(oxo) complex was reacted with Lawesson's reagent, following the general procedure. Only starting material was recovered.

6.5.5   With Phosphines

Reaction of [Mo(N(2-Me)C₆H₄)₂(etc)₂] with PPh₃

An excess amount of triphenylphosphine was added to a d⁶-benzene solution of **3** in a nmr tube; the tube was then flame-sealed. A change in colour of the solution was observed, initially to a dark-red colour; gradually, the solution became brighter, more transparent and eventually, became almost orange in colour. Its ^{1}H nmr spectrum was recorded on three occasions.

nmr: ^{31}P[^{1}H]: *1.* -5.0, (s, PPh₃); 43.1 (s, Ph₃P=NR)

2. -5.0 (s, PPh₃); 26.1 (s, Ph₃P=O); 43.1, (s, Ph₃P=NR)

3. -5.0 (s, PPh₃); 26.1 (s, Ph₃P=O); 43.1, (s, Ph₃P=NR)

Reaction of [Mo(N^{t}Bu)₂(etc)₂] with PPh₃

An excess amount of triphenylphosphine was added to a thf solution of **2**. Solvent was removed from the solution *in vacuo*.

nmr: ^{31}P[^{1}H]: 25.1 (s, Ph₃P=NR); -5.0 (PPh₃)

6.5.6   With Other Molecules
Photolysis reaction with C₂H₂

Using equipment suitable for uv irradiation, acetylene was bubbled continuously through a toluene solution of **1** (0.45 mmol). Solvent was removed under reduced pressure and the residue washed with petrol. The substance retrieved was highly impure and unsuitable for further analysis.

Reaction with DMAD, [(MeO₂C)₂C₂]

Five equivalents of DMAD was added *via* a degassed syringe to a solution of **2** (.33 mmol). The solution was stirred for twelve hours. Solvent was removed under reduced pressure and the residue washed with petrol. The substance retrieved was highly impure and unsuitable for further analysis.

Photolysis reaction with DMAD, [(MeO₂C)₂C₂]

Five equivalents of DMAD (1.5 mmol) was added *via* a degassed syringe to a solution of **1** (0.33 mmol). The solution was stirred for twelve hours whilst subject to uv irradiation. The solution was transferred to another schlenk tube and solvent removed *in vacuo*. The residue washed with petrol. The substance retrieved was highly impure and unsuitable for further analysis.

With sodium amalgam

Sodium amalgam was pipetted into a schlenk tube containing tetrahydrofuran solvent

---

and a stirrer bar. A tetrahydrofuran solution of **1** (0.50 mmol) was added to the sodium amalgam in solvent and the mixture was left to stir for three days. The solution was filtered to another schlenk tube and the solvent removed *in vacuo*. The oily brown solid was washed with petrol. The substance retrieved was highly impure and unsuitable for further analysis.

With Chlorine, Cl_2
Reaction with [Mo(NPh)$_2$(etc)$_2$]

Chlorine gas was bubbled through a dichloromethane solution of **1** (0.60 mmol). After stirring for twelve hours, solvent was removed *in vacuo* and the red solid washed with petrol and ether. The substance retrieved was highly impure and unsuitable for further analysis.

Reaction with [Mo(NPh)$_2$(etc)$_2$]

Chlorine gas was bubbled through a dichloromethane solution of **2** (0.50 mmol) for 30 seconds. After stirring for twelve hours the solution had changed colour to red and solvent was removed *in vacuo*. The red solid was washed with petrol. The substance retrieved was highly impure and unsuitable for further analysis.

With Hydrogen, H_2

Using photolysis equipment and a procedure as described above, hydrogen gas was bubbled continuously through a toluene solution of **1** (0.45 mmol); the solution was stirred for twelve hours whilst subject to uv irradiation. The solvent was removed *in vacuo* and the solid washed with petrol. The substance retrieved was highly impure and unsuitable for further analysis.

With methyl hydrazine, [CH_3NHNH_2]

Two equivalents of methyl hydrazine (0.03 ml, 0.7 mmol) was added via a degassed syringe to a toluene solution of **1** (0.33 mmol); the solution was stirred for twelve hours whilst subject to uv irradiation. Solvent was removed under reduced pressure and the residue washed with petrol. The substance retrieved was highly impure and unsuitable for further analysis.

With ethyldiazoacetate, [$CH(COOEt)N_2$]

Two equivalents of methyl hydrazine (0.85 mmol) was added via a degassed syringe to a toluene solution of **1** (0.4 mmol); the solution was stirred for twelve hours whilst subject to uv irradiation. After stirring, the solution had changed colour to yellow.

Solvent was removed under reduced pressure and the residue washed with petrol. The substance retrieved was highly impure and unsuitable for further analysis.

6.5.7   With Aniline
Reaction with [Mo(N^{t}Bu)$_2$(etc)$_2$]

In an nmr tube, aniline was added to a C_6D_6 solution of **2**. The reaction was monitored by ^{1}H nmr spectroscopy. A change in colour from orange was noted with the gradual darkening and reddening of the solution.

nmr: ^{1}H: (discernable peaks): 7.46 (d, J 7.3, H^{2,6}); 7.35 - 7.0 (m); 6.97 (t, J 7.5, H^{3,5}); 6.70 (t, J 7.4, H^4); 6.37 (d, J 7.3); 3.25 (q, J 7.1, CH_2CH_3); 3.10 (q, J 7.2); 1.56 (s), 1.47 (s), 1.3 - 1.1 (m); 0.74 (t, J 7.1, CH_2CH_3); 0.68 (t, J 7.2)

6.6   Experimental for Chapter 5

An nmr tube containing a d^8-toluene solution of **1** was exposed briefly to air and the tube resealed, to allow the hydrolysis (aerial oxidation) of **1** to the oxo-imido, [Mo(O)(NPh)(etc)$_2$]. The solution started to pale and turn yellow. When this change in colour was observed, the nmr solution was refluxed. On heating, the solution changed colour to a pale green.

nmr: ^{1}H (C$_7$D$_8$): ** denotes a new peak

1: after one hour.   7.47 (d, 2H, J 7.4, H^{2,6}); 6.68 (t, 1H, J 7.3, H^4); 3.11 (q, 8H, J 7.2, CH_2CH_3); 0.68 (t, 12H, J 7.2, CH_2CH_3)

2: after heating for 24h. ** 7.57 (d); 7.47 (d); ** 7.33 (t); ** 7.25 - 7.10 (m); ** 6.80 - 6.60 (m); **6.23 (d); ** 3.6 - 2.6 (m); ** 2.41 (q, J 7.2); **0.93 (t, J 7.0); ** 0.90 - 0.75 (m); 0.68 (t, J 7.1); ** 0.66 (t, J 7.65); ** 0.61 - 0.34 (m)

3: after heating for 48h. ** 7.56 (d); 7.47 (d); 7.34 (t); 7.25 (d); 7.25 - 7.1 (m); 6.77 - 6.58 (m); 6.24 (d); 3.60 - 2.67 (m); 2.41 (q); 0.93 (t); ** 0.86 (t); 0.66 (t); 0.64 - 0.34 (m)

4: after 72h. ** 7.57 (d); 7.33 (t); 7.22 (q?); 6.77 - 6.59 (m); 6.23 (d); 3.60 - 2.60 (m); 2.42 (q); 1.05 - 0.56 (m)

5: after 120h. 7.55 (d); 7.35 - 7.31 (m); 7.23 (d); 6.72 - 6.59 (m); 6.23 (d); 3.55 - 2.84 (m); 2.41 (q); 0.93 (t); 0.81 (t); 0.65 (q); 0.60 - 0.47 (m)

Appendix I   Solid State Nmr Spectroscopy

This appendix is designed to introduce the reader to solid state nmr spectroscopy at a simple level involving theory, technical procedure and terminology. Acknowledgements are due to Dr Patrick Barrie and his lecture course.

Nmr spectra of solids are not recorded in the same way as liquids due to the number of anisotropic interactions occurring in the solid state. The three main interactions are (direct) dipole-dipole coupling, chemical shift anisotropy and quadrupolar interaction. These effects are averaged out in solution by fast, random molecular motion but in the solid state, they lead to broadening of peaks in the spectra and obscurement of most of a spectrum's information.

Dipole-dipole coupling arises from neighbouring nuclei (which have a magnetic moment) exerting a magnetic field on other nuclei. The Hamiltonian is proportional to the multiple of the gyromagnetic ratio (γ) for each nucleus coupled to a spin geometry term (for either homo- or hetero-nuclear spins) and to the specific orientation (θ) between the two nuclei. It is inversely proportional to the cube of the internuclear distance (r), thus consideration is only needed for nuclei within a short range.

$$H_D = \frac{\gamma \cdot \gamma}{r^3} (1 - 3 \cos^2\theta) \cdot [\text{spin geometry term}]$$

To remove dipolar broadening from the spectrum, the term involving orientation must be averaged to zero, thus imitating the behaviour in solution nmr. The method most widely used is <u>magic-angle spinning (MAS)</u>. If the solid is set to spin at an angle to the magnetic field, β, then an expression can be set up for the average values of $(1 - 3 \cos^2\theta)$ linking it to the angle between the vector joining the spins and the rotation axis. This can be varied and if $(1 - 3 \cos^2\beta)$ can be set to zero then the orientation effect, $(1 - 3 \cos^2\theta)$, must also be zero. This angle is then the "magic angle" - 54.7°. Thus, if the sample can be spun so that is averaged quickly with the magnitude of the dipolar interaction, then the effect can be negated by magic-angle spinning and a higher resolution spectrum be obtained. By spinning quickly, the anisotropy effect can also be removed.

In reality, machines are capable of spinning speeds to remove the interaction except for where coupling to hydrogen or fluorine exists, due to their high gyromagnetic ratios. To counteract coupling to hydrogen, high power decoupling may be used which involves a strong radiofrequency pulse (at the frequency of proton) being applied. This makes the proton spins change so rapidly such that the influence of their magnetic moment is averaged to zero. It is termed high power decoupling because the strength of the pulse must be of the same order as the undesired interaction. Another way to

record spectra with hydrogen and fluorine coupling is to use a multiple-pulsing technique which will resolve the spin part of the Hamiltonian to be zero.

In solid state nmr spectra, the signals are weak and spin-lattice relaxation times are generally long, leading to long times between pulses. Cross-polarization (CP) is a technique that transfers magnetization from neighbouring hydrogen nuclei to the target atom (usually ^{13}C). This allows a shorter time between scans and enhances the signal. It is possible to regulate the orientation, timing and strength of the irradiation of the nuclei so that the two nuclei have the same quantization axis and the energy gap between the energy levels of the carbon and hydrogen atoms is identical. The dipole-dipole interaction that exists between them is used to transfer energy between the two nuclei, i.e. the excess magnetization of the hydrogen nuclei becomes ^{13}C magnetization and the populations of the two ^{13}C levels are changed. After allowing time for this transfer, the irradiation of the carbon nuclei is stopped and the ^{13}C signal is measured. This effect enhances the signal intensity by a factor of four for carbon; in general, the enhancement is the ratio of gyromagnetic factors, γ_H/γ_X (for any nucleus, X).

Not only is the signal enhanced but as the time between scans is determined by the relaxation time of hydrogen nuclei, not the target nucleus, then the time taken for the nmr experiment may be significantly shortened. The rate of cross-polarization depends mainly on the number of hydrogens nearby (available for magnetization transfer), the distance away and any molecular motion. For ^{13}C nmr, the CP rates are observed to decrease in the order : $CH_2 > CH > CH_3 > C_{quaternary}$. This follows the number of hydrogen nuclei available except for methyl groups whose high mobilities reduce the rate of cross-polarization.

The reliance of cross-polarization on the dipole-dipole interaction seems contrary to the action of MAS averaging out these interactions. However, the strength of coupling between the nuclei is such to allow spectra to be recorded at speeds up to 12 kHz. The exception to this involves the quaternary carbon when spinning speeds over 6 kHz will lead to intensity distortions in the spectrum.

Non-quaternary suppression (NQS) is possible, usually accompanied by the total suppppression of sidebands (TOSS). The dipolar dephasing suppresses CH and CH_2 signals, but leaves those for C_{quat} and CH_3. Spinning speeds achieved are ≈ 4 kHz. The final nmr experiment used in this work is FLIP, which is essentially the technique used in solution nmr spectroscopy.

References

(1)   Clifford A.F. and Kobayashi C.S., 1956, *Abstracts, 130th National meeting of the American Chemical Society, Atlantic City, NJ*, 50R

(2)   Clifford A.F. and Kobayashi C.S., 1960, *Inorganic Synthesis*, **6**, 207

(3)   Herranz E. and Sharpless K.B., 1978, *J.Org.Chem.*, **43**, 2544

(4)   Patrick D.W., Truesdale L.K., Biller S.A. and Sharpless K.B., 1978, *J.Org.Chem.*, **43**, 2628

(5)   Chan D.M.-T. and Nugent W.A., 1985, *Inorg.Chem.*, **24**, 1422

(6)   Schofield M.H., Schrock R.R., Kee T.P., Anhaus J.T., Johnson K.H. and Davis W.M., 1991, *Inorg.Chem.*, **30**, 3595

(7)   Nugent W.A. and Haymore B.L., 1980, *Coord.Chem.Rev.*, **31**, 123

(8)   Wigley D.E., 1994, *Progress in Inorganic Chemistry*, **42**, 239

(9)   Nugent W.A. and Mayer J.M., *Metal-Ligand Multiple Bonds*; Wiley Interscience, 1988

(10)   Miyaura N. and Kochi J.K., 1983, *J.Am.Chem.Soc.*, **105**, 2368

(11)   Groves J.T. and Quinn R., 1985, *J.Am.Chem.Soc.*, **107**, 5790

(12)   Sharpless K.B. and Michaelson R.C., 1973, *J.Am.Chem.Soc.*, **95**, 6136

(13)   Schröder M. and Constable E., 1982, *J.Chem.Soc., Chem.Commun.*, 734

(14)   Holm R.H., 1987, *Chem.Rev.*, **87**, 1401

(15)   Barral R., Bocard C., Seree de Roch I. and Sajus L., 1972, *Tetrahedron Letters*, 1693

(16)   Reynolds M.S., Berg J.M. and Holm R.H., 1984, *Inorg.Chem.*, **23**, 3057

(17)   Harmer M.A., Halbert T.R., Pan W.-H., Coyle C.L., Cohen S.A. and Stiefel E.L., 1986, *Polyhedron*, **6**, 341

(18)   Coffey T.A., Forster G.D. and Hogarth G., 1993, *J.Chem.Soc., Chem.Commun.*, 1524

(19)   Elder R.C. and Trkula M., 1977, *Inorg.Chem.*, **16**, 1048

(20)   Müller A., Nolte W.-O. and Krebs B., 1980, *Inorg.Chem.*, **19**, 2835

(21)   Müller A. and Diemann E. In *Comprehensive Coordination Chemistry* Pergamon: 1987; Vol. 2; pp 515-550.

(22)   Coffey T.A., Forster G.D. and Hogarth G., 1996, *J.Chem.Soc., Dalton Trans.*, 183

(23)   Rappé A.K. and Goddard III W.A., 1980, *J.Am.Chem.Soc.*, **102**, 5114

(24)   Rappé A.K. and Goddard III W.A., 1980, *Nature*, **285**, 311

(25)   Rappé A.K. and Goddard III W.A., 1982, *J.Am.Chem.Soc.*, **104**, 448

(26)   Gibson V.C., Marshall E.L., Redshaw C., Clegg W. and Elsegood M.R.J., 1996, *J.Chem.Soc., Dalton Trans.*, 4197

(27)   Schrock R.R., Murdzek J.S., Bazan G.C., Robbins J., DiMare M. and O'Regan M., 1990, *J.Am.Chem.Soc.*, **112**, 3870

(28)   Schrock R.R., De Pue R.T., Feldman J., Yap K.B., Yang D.C., Davis W.M., Park
       L.Y., DiMare M., Schofield M., Anhaus J., Walborsky E., Evitt E., Krüger C.
       and Betz P., 1990, *Organometallics*, **9**, 2262

(29)   Nugent W.A., McKinney R.J., Kasowski R.V. and Van-Catledge F.A., 1982,
       Inorganica Chimica Acta, **65**, L91

(30)   Cundari T.R., 1992, *J.Am.Chem.Soc.*, **114**, 7879

(31)   Cundari T.R., 1992, *J.Am.Chem.Soc.*, **114**, 10557

(32)   Cundari T.R., 1993, *Organometallics*, **12**, 1998

(33)   Hodgson D.J. and Ibers J.A., 1968, *Inorg.Chem.*, **18**, 2345

(34)   Mason J., Mingos D.M.P., Schaefer J., Sherman D. and Stejskal E.O., 1984,
       J.Chem.Soc., Chem.Commun., 444

(35)   Pierpont C.G. and Eisenberg E., 1972, *Inorg.Chem.*, **11**, 1088

(36)   Mason J., Mingos D.M.P., Sherman R. and Wardle R.W.M., 1984, *J.Chem.Soc.,
       Chem.Commun.*, 1223

(37)   Bell A., Clegg W., Dyer P.W., Elsegood M.R.J., Gibson V.C. and Marshall E.L.,
       1994, *J.Chem.Soc., Chem.Commun.*, 2547

(38)   Haymore B.L., Maatta E.A. and Wentworth R.A.D., 1979, *J.Am.Chem.Soc.*,
       101, 2063

(39)   Danopoulos A.A., Wilkinson G., Hussain-Bates B. and Hursthouse M.B., 1993,
       J.Chem.Soc., Chem.Commun., 495

(40)   Minelli M., Carson M.R., Whisenhunt D.W., Imhof W. and Hutter G., 1990,
       Inorg.Chem., **29**, 4801

(41)   Baranger A.M. and Bergman R.G., 1994, *J.Am.Chem.Soc.*, **116**, 3822

(42)   Coffey T.A., Forster G.D. and Hogarth G., 1995, *J.Chem.Soc., Dalton Trans.*,
       2337

(43)   Nugent W.A. and Harlow R.L., 1980, *J.Am.Chem.Soc.*, **102**, 1759

(44)   Thorn D.L., Nugent W.A. and Harlow R.L., 1981, *J.Am.Chem.Soc.*, **103**, 357

(45)   Saboonchian V., Gutierrez A., Wilkinson G., Hussain-Bates B. and Hurtshouse
       M.B., 1991, *Polyhedron*, **10**, 1423

(46)   Sun W., Yang S., Wang H., Yin Y. and Yu K., 1992, *Polyhedron*, **11**, 1143

(47)   Blohm M.L. and Gladfelter W.L., 1986, *Organometallics*, **5**, 1049

(48)   Cenini S. and La Monica G., 1976, *Inorg.Chim.Acta.*, **18**, 279

(49)   Chatt J. and Rowe G.A., 1962, *J.Chem.Soc.*, 4019

(50)   Rowbottom J.F. and Wilkinson G., 1972, *J.Chem.Soc., Dalton Trans.*, 826

(51)   Chisholm M.H. and Rothwell I.P. In *Comprehensive Coordination Chemistry*; G.
       Wilkinson, Gillard R.D. and McCleverty J.A., Ed.; Pergamon: Oxford, 1987;
       Vol. 2; pp 161.

(52)   Nugent W.A. and Harlow R.L., 1980, *Inorg.Chem.*, **19**, 777

(53)   Kolomnikov I.S., Koreshkov Y.D., Lobeeva T.S. and Volpin M.E., 1970, *J.Chem.Soc., Chem.Commun.*, 1432

(54)   Sappa E. and Milone L., 1973, *J. Organometallic Chem.*, **61**, 383

(55)   Bryan J.C., Geib S.J., Rheingold A.L. and Mayer J.M., 1987, *J.Am.Chem.Soc.*, **109**, 2826

(56)   Jernakoff P., Geoffroy G.L., Rheingold A.L. and Geib S.J., 1987, *J.Chem.Soc., Chem.Commun.*, 1610

(57)   Green J.C., Green M.L.H., James J.T., Konidaris P.C., Maunder G.H. and Mountford P., 1992, *J.Chem.Soc., Chem.Commun.*, 1361

(58)   Manuel T., 1963, *Inorg.Chem.*, **3**, 1703

(59)   Gambarotta S., Chiesi-Villa A. and Guastini C., 1984, *J. Organometallic Chem.*, **270**, C49-52

(60)   Edelblut A.W. and Wentworth R.A.D., 1980, *Inorg.Chem.*, **19**, 1110

(61)   Chao Y.-W., Rodgers P.M., Wigley D.E., Alexander S.J. and Rheingold A.L., 1991, *J.Am.Chem.Soc.*, **11**, 6326

(62)   Morrison D.L. and Wigley D.E., 1995, *Inorg.Chem.*, **34**, 2610

(63)   Danopoulos A.A., Wilkinson G., Hussain B. and Hursthouse M.B., 1989, *J.Chem.Soc., Chem.Commun.*, 896

(64)   Forster G.D. Ph.D. Thesis, London, 1995

(65)   Bell A., Clegg W., Dyer P.W., Elsegood M.R.J., Gibson V.C. and Marshall E.L., 1994, *J.Chem.Soc., Chem.Commun.*, 2247

(66)   Burrell A.K. and Bryan J.C., 1993, *Angew.Chem.Int.Ed.Engl.*, **32**, 94

(67)   Dirand-Colin J., Shappacher M., Ricard L. and Weiss R., 1977, *J. Less-Known Metals*, **54**, 91

(68)   Dehnicke K. and Strähle J., 1981, *Angew.Chem.Int.Ed.Engl.*, **20**, 413

(69)   Osborne J.H. and Trogler W.C., 1985, *Inorg.Chem.*, **24**, 3098

(70)   Korolev A.V., Rheingold A.L. and Williams D.S., 1997, *Inorg.Chem.*, **36**, 2647

(71)   Haymore B.L., Hughes M., Mason J. and Richards R.L., 1988, *J.Chem.Soc., Dalton Trans.*, 2935

(72)   Bell L.K., Mason J., Mingos D.M.P. and Tew D.G., 1983, *Inorg. Chem.*, **22**, 3497

(73)   Bradley D.C., Hodge S.R., Runnacles J.D., Hughes M., Mason J. and Richards R.L., 1992, *J.Chem.Soc., Dalton Trans.*, 1663

(74)   Nugent W.A., Harlow R.L. and McKinney R.J., 1979, *J.Am.Chem.Soc.*, **101**, 7265

(75)   Minelli M., Young C.G. and Enemark J.H., 1985, *Inorg.Chem.*, **24**, 1111

(76)   Maatta E.A. and Wentworth R.A.D., 1979, *Inorg.Chem.*, **18**, 2409

(77)   Glueck D.S., Wu J., Hollander F.J. and Bergman R.G., 1991, *J.Am.Chem.Soc.*, **113**, 2041

(78)   Forster G.D. and Hogarth G., 1997, *J.Chem.Soc., Dalton Trans.*, 2305

(79)   Chen G.J.-J., McDonald J.W. and Newton W.E., 1976, *Inorg.Chem.*, **15**, 2612

(80) Harlan E.W. and Holm R.H., 1990, *J.Am.Chem.Soc.*, **112**, 186

(81) Shapley P.A., Shusta J.M. and Hunt J.L., 1996, *Organometallics*, **15**, 1622

(82) Green M.L.H., Konidaris P.C. and Mountford P., 1992, *J.Chem.Soc., Chem.Commun.*, 256

(83) McCormick B.J., Bereman R. and Baird D., 1984, *Coord.Chem.Rev.*, **54**, 99

(84) Heckley P.R., Holah D.G. and Brown D., 1971, *Canadian Journal of Chemistry*, **49**, 1151

(85) Bond A.M. and Martin R.L., 1984, *Coord.Chem.Rev.*, **54**, 23

(86) Kondrateva O.I., Troitskaya A.D., Chadaeva N.A., Chuikova A.I., Usacheva G.M. and Ivantsov A.I., 1973, *Zh. Obshch. Khim.*, **43**, 2087

(87) Burns R.P., McCullough F.P. and McAuliffe C.A., 1980, *Advances in Inorganic and Radiochemistry*, **23**, 211

(88) Chong A.O., Oshima K. and Sharpless K.B., 1977, *J.Am.Chem.Soc.*, **99**, 3420

(89) Schrock R.R., 1990, *Acc.Chem.Res.*, **23**, 158

(90) de With J. and Horton A.D., 1993, *Angew.Chem.Int.Ed.Engl.*, **32**, 903

(91) Baldwin T.C., Huber S.R., Bruck M.A. and Wigley D.E., 1993, *Inorg.Chem.*, **31**, 1319

(92) Coffey T.A., Forster G.D., Hogarth G. and Sella A., 1993, *Polyhedron*, **12**, 2741

(93) Lam H.-W., Wilkinson G., Hussain-Bates B. and Hursthouse M.B., 1993, *J.Chem.Soc., Dalton Trans.*, 781

(94) Williams D.S., Schofield M.H. and Schrock R.R., 1993, *Organometallics*, **12**, 4560

(95) Danopoulos A.A., Wilkinson G. and Williams D.J., 1991, *J.Chem.Soc., Chem.Commun.*, 181

(96) Danopoulos A.A., Wilkinson G., Hussain-Bates B. and Hursthouse M.B., 1992, *Polyhedron*, **11**, 1961

(97) Huang J.-S., Chi C.-M. and Poon C.-K., 1992, *J.Chem.Soc., Chem.Commun.*, 161

(98) Nugent W.A. and Harlow R.L., 1979, *J.Chem.Soc., Chem.Commun.*, 342

(99) Robbins Wolf J., Bazan G.C. and Schrock R.R., 1993, *Inorg.Chem.*, **32**, 4155

(100) Fox H.H., Yap K.B., Robbins J., Cai S. and Schrock R.R., 1992, *Inorg.Chem.*, **31**, 2287

(101) Dyer P.W., Gibson V.C., Howard J.A.K., Whittle B. and Wilson C., 1992, *J.Chem.Soc., Chem.Commun.*, 1666

(102) Sundermeyer J. and Runge D., 1994, *Angew.Chem.Int.Ed.Engl.*, **33**, 1255

(103) Sundermeyer J., Runge D. and Field J.S., 1994, *Angew.Chem.Int.Ed.Engl.*, **33**, 678

(104) Hursthouse M.B., Motevalli M., Sullivan A.C. and Wilkinson G., 1986, *J.Chem.Soc., Chem.Commun.*, 1398

(105)   Bradley D.C., Errington R.J., Hursthouse M.B., Short R.L., Ashcroft B.R., Clark
         G.R., Nielson A.J. and Rickard C.E.F., 1987, *J.Chem.Soc., Dalton Trans.,* 2067

(106)   Clark G.R., Nielson A.J. and Rickard C.E.F., 1988, *Polyhedron,* **7**, 117

(107)   Ricard L., Estienne J., Karagiannidis P., Toledano P., Fischer J., Mitschler A.
         and Weiss R., 1974, *J.Coord.Chem.,* **3**, 277

(108)   Enemark J.H. and Feltham R.D., 1974, *Coord.Chem.Rev.,* **13**, 339

(109)   Green M.L.H., Hogarth G., Konidaris P.C. and Mountford P., 1990,
         J.Chem.Soc., Dalton Trans., 3781

(110)   Elian M., Chen M.M.L., Mingos D.M.P. and Hoffman R., 1976, *Inorg.Chem.,* **15**,
         1148

(111)   Clark G.R., Nielson A.J. and Rickard C.E.F., 1996, *J.Chem.Soc., Dalton Trans.,*
         4265

(112)   Galindo A., Montilla F., Pastor A., Carmona E., Gutiérrez-Puebla E., Monge A.
         and Ruiz C., 1997, *Inorg.Chem.,* **36**, 2379

(113)   Williams D.S., Schofield M.H., Anhaus J.T. and Schrock R.R., 1990,
         J.Am.Chem.Soc., **112**, 6728

(114)   Dyer P.W., Gibson V.C. and Clegg W., 1995, *J.Chem.Soc., Dalton Trans.,* 3313

(115)   Copley R.C.B., Dyer P.W., Gibson V.C., Howard J.A.K., Marshall E.L., Wang
         W. and Whittle B., 1996, *Polyhedron,* **15**, 3001

(116)   Collier P.E., Dunn S.C., Mountford P., Shishkin O.V. and Swallow D., 1995,
         J.Chem.Soc., Dalton Trans., 3743

(117)   Lowe J.P., *Quantum Chemistry;* Academic Press, 1991

(118)   Mealli C. and Proserpio D.M., 1990, *J.Chem.Ed.,* **67**, 399

(119)   Coles M.P., Dalby C.I., Gibson V.C., Clegg W. and Elsegood M.R.J., 1995,
         J.Chem.Soc., Chem.Commun., 1709

(120)   Danopoulos A.A., Wilkinson G., Sweet T.K.N. and Hursthouse M.B., 1995,
         J.Chem.Soc., Dalton Trans., 2111

(121)   Maatta E.A., Haymore B.L. and Wentworth R.A.D., 1980, *Inorg.Chem.,* **19**,
         1055

(122)   Oskam J.H. and Schrock R.R., 1993, *J.Am.Chem.Soc.,* **115**, 11831

(123)   Gagné M.R., Grubbs R.H., Feldman J. and Ziller J.W., 1992, *Organometallics,* **11**,
         3933

(124)   Leung W.-H., Chow E.K.F., Wu M.-C., Kum P.W.Y. and L-L. Y., 1995,
         Tetrahedron Letters, 107

(125)   Danopoulos A.A., Leung W.H., Wilkinson G., Hussain-Bates B. and
         Hursthouse M.B., 1990, *Polyhedron,* **9**, 2625

(126)   Nugent W.A., 1983, *Inorg.Chem.,* **22**, 965

(127)   Leung W.H., Danopoulos A.A., Wilkinson G., Hussain-Bates B. and
         Hursthouse M.B., 1991, *J.Chem.Soc., Dalton Trans.,* 2051

(128) Bishop M.R., Chatt J. and Dilworth J.R., 1979, *J.Chem.Soc., Dalton Trans.,* 1

(129) Chivers T. and Edelmann F., 1986, *Polyhedron,* **6,** 1661

(130) Hursthouse M.B. and Motevalli M., 1979, *J.Chem.Soc., Dalton Trans.,* 1362

(131) Wilkinson G.L., 1982, *Polyhedron,* **1,** 31

(132) Young C.G., Broomhead J.A. and Boreham C.J., 1983, *J.Chem.Soc., Dalton Trans.,* 2135

(133) Bryson N., Youinou M.-T. and Osborn J.A., 1991, *Organometallics,* **10,** 3389

(134) Gatehouse B.M. and Leverett P., 1969, *J.Chem.Soc. A,* 849

(135) Carofiglio T., Floriani C., Rosi M., Chiesi-Villa A. and Rizzoli C., 1991, *Inorg.Chem.,* **30,** 3245

(136) Armour A.W., Drew M.G.B. and Mitchell P.C.H., 1975, *J.Chem.Soc., Dalton Trans.,* 1493

(137) Hursthouse M.B., Short R.L., Piggott B., Tucher A. and Wong S.F., 1986, *Polyhedron,* **5,** 2121

(138) Schoettel G., Kress J. and Osborn J.A., 1988, *J.Chem.Soc., Chem.Commun.,* 914

(139) Peters J.C., Johnson A.R., Odom A.L., Wanandi P.W., Davis W.M. and Cummins C.C., 1996, *J.Am.Chem.Soc.,* **118,** 10175

(140) Bishop M.W., Chatt J., Dilworth J.R., Neaves B.D., Dahlstrom P., Hyde J. and Zubieta J., 1981, *J.Organometallic Chem.,* **213,** 109

(141) Chien F.Z., Moss S.C., Liang K.S. and Chianelli R.R., 1984, *Phys.Rev.,* **B29,** 4606

(142) Hibble S.J., Rice D.A., Pickup D.M. and Beer M.P., 1995, *Inorg.Chem.,* **34,** 5109

(143) Fletcher J., Hogarth G. and Tocher D.A., 1991, *J. Organometallic Chem.,* **204,** 227

(144) Pedersen P., Scheibye P., Nilsson P. and Lawesson S.O., 1978, *Bull.Soc.Chim.Belges,* **87,** 223

(145) Cheraksov R.A., Kutrev G.A. and Pudovik N., 1985, *Tetrahedron,* **14,** 2567

(146) Hill A.F. and Malget J.M., 1996, *J.Chem.Soc., Chem.Commun.,* 1177

(147) Schiebye P., Pedersen P. and Lawesson S.O., 1978, *Bull.Soc.Chim.Belges,* **87,** 229, 293

(148) Roof L. and Kolis J.W., 1993, *Chem. Rev.,* **93,** 1037

(149) Michelman R.I., Bergman R.G. and Andersen R.A., 1993, *Organometallics,* **12,** 2741

(150) Cantrell G.K. and Meyer T.Y., 1997, *J.Chem.Soc., Chem.Commun.,* 1551

(151) Meyer W.E., Walsh P.J. and Bergman R.J., 1994, *J.Am.Chem.Soc.,* **116,** 2669

(152) Ricard L., Estienne J. and Weiss R., 1973, *Inorg.Chem.,* **9,** 2182

(153) Ricard L., Estienne J. and Weiss R., 1972, *J.Chem.Soc., Chem.Commun.,* 906

(154) Brower D.C., Tonker T.L., Morrow J.R., Rivers D.S. and Templeton J.L., 1986, *Organometallics,* **5,** 1093

(155)   Drew M.G.B., Williams D.M. and Rice D.C., 1984, *Inorg.Chim.Acta*, **89**, L19-20

(156)   Deeming A.J. and Vaish R., 1993, *J.Organomet.Chem.*, **460**, C8

(157)   Dirand J., Ricard L. and Weiss R., 1975, *Transiton Metal Chemistry*, **1**, 2

(158)   Henshaw G., Parkin I.P. and Shaw G.A., 1997, *J.Chem.Soc., Dalton Trans.*, 231

(159)   Sheldrick G.M. In Siemens Analytical Instruments Co.: Madison, WI, 1990; pp .

(160)   Gibson V.C., 1995, *Polyhedron*, **14**, 2455

(161)   Coffey T.A. and Hogarth G., 1996, *Polyhedron*, **16**, 165

(162)   Coffey T.A., Forster G.D. and Hogarth G., 1996, *Acta.Cryst. Sect.C.*, 2157

Appendix II   Powder X-Ray Diffraction

X-rays are electromagnetic radiation with wavelength, ~1 Å, which are produced upon collision of high-energy charged particles with matter. In a molecule, the distance between atoms is of the order of the X-ray wavelength, so upon impingement of the radiation, ordered scattering yields discrete interference minima and maxima.

A typical X-ray spectrum has two components - white radiation and a number of monochromatic wavelengths. In a diffractometer, monochromatic radiation is produced by a beam of electrons being accelerated through a high voltage and striking a metal target, often molybdenum. The incident energy is high enough to ionise an electron from the K (1s) shell; an electron from an outer orbital falls into the vacancy and the energy from this transition appears as an X-ray. Crystal X-ray diffraction is an excellent technique to discern the structure of a given compound but, obviously, a good quality single crystal is needed. Such crystals may not be so easy to acquire. Instead, a good microcrystalline sample of a given complex may be used to obtain a powder diffraction spectrum. It is not simple to discern a molecular structure from such spectra but techniques are continually developing, with the intention of producing molecular structures as easily and as accurately as with a single crystal.

For a powder sample, radiation will hit randomly-orientated particles leading to X-ray diffraction in every conceivable direction with the effect of producing diffraction cones.
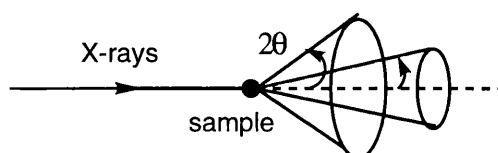
To determine the diffraction angle, 2θ, of these cones, a modern powder X-ray diffractometer measures the intensity of the scattered (reflected) X-rays as a function of 2θ to produce a diffraction pattern (with discrete peaks at specific values of 2θ, usually from 5 to 55°).
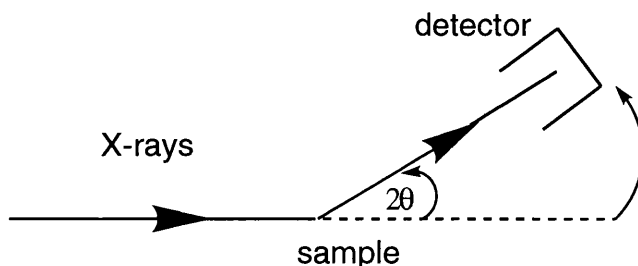
Due to the enormous range of structures a molecule can adopt, the near majority of crystalline solids has a unique powder X-ray diffraction pattern in terms of both the intensities of the peaks and of the positions of the observed reflections. To identify the unknown complex, a few intense peaks are studied and compared with known molecules. For more complicated molecules, comparisons are also made with known structures but considerably more peaks are considered.

Cell parameters can be determined if Miller indices can be assigned to some of the peaks from the diffraction pattern. However, as the symmetry of a structure decreases, so more lines in the pattern will result and it will be more difficult to assign the correct peaks. As in crystallography, systematic absences are important in structural determination as well as peak intensities. Reflections occur along the single 2θ axis and so they often overlap, particularly at high values of 2θ. One way of extracting intensities is to follow the Rietveld method in which a trial structure is used to calculate intensities for the various reflections expected. These intensities can combined with other determinant variables (like radiation wavelength and lattice parameters) to generate a calculated powder pattern. Comparison and adjustment of the parameters can then be made to make a best fit between the actual and the calculated data, helping to ascertain atomic positions in the unit cell.

Powder diffraction has been used to study other issues, like determining the size of crystallites in a given sample, or, by varying the temperature, identifying phase changes in a material.

To conclude, obtaining structures using powder X-ray diffraction is much more difficult than X-ray diffraction crystallography, due to the scattering of reflections of randomly-orientated particles. Cell parameters can be obtained from discrete peaks and using different methods, powder patterns can be calculated for a given structure and used for comparison in structural determination of characterised complexes.

Appendix III   Crystallography

The crystallographic parameters of each new structure introduced in this thesis are reproduced below. The structures of $[\{Mo(N(2,6\text{-}^iPr_2C_6H_3))_2(etc)\}_2(\mu\text{-S})(\mu^2\text{-}\eta^2\text{-}S_2)]^{161}$ and $[Mo(NS)(etc)_3]^{162}$ have already been published. Intensity data were collected on a Nicolet R3mV diffractometer, by the ω scan technique ($5 \leq 2\theta \leq 45°$). Structures were resolved by direct methods. Structure solution utilized the SHELXTL PLUS programme[159] on a Micro Vax II computer. All non-hydrogen atoms were refined anisotropically. Hydrogen atoms were placed in idealized positions (C-H 0.96è) and assigned a common isotropic thermal parameter ($U=0.08$ Å^2). The quantity minimized was $\Sigma w^{\Omega}.[\geq F_0| - |F_c|]/\Sigma w^{\Omega}.|F_0|$ $[w^{-1} = \sigma^2(F) + 0.000381F^2]$.

The structures detailed below are:

i) $[Mo(NPh)_2(S_2CNEt_2)_2]$ **(1)** (at room temperature)

ii) $[Mo(N^tBu)_2(etc)_2]$ **(2)**

iii) $[Mo(N(2\text{-}Me)C_6H_4)_2(etc)_2]$ **(3)**

iv) $[Mo(NS)(etc)_3]$ **(24)**

v) $[\{Mo(N(2,6\text{-}^iPr_2C_6H_3))_2(etc)(\mu\text{-}MoO_4)_2\}_2]$ **(27)**

vi) $[\{Mo(N(2,6\text{-}^iPr_2C_6H_3))_2(etc)\}_2(\mu\text{-S})(\mu^2\text{-}\eta^2\text{-}S_2)]$ **(37)**

vii) $[Mo(N(2,6\text{-}Cl_2C_6H_3))(S_2)(etc)_2]$ **(38)**
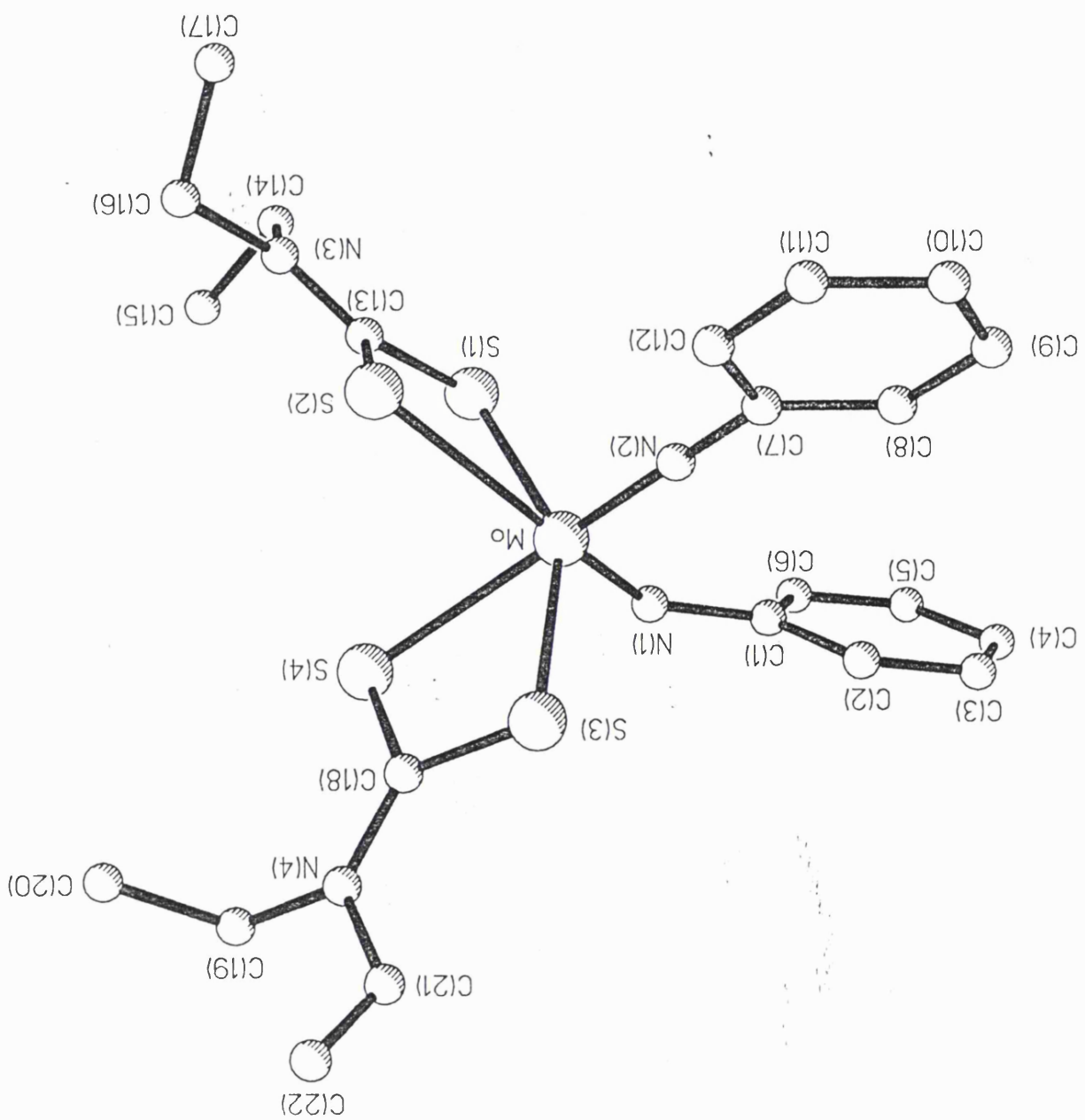
Table 1. Crystal data and structure refinement for 1.

Identification code	str509
Empirical formula	C22 H30 Mo N4 S4
Formula weight	574.68
Temperature	293(2) K
Wavelength	0.71073 A
Crystal system	Monoclinic
Space group	P21/a
Unit cell dimensions	a = 16.973(4) A alpha = 90 deg.
	b = 10.293(2) A beta = 116.01(2) deg
	c = 17.369(4) A gamma = 90 deg.
Volume	2727.1(10) A^3
Z	4
Density (calculated)	1.400 Mg/m^3
Absorption coefficient	0.804 mm^-1
F(000)	1184
Crystal size	0.42 x 0.40 x 0.28 mm
Theta range for data collection	2.61 to 25.05 deg.
Index ranges	0<=h<=20, 0<=k<=12, -20<=l<=18
Reflections collected	4937
Independent reflections	4759 [R(int) = 0.0476]
Absorption correction	None
Refinement method	Full-matrix least-squares on F^2
Data / restraints / parameters	4753 / 0 / 280
Goodness-of-fit on F^2	1.044
Final R indices [I>2sigma(I)]	R1 = 0.0591, wR2 = 0.1089
R indices (all data)	R1 = 0.1026, wR2 = 0.1254
Largest diff. peak and hole	0.460 and -0.610 e.A^-3

Table 2.   Atomic coordinates (x 10^4) and equivalent isotropic
displacement parameters (A^2 x 10^3) for 1.   U(eq) is defined
as one third of the trace of the orthogonalized Uij tensor.

	x	y	z	U(eq)
Mo	6556(1)	2157(1)	2365(1)	38(1)
S(1)	6466(1)	1169(2)	3616(1)	44(1)
S(2)	8052(1)	799(2)	3397(1)	47(1)
S(3)	6825(1)	1968(2)	1091(1)	50(1)
S(4)	6120(1)	-139(2)	1680(1)	45(1)
N(1)	5461(3)	2735(5)	1938(3)	43(1)
N(2)	7185(3)	3573(5)	2695(3)	44(1)
N(3)	7779(4)	-366(5)	4629(3)	52(1)
N(4)	6281(4)	-261(5)	224(3)	51(1)
C(1)	4975(4)	3882(6)	1759(3)	40(1)
C(2)	5159(5)	4885(8)	1331(5)	70(2)
C(3)	4688(6)	6029(8)	1171(6)	100(3)
C(4)	4043(5)	6186(8)	1425(6)	85(3)
C(5)	3849(5)	5196(7)	1833(5)	67(2)
C(6)	4299(4)	4030(6)	1984(4)	51(2)
C(7)	7766(4)	4606(6)	2893(4)	45(2)
C(8)	7463(5)	5871(6)	2807(4)	60(2)
C(9)	8053(6)	6900(7)	2991(5)	81(3)
C(10)	8908(7)	6672(10)	3288(7)	108(3)
C(11)	9204(6)	5426(10)	3380(7)	113(4)
C(12)	8644(5)	4394(8)	3187(6)	81(2)
C(13)	7496(4)	432(6)	3966(4)	42(2)
C(14)	7235(5)	-710(8)	5064(5)	76(2)
C(15)	6638(5)	-1832(8)	4647(6)	93(3)
C(16)	8637(4)	-997(7)	4946(4)	66(2)
C(17)	9310(6)	-328(10)	5713(5)	111(4)
C(18)	6395(4)	410(6)	910(4)	42(2)
C(19)	5874(5)	-1569(6)	69(4)	57(2)
C(20)	6534(5)	-2629(7)	458(5)	79(2)
C(21)	6491(8)	286(9)	-446(6)	112(4)
C(22)	6803(11)	-289(12)	-850(9)	239(10)

Table 3. Selected bond lengths [A] and angles [deg] for 1.

Mo-N(2)	1.749(5)
Mo-N(1)	1.776(5)
Mo-S(3)	2.455(2)
Mo-S(1)	2.464(2)
Mo-S(4)	2.603(2)
Mo-S(2)	2.761(2)
N(1)-C(1)	1.394(7)
N(2)-C(7)	1.387(7)
N(2)-Mo-N(1)	103.5(2)
N(2)-Mo-S(3)	91.9(2)
N(1)-Mo-S(3)	103.0(2)
N(2)-Mo-S(1)	108.7(2)
N(1)-Mo-S(1)	92.7(2)
S(3)-Mo-S(1)	150.49(6)
N(2)-Mo-S(4)	156.5(2)
N(1)-Mo-S(4)	94.5(2)
S(3)-Mo-S(4)	69.14(5)
S(1)-Mo-S(4)	85.06(5)
N(2)-Mo-S(2)	87.3(2)
N(1)-Mo-S(2)	159.6(2)
S(3)-Mo-S(2)	93.62(6)
S(1)-Mo-S(2)	67.29(5)
S(4)-Mo-S(2)	80.41(5)
C(1)-N(1)-Mo	141.8(4)
C(7)-N(2)-Mo	170.4(5)

Symmetry transformations used to generate equivalent atoms:

Table 4.   Bond lengths [A] and angles [deg] for 1.

Mo-N(2)	1.749(5)
Mo-N(1)	1.776(5)
Mo-S(3)	2.455(2)
Mo-S(1)	2.464(2)
Mo-S(4)	2.603(2)
Mo-S(2)	2.761(2)
S(1)-C(13)	1.751(6)
S(2)-C(13)	1.683(6)
S(3)-C(18)	1.732(6)
S(4)-C(18)	1.694(6)
N(1)-C(1)	1.394(7)
N(2)-C(7)	1.387(7)
N(3)-C(13)	1.321(7)
N(3)-C(16)	1.464(8)
N(3)-C(14)	1.470(8)
N(4)-C(18)	1.316(7)
N(4)-C(21)	1.470(9)
N(4)-C(19)	1.483(8)
C(1)-C(6)	1.373(8)
C(1)-C(2)	1.385(9)
C(2)-C(3)	1.381(10)
C(3)-C(4)	1.357(10)
C(4)-C(5)	1.361(10)
C(5)-C(6)	1.384(9)
C(7)-C(12)	1.365(9)
C(7)-C(8)	1.383(9)
C(8)-C(9)	1.396(10)
C(9)-C(10)	1.331(12)
C(10)-C(11)	1.361(13)
C(11)-C(12)	1.366(11)
C(14)-C(15)	1.497(11)
C(16)-C(17)	1.489(10)
C(19)-C(20)	1.496(9)
C(21)-C(22)	1.204(11)
N(2)-Mo-N(1)	103.5(2)
N(2)-Mo-S(3)	91.9(2)
N(1)-Mo-S(3)	103.0(2)
N(2)-Mo-S(1)	108.7(2)
N(1)-Mo-S(1)	92.7(2)
S(3)-Mo-S(1)	150.49(6)
N(2)-Mo-S(4)	156.5(2)
N(1)-Mo-S(4)	94.5(2)
S(3)-Mo-S(4)	69.14(5)
S(1)-Mo-S(4)	85.06(5)
N(2)-Mo-S(2)	87.3(2)
N(1)-Mo-S(2)	159.6(2)
S(3)-Mo-S(2)	93.62(6)
S(1)-Mo-S(2)	67.29(5)
S(4)-Mo-S(2)	80.41(5)
C(13)-S(1)-Mo	92.7(2)
C(13)-S(2)-Mo	84.3(2)
C(18)-S(3)-Mo	90.3(2)
C(18)-S(4)-Mo	86.3(2)
C(1)-N(1)-Mo	141.8(4)
C(7)-N(2)-Mo	170.4(5)
C(13)-N(3)-C(16)	121.7(6)
C(13)-N(3)-C(14)	121.8(6)
C(16)-N(3)-C(14)	116.4(5)
C(18)-N(4)-C(21)	121.7(6)

C(18)-N(4)-C(19)	120.9(5)
C(21)-N(4)-C(19)	117.3(5)
C(6)-C(1)-C(2)	118.9(6)
C(6)-C(1)-N(1)	121.1(5)
C(2)-C(1)-N(1)	120.1(6)
C(3)-C(2)-C(1)	119.8(7)
C(4)-C(3)-C(2)	120.9(8)
C(3)-C(4)-C(5)	119.6(7)
C(4)-C(5)-C(6)	120.5(7)
C(1)-C(6)-C(5)	120.2(6)
C(12)-C(7)-C(8)	119.0(7)
C(12)-C(7)-N(2)	120.7(6)
C(8)-C(7)-N(2)	120.3(6)
C(7)-C(8)-C(9)	119.6(7)
C(10)-C(9)-C(8)	120.4(8)
C(9)-C(10)-C(11)	119.7(9)
C(10)-C(11)-C(12)	121.5(9)
C(7)-C(12)-C(11)	119.7(8)
N(3)-C(13)-S(2)	124.6(5)
N(3)-C(13)-S(1)	119.9(5)
S(2)-C(13)-S(1)	115.5(3)
N(3)-C(14)-C(15)	112.4(7)
N(3)-C(16)-C(17)	112.2(6)
N(4)-C(18)-S(4)	123.8(5)
N(4)-C(18)-S(3)	122.2(5)
S(4)-C(18)-S(3)	114.0(3)
N(4)-C(19)-C(20)	112.5(6)
C(22)-C(21)-N(4)	126.5(10)

Symmetry transformations used to generate equivalent atoms:

Table 5.   Anisotropic displacement parameters (A^2 x 10^3) for 1.
The anisotropic displacement factor exponent takes the form:
-2 pi^2 [h^2 a*^2 U11 + ... + 2 h k a* b* U12]

	U11	U22	U33	U23	U13	U12
Mo	40(1)	30(1)	39(1)	0(1)	13(1)	-1(1)
S(1)	45(1)	45(1)	43(1)	2(1)	21(1)	6(1)
S(2)	45(1)	49(1)	49(1)	9(1)	22(1)	7(1)
S(3)	61(1)	43(1)	49(1)	0(1)	27(1)	-11(1)
S(4)	56(1)	35(1)	46(1)	-2(1)	25(1)	-6(1)
N(1)	33(3)	49(3)	42(3)	-6(2)	11(2)	6(3)
N(2)	52(3)	34(3)	42(3)	0(2)	18(3)	-5(3)
N(3)	60(4)	51(3)	40(3)	13(3)	17(3)	6(3)
N(4)	63(4)	52(3)	43(3)	-6(3)	30(3)	-10(3)
C(1)	38(4)	41(4)	33(3)	6(3)	9(3)	-2(3)
C(2)	54(5)	76(5)	93(6)	30(5)	44(4)	16(4)
C(3)	84(6)	67(6)	165(9)	74(6)	70(7)	40(5)
C(4)	76(6)	56(5)	139(8)	28(5)	62(6)	29(5)
C(5)	69(5)	61(5)	89(6)	11(4)	51(5)	13(4)
C(6)	53(4)	45(4)	58(4)	12(3)	28(3)	-1(3)
C(7)	59(5)	36(4)	40(3)	-7(3)	21(3)	-5(3)
C(8)	63(5)	46(4)	62(4)	-6(3)	20(4)	-6(4)
C(9)	105(7)	39(4)	87(6)	7(4)	30(5)	-16(5)
C(10)	88(8)	75(7)	141(9)	-28(6)	33(7)	-38(6)
C(11)	70(6)	86(7)	192(11)	-25(7)	67(7)	-26(6)
C(12)	57(5)	59(5)	120(7)	-8(5)	34(5)	-3(4)
C(13)	41(4)	38(3)	41(3)	-5(3)	13(3)	3(3)
C(14)	85(6)	94(6)	59(5)	45(5)	40(4)	20(5)
C(15)	77(6)	80(6)	120(7)	55(6)	40(5)	0(5)
C(16)	60(5)	77(5)	56(4)	26(4)	22(4)	29(4)
C(17)	81(6)	148(10)	72(6)	1(6)	2(5)	35(7)
C(18)	41(4)	42(4)	42(3)	1(3)	18(3)	-1(3)
C(19)	65(5)	52(4)	51(4)	-8(3)	24(4)	-8(4)
C(20)	77(6)	64(5)	85(6)	-3(4)	24(5)	1(5)
C(21)	190(11)	98(7)	99(7)	-40(6)	110(8)	-50(7)
C(22)	495(30)	111(10)	302(20)	-66(12)	350(23)	-93(15)

Table 6.   Hydrogen coordinates (x 10^4) and isotropic displacement parameters (A^2 x 10^3) for 1.

	x	y	z	U(eq)
H(2A)	5614(5)	4780(8)	1150(5)	80
H(3A)	4813(6)	6715(8)	866(6)	80
H(4A)	3720(5)	6984(8)	1315(6)	80
H(5A)	3409(5)	5311(7)	2033(5)	80
H(6A)	4134(4)	3317(6)	2238(4)	80
H(8A)	6850(5)	6038(6)	2623(4)	80
H(9A)	7837(6)	7776(7)	2895(5)	80
H(10A)	9309(7)	7391(10)	3443(7)	80
H(11A)	9820(6)	5268(10)	3580(7)	80
H(12A)	8858(5)	3519(8)	3248(6)	80
H(14A)	6880(5)	25(8)	5047(5)	80
H(14B)	7606(5)	-911(8)	5654(5)	80
H(15A)	6287(5)	-2032(8)	4939(6)	80
H(15B)	6263(5)	-1626(8)	4060(6)	80
H(15C)	6995(5)	-2569(8)	4671(6)	80
H(16A)	8827(4)	-1016(7)	4501(4)	80
H(16B)	8584(4)	-1878(7)	5100(4)	80
H(17A)	9864(6)	-765(10)	5910(5)	80
H(17B)	9369(6)	549(10)	5557(5)	80
H(17C)	9124(6)	-321(10)	6161(5)	80
H(19A)	5556(5)	-1717(6)	-536(4)	80
H(19B)	5464(5)	-1606(6)	312(4)	80
H(20A)	6248(5)	-3460(7)	349(5)	80
H(20B)	6938(5)	-2605(7)	208(5)	80
H(20C)	6846(5)	-2493(7)	1065(5)	80
H(21A)	6841(8)	1048(9)	-211(6)	80
H(21B)	5942(8)	575(9)	-891(6)	80
H(22A)	6872(11)	230(12)	-1275(9)	80
H(22B)	7369(11)	-560(12)	-425(9)	80
H(22C)	6455(11)	-1040(12)	-1116(9)	80

C(3)

C(4)

C(2)

C(5)

N(1)

C(12)

C(11)

C(13)

S(1)

C(1)

S(2)

N(3)

Mo(1)

C(14)

C(16)

C(15)

N(4)

S(4)

S(3)

C(6)

C(18)

N(2)

C(10)

C(7)

C(17)

C(9)

C(8)

154
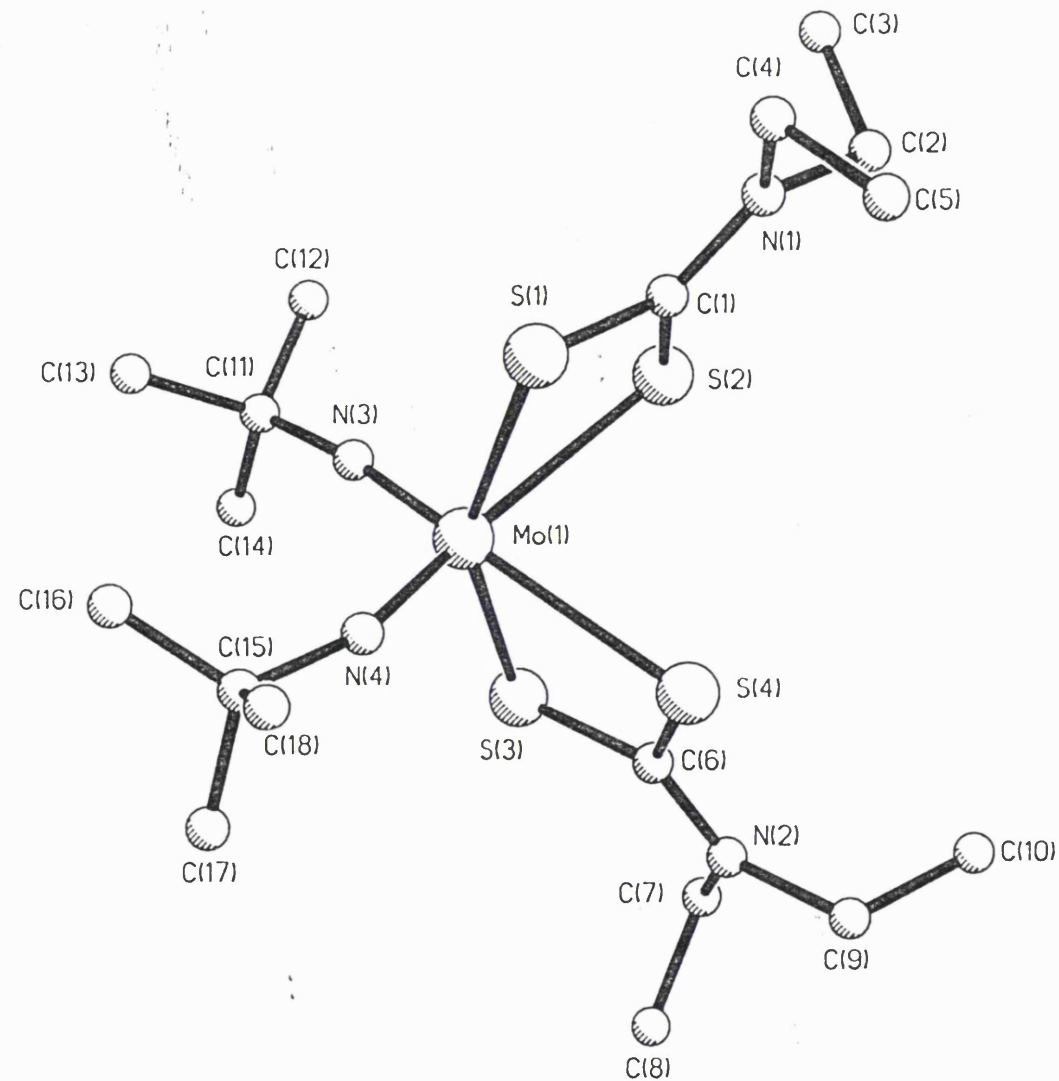
Table. Crystallographic data for [Mo(NBu^t)$_2$(η^2-S$_2$CNEt$_2$)$_2$]

Formula	Mo$_1$ C$_{18}$ H$_{38}$ N$_4$ S$_4$
Space group	P 2$_1$/c
a, Å	17.0144(71)
b, Å	9.1927(36)
c, Å	19.0640(65)
α, deg	90
ß, deg	115.088
γ, deg	90
V, Å^3	2700.46
Z	4
F(000)	1120
d$_{calc}$, g/cm^3	1.32
Cryst. size, mm	0.35 x 0.30 x 0.10
μ(Mo-K$_\alpha$), cm^{-1}	7.82
Data collection instrument	Nicolet R3mV
Radiation	Mo-K$_\alpha$ (λ = 0.71073)
Orientation reflections: no.;range	23; 13$\leq$2$\theta$$\leq$23
Temp., °C	19
Data measured	5463
Unique data	5061
No. of unique with I$\geq$3.0σ(I)	2359
No. of parameters	244
R ^{a}	0.049
R$_w$ ^{b}	0.050
Weighting scheme	w^{-1} = σ^2(F) + 0.000321F^2
Largest shift/esd, final cycle	0.002
Largest peak, e/Å^3	0.46

[a] $R = \Sigma[|F_o| - |F_c|]/\Sigma|F_o|$

[b] $R_w = \Sigma w^{1/2}.[|F_o| - |F_c|]/\Sigma w^{1/2}.|F_o|$

Table 1. Atomic coordinates ($\times 10^4$) and equivalent isotropic
displacement parameters ($\text{Å}^2 \times 10^3$)

	x	y	z	U(eq)
Mo(1)	2539(1)	2019(1)	2339(1)	55(1)
S(1)	1379(1)	1364(3)	2736(1)	54(1)
S(2)	1183(1)	651(3)	1196(1)	59(1)
S(3)	3016(1)	2951(3)	1368(1)	66(1)
S(4)	1608(1)	4342(3)	1567(1)	63(1)
N(1)	-91(4)	281(7)	1643(3)	49(3)
N(2)	2172(5)	5278(9)	543(4)	69(4)
N(3)	3162(4)	481(9)	2470(4)	71(4)
N(4)	3061(4)	3121(9)	3158(3)	70(3)
C(1)	720(5)	690(9)	1824(4)	47(3)
C(2)	-649(6)	-265(10)	867(4)	65(4)
C(3)	-603(7)	-1914(10)	805(5)	79(5)
C(4)	-493(5)	378(9)	2191(4)	54(4)
C(5)	-973(6)	1792(10)	2103(5)	72(5)
C(6)	2248(5)	4334(10)	1098(4)	54(4)
C(7)	2683(7)	5128(13)	77(6)	89(6)
C(3)	3333(9)	6255(16)	248(8)	150(10)
C(9)	1519(6)	6458(11)	301(5)	77(5)
C(10)	744(7)	6062(13)	-401(6)	105(6)
C(11)	3761(8)	-683(14)	2585(6)	89(6)
C(12)	3321(12)	-1982(18)	2196(11)	271(16)
C(13)	4225(11)	-1115(16)	3390(9)	203(12)
C(14)	4372(14)	-292(23)	2323(14)	406(37)
C(15)	3640(6)	3626(10)	3901(5)	61(4)
C(16)	4114(10)	2497(14)	4415(7)	175(10)
C(17)	4265(11)	4535(20)	3798(8)	249(15)
C(18)	3208(11)	4405(23)	4256(9)	300(18)

* Equivalent isotropic U defined as one third of the trace of
the orthogonalized U_{ij} tensor

Table 2. Bond lengths (Å)

Mo(1)-S(1)	2.469	(3)	Mo(1)-S(2)	2.719	(2)
Mo(1)-S(3)	2.468	(3)	Mo(1)-S(4)	2.694	(3)
Mo(1)-N(3)	1.721	(8)	Mo(1)-N(4)	1.753	(7)
S(1)-C(1)	1.735	(7)	S(2)-C(1)	1.690	(10)
S(3)-C(6)	1.738	(9)	S(4)-C(6)	1.677	(10)
N(1)-C(1)	1.327	(11)	N(1)-C(2)	1.467	(9)
N(1)-C(4)	1.474	(13)	N(2)-C(6)	1.331	(12)
N(2)-C(7)	1.489	(17)	N(2)-C(9)	1.480	(13)
N(3)-C(11)	1.429	(15)	N(4)-C(15)	1.418	(10)
C(2)-C(3)	1.525	(14)	C(4)-C(5)	1.506	(13)
C(7)-C(8)	1.447	(19)	C(9)-C(10)	1.473	(12)
C(11)-C(12)	1.438	(20)	C(11)-C(13)	1.453	(18)
C(11)-C(14)	1.376	(32)	C(15)-C(16)	1.420	(15)
C(15)-C(17)	1.429	(23)	C(15)-C(18)	1.391	(24)

Table 3. Bond angles (°)

S(1)-Mo(1)-S(2)	67.4(1)	S(1)-Mo(1)-S(3)	151.0(1)
S(2)-Mo(1)-S(3)	89.8(1)	S(1)-Mo(1)-S(4)	90.0(1)
S(2)-Mo(1)-S(4)	80.0(1)	S(3)-Mo(1)-S(4)	67.6(1)
S(1)-Mo(1)-N(3)	106.2(3)	S(2)-Mo(1)-N(3)	89.8(2)
S(3)-Mo(1)-N(3)	90.8(3)	S(4)-Mo(1)-N(3)	156.0(3)
S(1)-Mo(1)-N(4)	92.1(3)	S(2)-Mo(1)-N(4)	156.7(3)
S(3)-Mo(1)-N(4)	105.3(3)	S(4)-Mo(1)-N(4)	89.3(2)
N(3)-Mo(1)-N(4)	107.3(3)	Mo(1)-S(1)-C(1)	92.3(3)
Mo(1)-S(2)-C(1)	85.1(2)	Mo(1)-S(3)-C(6)	91.8(3)
Mo(1)-S(4)-C(6)	85.6(3)	C(1)-N(1)-C(2)	121.1(8)
C(1)-N(1)-C(4)	122.9(6)	C(2)-N(1)-C(4)	116.0(7)
C(6)-N(2)-C(7)	122.0(8)	C(6)-N(2)-C(9)	122.1(9)
C(7)-N(2)-C(9)	115.7(8)	Mo(1)-N(3)-C(11)	173.2(8)
Mo(1)-N(4)-C(15)	162.5(7)	S(1)-C(1)-S(2)	114.9(5)
S(1)-C(1)-N(1)	121.4(7)	S(2)-C(1)-N(1)	123.7(5)
N(1)-C(2)-C(3)	112.7(6)	N(1)-C(4)-C(5)	111.5(7)
S(3)-C(6)-S(4)	114.9(5)	S(3)-C(6)-N(2)	121.3(8)
S(4)-C(6)-N(2)	123.7(7)	N(2)-C(7)-C(8)	112.5(11)
N(2)-C(9)-C(10)	111.5(8)	N(3)-C(11)-C(12)	111.2(11)
N(3)-C(11)-C(13)	113.5(12)	C(12)-C(11)-C(13)	104.4(12)
N(3)-C(11)-C(14)	110.4(13)	C(12)-C(11)-C(14)	109.8(16)
C(13)-C(11)-C(14)	107.4(14)	N(4)-C(15)-C(16)	113.6(9)
N(4)-C(15)-C(17)	107.3(9)	C(16)-C(15)-C(17)	106.5(11)
N(4)-C(15)-C(18)	111.6(9)	C(16)-C(15)-C(18)	107.6(12)
C(17)-C(15)-C(18)	110.1(13)		

Table 4.   Anisotropic displacement parameters (Å²x10³)

	U_{11}	U_{22}	U_{33}	U_{23}	U_{13}	U_{12}
Mo(1)	42(1)	74(1)	46(1)	2(1)	16(1)	0(1)
S(1)	55(1)	72(2)	39(1)	-12(1)	22(1)	-10(1)
S(2)	62(1)	80(2)	42(1)	-14(1)	29(1)	-14(1)
S(3)	57(1)	79(2)	75(1)	12(1)	41(1)	16(1)
S(4)	57(1)	74(2)	67(1)	7(1)	35(1)	14(1)
N(1)	59(4)	52(4)	38(3)	0(3)	22(3)	-10(4)
N(2)	74(5)	69(5)	74(5)	12(4)	43(4)	13(5)
N(3)	57(5)	76(6)	85(5)	34(4)	35(4)	20(5)
N(4)	55(4)	96(6)	49(4)	-3(4)	13(3)	-22(5)
C(1)	52(5)	47(5)	42(4)	6(4)	20(4)	2(4)
C(2)	65(6)	84(7)	41(4)	-8(5)	18(4)	-24(5)
C(3)	103(8)	88(8)	51(5)	-13(6)	38(5)	-37(7)
C(4)	55(5)	59(6)	55(5)	2(4)	31(4)	-12(5)
C(5)	69(6)	72(7)	88(7)	5(6)	47(5)	3(6)
C(6)	43(5)	62(6)	54(5)	3(5)	17(4)	2(5)
C(7)	95(8)	104(9)	90(7)	26(7)	61(7)	10(7)
C(8)	147(13)	166(15)	184(14)	3(12)	116(12)	-9(12)
C(9)	81(7)	78(7)	77(6)	15(6)	40(6)	-4(6)
C(10)	88(8)	114(10)	101(8)	26(8)	27(7)	-14(8)
C(11)	99(9)	85(8)	77(7)	0(7)	31(7)	11(8)
C(12)	215(21)	164(19)	272(24)	-77(19)	-53(18)	66(18)
C(13)	227(19)	129(14)	178(16)	-19(12)	12(14)	105(14)
C(14)	484(43)	232(30)	754(63)	321(38)	554(50)	268(32)
C(15)	62(6)	60(6)	54(5)	1(5)	17(5)	-10(5)
C(16)	235(19)	117(13)	88(9)	-10(8)	-14(10)	0(12)
C(17)	283(24)	332(28)	108(11)	-40(14)	59(13)	-233(23)
C(18)	169(18)	482(41)	174(17)	-172(22)	1(14)	130(23)

The anisotropic displacement exponent takes the form:
$-2\pi^2(h^2a^{*2}U_{11} + \ldots + 2hka^*b^*U_{12})$

153

Table 5. H-Atom coordinates (x10⁴) and isotropic displacement parameters ($Å^2$x10³)

	x	y	z	U
H(2A)	-498	197	490	80
H(2B)	-1239	-17	753	80
H(3A)	-982	-2243	295	80
H(3B)	-15	-2160	913	80
H(3C)	-762	-2376	1178	80
H(4A)	-56	285	2712	80
H(4B)	-898	-408	2091	80
H(5A)	-1237	1836	2459	80
H(5B)	-565	2575	2209	80
H(5C)	-1413	1877	1582	80
H(7A)	2304	5176	-465	80
H(7B)	2959	4192	182	80
H(8A)	3659	6124	-52	80
H(8B)	3056	7190	137	80
H(8C)	3716	6197	790	80
H(9A)	1768	7323	198	80
H(9B)	1356	6663	715	80
H(10A)	327	6837	-550	80
H(10B)	910	5868	-815	80
H(10C)	493	5203	-294	80
H(12A)	3014	-1807	1649	80
H(12B)	3715	-2781.	2282	80
H(12C)	2914	-2215	2406	80
H(13A)	3808	-1500	3558	80
H(13B)	4661	-1834	3463	80
H(13C)	4491	-264	3688	80
H(14A)	4156	1	1791	80
H(14B)	4630	529	2652	80
H(14C)	4800	-1041	2426	80
H(16A)	3712	1870	4501	80
H(16B)	4418	1952	4178	80
H(16C)	4522	2884	4901	80
H(17A)	3959	5323	3463	80
H(17B)	4673	4918	4286	80
H(17C)	4569	3985	3563	80
H(18A)	2803	3776	4336	80
H(18B)	3612	4788	4744	80
H(18C)	2899	5193	3921	80
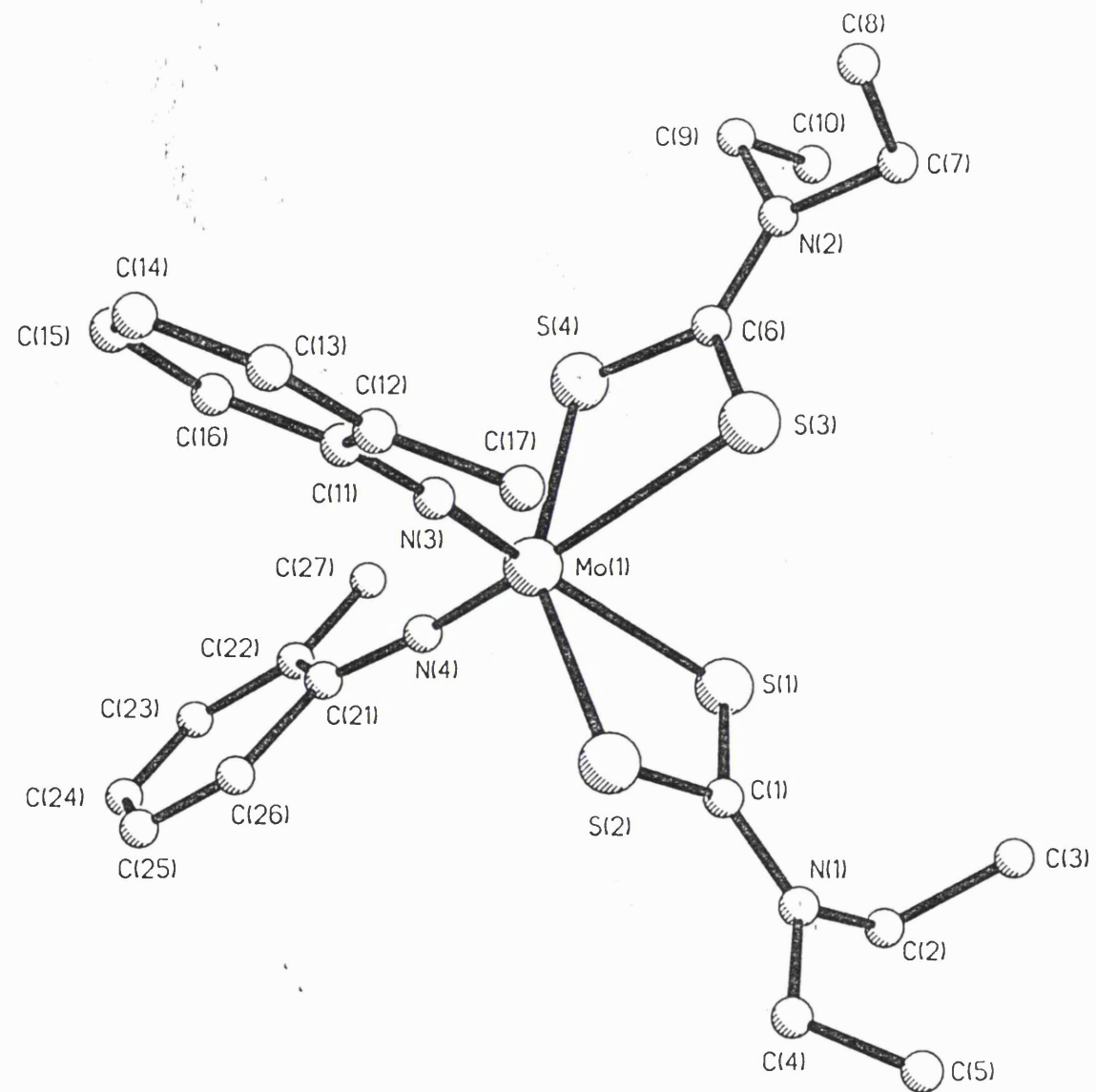
Table. Crystallographic data for [Mo(N-2-MeC$_6$H$_4$)$_2$(η^2-S$_2$CNEt$_2$)$_2$]

Formula	Mo$_1$ C$_{24}$ H$_{34}$ N$_4$ S$_4$
Space group	P $\bar{1}$
a, Å	8.4672(20)
b, Å	10.4857(30)
c, Å	16.3883(44)
α, deg	73.316(21)
β, deg	86.184(20)
γ, deg	89.127(22)
V, Å^3	1390.67
Z	2
F(000)	624
d$_{calc}$, g/cm^3	1.44
Cryst. size, mm	0.42 x 0.26 x 0.22
μ(Mo-K$_\alpha$), cm^{-1}	7.68
Data collection instrument	Nicolet R3mV
Radiation	Mo-K$_\alpha$ (λ = 0.71073)
Orientation reflections: no.;range	25; 19$\leq$2$\theta\leq$29
Temp., °C	19
Data measured	5442
Unique data	5140
No. of unique with I$\geq$3.0σ(I)	3801
No. of parameters	298
R ^{a}	0.050
R$_w$ ^{b}	0.054
Weighting scheme	w^{-1} = σ^2(F) + 0.000779F^2
Largest shift/esd, final cycle	0.03
Largest peak, e/Å^3	0.89

[a] R = $\Sigma[\,|F_o|\!-\!|F_c|\,]/\Sigma|F_o|$

[b] R$_w$ = $\Sigma w^{1/2}.[\,|F_o|\!-\!|F_c|\,]/\Sigma w^{1/2}.|F_o|$

Table 1. Atomic coordinates (x10^4) and equivalent isotropic
displacement parameters (Å^{2}x10^3)

	x	y	z	U(eq)
Mo(1)	2587(1)	6291(1)	2245(1)	42(1)
S(1)	2212(2)	6804(2)	3740(1)	55(1)
S(2)	-230(2)	6287(2)	2727(1)	52(1)
S(3)	2576(2)	8962(1)	1735(1)	50(1)
S(4)	5277(2)	7215(1)	2094(1)	48(1)
N(1)	-849(6)	6652(5)	4268(3)	50(2)
N(2)	5562(6)	9864(5)	1524(3)	50(2)
N(3)	2198(5)	6287(5)	1206(3)	49(2)
N(4)	3204(6)	4649(5)	2765(3)	58(2)
C(1)	241(7)	6596(5)	3665(4)	46(2)
C(2)	-382(8)	6893(7)	5060(4)	62(3)
C(3)	-153(12)	8341(8)	4975(6)	92(4)
C(4)	-2520(8)	6379(9)	4221(5)	73(3)
C(5)	-3610(12)	7274(13)	4430(8)	124(6)
C(6)	4568(6)	8835(5)	1751(3)	42(2)
C(7)	4958(8)	11249(6)	1227(4)	56(2)
C(3)	4728(9)	11648(7)	288(5)	68(3)
C(9)	7291(7)	9711(7)	1478(5)	61(3)
C(10)	8033(9)	9956(9)	2228(6)	84(4)
C(11)	1924(7)	6169(5)	414(4)	45(2)
C(12)	763(7)	6932(6)	-84(4)	53(2)
C(13)	591(8)	6781(7)	-871(4)	61(3)
C(14)	1523(9)	5942(8)	-1194(5)	69(3)
C(15)	2699(9)	5216(7)	-721(5)	68(3)
C(16)	2892(7)	5312(6)	81(4)	56(2)
C(17)	-258(8)	7856(7)	273(5)	66(3)
C(21)	3527(11)	3332(8)	3009(5)	76(3)
C(22)	4778(14)	2740(11)	3343(7)	106(5)
C(23)	4950(18)	1291(9)	3625(7)	118(5)
C(24)	3739(17)	585(13)	3502(8)	118(6)
C(25)	2352(16)	1128(12)	3135(7)	123(6)
C(26)	2177(14)	2432(7)	2893(5)	98(4)
C(27)	6021(13)	3552(11)	3436(8)	118(5)

* Equivalent isotropic U defined as one third of the trace of
the orthogonalized U$_{ij}$ tensor

Table 2. Bond lengths (Å)

Mo(1)-S(1)	2.654	(2)	Mo(1)-S(2)	2.462	(2)
Mo(1)-S(3)	2.682	(2)	Mo(1)-S(4)	2.458	(2)
Mo(1)-N(3)	1.757	(6)	Mo(1)-N(4)	1.776	(5)
S(1)-C(1)	1.703	(6)	S(2)-C(1)	1.732	(7)
S(3)-C(6)	1.691	(6)	S(4)-C(6)	1.740	(5)
N(1)-C(1)	1.320	(8)	N(1)-C(2)	1.471	(9)
N(1)-C(4)	1.459	(9)	N(2)-C(6)	1.329	(7)
N(2)-C(7)	1.488	(7)	N(2)-C(9)	1.470	(8)
N(3)-C(11)	1.373	(8)	N(4)-C(21)	1.352	(9)
C(2)-C(3)	1.499	(11)	C(4)-C(5)	1.403	(15)
C(7)-C(8)	1.500	(10)	C(9)-C(10)	1.504	(13)
C(11)-C(12)	1.408	(8)	C(11)-C(16)	1.407	(9)
C(12)-C(13)	1.361	(10)	C(12)-C(17)	1.503	(10)
C(13)-C(14)	1.366	(11)	C(14)-C(15)	1.383	(10)
C(15)-C(16)	1.368	(11)	C(21)-C(22)	1.292	(14)
C(21)-C(26)	1.549	(14)	C(22)-C(23)	1.464	(14)
C(22)-C(27)	1.406	(17)	C(23)-C(24)	1.333	(20)
C(24)-C(25)	1.393	(19)	C(25)-C(26)	1.320	(14)

Table 3. Bond angles (°)

S(1)-Mo(1)-S(2)	68.6(1)	S(1)-Mo(1)-S(3)	79.4(1)
S(2)-Mo(1)-S(3)	89.9(1)	S(1)-Mo(1)-S(4)	88.0(1)
S(2)-Mo(1)-S(4)	150.9(1)	S(3)-Mo(1)-S(4)	68.3(1)
S(1)-Mo(1)-N(3)	159.1(2)	S(2)-Mo(1)-N(3)	94.1(2)
S(3)-Mo(1)-N(3)	89.4(2)	S(4)-Mo(1)-N(3)	104.3(2)
S(1)-Mo(1)-N(4)	90.0(2)	S(2)-Mo(1)-N(4)	103.2(2)
S(3)-Mo(1)-N(4)	159.0(2)	S(4)-Mo(1)-N(4)	93.4(2)
N(3)-Mo(1)-N(4)	105.7(3)	Mo(1)-S(1)-C(1)	85.7(2)
Mo(1)-S(2)-C(1)	91.3(2)	Mo(1)-S(3)-C(6)	85.2(2)
Mo(1)-S(4)-C(6)	91.5(2)	C(1)-N(1)-C(2)	119.9(5)
C(1)-N(1)-C(4)	122.9(6)	C(2)-N(1)-C(4)	117.1(5)
C(6)-N(2)-C(7)	120.6(5)	C(6)-N(2)-C(9)	122.9(5)
C(7)-N(2)-C(9)	116.2(5)	Mo(1)-N(3)-C(11)	175.1(4)
Mo(1)-N(4)-C(21)	166.8(6)	S(1)-C(1)-S(2)	114.4(3)
S(1)-C(1)-N(1)	123.6(5)	S(2)-C(1)-N(1)	122.1(5)
N(1)-C(2)-C(3)	112.9(5)	N(1)-C(4)-C(5)	116.6(9)
S(3)-C(6)-S(4)	114.9(3)	S(3)-C(6)-N(2)	124.5(4)
S(4)-C(6)-N(2)	120.6(4)	N(2)-C(7)-C(8)	111.2(6)
N(2)-C(9)-C(10)	112.4(6)	N(3)-C(11)-C(12)	121.7(6)
N(3)-C(11)-C(16)	118.6(5)	C(12)-C(11)-C(16)	119.6(6)
C(11)-C(12)-C(13)	118.2(6)	C(11)-C(12)-C(17)	119.3(6)
C(13)-C(12)-C(17)	122.5(6)	C(12)-C(13)-C(14)	122.3(6)
C(13)-C(14)-C(15)	120.1(7)	C(14)-C(15)-C(16)	119.6(7)
C(11)-C(16)-C(15)	120.1(6)	N(4)-C(21)-C(22)	128.6(9)
N(4)-C(21)-C(26)	114.5(7)	C(22)-C(21)-C(26)	116.9(8)
C(21)-C(22)-C(23)	123.4(11)	C(21)-C(22)-C(27)	117.2(10)
C(23)-C(22)-C(27)	119.4(11)	C(22)-C(23)-C(24)	116.2(12)
C(23)-C(24)-C(25)	124.8(12)	C(24)-C(25)-C(26)	119.4(13)
C(21)-C(26)-C(25)	119.3(10)		

Table 4.   Anisotropic displacement parameters ($\text{Å}^2\text{x}10^3$)

	U_{11}	U_{22}	U_{33}	U_{23}	U_{13}	U_{12}
Mo(1)	43(1)	33(1)	50(1)	-15(1)	5(1)	-2(1)
S(1)	47(1)	68(1)	54(1)	-23(1)	4(1)	-12(1)
S(2)	44(1)	62(1)	56(1)	-24(1)	3(1)	-8(1)
S(3)	42(1)	38(1)	69(1)	-14(1)	5(1)	1(1)
S(4)	41(1)	40(1)	62(1)	-14(1)	3(1)	1(1)
N(1)	51(3)	49(3)	52(3)	-18(2)	8(2)	-3(2)
N(2)	49(3)	37(2)	64(3)	-16(2)	8(2)	-6(2)
N(3)	41(3)	45(3)	65(3)	-24(2)	5(2)	-7(2)
N(4)	65(3)	33(2)	75(4)	-14(2)	0(3)	-5(2)
C(1)	47(3)	36(3)	54(3)	-13(2)	6(3)	-6(2)
C(2)	68(4)	65(4)	53(4)	-21(3)	14(3)	-2(3)
C(3)	121(7)	67(5)	98(6)	-45(4)	28(5)	-20(5)
C(4)	49(4)	101(6)	77(5)	-40(4)	9(3)	-7(4)
C(5)	76(6)	176(11)	140(9)	-76(9)	-12(6)	32(7)
C(6)	40(3)	42(3)	45(3)	-18(2)	11(2)	0(2)
C(7)	65(4)	37(3)	67(4)	-18(3)	12(3)	-8(3)
C(8)	75(5)	46(4)	76(5)	-9(3)	3(4)	-6(3)
C(9)	43(3)	52(4)	89(5)	-24(3)	18(3)	-14(3)
C(10)	57(4)	84(5)	113(7)	-27(5)	-14(4)	-9(4)
C(11)	42(3)	43(3)	52(3)	-20(3)	11(3)	-13(2)
C(12)	46(3)	47(3)	67(4)	-20(3)	2(3)	-13(3)
C(13)	59(4)	66(4)	59(4)	-21(3)	-6(3)	-7(3)
C(14)	78(5)	79(5)	62(4)	-36(4)	-3(4)	-15(4)
C(15)	72(5)	63(4)	80(5)	-44(4)	20(4)	-12(4)
C(16)	48(3)	51(3)	72(4)	-26(3)	5(3)	0(3)
C(17)	57(4)	63(4)	81(5)	-26(4)	-5(4)	12(3)
C(21)	106(6)	69(5)	53(4)	-22(3)	12(4)	28(5)
C(22)	112(8)	93(7)	117(8)	-38(6)	6(6)	17(6)
C(23)	174(12)	52(5)	123(8)	-28(5)	31(8)	19(6)
C(24)	133(10)	92(8)	124(9)	-23(7)	-4(8)	21(8)
C(25)	151(11)	107(8)	127(9)	-64(7)	27(8)	-57(8)
C(26)	176(10)	38(4)	78(5)	-22(3)	43(6)	-17(5)
C(27)	106(8)	108(8)	147(10)	-55(7)	16(7)	-6(7)

The anisotropic displacement exponent takes the form:
$-2\pi^2(h^2a^{*2}U_{11} + \ldots + 2hka^*b^*U_{12})$

Table 5. H-Atom coordinates (x10⁴) and isotropic
displacement parameters (Å²x10³)

	x	y	z	U
H(2A)	593	6438	5218	80
H(2B)	-1175	6533	5511	80
H(3A)	153	8452	5504	80
H(3B)	655	8703	4533	80
H(3C)	-1131	8799	4829	80
H(4A)	-2760	5507	4596	80
H(4B)	-2678	6355	3650	80
H(5A)	-4667	7003	4379	80
H(5B)	-3493	7289	5006	80
H(5C)	-3410	8148	4048	80
H(7A)	5690	11849	1349	80
H(7B)	3965	11310	1532	80
H(8A)	4335	12543	115	80
H(8B)	5723	11602	-19	80
H(8C)	3982	11058	166	80
H(9A)	7735	10323	962	80
H(9B)	7541	8825	1454	80
H(10A)	9158	9841	2171	80
H(10B)	7806	10847	2248	80
H(10C)	7609	9333	2745	80
H(13A)	-219	7274	-1210	80
H(14A)	1370	5862	-1752	80
H(15A)	3373	4646	-955	80
H(16A)	3689	4792	417	80
H(17A)	-989	8304	-137	80
H(17B)	-833	7355	787	80
H(17C)	406	8500	399	80
H(23A)	5890	887	3883	80
H(24A)	3835	-367	3680	80
H(25A)	1542	546	3063	80
H(26A)	1221	2818	2646	80
H(27A)	5745	4474	3225	80
H(27B)	6220	3348	4029	80
H(27C)	6954	3376	3120	80
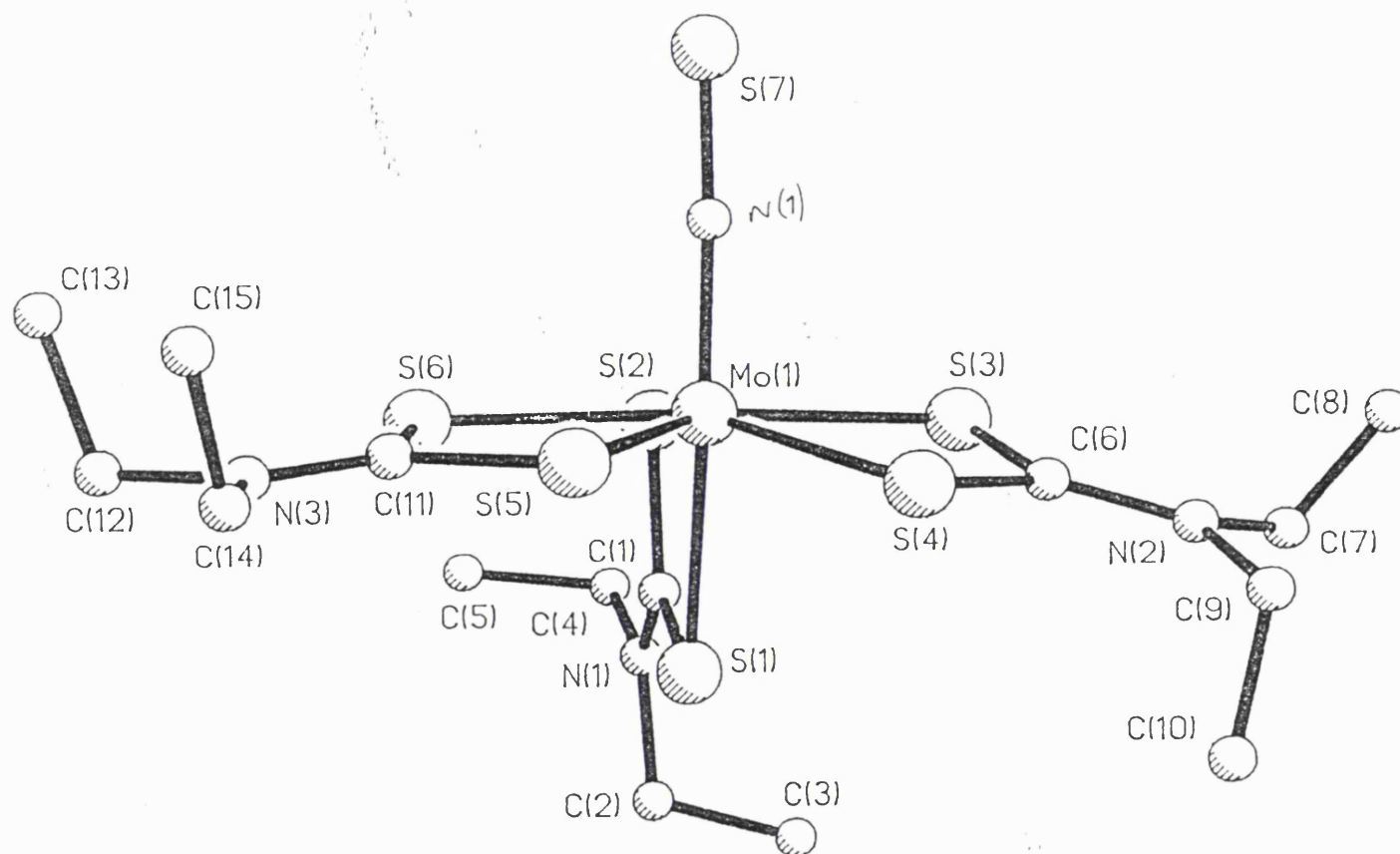
Table 1. Crystal data and structure refinement for 24

Identification code	str426
Empirical formula	C15 H30 Mo N4₃ S7
Formula weight	586.79
Temperature	293(2) K
Wavelength	0.71073 A
Crystal system	Monoclinic
Space group	P 21/c
Unit cell dimensions	a = 9.686(3) A alpha = 90 deg.
	b = 17.512(4) A beta = 96.35(2) deg.
	c = 15.470(5) A gamma = 90 deg.
Volume	2608.0(12) A^3
Z	4
Density (calculated)	1.494 Mg/m^3
Absorption coefficient	1.073 mm^-1
F(000)	1208
Crystal size	0.50 x 0.40 x 0.30 mm
Theta range for data collection	2.64 to 25.07 deg.
Index ranges	0<=h<=11, 0<=k<=20, -18<=l<=18
Reflections collected	4869
Independent reflections	4588 [R(int) = 0.0199]
Refinement method	Full-matrix least-squares on F^2
Data / restraints / parameters	4574 / 0 / 253
Goodness-of-fit on F^2	0.979
Final R indices [I>2sigma(I)]	R1 = 0.0410, wR2 = 0.0858
R indices (all data)	R1 = 0.0623, wR2 = 0.1033
Largest diff. peak and hole	0.353 and -0.411 e.A^-3

Table 2. Atomic coordinates (x 10^4) and equivalent isotropic displacement parameters (A^2 x 10^3) for 2₄. U(eq) is defined as one third of the trace of the orthogonalized Uij tensor.

	x	y	z	U(eq)
Mo(1)	8034(1)	874(1)	7835(1)	49(1)
S(1)	6962(1)	-150(1)	6733(1)	58(1)
S(2)	8279(1)	1268(1)	6319(1)	58(1)
S(3)	10311(1)	274(1)	7534(1)	60(1)
S(4)	8810(1)	-140(1)	8921(1)	61(1)
S(5)	6251(1)	749(1)	8892(1)	71(1)
S(6)	5858(1)	1617(1)	7355(1)	67(1)
S(7)	9615(1)	2437(1)	8676(1)	67(1)
N(1)	7292(4)	278(2)	5100(2)	55(1)
N(2)	11049(4)	-924(2)	8574(2)	64(1)
N(3)	3874(4)	1504(3)	8441(3)	73(1)
N(4)	8881(4)	1682(2)	8324(2)	50(1)
C(1)	7468(4)	430(3)	5943(3)	51(1)
C(2)	6710(6)	-451(3)	4768(3)	72(1)
C(3)	7823(8)	-1024(4)	4668(4)	104(2)
C(4)	7700(5)	827(3)	4456(3)	64(1)
C(5)	6548(6)	1367(3)	4163(4)	83(2)
C(6)	10205(5)	-347(3)	8377(3)	55(1)
C(7)	12142(6)	-1127(4)	8029(4)	80(2)
C(8)	13437(16)	-741(8)	8287(11)	100(4)
C(8A)	13556(35)	-1165(16)	8512(23)	114(11)
C(9)	10784(6)	-1468(3)	9256(3)	71(1)
C(10)	9760(7)	-2076(3)	8916(4)	89(2)
C(11)	5140(5)	1319(3)	8256(3)	64(1)
C(12)	2970(6)	1991(3)	7830(4)	82(2)
C(13)	3225(7)	2819(4)	7992(5)	101(2)
C(14)	3356(6)	1246(4)	9248(4)	97(2)
C(15)	3617(9)	1800(5)	9965(5)	127(3)

Table 4.   Bond lengths [A] and angles [deg] for 24.

Mo(1)-N(4)	1.765(4)
Mo(1)-S(2)	2.4817(14)
Mo(1)-S(4)	2.5016(13)
Mo(1)-S(5)	2.515(2)
Mo(1)-S(6)	2.5182(14)
Mo(1)-S(3)	2.5320(13)
Mo(1)-S(1)	2.6083(14)
S(1)-C(1)	1.703(4)
S(2)-C(1)	1.734(5)
S(3)-C(6)	1.710(5)
S(4)-C(6)	1.707(5)
S(5)-C(11)	1.700(5)
S(6)-C(11)	1.706(5)
S(7)-N(4)	1.568(4)
N(1)-C(1)	1.324(5)
N(1)-C(2)	1.465(6)
N(1)-C(4)	1.469(5)
N(2)-C(6)	1.314(6)
N(2)-C(9)	1.467(6)
N(2)-C(7)	1.468(6)
N(3)-C(11)	1.330(6)
N(3)-C(14)	1.466(7)
N(3)-C(12)	1.486(7)
C(2)-C(3)	1.494(8)
C(4)-C(5)	1.495(7)
C(7)-C(8)	1.44(2)
C(7)-C(8A)	1.49(3)
C(8)-C(8A)	0.82(3)
C(9)-C(10)	1.509(8)
C(12)-C(13)	1.487(8)
C(14)-C(15)	1.475(9)
N(4)-Mo(1)-S(2)	95.36(11)
N(4)-Mo(1)-S(4)	100.98(12)
S(2)-Mo(1)-S(4)	141.17(4)
N(4)-Mo(1)-S(5)	96.35(12)
S(2)-Mo(1)-S(5)	141.53(5)
S(4)-Mo(1)-S(5)	71.29(5)
N(4)-Mo(1)-S(6)	92.64(12)
S(2)-Mo(1)-S(6)	75.06(5)
S(4)-Mo(1)-S(6)	138.09(5)
S(5)-Mo(1)-S(6)	67.90(5)
N(4)-Mo(1)-S(3)	92.19(12)
S(2)-Mo(1)-S(3)	76.41(5)
S(4)-Mo(1)-S(3)	68.05(4)
S(5)-Mo(1)-S(3)	139.33(5)
S(6)-Mo(1)-S(3)	151.38(4)
N(4)-Mo(1)-S(1)	164.62(11)
S(2)-Mo(1)-S(1)	69.29(4)
S(4)-Mo(1)-S(1)	91.12(5)
S(5)-Mo(1)-S(1)	96.51(5)
S(6)-Mo(1)-S(1)	84.43(5)
S(3)-Mo(1)-S(1)	83.50(5)
C(1)-S(1)-Mo(1)	86.2(2)
C(1)-S(2)-Mo(1)	89.7(2)
C(6)-S(3)-Mo(1)	89.8(2)
C(6)-S(4)-Mo(1)	90.9(2)
C(11)-S(5)-Mo(1)	90.5(2)
C(11)-S(6)-Mo(1)	90.3(2)
C(1)-N(1)-C(2)	121.6(4)

C(1)-N(1)-C(4)	121.4(4)
C(2)-N(1)-C(4)	117.0(4)
C(6)-N(2)-C(9)	120.8(4)
C(6)-N(2)-C(7)	121.6(4)
C(9)-N(2)-C(7)	116.7(4)
C(11)-N(3)-C(14)	121.2(5)
C(11)-N(3)-C(12)	119.7(5)
C(14)-N(3)-C(12)	119.1(4)
S(7)-N(4)-Mo(1)	174.8(2)
N(1)-C(1)-S(1)	124.8(3)
N(1)-C(1)-S(2)	120.4(3)
S(1)-C(1)-S(2)	114.8(2)
N(1)-C(2)-C(3)	111.6(5)
N(1)-C(4)-C(5)	111.8(4)
N(2)-C(6)-S(4)	123.7(4)
N(2)-C(6)-S(3)	125.2(4)
S(4)-C(6)-S(3)	111.0(3)
C(8)-C(7)-N(2)	112.8(8)
C(8)-C(7)-C(8A)	32.6(12)
N(2)-C(7)-C(8A)	114(2)
C(8A)-C(8)-C(7)	77(3)
C(8)-C(8A)-C(7)	71(3)
N(2)-C(9)-C(10)	111.6(4)
N(3)-C(11)-S(5)	124.0(4)
N(3)-C(11)-S(6)	124.8(4)
S(5)-C(11)-S(6)	111.2(3)
N(3)-C(12)-C(13)	112.2(5)
N(3)-C(14)-C(15)	113.0(6)

Symmetry transformations used to generate equivalent atoms:

Table 5.   Anisotropic displacement parameters (A^2 x 10^3) for 24.
The anisotropic displacement factor exponent takes the form:
-2 pi^2 [h^2 a*^2 U11 + ... + 2 h k a* b* U12]

	U11	U22	U33	U23	U13	U12
Mo(1)	50(1)	50(1)	48(1)	1(1)	6(1)	2(1)
S(1)	68(1)	54(1)	53(1)	8(1)	10(1)	-13(1)
S(2)	66(1)	52(1)	56(1)	8(1)	7(1)	-11(1)
S(3)	54(1)	67(1)	60(1)	6(1)	13(1)	5(1)
S(4)	70(1)	65(1)	51(1)	9(1)	16(1)	17(1)
S(5)	62(1)	86(1)	68(1)	14(1)	20(1)	13(1)
S(6)	61(1)	72(1)	67(1)	8(1)	6(1)	15(1)
S(7)	72(1)	55(1)	72(1)	-8(1)	6(1)	0(1)
N(1)	58(2)	64(2)	45(2)	3(2)	6(2)	-8(2)
N(2)	66(2)	74(3)	52(2)	1(2)	9(2)	19(2)
N(3)	50(2)	76(3)	94(3)	-12(3)	14(2)	4(2)
N(4)	53(2)	51(2)	46(2)	1(2)	6(2)	8(2)
C(1)	51(2)	54(3)	49(2)	4(2)	7(2)	-6(2)
C(2)	87(4)	77(4)	55(3)	-4(3)	10(3)	-20(3)
C(3)	134(6)	82(4)	103(5)	-11(4)	43(4)	6(4)
C(4)	66(3)	80(3)	47(2)	12(2)	13(2)	-10(3)
C(5)	71(4)	93(4)	84(4)	33(3)	6(3)	-7(3)
C(6)	54(3)	60(3)	51(2)	-5(2)	4(2)	8(2)
C(7)	74(4)	91(4)	78(4)	3(3)	16(3)	27(3)
C(8)	66(8)	116(12)	115(12)	-26(10)	8(7)	-3(8)
C(8A)	100(17)	130(27)	111(21)	-16(19)	3(14)	44(21)
C(9)	84(4)	77(4)	51(3)	6(3)	4(3)	26(3)
C(10)	124(5)	64(4)	79(4)	1(3)	17(4)	21(4)
C(11)	57(3)	63(3)	71(3)	-4(2)	1(2)	4(2)
C(12)	59(3)	70(4)	116(5)	-19(3)	4(3)	7(3)
C(13)	95(5)	84(4)	120(5)	-11(4)	-8(4)	0(4)
C(14)	69(4)	108(5)	121(5)	-1(4)	39(4)	15(4)
C(15)	150(7)	132(7)	104(5)	3(5)	40(5)	34(6)

Table 6.   Hydrogen coordinates (x 10^4) and isotropic
displacement parameters (A^2 x 10^3) for 24.

	x	y	z	U(eq)
H(2A)	6180(6)	-373(3)	4213(3)	80
H(2B)	6098(6)	-647(3)	5163(3)	80
H(3A)	7429(8)	-1500(4)	4453(4)	80
H(3B)	8427(8)	-829(4)	4268(4)	80
H(3C)	8344(8)	-1105(4)	5225(4)	80
H(4A)	7955(5)	555(3)	3958(3)	80
H(4B)	8495(5)	1109(3)	4704(3)	80
H(5A)	6838(6)	1720(3)	3744(4)	80
H(5B)	5758(6)	1084(3)	3907(4)	80
H(5C)	6303(6)	1643(3)	4660(4)	80
H(7A)	11908(6)	-925(4)	7455(4)	80
H(7B)	12184(6)	-1674(4)	7986(4)	80
H(8A)	14109(16)	-906(8)	7915(11)	80
H(8B)	13129(16)	-235(8)	8125(11)	80
H(8C)	13852(16)	-740(8)	8880(11)	80
H(8AD)	13986(35)	-1515(16)	8938(23)	80
H(8AA)	14120(35)	-1118(16)	8043(23)	80
H(8AB)	13462(35)	-675(16)	8776(23)	80
H(9A)	10427(6)	-1202(3)	9727(3)	80
H(9B)	11641(6)	-1709(3)	9479(3)	80
H(10A)	9600(7)	-2429(3)	9369(4)	80
H(10B)	8901(7)	-1834(3)	8700(4)	80
H(10C)	10125(7)	-2345(3)	8450(4)	80
H(12A)	2013(6)	1877(3)	7881(4)	80
H(12B)	3150(6)	1874(3)	7247(4)	80
H(13A)	2633(7)	3118(4)	7583(5)	80
H(13B)	3032(7)	2938(4)	8572(5)	80
H(13C)	4179(7)	2935(4)	7932(5)	80
H(14A)	3816(6)	776(4)	9422(4)	80
H(14B)	2377(6)	1145(4)	9144(4)	80
H(15A)	3280(9)	1607(5)	10483(5)	80
H(15B)	4597(9)	1895(5)	10075(5)	80
H(15C)	3145(9)	2268(5)	9795(5)	80

C(5) C(3)
C(2)
C(4) N(1)
C(1)
S(1)
S(2)
O(3a) S(4a)
Mo(2a) O(2a)
C(22)
O(1) Mo(1a)
C(19)
C(17)
C(13) C(12) C(11)
N(3) Mo(1) O(4)
C(14)
C(15) C(16) C(20)
S(3) O(2) O(1a)
C(18)
Mo(2)
S(1a) S(2a)
C(21)
C(6) S(4)
C(7)
C(8) N(2) O(3)

22

C(9) C(10)
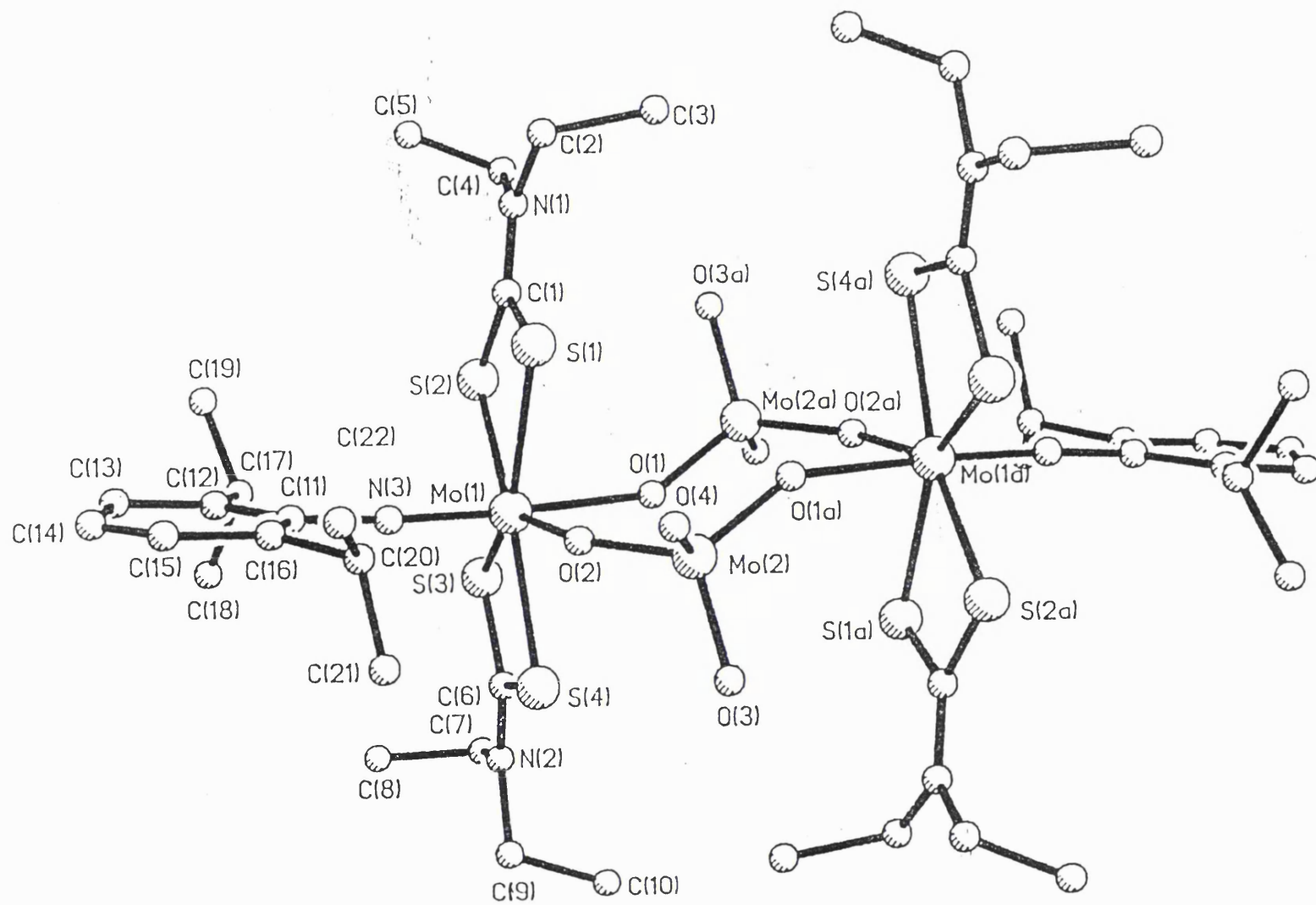
Table 1. Crystallographic data for $[Mo(\eta^2\text{-}S_2CNEt_2)_2(N\text{-}2,6\text{-}^iPr_2C_6H_3)(\mu\text{-}MoO_4)]_2.2H_2O$

Formula	$Mo_4 C_{44} H_{72} N_6 O_{10} S_8$
Space group	$P\,2_1/a$
a, Å	11.5694(17)
b, Å	23.0105(66)
c, Å	12.7226(33)
α, deg	90
ß, deg	103.16(2)
γ, deg	90
V, Å^3	3298.19
Z	2
F(000)	1508
d_{calc}, g/cm^3	1.50
Cryst. size, mm	0.80 x 0.20 x 0.08
μ(Mo-K$_\alpha$), cm^{-1}	10.17
Data collection instrument	Nicolet R3mV
Radiation	Mo-K$_\alpha$ (λ = 0.71073)
Orientation reflections: no.;range	27; $11 \leq 2\theta \leq 23$
Temp., °C	19
Data measured	6337
Unique data	5934
No. of unique with $I \geq 3.0\sigma(I)$	3377
No. of parameters	334
R ^{a}	0.057
R$_w$ ^{b}	0.064
Weighting scheme	$w^{-1} = \sigma^2(F) + 0.003794F^2$
Largest shift/esd, final cycle	0.1
Largest peak, e/Å^3	0.86

^{a} $R = \Sigma[|F_o| - |F_c|]/\Sigma|F_o|$

^{b} $R_w = \Sigma w^{1/2}.[|F_o| - |F_c|]/\Sigma w^{1/2}.|F_o|$

Table 1. Atomic coordinates (x10⁴) and equivalent isotropic
displacement parameters (Å²x10³)

	x	y	z	U(eq)
Mo(1)	3285(1)	523(1)	-1834(1)	42(1)
Mo(2)	5894(1)	885(1)	327(1)	43(1)
S(1)	5030(2)	145(1)	-2493(3)	61(1)
S(2)	2711(2)	-304(1)	-3157(2)	49(1)
S(3)	1140(2)	269(1)	-1946(2)	52(1)
S(4)	2429(2)	1088(1)	-512(2)	57(1)
N(1)	4581(9)	-792(5)	-3770(8)	72(4)
N(2)	97(9)	898(4)	-627(7)	58(3)
N(3)	3008(7)	1055(3)	-2834(6)	45(3)
O(1)	3624(7)	-158(3)	-703(6)	54(2)
O(2)	4703(6)	894(3)	-879(6)	55(2)
O(3)	5426(9)	1226(3)	1350(6)	78(4)
O(4)	7053(7)	1278(3)	93(8)	82(4)
C(1)	4154(9)	-377(5)	-3234(9)	53(4)
C(2)	5840(12)	-823(7)	-3787(14)	92(6)
C(3)	6523(12)	-1215(10)	-2854(16)	135(10)
C(4)	3794(11)	-1262(5)	-4312(10)	69(5)
C(5)	3346(15)	-1147(8)	-5443(13)	112(8)
C(6)	1073(9)	776(4)	-987(8)	49(4)
C(7)	-999(11)	577(6)	-999(12)	79(5)
C(8)	-1768(14)	827(8)	-1970(13)	108(7)
C(9)	86(12)	1384(5)	132(11)	71(5)
C(10)	276(16)	1181(6)	1261(11)	93(6)
C(11)	2897(9)	1463(4)	-3650(9)	47(3)
C(12)	1934(10)	1413(4)	-4572(8)	51(4)
C(13)	1884(13)	1836(5)	-5356(9)	69(5)
C(14)	2720(14)	2268(6)	-5261(12)	92(6)
C(15)	3650(14)	2302(5)	-4353(13)	91(6)
C(16)	3751(11)	1915(5)	-3507(11)	65(5)
C(17)	1021(10)	942(5)	-4667(8)	56(4)
C(18)	-190(14)	1154(7)	-4648(15)	102(7)
C(19)	984(15)	580(6)	-5705(10)	87(6)
C(20)	4711(11)	1982(5)	-2489(10)	67(4)
C(21)	4205(12)	2267(6)	-1657(11)	83(5)
C(22)	5827(12)	2299(7)	-2642(14)	98(7)
O(100)	2283(29)	-2298(13)	-1428(42)	287(29)
O(101)	4612(26)	-2357(7)	-2103(18)	120(12)

* Equivalent isotropic U defined as one third of the trace of
the orthogonalized U_{ij} tensor

Table 2. Bond lengths (Å)

Mo(1)-S(1)	2.511	(3)	Mo(1)-S(2)	2.528	(3)
Mo(1)-S(3)	2.522	(3)	Mo(1)-S(4)	2.502	(3)
Mo(1)-N(3)	1.740	(8)	Mo(1)-O(1)	2.103	(7)
Mo(1)-O(2)	1.997	(6)	Mo(2)-O(2)	1.814	(6)
Mo(2)-O(3)	1.710	(9)	Mo(2)-O(4)	1.698	(9)
Mo(2)-O(1A)	1.794	(7)	S(1)-C(1)	1.709	(10)
S(2)-C(1)	1.702	(12)	S(3)-C(6)	1.703	(11)
S(4)-C(6)	1.706	(10)	N(1)-C(1)	1.333	(16)
N(1)-C(2)	1.464	(18)	N(1)-C(4)	1.479	(16)
N(2)-C(6)	1.340	(15)	N(2)-C(7)	1.450	(15)
N(2)-C(9)	1.480	(16)	N(3)-C(11)	1.384	(13)
O(1)-Mo(2A)	1.794	(7)	C(2)-C(3)	1.555	(24)
C(4)-C(5)	1.438	(20)	C(7)-C(8)	1.467	(20)
C(9)-C(10)	1.473	(19)	C(11)-C(12)	1.426	(13)
C(11)-C(16)	1.418	(15)	C(12)-C(13)	1.386	(15)
C(12)-C(17)	1.498	(15)	C(13)-C(14)	1.373	(20)
C(14)-C(15)	1.390	(20)	C(15)-C(16)	1.381	(19)
C(16)-C(20)	1.510	(16)	C(17)-C(18)	1.489	(20)
C(17)-C(19)	1.554	(17)	C(20)-C(21)	1.474	(20)
C(20)-C(22)	1.533	(20)			

Table 3. Bond angles (°)

S(1)-Mo(1)-S(2)	68.1(1)	S(1)-Mo(1)-S(3)	139.2(1)
S(2)-Mo(1)-S(3)	71.4(1)	S(1)-Mo(1)-S(4)	151.2(1)
S(2)-Mo(1)-S(4)	139.0(1)	S(3)-Mo(1)-S(4)	67.8(1)
S(1)-Mo(1)-N(3)	91.6(3)	S(2)-Mo(1)-N(3)	93.8(3)
S(3)-Mo(1)-N(3)	96.1(3)	S(4)-Mo(1)-N(3)	95.3(3)
S(1)-Mo(1)-O(1)	86.1(2)	S(2)-Mo(1)-O(1)	82.8(2)
S(3)-Mo(1)-O(1)	83.9(2)	S(4)-Mo(1)-O(1)	88.1(2)
N(3)-Mo(1)-O(1)	176.4(3)	S(1)-Mo(1)-O(2)	74.9(2)
S(2)-Mo(1)-O(2)	141.5(2)	S(3)-Mo(1)-O(2)	142.6(2)
S(4)-Mo(1)-O(2)	76.4(2)	N(3)-Mo(1)-O(2)	97.7(3)
O(1)-Mo(1)-O(2)	84.4(3)	O(2)-Mo(2)-O(3)	109.1(4)
O(2)-Mo(2)-O(4)	108.9(4)	O(3)-Mo(2)-O(4)	106.8(5)
O(2)-Mo(2)-O(1A)	111.5(3)	O(3)-Mo(2)-O(1A)	110.9(4)
O(4)-Mo(2)-O(1A)	109.5(4)	Mo(1)-S(1)-C(1)	90.4(4)
Mo(1)-S(2)-C(1)	90.0(4)	Mo(1)-S(3)-C(6)	90.4(4)
Mo(1)-S(4)-C(6)	91.0(4)	C(1)-N(1)-C(2)	121.8(11)
C(1)-N(1)-C(4)	120.2(10)	C(2)-N(1)-C(4)	117.9(11)
C(6)-N(2)-C(7)	121.6(10)	C(6)-N(2)-C(9)	120.9(9)
C(7)-N(2)-C(9)	117.4(11)	Mo(1)-N(3)-C(11)	174.2(8)
Mo(1)-O(1)-Mo(2A)	151.1(4)	Mo(1)-O(2)-Mo(2)	150.4(4)
S(1)-C(1)-S(2)	111.5(6)	S(1)-C(1)-N(1)	122.9(9)
S(2)-C(1)-N(1)	125.6(8)	N(1)-C(2)-C(3)	110.5(13)
N(1)-C(4)-C(5)	112.0(12)	S(3)-C(6)-S(4)	110.7(6)
S(3)-C(6)-N(2)	124.5(7)	S(4)-C(6)-N(2)	124.8(8)
N(2)-C(7)-C(8)	113.1(12)	N(2)-C(9)-C(10)	112.0(10)
N(3)-C(11)-C(12)	118.9(8)	N(3)-C(11)-C(16)	117.3(9)
C(12)-C(11)-C(16)	123.8(10)	C(11)-C(12)-C(13)	115.6(10)
C(11)-C(12)-C(17)	121.9(9)	C(13)-C(12)-C(17)	122.5(9)
C(12)-C(13)-C(14)	122.2(11)	C(13)-C(14)-C(15)	120.6(13)
C(14)-C(15)-C(16)	121.6(13)	C(11)-C(16)-C(15)	116.1(11)
C(11)-C(16)-C(20)	122.7(11)	C(15)-C(16)-C(20)	121.2(11)
C(12)-C(17)-C(18)	114.2(10)	C(12)-C(17)-C(19)	109.9(10)
C(18)-C(17)-C(19)	110.2(11)	C(16)-C(20)-C(21)	109.1(11)
C(16)-C(20)-C(22)	114.6(12)	C(21)-C(20)-C(22)	111.3(11)

Table 4. Anisotropic displacement parameters ($\text{Å}^2 \times 10^3$)

	U_{11}	U_{22}	U_{33}	U_{23}	U_{13}	U_{12}
Mo(1)	34(1)	41(1)	45(1)	-1(1)	-3(1)	0(1)
Mo(2)	34(1)	40(1)	49(1)	-5(1)	-1(1)	0(1)
S(1)	39(1)	67(2)	76(2)	-14(2)	10(1)	-7(1)
S(2)	38(1)	53(1)	54(1)	-12(1)	3(1)	-3(1)
S(3)	40(1)	57(2)	55(2)	-10(1)	6(1)	-8(1)
S(4)	46(1)	58(2)	61(2)	-15(1)	-1(1)	-3(1)
N(1)	63(6)	80(7)	71(6)	-22(6)	12(5)	6(5)
N(2)	52(5)	62(5)	61(6)	-4(5)	12(4)	-1(5)
N(3)	43(4)	43(4)	45(5)	-6(4)	1(4)	-7(4)
O(1)	60(4)	50(4)	49(4)	-4(3)	5(3)	4(3)
O(2)	44(4)	47(4)	62(4)	-3(3)	-10(3)	-1(3)
O(3)	112(7)	66(5)	57(5)	-7(4)	24(5)	25(5)
O(4)	54(5)	58(5)	126(8)	-4(5)	4(5)	-18(4)
C(1)	46(6)	55(6)	56(6)	1(5)	11(5)	0(5)
C(2)	58(8)	109(11)	112(12)	-30(10)	29(8)	13(8)
C(3)	43(8)	215(22)	143(16)	-41(16)	14(9)	37(11)
C(4)	67(8)	69(7)	70(8)	-25(6)	17(6)	4(6)
C(5)	90(12)	144(15)	104(13)	-22(12)	28(10)	-14(11)
C(6)	43(6)	47(6)	55(6)	11(5)	5(5)	6(4)
C(7)	52(7)	98(10)	92(10)	-25(8)	26(7)	2(7)
C(8)	67(9)	157(16)	93(11)	3(11)	4(8)	-2(10)
C(9)	61(7)	61(7)	88(9)	-8(7)	15(7)	17(6)
C(10)	129(14)	80(9)	66(8)	-9(7)	15(9)	-3(9)
C(11)	52(6)	32(5)	62(6)	1(5)	23(5)	8(4)
C(12)	61(6)	51(6)	37(5)	3(5)	3(5)	4(5)
C(13)	95(9)	57(7)	48(6)	4(5)	1(6)	7(7)
C(14)	109(12)	74(9)	81(10)	26(8)	0(9)	-9(9)
C(15)	110(11)	45(7)	109(11)	23(7)	9(9)	-28(7)
C(16)	71(8)	43(6)	86(8)	-5(6)	27(7)	-14(5)
C(17)	57(6)	51(6)	47(6)	-4(5)	-13(5)	-4(5)
C(18)	78(10)	80(9)	142(15)	17(10)	11(10)	22(8)
C(19)	121(12)	76(8)	65(8)	-17(7)	20(8)	-31(8)
C(20)	63(7)	53(6)	76(8)	-3(6)	1(6)	-11(6)
C(21)	82(9)	68(8)	85(9)	-24(7)	-10(8)	4(7)
C(22)	63(8)	95(10)	133(14)	-7(10)	16(9)	-21(8)
O(100)	152(28)	150(24)	562(71)	-247(37)	84(36)	-85(21)
O(101)	212(27)	40(9)	112(16)	-21(10)	42(18)	8(13)

The anisotropic displacement exponent takes the form:
$-2\pi^2(h^2 a^{*2} U_{11} + \ldots + 2hka^*b^* U_{12})$

178

Table 5. H-Atom coordinates (x10⁴) and isotropic
displacement parameters (Å²x10³)

	x	y	z	U
H(2A)	6162	-436	-3719	80
H(2B)	5929	-979	-4463	80
H(3B)	7345	-1222	-2880	80
H(3C)	6445	-1055	-2177	80
H(3D)	6211	-1603	-2927	80
H(4B)	3117	-1301	-3999	80
H(4C)	4225	-1622	-4225	80
H(5A)	2839	-1445	-5827	80
H(5B)	2923	-785	-5511	80
H(5C)	4035	-1108	-5739	80
H(7A)	-1440	584	-445	80
H(7B)	-815	180	-1125	80
H(8A)	-2491	611	-2203	80
H(8B)	-1953	1223	-1837	80
H(8C)	-1325	816	-2522	80
H(9A)	-656	1588	-65	80
H(9B)	716	1649	97	80
H(10A)	276	1489	1769	80
H(10B)	-360	916	1282	80
H(10C)	1019	977	1445	80
H(13A)	1233	1831	-5977	80
H(14A)	2702	2539	-5837	80
H(15A)	4217	2612	-4277	80
H(17A)	1274	679	-4073	80
H(18A)	-126	1366	-3987	80
H(18B)	-474	1408	-5250	80
H(18C)	-734	837	-4673	80
H(19A)	1758	436	-5722	80
H(19B)	446	259	-5736	80
H(19C)	706	830	-6313	80
H(20A)	4957	1599	-2239	80
H(21A)	3527	2052	-1556	80
H(21B)	4790	2282	-988	80
H(21C)	3966	2654	-1889	80
H(22A)	6138	2102	-3182	80
H(22B)	5600	2687	-2881	80
H(22C)	6424	2315	-1981	80

179

----
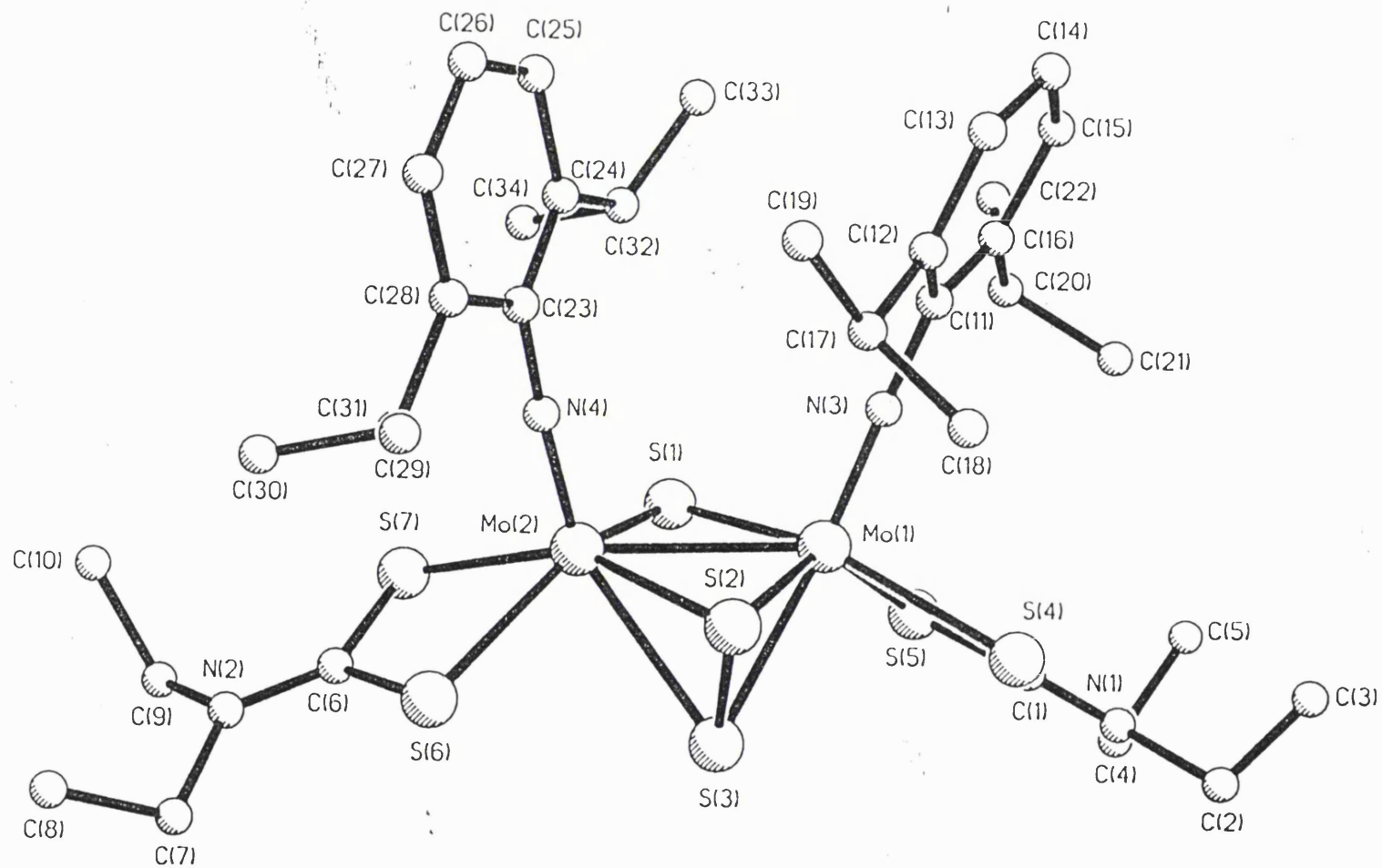
t contents: C(136) H(216) N(16) S(28) Mo(8)

ce group: P 21/n,   Z = 1

= 17.824(6)A   Alpha =   90 deg.   Vol. = 4296.4(4.1)A^3
= 10.984(4)A   Beta   = 102.72(2)deg.   Dens. = 1.446 g/cm3
= 22.497(4)A   Gamma =   90 deg.   Mu   = 9.25   cm-1

fractometer: Nicolet P3   Scan technique : Theta/2*Theta
ochromator : none   sin(Th)/WL(max): .5384
bda   : Mo (K-alpha)   Number of refl.: 3229 I >******Sig(I)

grams   : SHELXTL   Solution   : Patterson

           : .058   GOOF   = 1.61
           : .058   Weight = 1/(sigma**(F) + .000381*F*F)

le 1.   Atom coordinates (x10^4) and temperature factors (A^2 x10^3)

m	x	y	z	U
(1)	6007(1)	814(1)	3653(1)	43(1)*
(2)	6249(1)	2112(1)	4749(1)	43(1)*
1)	6371(2)	2866(3)	3803(1)	49(1)*
2)	5698(2)	133(4)	4570(2)	66(1)*
3)	4896(3)	1234(4)	4171(2)	92(2)*
4)	5149(2)	-827(4)	3104(2)	74(2)*
5)	5358(2)	1544(3)	2638(2)	62(1)*
6)	5518(2)	2353(3)	5563(2)	63(1)*
7)	6201(2)	4290(3)	5030(2)	61(1)*
1)	4464(8)	-151(13)	1975(5)	81(6)*
2)	5561(6)	4606(9)	5982(5)	56(4)*
3)	6855(5)	59(9)	3614(4)	49(4)*
4)	7157(6)	1746(9)	5147(4)	48(4)*
1)	4932(8)	-151(13)	2499(6)	68(6)*
2)	4060(14)	-1338(20)	1892(9)	119(11)*
3)	4503(15)	-2094(23)	1655(11)	179(17)*
4)	4233(22)	694(27)	1471(9)	198(19)*
5)	4784(21)	631(33)	1079(15)	475(47)*
6)	5737(7)	3858(11)	5587(5)	46(5)*
7)	5055(9)	4269(14)	6405(6)	84(7)*
8)	5348(12)	4426(18)	7027(7)	134(11)*
9)	5773(10)	5909(14)	5987(7)	84(7)*
10)	6545(11)	6193(17)	6319(8)	125(10)*
11)	7506(7)	-587(11)	3593(5)	47(5)*
12)	7826(8)	-1410(13)	4062(6)	60(6)*
13)	8477(8)	-2043(14)	4005(7)	72(6)*
14)	8792(8)	-1915(15)	3504(7)	77(7)*
15)	8477(10)	-1117(14)	3051(7)	80(7)*
16)	7840(8)	-410(12)	3090(6)	57(5)*
17)	7417(9)	-1662(14)	4570(6)	72(6)*
18)	6773(9)	-2567(14)	4378(7)	90(7)*
19)	7979(10)	-2043(15)	5167(6)	96(8)*
20)	7494(8)	392(14)	2573(7)	68(6)*
21)	6936(10)	-259(16)	2087(6)	99(8)*
22)	8089(10)	1095(16)	2304(8)	114(9)*

23)	7860(8)	1337(11)	5463(6)	56(5)*
24)	8512(8)	1461(13)	5193(6)	69(6)*
25)	9233(9)	1053(15)	5524(8)	90(8)*
26)	9295(9)	600(16)	6092(8)	95(8)*
27)	8687(10)	529(16)	6360(7)	92(8)*
28)	7958(8)	867(13)	6057(6)	66(6)*
29)	7272(10)	799(16)	6361(6)	87(7)*
30)	7239(13)	1928(19)	6731(9)	148(13)*
31)	7277(12)	-283(19)	6759(8)	144(12)*
32)	8417(8)	2041(15)	4567(6)	71(6)*
33)	9019(9)	1631(20)	4225(7)	126(10)*
34)	8421(10)	3424(17)	4628(7)	101(8)*

Equivalent isotropic U defined as one third of the
trace of the orthogonalised U(i,j) tensor

Table 2.   Bond lengths (A)

Mo(1)-Mo(2)	2.797(2)	Mo(1)-S(1)	2.349(3)
Mo(1)-S(2)	2.370(4)	Mo(1)-S(3)	2.551(5)
Mo(1)-S(4)	2.507(4)	Mo(1)-S(5)	2.456(3)
Mo(1)-N(3)	1.74(1)	Mo(2)-S(1)	2.337(3)
Mo(2)-S(2)	2.383(4)	Mo(2)-S(3)	2.657(5)
Mo(2)-S(6)	2.485(4)	Mo(2)-S(7)	2.481(4)
Mo(2)-N(4)	1.716(9)	S(2)-S(3)	1.936(6)
S(4)-C(1)	1.71(1)	S(5)-C(1)	1.71(2)
S(6)-C(6)	1.70(1)	S(7)-C(6)	1.71(1)
N(1)-C(1)	1.33(2)	N(1)-C(2)	1.48(3)
N(1)-C(4)	1.45(3)	N(2)-C(6)	1.30(2)
N(2)-C(7)	1.49(2)	N(2)-C(9)	1.48(2)
N(3)-C(11)	1.37(2)	N(4)-C(23)	1.37(2)
C(2)-C(3)	1.34(4)	C(4)-C(5)	1.46(5)
C(7)-C(8)	1.39(2)	C(9)-C(10)	1.45(2)
C(11)-C(12)	1.41(2)	C(11)-C(16)	1.40(2)
C(12)-C(13)	1.38(2)	C(12)-C(17)	1.51(2)
C(13)-C(14)	1.37(2)	C(14)-C(15)	1.37(2)
C(15)-C(16)	1.39(2)	C(16)-C(20)	1.48(2)
C(17)-C(18)	1.51(2)	C(17)-C(19)	1.54(2)
C(20)-C(21)	1.49(2)	C(20)-C(22)	1.54(3)
C(23)-C(24)	1.43(2)	C(23)-C(28)	1.41(2)
C(24)-C(25)	1.41(2)	C(24)-C(32)	1.52(2)
C(25)-C(26)	1.35(3)	C(26)-C(27)	1.35(3)
C(27)-C(28)	1.38(2)	C(28)-C(29)	1.53(2)
C(29)-C(30)	1.50(3)	C(29)-C(31)	1.49(3)
C(32)-C(33)	1.52(2)	C(32)-C(34)	1.52(3)

183

Table 3. Bond angles (deg.)

Mo(2)-Mo(1)-S(1)	53.2(1)	Mo(2)-Mo(1)-S(2)	54.2(1)
S(1)-Mo(1)-S(2)	106.7(1)	Mo(2)-Mo(1)-S(3)	59.4(1)
S(1)-Mo(1)-S(3)	88.8(1)	S(2)-Mo(1)-S(3)	46.1(1)
Mo(2)-Mo(1)-S(4)	139.5(1)	S(1)-Mo(1)-S(4)	151.6(1)
S(2)-Mo(1)-S(4)	88.2(1)	S(3)-Mo(1)-S(4)	84.5(1)
Mo(2)-Mo(1)-S(5)	127.1(1)	S(1)-Mo(1)-S(5)	83.0(1)
S(2)-Mo(1)-S(5)	139.5(1)	S(3)-Mo(1)-S(5)	96.4(1)
S(4)-Mo(1)-S(5)	70.4(1)	Mo(2)-Mo(1)-N(3)	108.7(3)
S(1)-Mo(1)-N(3)	104.4(3)	S(2)-Mo(1)-N(3)	105.4(3)
S(3)-Mo(1)-N(3)	151.5(3)	S(4)-Mo(1)-N(3)	94.2(3)
S(5)-Mo(1)-N(3)	110.1(3)	Mo(1)-Mo(2)-S(1)	53.5(1)
Mo(1)-Mo(2)-S(2)	53.7(1)	S(1)-Mo(2)-S(2)	106.7(1)
Mo(1)-Mo(2)-S(3)	55.7(1)	S(1)-Mo(2)-S(3)	86.5(1)
S(2)-Mo(2)-S(3)	44.8(1)	Mo(1)-Mo(2)-S(6)	134.4(1)
S(1)-Mo(2)-S(6)	143.3(1)	S(2)-Mo(2)-S(6)	87.6(1)
S(3)-Mo(2)-S(6)	80.4(1)	Mo(1)-Mo(2)-S(7)	135.1(1)
S(1)-Mo(2)-S(7)	84.6(1)	S(2)-Mo(2)-S(7)	152.4(1)
S(3)-Mo(2)-S(7)	113.3(1)	S(6)-Mo(2)-S(7)	69.9(1)
Mo(1)-Mo(2)-N(4)	106.6(3)	S(1)-Mo(2)-N(4)	107.0(3)
S(2)-Mo(2)-N(4)	100.4(3)	S(3)-Mo(2)-N(4)	145.2(3)
S(6)-Mo(2)-N(4)	103.1(3)	S(7)-Mo(2)-N(4)	100.1(3)
Mo(1)-S(1)-Mo(2)	73.3(1)	Mo(1)-S(2)-Mo(2)	72.1(1)
Mo(1)-S(2)-S(3)	71.8(2)	Mo(2)-S(2)-S(3)	75.2(2)
Mo(1)-S(3)-Mo(2)	64.9(1)	Mo(1)-S(3)-S(2)	62.0(2)
Mo(2)-S(3)-S(2)	60.1(2)	Mo(1)-S(4)-C(1)	87.0(5)
Mo(1)-S(5)-C(1)	88.7(5)	Mo(2)-S(6)-C(6)	88.4(5)
Mo(2)-S(7)-C(6)	88.2(4)	C(1)-N(1)-C(2)	121.6(13)
C(1)-N(1)-C(4)	123.3(16)	C(2)-N(1)-C(4)	114.6(16)
C(6)-N(2)-C(7)	123.4(11)	C(6)-N(2)-C(9)	121.1(12)
C(7)-N(2)-C(9)	115.0(11)	Mo(1)-N(3)-C(11)	177.0(9)
Mo(2)-N(4)-C(23)	174.4(9)	S(4)-C(1)-S(5)	113.8(7)
S(4)-C(1)-N(1)	122.6(12)	S(5)-C(1)-N(1)	123.6(11)
N(1)-C(2)-C(3)	106.5(20)	N(1)-C(4)-C(5)	109.1(27)
S(6)-C(6)-S(7)	113.1(7)	S(6)-C(6)-N(2)	123.3(10)
S(7)-C(6)-N(2)	123.6(10)	N(2)-C(7)-C(8)	117.7(14)
N(2)-C(9)-C(10)	115.1(13)	N(3)-C(11)-C(12)	120.8(12)
N(3)-C(11)-C(16)	117.9(10)	C(12)-C(11)-C(16)	121.2(12)
C(11)-C(12)-C(13)	117.4(13)	C(11)-C(12)-C(17)	120.1(13)
C(13)-C(12)-C(17)	122.2(12)	C(12)-C(13)-C(14)	121.9(13)
C(13)-C(14)-C(15)	120.2(15)	C(14)-C(15)-C(16)	121.2(15)
C(11)-C(16)-C(15)	118.0(12)	C(11)-C(16)-C(20)	122.5(12)
C(15)-C(16)-C(20)	119.2(13)	C(12)-C(17)-C(18)	111.6(12)
C(12)-C(17)-C(19)	112.3(13)	C(18)-C(17)-C(19)	112.2(12)
C(16)-C(20)-C(21)	112.7(12)	C(16)-C(20)-C(22)	113.7(12)
C(21)-C(20)-C(22)	111.1(13)	N(4)-C(23)-C(24)	118.9(11)
N(4)-C(23)-C(28)	121.3(13)	C(24)-C(23)-C(28)	119.7(12)
C(23)-C(24)-C(25)	118.5(13)	C(23)-C(24)-C(32)	119.9(12)
C(25)-C(24)-C(32)	121.6(15)	C(24)-C(25)-C(26)	119.4(16)
C(25)-C(26)-C(27)	122.3(15)	C(26)-C(27)-C(28)	121.5(15)
C(23)-C(28)-C(27)	118.4(14)	C(23)-C(28)-C(29)	120.0(12)
C(27)-C(28)-C(29)	121.6(13)	C(28)-C(29)-C(30)	109.9(15)
C(28)-C(29)-C(31)	114.2(15)	C(30)-C(29)-C(31)	108.8(14)
C(24)-C(32)-C(33)	113.4(13)	C(24)-C(32)-C(34)	109.7(12)
C(33)-C(32)-C(34)	110.6(14)		
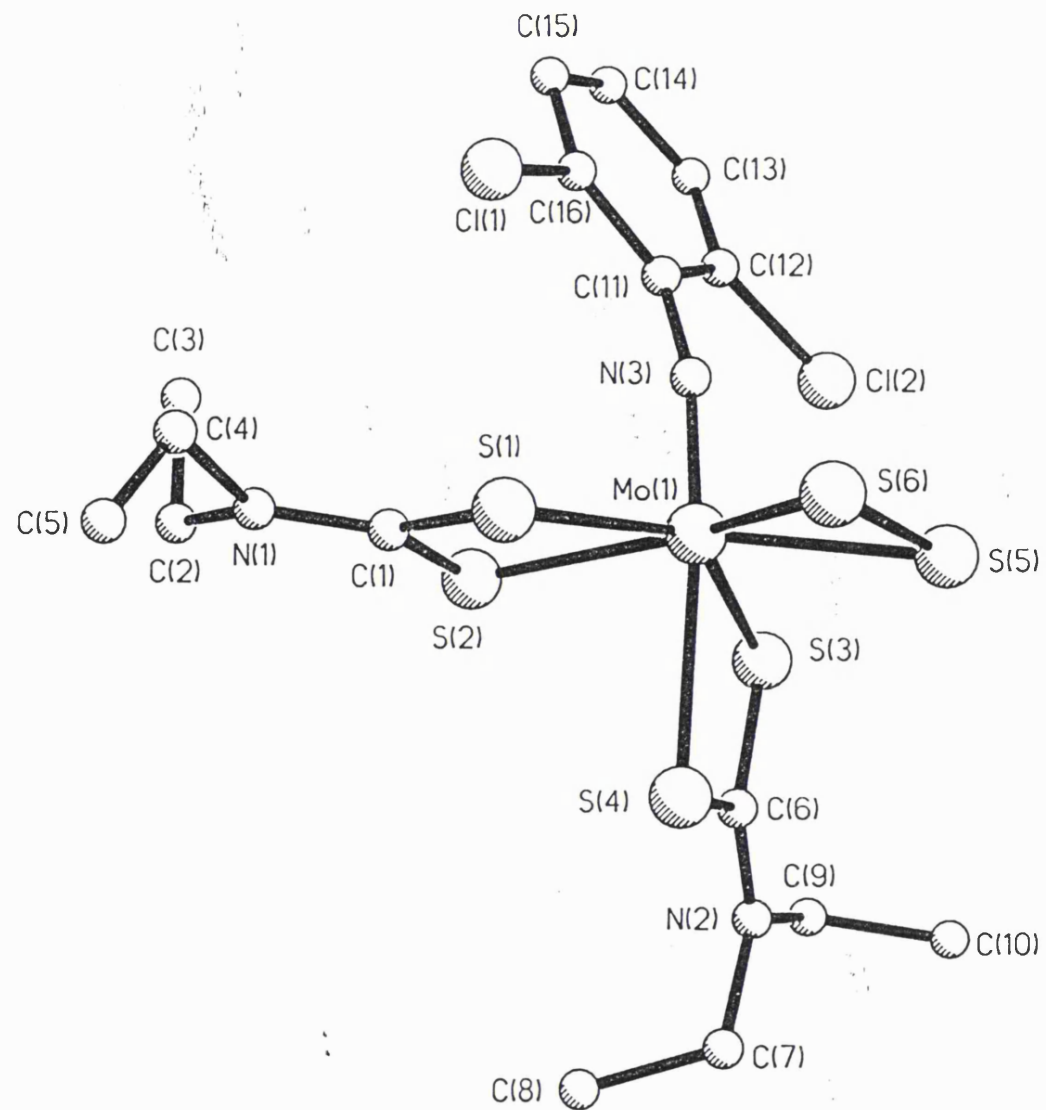
Table 1. Crystal data and structure refinement for 38.

Identification code   str539

Empirical formula   C16 H23 Cl2 Mo N3 S6

Formula weight   616.57

Temperature   293(2) K

Wavelength   0.71073 A

Crystal system   Orthorhombic

Space group   Pcab

Unit cell dimensions   a = 15.612(4) A   alpha = 90 deg.
                                        b = 17.646(4) A   beta = 90 deg.
                                        c = 18.024(3) A   gamma = 90 deg.

Volume   4965(2) A^3

Z   8

Density (calculated)   1.650 Mg/m^3

Absorption coefficient   1.258 mm^-1

F(000)   2496

Crystal size   0.44 x 0.31 x 0.03 mm

Theta range for data collection   2.54 to 25.05 deg.

Index ranges   0<=h<=18, 0<=k<=21, 0<=l<=21

Reflections collected   4145

Independent reflections   4145 [R(int) = 0.0000]

Refinement method   Full-matrix least-squares on F^2

Data / restraints / parameters   4145 / 0 / 253

Goodness-of-fit on F^2   1.219

Final R indices [I>2sigma(I)]   R1 = 0.0794, wR2 = 0.1624

R indices (all data)   R1 = 0.1266, wR2 = 0.2122

Largest diff. peak and hole   0.985 and -0.789 e.A^-3

Table 2. Atomic coordinates (x 10^4) and equivalent isotropic displacement parameters (A^2 x 10^3) for 36. U(eq) is defined as one third of the trace of the orthogonalized Uij tensor.

	x	y	z	U(eq)
Mo(1)	1440(1)	1828(1)	839(1)	37(1)
S(1)	11(2)	1654(2)	1385(2)	49(1)
S(2)	1293(2)	2597(2)	2013(2)	50(1)
S(3)	2609(2)	2793(2)	653(2)	44(1)
S(4)	843(2)	3072(2)	270(2)	44(1)
S(5)	1871(2)	1497(2)	-409(2)	54(1)
S(6)	727(2)	1068(2)	-70(2)	53(1)
N(1)	-120(7)	2210(6)	2770(6)	67(3)
N(2)	2076(6)	4108(5)	64(5)	47(2)
N(3)	2057(5)	1195(5)	1359(5)	36(2)
Cl(1)	1099(2)	267(2)	2466(2)	72(1)
Cl(2)	3949(2)	1454(2)	1240(2)	68(1)
C(1)	320(7)	2165(6)	2152(6)	46(3)
C(2)	221(8)	2641(8)	3411(7)	59(3)
C(3)	815(11)	2167(9)	3881(8)	83(5)
C(4)	-874(10)	1746(13)	2947(10)	113(8)
C(5)	-1595(14)	2011(19)	2880(16)	254(24)
C(6)	1863(7)	3418(6)	285(6)	38(2)
C(7)	1433(8)	4630(7)	-217(7)	54(3)
C(8)	1061(9)	5116(8)	406(8)	71(4)
C(9)	2980(7)	4352(6)	28(7)	53(3)
C(10)	3358(10)	4223(8)	-726(8)	72(4)
C(11)	2552(7)	859(6)	1892(6)	41(2)
C(12)	3446(7)	921(6)	1906(6)	46(3)
C(13)	3942(9)	584(8)	2453(8)	67(4)
C(14)	3553(10)	149(9)	2990(8)	77(5)
C(15)	2680(9)	47(8)	2977(8)	68(4)
C(16)	2185(8)	388(7)	2460(7)	53(3)

Table 4.   Bond lengths [A] and angles [deg] for 3%.

Mo(1)-N(3)	1.747(8)
Mo(1)-S(6)	2.392(3)
Mo(1)-S(5)	2.419(3)
Mo(1)-S(1)	2.458(3)
Mo(1)-S(3)	2.519(3)
Mo(1)-S(2)	2.525(3)
Mo(1)-S(4)	2.596(3)
S(1)-C(1)	1.720(12)
S(2)-C(1)	1.718(11)
S(3)-C(6)	1.735(11)
S(4)-C(6)	1.707(11)
S(5)-S(6)	2.034(5)
N(1)-C(1)	1.311(14)
N(1)-C(2)	1.48(2)
N(1)-C(4)	1.47(2)
N(2)-C(6)	1.322(13)
N(2)-C(7)	1.454(14)
N(2)-C(9)	1.478(14)
N(3)-C(11)	1.369(13)
Cl(1)-C(16)	1.709(13)
Cl(2)-C(12)	1.716(13)
C(2)-C(3)	1.51(2)
C(4)-C(5)	1.22(3)
C(7)-C(8)	1.53(2)
C(9)-C(10)	1.50(2)
C(11)-C(12)	1.40(2)
C(11)-C(16)	1.44(2)
C(12)-C(13)	1.39(2)
C(13)-C(14)	1.38(2)
C(14)-C(15)	1.37(2)
C(15)-C(16)	1.35(2)
N(3)-Mo(1)-S(6)	105.5(3)
N(3)-Mo(1)-S(5)	101.0(3)
S(6)-Mo(1)-S(5)	50.02(11)
N(3)-Mo(1)-S(1)	101.9(3)
S(6)-Mo(1)-S(1)	77.40(11)
S(5)-Mo(1)-S(1)	126.50(11)
N(3)-Mo(1)-S(3)	96.0(3)
S(6)-Mo(1)-S(3)	128.67(11)
S(5)-Mo(1)-S(3)	80.67(11)
S(1)-Mo(1)-S(3)	142.65(10)
N(3)-Mo(1)-S(2)	86.8(3)
S(6)-Mo(1)-S(2)	146.44(11)
S(5)-Mo(1)-S(2)	159.10(11)
S(1)-Mo(1)-S(2)	69.45(10)
S(3)-Mo(1)-S(2)	79.24(10)
N(3)-Mo(1)-S(4)	161.8(3)
S(6)-Mo(1)-S(4)	92.05(10)
S(5)-Mo(1)-S(4)	86.38(10)
S(1)-Mo(1)-S(4)	86.40(10)
S(3)-Mo(1)-S(4)	68.61(9)
S(2)-Mo(1)-S(4)	80.98(10)
C(1)-S(1)-Mo(1)	90.1(4)
C(1)-S(2)-Mo(1)	87.9(4)
C(6)-S(3)-Mo(1)	89.7(3)
C(6)-S(4)-Mo(1)	87.8(4)
S(6)-S(5)-Mo(1)	64.28(13)
S(5)-S(6)-Mo(1)	65.70(13)
C(1)-N(1)-C(2)	120.3(10)

C(1)-N(1)-C(4)	124.9(12)
C(2)-N(1)-C(4)	113.8(11)
C(6)-N(2)-C(7)	121.0(10)
C(6)-N(2)-C(9)	121.4(9)
C(7)-N(2)-C(9)	117.3(9)
C(11)-N(3)-Mo(1)	164.9(8)
N(1)-C(1)-S(2)	124.2(9)
N(1)-C(1)-S(1)	124.5(9)
S(2)-C(1)-S(1)	111.3(6)
N(1)-C(2)-C(3)	112.0(11)
C(5)-C(4)-N(1)	120(3)
N(2)-C(6)-S(4)	124.0(9)
N(2)-C(6)-S(3)	122.1(8)
S(4)-C(6)-S(3)	113.9(6)
N(2)-C(7)-C(8)	111.2(10)
N(2)-C(9)-C(10)	111.8(11)
N(3)-C(11)-C(12)	122.8(10)
N(3)-C(11)-C(16)	121.7(10)
C(12)-C(11)-C(16)	115.5(10)
C(13)-C(12)-C(11)	122.3(12)
C(13)-C(12)-Cl(2)	118.5(10)
C(11)-C(12)-Cl(2)	119.2(9)
C(14)-C(13)-C(12)	119.5(13)
C(13)-C(14)-C(15)	119.9(12)
C(14)-C(15)-C(16)	121.3(14)
C(15)-C(16)-C(11)	121.3(12)
C(15)-C(16)-Cl(1)	120.5(10)
C(11)-C(16)-Cl(1)	118.1(9)

Symmetry transformations used to generate equivalent atoms:

189

Table 5.   Anisotropic displacement parameters (A^2 x 10^3) for 3̌§.
The anisotropic displacement factor exponent takes the form:
-2 pi^2 [h^2 a*^2 U11 + ... + 2 h k a* b* U12]

	U11	U22	U33	U23	U13	U12
Mo(1)	34(1)	37(1)	38(1)	4(1)	0(1)	0(1)
S(1)	37(1)	50(2)	59(2)	-9(1)	5(1)	-8(1)
S(2)	48(2)	56(2)	44(2)	-4(1)	2(1)	-12(1)
S(3)	36(1)	43(2)	53(2)	10(1)	-2(1)	-3(1)
S(4)	38(1)	43(2)	52(2)	4(1)	-2(1)	4(1)
S(5)	61(2)	53(2)	47(2)	1(1)	7(2)	7(2)
S(6)	53(2)	49(2)	56(2)	-5(1)	-11(2)	3(1)
N(1)	69(7)	68(7)	65(7)	-13(6)	34(6)	-26(6)
N(2)	67(6)	31(5)	44(5)	5(4)	-1(5)	-6(5)
N(3)	35(4)	36(5)	36(5)	-3(4)	2(4)	-4(4)
Cl(1)	61(2)	86(3)	70(2)	26(2)	14(2)	-3(2)
Cl(2)	45(2)	65(2)	93(3)	3(2)	5(2)	-7(2)
C(1)	45(6)	40(6)	53(7)	-4(5)	11(5)	-9(5)
C(2)	67(8)	62(8)	48(7)	4(6)	13(6)	14(7)
C(3)	94(11)	93(12)	62(9)	7(9)	1(9)	-12(10)
C(4)	66(10)	188(21)	85(12)	-56(13)	50(9)	-47(12)
C(5)	85(16)	456(63)	221(33)	-203(38)	26(19)	-71(27)
C(6)	45(6)	35(6)	35(5)	5(4)	-5(5)	-9(5)
C(7)	66(8)	47(7)	50(7)	20(6)	-8(6)	1(6)
C(8)	65(9)	58(8)	90(11)	-14(8)	-9(8)	10(7)
C(9)	53(7)	27(6)	77(9)	4(6)	-3(6)	-3(5)
C(10)	88(10)	58(8)	70(9)	11(7)	19(8)	8(8)
C(11)	38(6)	43(6)	43(6)	0(5)	6(5)	9(5)
C(12)	54(7)	40(6)	46(6)	-14(5)	-7(5)	7(5)
C(13)	64(8)	77(10)	59(8)	-7(8)	-16(7)	18(7)
C(14)	82(10)	96(11)	55(9)	16(8)	-21(8)	42(9)
C(15)	74(10)	74(9)	56(8)	11(7)	4(7)	18(8)
C(16)	74(8)	43(7)	43(6)	9(5)	1(6)	13(6)

Table 6. Hydrogen coordinates (x 10^4) and isotropic displacement parameters (A^2 x 10^3) for 28.

	x	y	z	U(eq)
H(2A)	-244(8)	2817(8)	3714(7)	80
H(2B)	523(8)	3077(8)	3231(7)	80
H(3A)	1022(11)	2471(9)	4285(8)	80
H(3B)	514(11)	1735(9)	4074(8)	80
H(3C)	1290(11)	1998(9)	3586(8)	80
H(4A)	-860(10)	1589(13)	3457(10)	80
H(4B)	-856(10)	1305(13)	2635(10)	80
H(5A)	-2101(14)	1718(19)	2975(16)	80
H(5B)	-1592(14)	2450(19)	3193(16)	80
H(5C)	-1589(14)	2166(19)	2369(16)	80
H(7A)	983(8)	4351(7)	-456(7)	80
H(7B)	1689(8)	4959(7)	-579(7)	80
H(8A)	638(9)	5459(8)	214(8)	80
H(8B)	799(9)	4785(8)	764(8)	80
H(8C)	1511(9)	5399(8)	639(8)	80
H(9A)	3305(7)	4079(6)	393(7)	80
H(9B)	3015(7)	4882(6)	145(7)	80
H(10A)	3944(10)	4388(8)	-728(8)	80
H(10B)	3333(10)	3692(8)	-840(8)	80
H(10C)	3040(10)	4502(8)	-1091(8)	80
H(13A)	4551(9)	659(8)	2450(8)	80
H(14A)	3894(10)	-61(9)	3382(8)	80
H(15A)	2421(9)	-290(8)	3329(8)	80